DECISION-MAKING FRAMEWORK FOR WATER TRANSMISSION MAIN MANAGEMENT USING DEEP LEARNING AND ECONOMIC EVALUATION

by

Hong Jin Jun

A dissertation submitted in partial fulfillment

of the requirements for the degree of

Doctor of Philosophy

(Civil and Environmental Engineering)

at the

UNIVERSITY OF WISCONSIN-MADISON

2019

Date of final oral examination: 11/14/2018

The dissertation is approved by the following members of the Final Oral Committee:

Park, Jim, Professor, Civil and Environmental Engineering
Harrington, Gregory, Professor, Civil and Environmental Engineering
Wu, Chin, Professor, Civil and Environmental Engineering
Ahn, Soyoung, Associate Professor, Civil and Environmental Engineering
Kim, Chanwoo, Assistant Professor, Mathematics

To

My beloved Parents and

My lovely Wife and Son

ABSTRACT

As water networks get older, water main breaks become far more likely, resulting in water service interruption, property flooding, traffic disruption, claims and considerable inconvenience to end users. In the United States (U.S.), water main breaks occur at the high rate of 240,000 per year (EPA 2007). Accordingly, it is not surprising that the reported infrastructure grade of the U.S. in the drinking water category is "D (Poor - At Risk)", implying that the infrastructure is approaching the end of its service life with a high risk of failure (American Water Works Association 2014). Failures in drinking water infrastructure can cause water service outages as well as obstacles to emergency preparedness and can affect other infrastructure systems such as damage to the road. Unscheduled pipe repair work may bring about additional interruptions to transportation and commerce (American Water Works Association 2014). Similarly, the multi-regional water transmission mains (WTMs) (approximately 5,000 km and 50 water supply facilities) installed in the 1960s in the Republic of Korea (ROK) are experiencing increased water main breaks.

The problems associated with the management of aging WTMs that need to be solved are: (1) lack of study on understanding the main factors affecting steel WTMs in practice and their failure mechanisms, (2) lack of analysis on comprehensive factor affecting pipe failures, (3) no predictive model forecasting a service life of aging steel WTMs, and (4) no methodology to valuate the intangible benefits of water main improvement projects into monetary units to assess their economic feasibility study.

To solve the above addressed problems, the following four tasks were studied: (1) determination of primary factors affecting failures in installed steel WTMs, (2) establishment of scientific causal mechanisms of the identified factors with WTM failure, (3) development of a predictive model for large diameter

steel WTM breaks, which includes both physical factors as well as water quality factors, with the aid of Deep Neural Network algorithms, and (4) establishment of an economic feasibility assessment framework for the budget justification of water main improvement and rehabilitation projects by developing a methodology to convert intangible public benefits of water main improvement into monetary units.

From the study, the holistic model for chemistry-based mechanisms between the key factors and deterioration of steel WTMs was formulated, the DNN-based predictive model suitable for steel WTMs was developed, and an economic feasibility study framework based on the developed economic valuation techniques of aging pipe improvements was proposed. These outcomes should allow water utilities to successfully establish optimal water transmission mains management strategies for multi-regional water supply facilities by: (1) predicting replacement timing of aging steel WTMs through input of physical, environmental and operational data, (2) assessing an economic feasibility on aging pipeline improvement projects including social and environmental benefits to public, and (3) supporting a long-term strategic investment planning of underground pipeline asset improvement projects. Thus, the study outcomes will contribute to public budget savings, proper decision making on securing funds, an extended water main service life, and reduced water supply service disruptions.

ACKNOWLEDGMENTS

Completion of this doctoral dissertation was possible with the support of several people.

First, I am extremely grateful to my advisor, Dr. Jim Park. He has been a tremendous mentor for me. I greatly appreciate his valuable guidance and consistent encouragement throughout my study. His patience and effort were essential to the birth of my dissertation. I will never be able to thank him enough.

Also, I would like to thank my committee members, Dr. Gregory Harrington, Dr. Chin Wu, Dr. Soyoung Ahn, and Dr. Chanwoo Kim for serving as my committee members. I want to thank you for letting my defense be an enjoyable moment, and for their brilliant comments and suggestions that enriched my work.

Additionally, my gratitude is extended to K-water for the financial support and data, Dr. CH Bae for valuable suggestion and resources, Dr. MK Kang for counseling and encouragement, Gary K. Klemp for proofreading this dissertation.

Finally, I give my full gratitude to my parents, parents-in-law, my sister for taking care of my parents, my brother, and brother-in-law for financial support throughout my study. Most of all, I would like to express my deepest love and appreciation to my beloved wife, Yougsuk, Seo and my son, Jaesung Jun. Thank you for your patience and steady belief in me.

Above all, I owe it all to Almighty God for granting me the wisdom, health, and strength to undertake this research task and caring for me every moment to its completion.

TABLE OF CONTENTS

LIST OF FIGURES

LIST OF TABLES

ACRONYMS

ANN	Artificial Neural Network
ASCE	American Society for Civil Engineers
AWWA	American Water Works Association
BC	Benefit to Cost
CNN	Convolutional Neural Network
CVM	Contingent Valuation Method
DBN	Deep Belief Network
DC	Direct Current
DNN	Deep Neural Network
DO	Dissolved Oxygen
DWTP	Drinking Water Treatment Plant
EC	Electoral Conductivity
ECP	Electrochemical Corrosion Potential
EPA	Environmental Protection Agency
MIC	Microbiologically Influenced Corrosion
MLNN	Multiple hidden-Layered Neural Network
NN	Neural Network
PAC	Poly Aluminum Chloride
pH	Potential of Hydrogen
PVC	Polyvinyl Chloride
RDM	Robust Decision Making
RMSE	Rooted Mean Squared Errors

ROCOF	Rate of Occurrence of Failure
SOM	Self-Organizing Map
SRB	Sulfate Reducing Bacteria
WTM	Water Transmission Mains
WTP	Willingness to Pay

1 INTRODUCTION

1.1 Background and Research Motivation

A water network consists of transmission mains and a distribution network. Water transmission mains are pipe diameter larger than 61 cm that transport large volumes of water, including both raw water from natural water sources destined for a treatment plant, as well as treated water en route to storage reservoirs or to smaller-diameter distribution networks connected to customers (National Research Council 2006). WTMs include pipes of various diameters and materials (steel, iron, plastics, etc.), chosen to suit the characteristics of the various regional water resources and supply systems. For example, in the United States (U.S.), non-steel pipes (iron and plastics) account for 96% of water networks since there are an abundance of local water supplies (US EPA 2009); this contrasts with the predominance (54%) of large diameter steel transmission mains in the ROK where there is a relative paucity of local water supply and a consequent reliance upon long conveyance and a multi-regional water supply system (about 5,000 km and 50 water supply facilities). WTMs are an important component of the water supply system and play a key role in conveying large volumes of water like an artery conveying blood in our circulatory network.

In the U.S., water main breaks occur at the rate of 240,000 per year (EPA 2007). Accordingly, it is not surprising that the reported infrastructure grade of the United States in the drinking water category is “D (Poor: At Risk)”, implicating that the infrastructure is approaching the end of its service life with a high risk of failure (American Water Works Association 2014).

Also, it was projected that the annual replacements for water mains and their costs would increase over time, as shown in Figure 1.1 and Figure 1.2 (AWWA 2012; EPA 2002). Additionally, Figure 1.3 demonstrates that operations and maintenance expenditures are growing over time and the aging infrastructures pushed up the maintenance spending (Congressional Budget Office 2015). This growing trend of maintenance spending corresponds with U.S. EPA's projections on water main replacement, implying that main breaks are supposed to increase as they approach the end of their service lives. This makes sense considering that most of the nation's drinking water lines were installed after the 1940s.

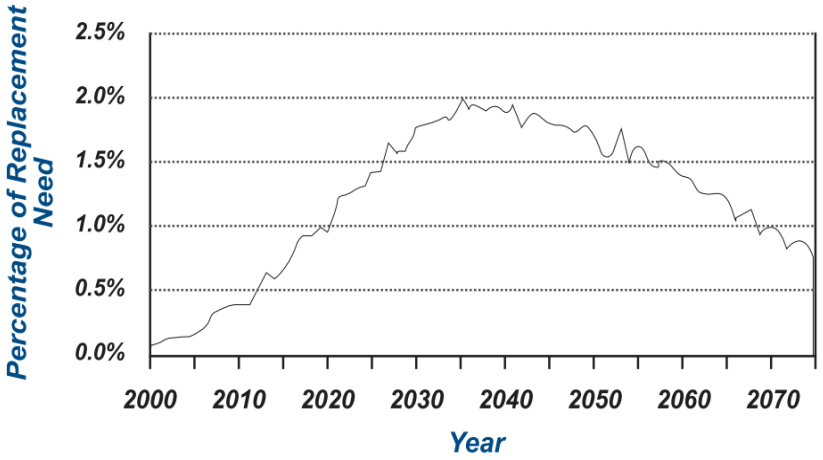

Figure 1.1. Projected annual replacement needs for water mains, 2000-2075 [source from (EPA 2002)]

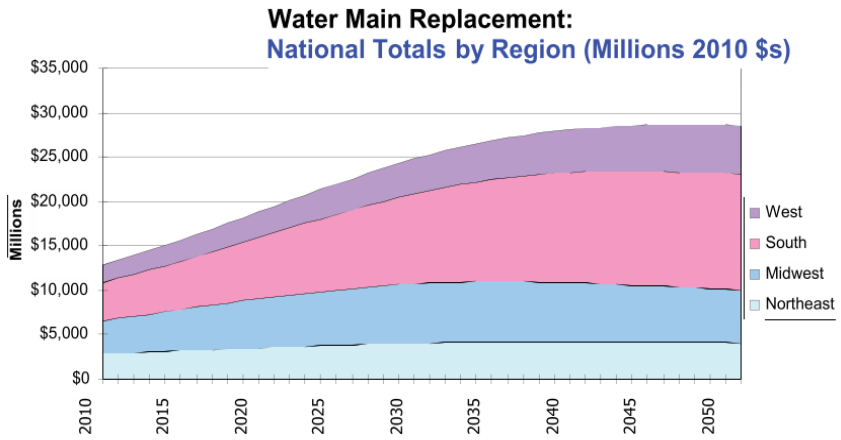

Figure 1.2. Water main replacement costs per region [source from (AWWA 2012)]

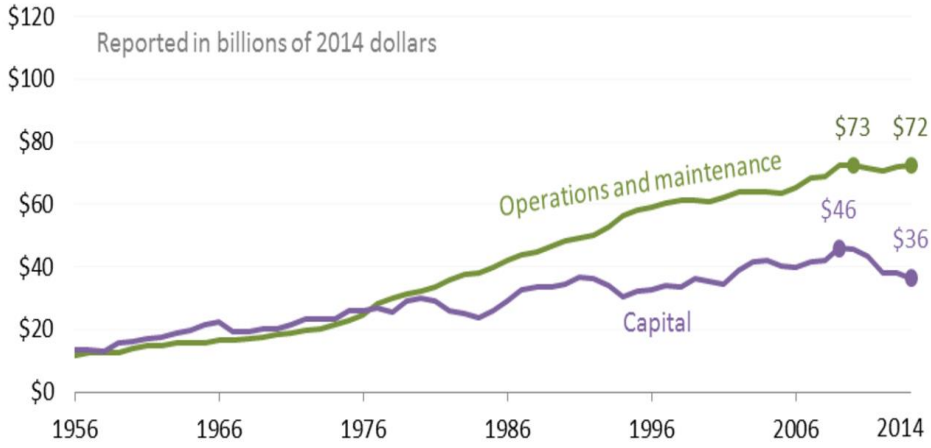

Figure 1.3 Public spending on water infrastructures [source from Congressional Budget Office (2015)]

The number of breaks increases substantially near the end of the system's service life (EPA 2007). The nation's drinking water utilities need 384.2 billion USD in infrastructure investments over the next 20 years for the national public water system infrastructure to ensure the public health (EPA 2013): (1) Large utility breaks in the Midwest increased from 250 per year to 2,200 per year during a 19-year period; (2) In 2003, Baltimore, Maryland, reported 1,190 water main breaks (more than three per day); (3) The U.S.

Geological Survey estimates that water lost from water distribution systems is 38 billion m^3 (1.7 trillion gallons) per year at a national cost of 2.6 billion USD per year.

As water mains age, they become far more likely to fail, resulting in water service disruption, traffic disruption, and considerable inconvenience to end users as seen in Figure 1.4. Besides, failures in drinking water infrastructure can cause water outage as well as obstacles to emergency preparedness and can affect other infrastructure systems such as damage to the road. Unscheduled pipe repair work may cause additional interruptions to transportation and commerce (American Water Works Association 2014). Especially, since large diameter WTMs transport a huge amount of water through a single-track pipeline, the breaks of those WTMs cause more catastrophic damages with far-reaching effects including serious social and economic losses to water consumers than small-diameter based water distribution networks. The risk posed by the failure of large diameter WTMs can be orders of magnitude higher due to the significant damage and loss of service that can occur (US EPA 2009). The postponement of the replacement or rehabilitation of aging WTMs could cause service disruptions that may cost more money, along with inconvenience to the public.

Figure 1.4. Water main break damages in the U.S. (sourced from CNN.com)

Similarly, the multi-regional WTMs (about 5,000 km and 50 water supply facilities) installed in the 1960s in the ROK are experiencing increased WTM breaks, as revealed in Figure 1.5. In the wake of the increased

breaks, in 2015, Korea Water Resources Corporation (K-water) initiated the Aging WTM Improvement Plan (estimated at 3.3 billion USD), which replaces aging pipes and converts existing single to double-track pipelines in order to ensure the stability of the water supply. The scale of the multi-regional WTM improvement projects is so large that the economic feasibility for each project (43.7million USD or more) must be conducted and approved by Ministry of Strategy and Finance of Republic of Korea (ROK) according to relevant statutes. However, surprisingly, a guideline or methodology suitable for aging pipeline improvement has not been established yet, which causes their economic feasibilities to be commonly assessed as low (i.e., BCR < 1), due to their unrecognized social benefits. As a result, K-water has suffered from difficulty in justifying the need of the WTM improvement projects funded by the government, such that a preventive replacement on aging WTMs has not been promoted proactively.

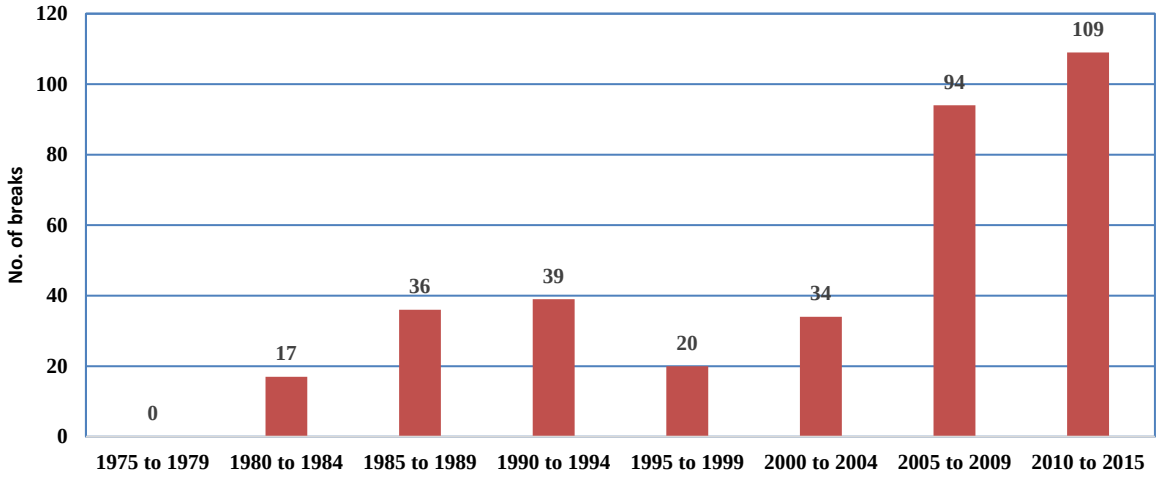

Figure 1.5. The ROK's multi-regional water main breaks caused by deterioration over time [source from (K-water's Operation and Management Services System)]

If water main breaks could be accurately anticipated and a new methodology converting intangible social benefits of WTM improvement into monetary units, water service outages and end-user inconvenience could all be minimized. To this end, a reliable prediction model as well as a methodology to be able to

valuate hidden social benefits into monetary units, are needed in order to make the process of water main replacement as economical as possible and aid in computing an economic validity (i.e., BC >1).

1.2 Problem Statement

Through a review of published literature on the management of water networks, the problems relating to the management of aging WTMs, which need to be solved, are revealed as: (1) lack of study on understanding the main factors affecting steel WTMs in practice and their failure mechanisms, (2) lack of analysis on comprehensive factor affecting pipe failures, (3) no predictive model forecasting breaks of aging steel WTMs, and (4) no methodology to valuate the intangible benefits of water main improvement projects into monetary units to assess their economic feasibility study.

1.2.1 Lack of Study on Understanding Main Factors Affecting Steel WTM failure and Their Failure Mechanisms

Management data and historical records of steel WTMs are scarce (Kleiner and Rajani 2007). Previous studies on the factors contributing to pipeline failure have been concentrated on small diameter water distribution networks composed of iron or PVC pipelines. No studies have so far been conducted in investigating steel WTMs. As WTMs transport a much larger volume of water and their failure leads to even greater damages than those seen in small diameter iron or PVC water main breaks, such studies are much needed. The need for studies focused on steel water mains is further underscored by the fact that extrapolation of the results of previous studies focusing on iron pipes may not be valid. This is due to the fact that iron and steel pipes are quite different in their composition, properties, lining and welding system, the chemical reactions associated with their corrosion and their failure characteristics (American Water Works Association Research Foundation 1996).

Furthermore, the mechanisms that lead to pipe breaks are very complicated and not well understood (Kleiner and Rajani 2007). Nonetheless, previous research on the main factors affecting water main failure has not yet been conducted in connection with identifying the failure mechanisms of the key factors derived, resulting in not presenting proper solutions to extend a service life of WTMs. Thus, present knowledge on the mechanisms between the key factors and failure in steel WTMs is still limited to use for steel WTMs management work efficiently, because it does not cover all factors contributing to water mains failure comprehensively.

1.2.2 Lack of Analysis on Comprehensive Factors Affecting Pipe Failures

Previous research has addressed physical factors such as pipe thickness and diameter and/or environmental factors such as soil characteristics when determining the main causes of failure in aging WTMs. However, these studies did not address water quality factors that may lead to internal corrosion as contributors to the failure of pipes, although internal corrosion has been well known as the most dominant cause of deterioration of steel WTMs (Hou et al. 2016). That is why the existing failure predictive models have not included significant factors affecting water main failures such as water quality and coating methods. This might cause inaccurate prediction results, thereby leading to the premature replacement of aging WTMs or, otherwise, WTM breaks, resulting in serious social and economic losses.

1.2.3 No Predictive Model of Aging Steel Pipeline Breakage

The existing predictive models have been based on small diameter water distribution networks composed of iron or PVC pipelines. No studies have so far been conducted in developing a predictive model for water main breaks in steel WTMs. The lack of predictive models specifically targeting steel WTMs necessitates alternative assessment methods such as the “Man Entry & Visual Inspection” method. This method, though accurate in determining the extent of deterioration at a given point in time, results in water service

interruption, is time-consuming, intrusive and costly, and is limited by very small sample counts. It is necessary to adopt a reasonable and faster method so as to assess the lifespan of aging WTMs and to make a quick decision for potential pipeline failure instead of this manual inspection method (US EPA 2012a).

1.2.4 No Valuating Methodology of Intangible Social Benefits from Water Main Improvements in Monetary Units

Although the timely improvement of aging WTMs is indispensable, its economic feasibility known as Benefit/Cost is generally assessed to be less than 1 due to the inability of considering intangible social impacts, causing the capital investment on water main improvements to fall behind in priority. This is thought to happen because the social and environmental benefits to the public have not been included in the total benefits systematically and institutionally yet despite their contributions. To be specific, there is no clear methodologies (e.g., benefits, calculation methods, specific criteria, etc.) on indirect (e.g., industrial, commercial) and social benefits (e.g., water quality, traffic, footprint, environment, etc.). This delays a timely maintenance or improvement, leading to break accidents in aging water mains. Also, the existing decision support models for water main improvements have not included indirect and social costs despite their significant contribution to the prioritization of water main improvements. This could result in unreasonable decision-making of the aging water main improvements. Thus, this might result in improper decision-making of water mains improvements.

1.3 Research Objectives

The principal objective of this study is to develop a decision support framework for proactive WTM management in multi-regional water supply facilities, which can predict reasonable and cost-effective service life of large diameter steel WTMs, can establish a long-term investment strategy on their improvements

using a newly developed feasibility study methodology for underground pipeline improvement projects. To achieve the principal objective, the study has the following four specific objectives:

(1) To determine key factors affecting failures in installed steel WTMs with analysis of general factors, which include both physical data and water quality data,

(2) To establish scientific causal mechanisms of the identified factors with WTM failure by literature review and by quantifying the failure causes based on the historical break data so that the results can be used for advancing failure prediction of steel pipes as well as for the management to extend a service life of WTMs.

(3) To develop a predictive model for large diameter steel WTM breaks, which includes both physical factors as well as water quality factors, with the aid of Deep Neural Network algorithms.

(4) To develop a methodology to convert intangible public benefits of water main improvement (e.g., implied a cost of averting fatality or water service outage, traffic & water quality improvement, footprint, etc.) into monetary units; and to establish a feasibility assessment methodology for the budget justification of water main improvement and rehabilitation projects.

1.4 Scope of Work and Methodology

The study will be preceded by four tasks listed below:

Task 1: Determine factors influencing deterioration in steel WTMs and their failure mechanisms.

This task identifies significant factors affecting failures in multi-regional steel WTMs by a statistical method using the data supplied from the database of K-water, which maintains 32 drinking water treatment plants and supply facilities (50% of the ROK's drinking water) as a government-owned public utility. Data consist of historical breaks of steel WTMs over the observation period (1969 – 2015) with a total length of 2,783 km. The collected data include pipe diameter, pipe thickness, age, coating, service type, depth of cover,

traffic loading, and water quality (pH, alkalinity, dissolved oxygen, residual chlorine, temperature, and electoral conductivity), and a pipe break rate (number of breaks divided by total length of sectional pipelines of WTMs). Also, this task includes an investigation into how the identified main factors through Pearson's Correlation analysis cause failure in steel WTMs by a comprehensive literature review, and failure cause analysis based on the historical WTM break data. The methodology used for task 1 is as shown in Figure 3.1.

Task 2: Develop a Deep Neural Network-based model to predict a break rate of aging steel WTMs.

This task develops a computational predictive model forecasting a break rate of aging multi-regional steel WTMs so as to determine their replacement timing, using Deep Neural Networks (DNNs), known as powerful tools used to accurately predict outcomes in complex systems involving multiple parameters. This task was performed with the same physical and water quality data used in task 1.

Also, the model was developed in four steps: (1) establish available scenarios (input and target variables) by the main factors obtained through Task 1, (2) determine the best model by comparing performances of three neural networks (NNs) (a shallow artificial NN, multiple hidden layered NN, Stacked autoencoder NN), (3) classify the data into homogeneous groups by an Artificial Neural Network-based clustering technique, and (4) perform the developed model for each group.

Task 3: Develop an economic feasibility study framework suitable to convert intangible public benefits into monetary units to justify the budgets of aging WTM improvements.

This task quantifies the public impacts and benefits of water main improvement and rehabilitation by reducing pipeline damage through the avoidance of failure in WTMs. It calculates repair cost savings of broken pipelines, damage savings of water supply shut-off, reduction in industrial loss, accidents, injuries and fatalities that would result from proactive maintenance and improvements, etc. The damage scope

of pipeline failure for the intangible benefit calculation is assumed to be a water service area of WTMs. Thus, this task provides water utility engineers with an economic feasibility study framework suitable for WTM improvement projects.

The typical valuation methods such as the cost of savings approach, the Replacement Cost Approach, the Market Demand Approach, and the Benefit Transfer are to be used for the intangible benefit valuation from WTM improvements. The direct survey methods such as the Contingent Valuation Method (CVM) of which survey data might be controversial are not to be used in this study.

Task 4: Validate the economic feasibility study framework developed.

This task validates the developed economic feasibility study framework by applying this methodology to an actual WTM improvement project. A sample WTM was selected from the WTMs of the ROK. This task involves: (1) to forecast a break rate of the sample WTM with the Deep Neural Network model developed in Task 2, (2) to decide an economical service life of the pipeline, (3) to compute the BCRs based on the quantified benefits from the WTM improvement project, and (4) to evaluate the validity by comparing before and after the developed valuation framework for economic feasibility study on aging WTM improvements.

1.5 Organization of the Dissertation

Figure 1.6 shows an overview of the organization of this dissertation. The organization of the dissertation is explained below.

Chapter 2 describes a comprehensive review of published literature on pipe deterioration, factors affecting deterioration and failure in drinking water networks, various predictive models (statistical, physical, and Artificial Intelligence) to forecast a break of pipes, and valuation of the benefits from public services.

Chapter 3, “Factors Affecting Steel Water Transmission Pipe Failure and Failure Mechanisms,” has been submitted to the *Journal of Water Research*. This chapter evaluates the primary factors affecting deterioration installed steel WTMs by statistical correlation analysis, presents a chemistry-based model on the causal relationships and mechanisms of the influential factors with the steel WTM failure by literature review, and quantifies the failure causes by the steel WTM failure cause analysis based on the historical break data.

Chapter 4, “Forecasting a Break Rate of Steel Water Transmission Pipe Using Deep Neural Networks” has been published in the *International Journal of Neural Networks and Advanced Applications*. This chapter presents the established methodology to forecast a break rate of large-diameter steel WTMs based on physical and environmental factors, using Deep Neural Network algorithms. The performances of three NNs (a shallow Artificial Neural Network, multi-layered NN, and stacked autoencoder NN) are compared. The performance and application results of ANN-based clustering technique to bundle data into homogeneous groups are discussed.

Chapter 5, “Economic Valuation of Aging Water Main Improvements,” has been submitted to the *Journal of Pipeline Systems Engineering and Practice* (ASCE). This chapter establishes valuation methodologies of benefits from aging water main improvements, propose an economic feasibility study framework on aging WTM improvements, carries out the economic feasibility assessment on a sample WTM improvement project, and evaluates the validity by comparing BCRs before and after the developed valuation framework for an economic feasibility study.

Lastly, Chapter 6 includes the conclusions of this dissertation and recommendation for future studies.

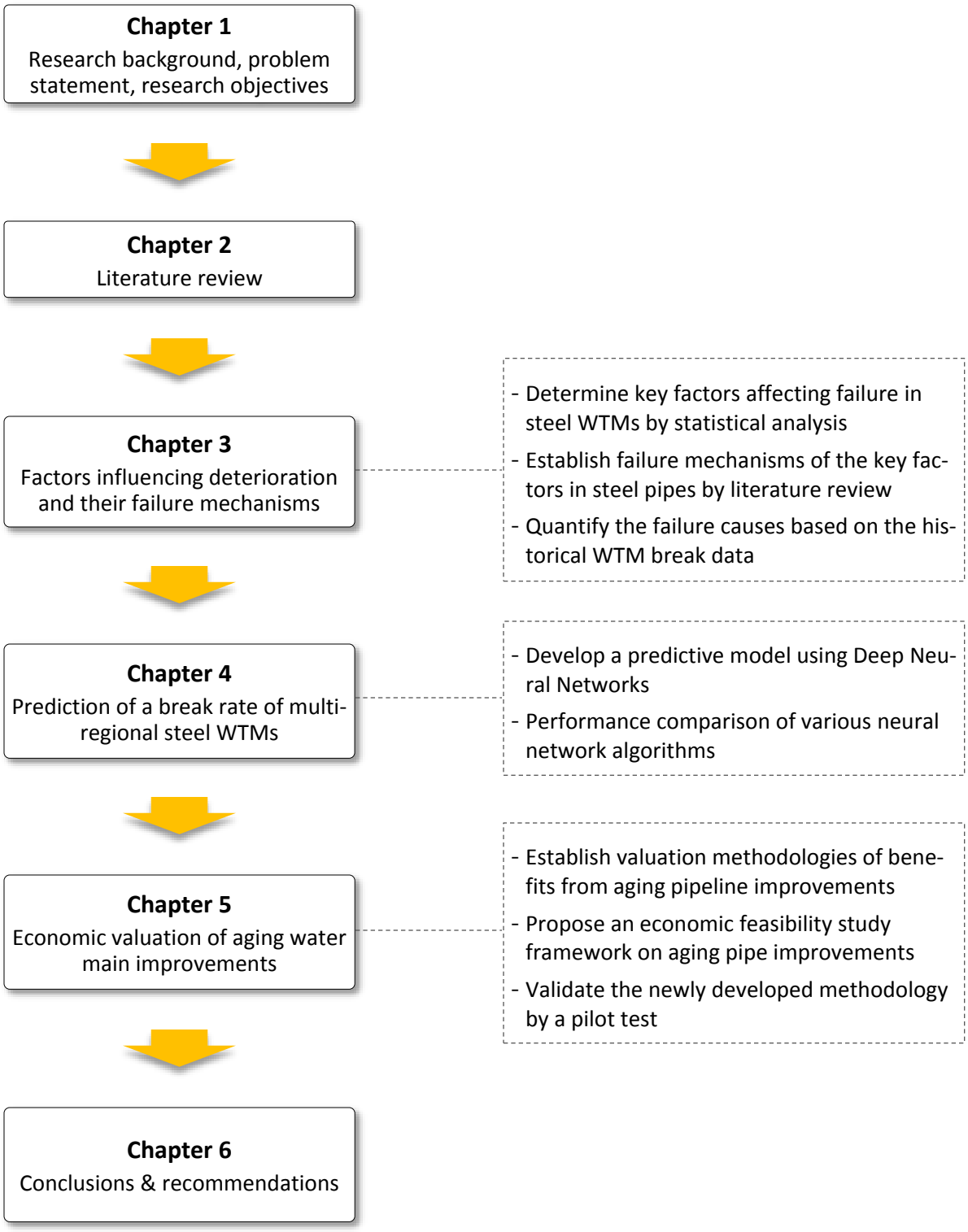

Figure 1.6. Organization of the dissertation

1.6 Summary

The failures of WTMs transporting a huge volume of water cause more catastrophic damages with far-reaching effects including serious social and economic losses to water consumers than small-diameter based water distribution networks. Thus, proactive maintenance on aging WTMs including timely replacement is required to avoid the tremendous damages and inconveniences to drinking water customers.

Since the previous studies and current practices lack the understanding of the main factors affecting steel WTM failure, a predictive model on steel WTMs, and an economic feasibility study guideline on aging pipe improvements, this research developed a failure mechanism model, a Deep Neural Network-based predictive model, and an economic feasibility study framework suitable for steel WTMs.

The study provided the reliable and robust approach to manage aging WTMs properly and proactively by offering the water utility engineers the advanced knowledge and tools for water network assets, resulting in maintaining a healthy water supply system with the least cost and social damage while satisfying the drinking water customers.

Figure 1.7 describes the intuitive flowchart of this study including the problems, the causes, the approaches to solve, the solutions, outcomes, and impacts.

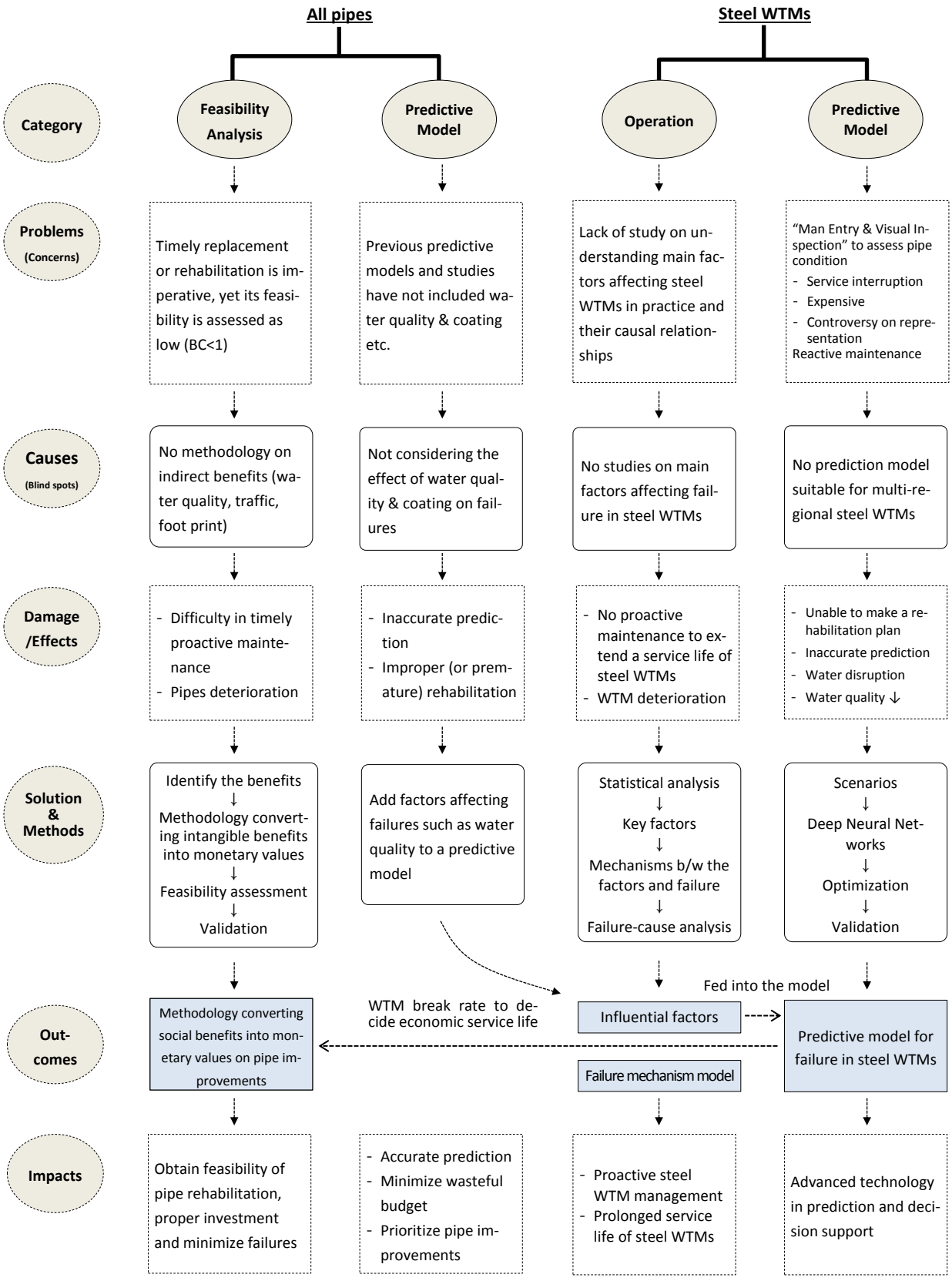

Figure 1.7. Schematic flowchart of this study

2 LITERATURE REVIEW

2.1 Types and Failures of Ferrous Pipes

2.1.1 Types of Ferrous Pipes

Iron pipes in service are composed of gray cast iron and ductile iron pipes. Gray cast iron pipes were typically used as transmission pipes for gas and water and as a water drainage pipe until they were replaced by ductile iron pipes in the late 1940s (Makar and Rajani 2000). Gray cast iron is very brittle and breaks when bent. Gray cast iron pipes are more likely to corrode than ductile iron pipes (US EPA 2009).

Ductile iron is a mainly iron-carbon-silicon alloy. The addition of magnesium transformed the graphite flakes of cast irons into the spherical shape of the graphite, which improved the ductility, the strength and the corrosion resistance of the iron, eventually leading the wide uses of ductile iron pipes in the water industry after the 1950s. Ductile iron pipes are available in the range of 80 to 1,000 mm diameter, in length of 5.5 to 6 m (Canada Pipe Compay 2012).

The carbon content tells steel pipes from iron pipes. Steel pipes contain fewer carbon contents (0.08 ~ 0.25%) by weight than iron pipes in excess of 2%. This enables steel pipes to exhibit substantially better mechanical characteristics (ductility, toughness and tensile elongations) than iron pipes (Keil and Devletian 2011).

Table 2-1 shows a summary of the overview and characteristics of ferrous pipes. Larger diameter pipes such as WTMs require better durability against higher water pressure and heavier external loads. To meet this requirement, iron pipe walls must be thicker as the pipe size increases. Iron pipes are not strong

enough to sustain heavy load and high water pressure compared with steel pipes. Furthermore, iron pipes are more expensive than steel pipes. Thus, steel pipes are better suited for larger size pipes. That is why steel pipes are more widely used for WTMs.

Table 2-1 Advantages, limitations, and graphite structures of ferrous (grey cast iron, ductile, and steel) pipes

Types	Overview	Characteristics	Graphite structures
Gray cast iron pipes	• 2.5 – 4.0% in carbon • Provided with cement mortar lining • Contains graphite flakes	• Thicker wall than ductile iron or steel • Weak in tension, bending, and corrosion resistance • High brittleness and heavy	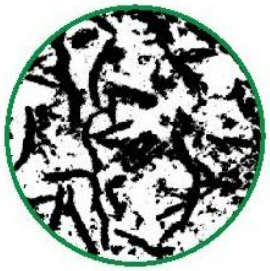
Ductile iron Pipes	• 2.5 - 4.0% carbon with the addition of magnesium • Cement mortar lining • Spherical graphite • 80 - 1,200 mm in diameter	• Susceptible to corrosion • Greater ductility than iron • Greater impact resistance than grey iron • Corrosion resistance	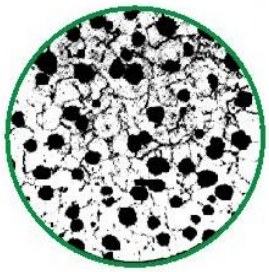
Steel pipes	• 0.08 - 0.25% in carbon • Epoxy Lining • A wide range of diameter available (Large diameter transmission pipes)	• Prone to external corrosion • Electrolysis prone • High tensile strength • High compressive strength	

2.1.2 Failure Causes of Ferrous Pipes

Causes of ferrous pipe breaks can mainly be categorized into corrosion and structural failures. Corrosion of the pipe may result in hole and leakage. Leakage can be considered as an indicator of pitting corrosion (US EPA 2009).

2.1.2.1 Corrosion

Corrosion can be defined as the deterioration of a metal by the reaction to its environment. The corrosion by oxidation requires oxygen, moisture, soluble salts, cathodic and anodic sites, etc. (Fontana 1988). Modes of corrosion include graphitization, pitting corrosion, microbiologically influenced corrosion, electrolytic corrosion, tuberculation, etc.

2.1.2.1.1 Graphitization

Graphitization known as graphitic corrosion is a type of corrosion of cast iron pipes. This type of corrosion occurs where the appropriate soil conditions of pH, dissolved salts, and organic compounds are advantageous to anaerobic bacteria growth, causing the metal to become brittle and be susceptible to cracking failure. In contrast, this form of corrosion does not take place in steel pipes (Illinois State Water Survey 1975).

2.1.2.1.2 Pitting Corrosion

Pitting corrosion is a form of highly localized corrosion with deep holes (Ma 2012). This type of deterioration is more destructive than uniform corrosion because pits are more difficult to be identified due to corrosion products such as rust covering the pits (National Research Council 2003). Pitting corrosion is the most common cause of ferrous pipe deterioration, which can lead to leakage or failure. It can be found on both the internal and external surfaces of the ferrous pipes (Nimmo and Hinds 2003).

In many cases, pitting corrosion results in pipe failure in the form of pinhole leaks. Leakage through holes in the pipe wall is common to ferrous pipes. Such leakage can cause erosion of the pipe bedding and water loss, eventually, leading to structural failure of the pipes (US EPA 2009).

2.1.2.1.3 Microbiologically Induced Corrosion

Microbiologically induced corrosion (MIC) known as biocorrosion is recognized as deterioration of metallic material caused by anaerobic bacteria such as sulfate-reducing bacteria (SRB). Ferrous pipes can be subject to MIC under the condition of sulfates, nitrates, and carbonates (US EPA 2009). This causes ferrous pipes to be weak and brittle, leading to pipe failure (Videla and Herrera 2005).

2.1.2.1.4 Electrolytic Corrosion

Electrolytic corrosion known as stray current corrosion takes places when the pipe picks up stray electrical current from an external direct current (DC) source such as subway or electric railway systems. Underground ferrous pipelines can offer a better path for conducting return currents from electrified transport systems and electrical installations systems. The corrosion occurs at the point where the positive current leaves the pipeline and joins the electrical current source (National Research Council 2003).

2.1.2.1.5 Tuberculation

Tuberculation can be regarded as a secondary result of corrosion and is a common problem occurring in ferrous pipes over time, causing small mounds of corrosive products on the inside of ferrous pipes (Knudsen 1940). Internal corrosion of the ferrous pipes forms porous rust (i.e., $Fe(OH)_3$), transforming into tubercles on the internal surface of the ferrous pipes (AWWA Research Foundation 1996). Various precipitates can combine with tubercles, depending on the pH and other ions present (US EPA 2009). Pitting is usually observed below the tubercles. Builds-up of tubercles reduce the cross-sectional area of a pipe, increase pipe roughness, and deteriorate water quality.

2.1.2.2 Structural Failures

It is often difficult to distinguish between structural failure and corrosion in ferrous pipes. Aging pipes typically break when various corrosion such as tuberculation or pitting weaken the metallic structure so that external or internal stress acting on it exceed remaining strength of the ferrous pipes. In general, circular failures are observed in small diameter pipes of water distribution networks associated with bending stresses, bad installation practices, or internal pressure, thermal contraction, or longitudinal stresses near values and fittings while longitudinal failures found in large diameter pipes of WTMs are caused by transverse stresses, internal pressure, or increased ring stress due to thermal changes (National Research Council 2003).

2.2 Factors Affecting Pipe Deterioration and Failure Mechanisms

2.2.1 Factors Affecting Deterioration in Drinking Water Pipes

A wide variety of physical, environmental, and operational factors are known to affect failure and deterioration in pipes as shown in Table 2-2.

Table 2-2 Factors affecting pipe failures [Modified from (Al-Barqawi and Zayed 2008)]

Categories	Factors
Physical	Pipe material, thickness, age, diameter, length, type of joints, lining and coating, vintage, traffic load, and manufacturing processes
Environmental	Soil type, soil moisture, soil load, microbes, stray electrical currents, water quality (pH, residual chlorine, dissolved oxygen, etc.).
Operational	Internal water pressure, flow velocity, and operational and maintenance practices

Major causes of reinforced concrete and cast iron pipes are found to be attributed to soil moisture content causing soil expansion and soil corrosivity, respectively (Pratt et al. 1996). It was reported that the factors (pipe material, pipe diameter, pipe installation vintage, traffic loading) have a relatively substantial effect on deterioration in pipes (iron, PVC, and concrete) (UNESCO 2014). It was identified that the diameter and burial depth have a relatively high impact on the failure in cast iron water mains, based on one city's limited data composed of 20 pipes with less than 500 mm (Wilson et al. 2015). A comprehensive review of previous research investigating relationships between the physical characteristics of pipes, climatic conditions and pipe failure (iron and plastic) can be found elsewhere (Kleiner and Rajani 2001).

Also, the studies on the identification of pipe deterioration mechanisms were carried out by various lab-scale experiments. The effect of water temperature on corrosion rate and tuberculation of cast iron samples was investigated at the lab experiments (McNeill and Edwards 2002). The effect of chlorides on pitting corrosion of steel specimens was examined, describing that the lifetime of steel under the corrosive condition is in a range of only 2.5 - 27% of that of the uncorroded condition (Ma 2012).

2.2.2 Failure Mechanisms of Ferrous Pipes by Influential Factors

2.2.2.1 pH and Alkalinity

pH and alkalinity are known as key water quality factors that affect steel corrosion (McNeill 2000). pH is a measure of the hydrogen ion (H^+) content of a solution. pH is used universally to represent the intensity of the acidity of a solution.

First, the pH dependency of iron oxidation can be described in the following three steps of iron corrosion reaction in which OH^- takes part in (Bockris et al. 1961):

$$Fe + OH^- \rightarrow FeOH + e^- \quad (2\text{-}1)$$

$$FeOH \rightarrow FeOH^+ + e^- \quad (2\text{-}2)$$

$$FeOH^+ \rightarrow Fe^{2+} + OH^- \quad (2\text{-}3)$$

$$Fe \rightarrow Fe^{2+} + 2e^- \ (Overall\ reaction) \quad (2\text{-}4)$$

Secondly, OH^- is commonly generated in drinking water networks by a reduction reaction as follows:

$$e^- + \tfrac{1}{4}O_2 + \tfrac{1}{2}H_2O \rightarrow OH^- \quad (2\text{-}5)$$

This reaction increases pH, forming $CaCO_3$ as follows (AWWA Research Foundation 1996):

$$OH^- + HCO_3^- \rightarrow CO_3^{2-} + H_2O \quad (2\text{-}6)$$

$$Ca^{2+} + CO_3^{2-} \rightarrow CaCO_3\,(s) \quad (2\text{-}7)$$

$CaCO_3$ precipitates on a surface of steel pipes. A surface is coated with $CaCO_3$ films (calcites) and passivated, inhibiting the corrosion rate.

Third, as pH increases, HCO_3^- concentrations will decrease and CO_3^{2-} will increase as shown in Equation *(2-8)*, producing insoluble $CaCO_3$ and $FeCO_3$ as shown in Equations (2-7) and *(2-9)* respectively. The pipe

wall is coated with the buildup of the precipitates ($CaCO_3$ and $FeCO_3$), thereby retarding the iron corrosion (American Water Works Association Research Foundation 1996).

$$HCO_3^- \rightarrow H^+ + CO_3^{2-} \quad (2\text{-}8)$$

$$Fe^{2+} + CO_3^{2-} \rightarrow FeCO_{3(S)}(siderite) \quad (2\text{-}9)$$

In addition to the increase in CO_3^{2-}, as pH increases, OH^- concentrations will increase. This triggers precipitations of ferrous hydroxide [$Fe(OH)_2$] and amorphous ferric hydroxide [$Fe(OH)_3$] as shown in Equations (2-10) and (2-11), developing protective scales on the pipe wall surface and ultimately inhibiting steel corrosion (American Water Works Association Research Foundation 1996):

$$Fe^{+2} + 2OH^- \rightarrow Fe(OH)_2\,(s) \quad (2\text{-}10)$$

$$Fe^{2+} + \tfrac{1}{4}\,O_2 + \tfrac{1}{2}\,H_2O + 2OH^- \rightarrow Fe(OH)_3\,(s) \quad (2\text{-}11)$$

The above description provides a full understanding of the mechanism of pH effect on steel corrosion. This is consistent with the experimental results indicated in Figure 2.1 (Maughan 2000).

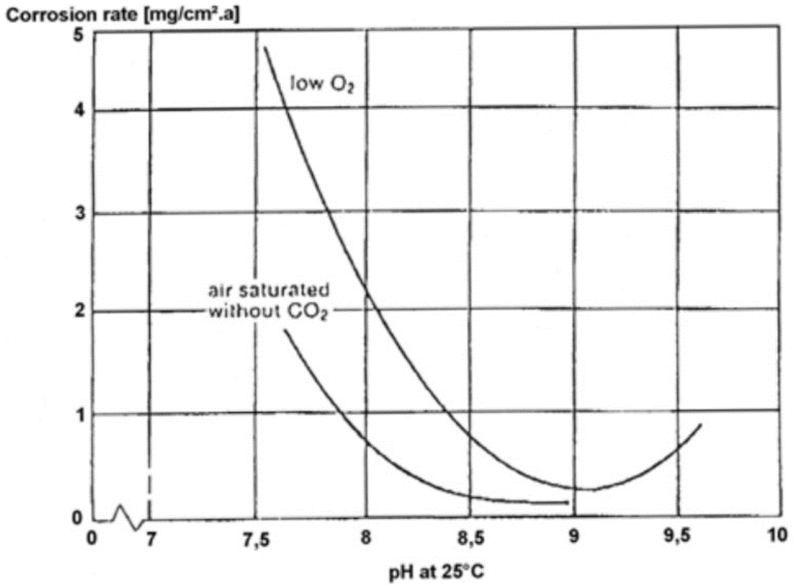

Figure 2.1. The relationship of corrosion rate and pH [Sourced from Maughan (2000)]

Alkalinity refers to water's quantitative capability to neutralize acids. It represents buffering capacity against a pH drop in the water. Total alkalinity includes bicarbonate (HCO_3^-), carbonate (CO_3^{2-}) and hydroxide (OH^-) ions (Muylwyk et al 2014).

First, bicarbonate and carbonate affect the mechanism of steel corrosion such as a capability of water to form a protective carbonate film or passivating scale on a steel surface as follows (AWWA Research Foundation 1996):

$$Ca^{2+} + HCO_3^- \rightarrow CaCO_3(s) + H^+ \qquad (2\text{-}12)$$

As the above reaction proceeds, $CaCO_3$ scales deposits on a surface of steel pipes. A surface is coated with $CaCO_3$ films (calcites) and passivated, inhibiting the corrosion rate. The relationship between alkalinity and steel corrosivity can also be described by the Langelier Index (LI) (Ahmad 2006):

$$LI = pH + \log[Ca^{2+}] + \log[toal\ alkalinity] + \log \gamma_{Ca2+} + \log \gamma_{Total\ Alkalinity} + \log K \qquad (2\text{-}13)$$

where:

[] = Brackets indicate molar concentration of the Ca^{2+} and total alkalinity as $CaCO_3$;

K = Ionized constant; and

γ = Activity coefficient;

Equation *(2-13)* has known as one of the representative corrosivity of water and saturation indices. The equation represents that an increase in pH and alkalinity leads to an increase in LI, indicating that the water tends precipitate $CaCO_3$, whereas a decrease in pH and alkalinity leads to a decrease LI, indicating undersaturation with $CaCO_3$ (AWWA Research Foundation 1996).

Second, high alkalinity provides a less corrosive condition and encourages the formation of a protective film such as $CaCO_3$ or $FeCO_3$ against oxygen diffusion on a steel surface, thereby eventually limiting corrosion rate (American Water Works Association Research Foundation 1996). The reactions taking place at the anode and cathode of the steel surface in the absence of a buffer are as follows:

Anode:

$$Fe \rightarrow Fe^{2+} + 2e^- \qquad (2\text{-}4)$$

$$2Fe^{2+} + \tfrac{1}{2}\, O_2 + 5H_2O \rightarrow 2Fe(OH)_3 + 4H^+ \qquad (2\text{-}14)$$

$$Fe^{+2} + 2OH^- \rightarrow Fe(OH)_2\,(s) \qquad (2\text{-}10)$$

Cathode:

$$O_2 + 2H_2O + 4e^- \rightarrow 4OH^- \qquad (2\text{-}15)$$

$$2H_2O + 2e^- \rightarrow H_2 + 2OH^- \qquad (2\text{-}16)$$

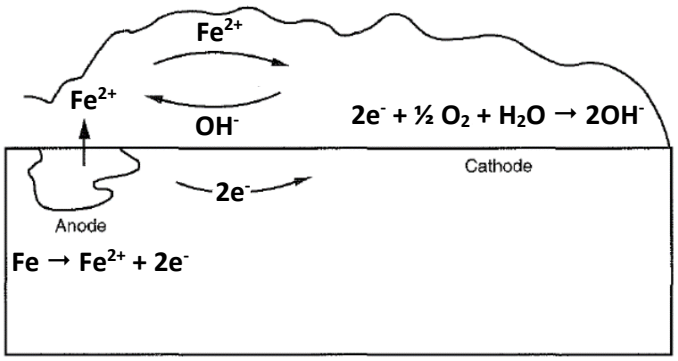

Figure 2.2 Schematic of a corrosion cell [Sourced from AWWA (1996)]

The anode is the site of corrosion. The atoms of the steel are ionized and release electrons as shown in Figure 2.2 and Equation *(2-4)*. Simultaneously, the positive ferrous ions diffuse through the water to the cathode, starting to corrode. The ferrous ions react further with dissolved oxygen (DO) to form ferric hydroxide [$Fe(OH)_3$] as shown in Equation (2-11). At the cathode, the electrons react with DO in the water to form hydroxide ions as shown in Equation (2-15) and (2-16). The negative hydroxide ions move from water to the anode and quickly precipitate as the form of ferrous hydroxide [$Fe(OH)_2$] as shown in Equation (2-10) (AWWA Research Foundation 1996).

The following reactions occur in the presence of a buffer:

Anode:

$$Fe \rightarrow Fe^{2+} + 2e^- \qquad (2\text{-}4)$$

$$2Fe^{2+} + \tfrac{1}{2}\, O_2 + 4HCO_3^- + 5H_2O \rightarrow 2Fe(OH)_3 + 4H_2CO_3 \qquad (2\text{-}17)$$

Cathode:

$$O_2 + 2H_2O + 4e^- \rightarrow 4OH^- \qquad (2\text{-}15)$$

$$2H_2O + 2e^- \rightarrow H_2 + 2OH^- \qquad (2\text{-}16)$$

$$2OH^- + 2Ca^{2+} + 2HCO_3^- \rightarrow 2CaCO_3(s) + 2H_2O \quad (2\text{-}18)$$

$$2OH^- + 2Fe^{2+} + 2HCO_3^- \rightarrow 2FeCO_3(s) + 2H_2O \quad (2\text{-}19)$$

At the anode, ferrous ions react with carbonate ion (HCO_3^-), producing carbonic acid (H_2CO_3) as shown in Equation (2-17). The hydroxide ions at the cathode are consumed through a neutralization reaction, thereby leading to the buildup of the precipitates such as $CaCO_3$ or $FeCO_3$, as shown in Equations (2-18) and (2-19). As a result, the catholyte in a buffer system does not become as basic as it is in the absence of a buffer while the anolyte does not remain as acidic as it is without alkalinity. Thus, steel in the water without alkalinity comes to be relatively more easily corroded while, in the alkaline condition with sufficient Ca^{2+} ions, $CaCO_3$ can be deposited and can retard steel corrosion (Rodolfo and Singley 2016).

In addition, high alkalinity contributes to forming a good barrier on a steel surface. The rapid oxidation of ferrous (Fe^{2+}) to ferric ions (Fe^{3+}) and the formation of ferric oxides (e.g., $Fe(OH)_3$) near pipe wall produces a more porous and fragile scale while siderite ($FeCO_3$) forms to a tight and more protective scale. pH and alkalinity play a role in deciding whether siderite forms or not (American Water Works Association Research Foundation 1996). As pH increases, the rate of formation of ferrous (Fe^{2+}) to ferric ions (Fe^{3+}) becomes faster, escalating the formation of nonprotective scale layers as shown in Equation (2-20), with the aid of hydroxide ions (OH^-). High alkalinity offsets this tendency, keeping the pH in a range where siderite formation might be kinetically favored over iron oxidation (Rossum 1983).

$$Fe^{3+} + 3OH^- \rightarrow Fe(OH)_3\,(s) \quad (2\text{-}20)$$

2.2.2.2 Temperature

Temperature variation in water sources (river, reservoir, etc.) leads to temperature changes in WTM systems. Temperature is expected to affect the corrosion of steel pipes by influencing several factors: electrochemical potential, DO solubility, thermal expansion, diffusivity, viscosity, and biological activity of iron-oxidizing bacteria. When the corrosion is due to DO in water, corrosion rate generally decreases as temperature rises. In contrast, if corrosion is due to mineral acids (e.g., hydrochloric acid) dissolving in water, resulting in hydrogen evolution, the corrosion rate increases with increasing temperatures (Ahmad 2006).

2.2.2.2.1 Electrochemical Potential

In natural systems, the equilibrium rarely occurs where the anodic reaction rate is equal to the cathodic reaction rate. In the view of electrochemistry, metals corrode only if the potential is above the equilibrium potential. The equilibrium potential can be calculated by using the Nernst equation for the reaction as follows (AWWA Research Foundation 1996):

$$E_H = E^0 - \frac{RT}{zF} ln\, aMe^{z+} \qquad (2\text{-}21)$$

where:

E_H = potential relative to a standard hydrogen electrode (SHE);

E_0 = standard potential, a constant that can be obtained from tables of electrochemical data;

R = ideal gas constant;

T = absolute temperature, K;

z = number of electrons transferred in the reaction;

F = Faraday constant; and

$a\, Me^{z+}$ = activity of the ion Me^{z+}.

It is noted that an increase in temperature leads to a decrease of the equilibrium potential since the potential is a function of temperature, i.e., corrosion rate decreases as temperature increases.

2.2.2.2.2 DO Solubility

The solubility of oxygen in water decreases as temperature increases, because increased temperature causes an increase in kinetic energy, leading to more motion in the oxygen molecules which break intermolecular bonds and escape from solution (Buckley 1971). The temperature dependence of the equilibrium constant K (solubility product) can generally be described with the Van't Hoff equation as follows:

$$ln\frac{K_T}{K_{To}} = -\frac{\Delta H_R^o}{R}\left(\frac{1}{T} - \frac{1}{T_0}\right) \qquad (2\text{-}22)$$

where:

K_T and K_{T0} = equilibrium constants at temperatures T and T_0, respectively;

ΔH_R^o = enthalpy of reaction which can be regarded as constant between 5 - 35°C (Stumm and Morgan 1996); and

R = gas constant (8.314 J/K/mole).

According to the Van't Hoff equation, solubility decreases as temperature increases, implicating that DO decreases with increasing temperature. As water temperature increases, it is more likely to inhibit the roles of DO in both accepting electrons and oxidizing ferrous compounds. Therefore, changes in DO solubility can have a significant impact on chemical reactions associated with steel corrosion such as oxidation and reduction as well as precipitation reactions.

2.2.2.2.3 Thermal Expansion and Constriction

WTM systems including various oxides and steel are subject to thermal expansion: a tendency to expand or constrict with a change in temperature. Ferrous compounds have a different coefficient of thermal expansion compared to metal as shown in Table 2-3. The differential thermal expansion properties of the scales lead to their physical stresses and deformation as temperature changes, and can develop critical crack propagation (Schutze 1997). This phenomenon can be important in cases where the oxide scales are heterogeneous. In addition, the cracks might expose the unprotected bare metal surface to the external corrosive environments, triggering steel corrosion. It is reported that oxide scales with many cracks causing paths for water have the poor capability for protection of steel against corrosion (Misawa et al. 1974).

Table 2-3. Coefficients of thermal expansion (α) values [Source from (Schutze 1997)]

Components	Coefficients of thermal expansion values
Fe	15.3×10^{-6}
FeO	12.2×10^{-6}
Fe_2O_3	10.96×10^{-6}
Fe_3O_4	10.5×10^{-6}

2.2.2.2.4 Other Effects of Temperature

Water temperature affects diffusivity and viscosity, both of which tend to influence the oxygen mass transfer and transport of ferrous ions to and from the steel surface, thereby altering corrosion rate (Davalos and Gracia 1991).

Also, it is observed that temperature has a major effect on microbiological oxidation of ferrous iron because it affects biological activities of iron-oxidizing bacteria, enabling them to alter DO depletion and the

reduction-oxidation reaction conditions (Ahonen and Tuovinen 1989). It is found that microbiological ferrous oxidation rate is dependent on temperature, the concentrations of hydrogen ion, DO, and ferrous iron (Stumm and Morgan 1996).

Furthermore, it was reported that there is a negative correlation between ferrous pipe breaks and water temperature from analytical correlation analysis based on historical break data as shown in Figure 2.3 (Milone 2012). Besides, the oxidation rate of iron pipes was found to increase with decreasing temperature in a series of experiments simulating water networks (McNeill and Edwards 2002). These observations indicate that the water temperature is a dominant factor affecting failure and deterioration in steel WTMs.

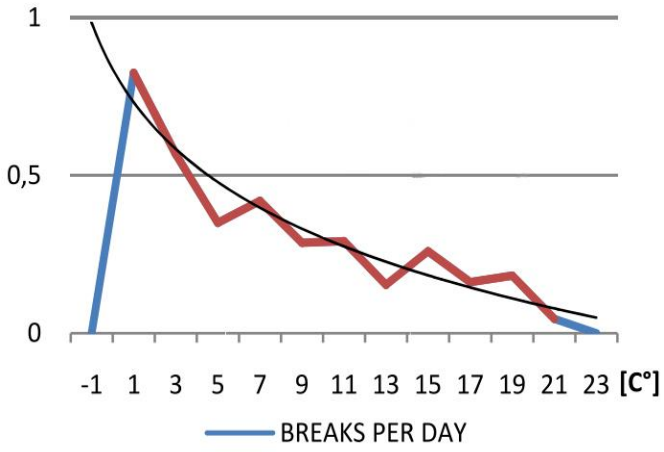

Figure 2.3. The relationship between ferrous water mains breakage rate and water temperature [Sourced from (Milone 2012)]

2.2.2.3 Residual Chlorine

Water chlorination is the final drinking water process, in which chlorine gas (Cl_2) is typically used to deactivate certain bacteria and other microbes in tap water to prevent waterborne diseases for public health.

Chlorine is a powerful oxidizing agent for metallic pipes. When chlorine is liquefied, it readily forms hydrochloric acid (HCl) and hypochlorous acid (HOCl) or hypochlorite (OCl^-) depending on pH as follows (Rodolfo and Singley 2016):

$$Cl_2 + H_2O \rightarrow HOCl + HCl\,(pH < 7.5) \qquad (2\text{-}23)$$

$$HOCl \rightarrow H^+ + OCl^-\,(pH > 7.5) \qquad (2\text{-}24)$$

HCl increases the acidity of the water and HOCl reacts with ferrous ion, precipitating ferric hydroxide [$Fe[OH]_3$], and thereby increasing corrosion rate as follows (Tuthill et al. 1998):

$$2Fe^{2+} + HOCl + 5H_2O \rightarrow 2Fe(OH)_3(S) + Cl^- + 5H^+ \qquad (2\text{-}25)$$

where HOCl as Cl_2 stoichiometrically oxidizes 1.56 mg of iron (Reckhow 2009).

Also, the above reactions accelerate a decrease in pH, leading to a decrease in LI index and the undersaturation with $CaCO_3$, and thereby rising corrosivity.

In addition, chloride ion generated by reaction in Equation (2-23) causes pitting corrosion. Pitting corrosion is a form of highly localized corrosion with deep holes. Iron is dissolved into ferrous ion inside the pit through the anodic reaction as shown in Equation *(2-4)* and the electrons flow to the cathodes. The water enclosed in the pit has a net positive charge. The positively charged pit attracts negative chloride ions (Cl^-), reacting with ferrous ion, as follows (Ma 2012):

$$Fe^{2+} + 2Cl^- \rightarrow FeCl_2 \qquad (2\text{-}26)$$

The formed $FeCl_2$ increases acidity of the water, resulting in further iron corrosion as follows (Ma 2012):

$$FeCl_2 + 2H_2O \rightarrow Fe(OH)_2\,(S) + 2HCl \qquad (2\text{-}27)$$

Figure 2.4 illustrates that pits are being developed by the autocatalytic reaction as described above.

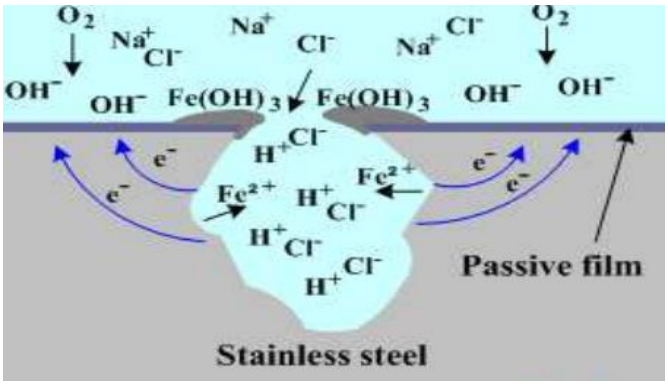

Figure 2.4. Pitting growth by chloride ions [Source from (Ma 2012)]

Besides, the relationship between steel corrosion rate and residual chlorine was verified from the laboratory experiment describing that the corrosion rate of steel is proportional to chlorine concentration ranging between 0.5 and 1.0 mg/L, which is a typical range of residual chlorine throughout drinking water network as shown in Figure 2.5 (Boffardi 1992).

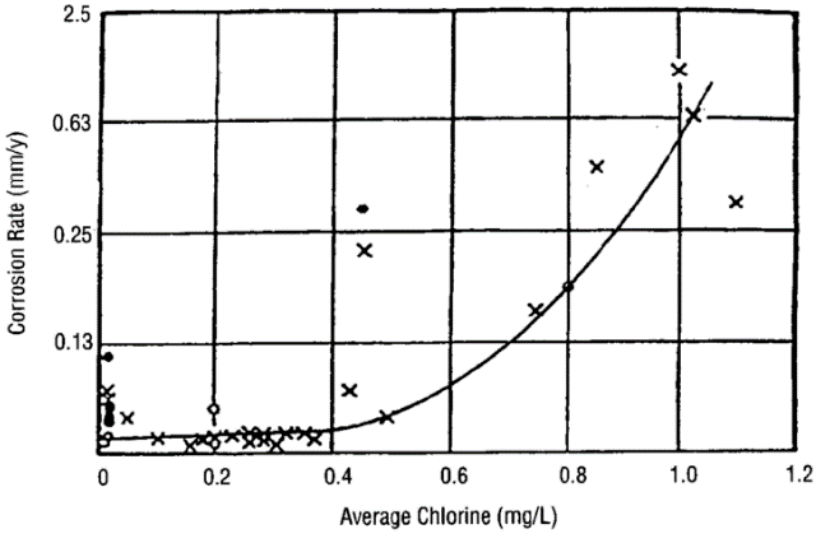

Figure 2.5. Effect of free chlorine on steel corrosion [Sourced from (Boffardi 1992)]

2.2.2.4 Electrical Conductivity

Electrical conductivity (EC) is defined as the reciprocal of the resistance measured between the opposing flats, implicating water's ability to allow the transport of charged ions (Ionode 2017):

$$EC = \frac{1}{R} \times \frac{D}{A} = \frac{I}{V} \times \frac{D}{A} \qquad (2\text{-}28)$$

where

EC = electrical conductivity (S/cm);

R = Resistance of the solution (ohms = 1/S);

V = voltage (volts);

I = current (amperes);

D = distance between the electrodes (cm); and

A = area of the electrodes (cm^2).

EC is generally calculated by measuring the resulting current (*I*) after entering other values (*V, D, A*) as shown in Equation (2-28). The current (*I*) is carried by charged ions. Thus, EC is determined by the number of charge carriers, implicating that EC is proportional to the concentration of ions present in the water (US EPA 2012b). These ions originate from dissolved salts and inorganic materials such as alkalis (OH^-), chlorides (Cl^-), sulfides (SO_4^{2-}) and carbonate compounds (CO_3^{2-}) (Miller et al. 1988).

EC is often associated with the corrosivity of steel in the water. Because the corrosion current must pass through the water by ionic conduction, EC will influence the way in which corrosion occurs in the water (Ahmad 2006). It is known that highly conductive water tends to be more corrosive than less conductive waters (Rossum 1983) and a positive relationship was identified between EC and corrosion rate (Rodolfo and Singley 2016). Consequently, the higher the dissolved salts, the higher the ionic strength, i.e., EC, and faster steel is corroded (Muylwyk et al. 2014).

EC is not detailed since it only measures the ionic content in a solution (Roisemount Analytical Inc. 2010). The ions contributing to EC contain their different corrosive characteristics. To be specific, some ions such as chlorides (Cl^-) and sulfides (SO_4^{2-}) are contributors to corrosion. This is because these ions react with ferrous ion, forming ferrous chloride ($FeCl_2$) or ferrous sulfate ($FeSO_4$) as described in Equation (2-26) and *(2-29)*. This eventually increases the acidity of the water (Bohnet 2003; Ma 2012), accelerating steel corrosion and pitting as shown in Equation (2-27) (Illinois State Water Survey 1975):

$$Fe^{2+} + 2Cl^- \rightarrow FeCl_2 \qquad (2\text{-}26)$$

$$FeCl_2 + 2H_2O \rightarrow Fe(OH)_2(S) + 2HCl \qquad (2\text{-}27)$$

$$Fe^{2+} + SO_4^{2-} \rightarrow FeSO_4(s) \qquad (2\text{-}29)$$

On the other hand, other ions such as alkalis (OH^-) and carbonate compounds (CO_2^{3-}) by reacting with calcium ions, forming carbonate films and ferrous oxides on a pipe wall, thereby retarding steel corrosion (Rossum 1983).

Figure 2.6 shows the relationship between the electrical resistivity (the reciprocal of EC) and the corrosion potential obtained by the experiment (Ribeiro et al. 2012). This result provides experimental evidence to suggest that the corrosion rate of steel WTMs increases as EC in the water increases because potable water passing through steel WTMs holds ions contributing to corrosion.

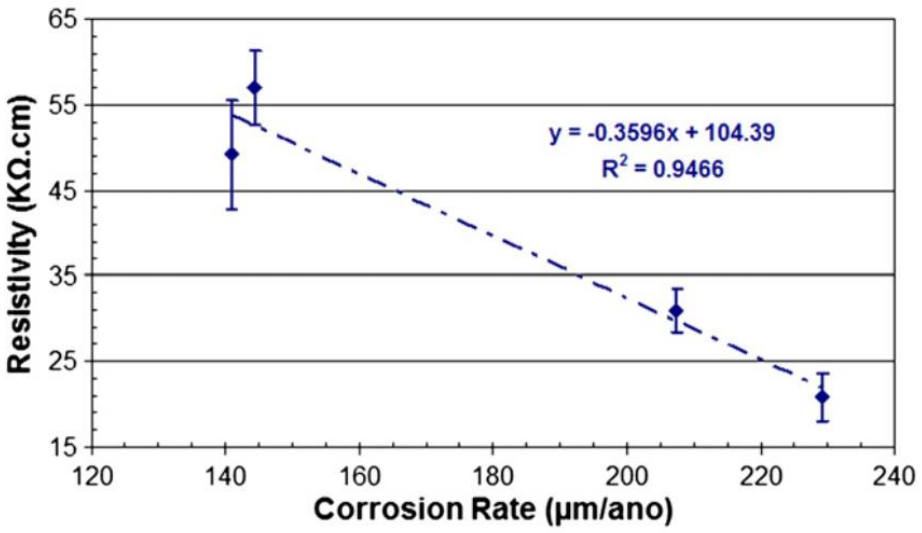

Figure 2.6. Correlation between electrical resistivity and corrosion rate [Sourced from (Ribeiro et al. 2012)]

2.2.2.5 Pipe Age

Pipe age can be determined from the installation year of WTMs. The pipe age indicates the length of time that WTMs have been in operation, exposed to the surrounding environment. Most predictive models have introduced pipe age as one of the most influential factors to forecast failure or deterioration of pipes in water networks. They assumed that increased frequency of pipe breaks was associated with pipe age. (UNESCO 2014).

The relationship between pipe failure and age is typically described by a so-called “bathtub curve” as is illustrated in Figure 2.7. The curve of the rate of occurrence of a failure (ROCOF) is usually associated with

its age. This curve includes three phases in the life of a buried pipe: 1) Burn-in phase, in which breaks occur mainly as a result of faulty installation; 2) In-usage phase, in which pipes operate relatively trouble-free; and 3) Wear-out phase, in which breaks increase due to deterioration and aging over time (Kleiner and Rajani 2001).

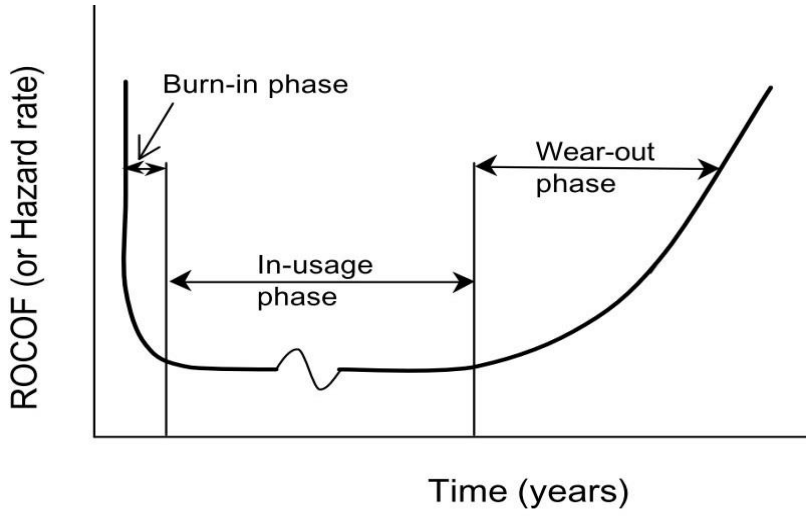

Figure 2.7. The bathtub curve of the life cycle of a buried pipe [Sourced from (Kleiner and Rajani 2001)]

It was found that the number of breaks in water mains increased with age (Gerhold 1976). Also, it was reported that corrosion-induced breaks increase over time, while breaks resulting from other causes were hard to find a relevance to pipe age (Fitzgerald 1968). The increase in metallic pipe break rates with age is generally ascribed to strength reduction because of corrosion (Boxall et al. 2007).

Additionally, the correlation of corrosion and age in metallic pipes over time was investigated in corrosive environments by monitoring in buried pipes for up to 14 years. The result reveals that the maximum pit depth and weight loss of metallic pipes increased over time and the rate of pitting on cast iron was greater than that of steel as shown in Figure 2.8 (Romanoff 1964). This observation experimentally supports that pipe age is associated with an increase in breakage of steel WTMs.

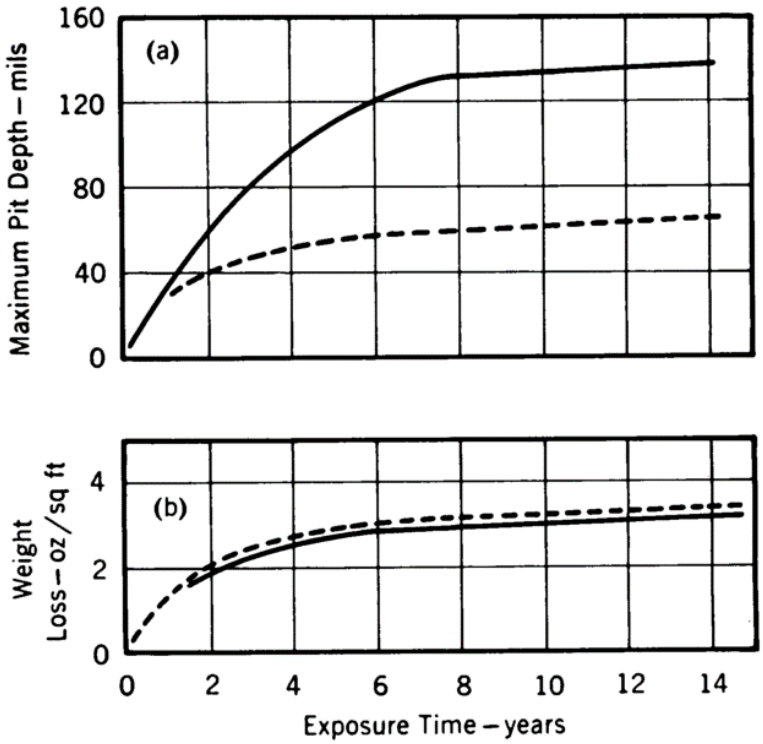

Figure 2.8 Weight loss and a maximum pit depth of cast-iron and steel pipe plotted against time [Sourced from Romanoff (1964)]: Solid curve - cast-iron pipe; the dashed - steel

2.2.2.6 Pipe Diameter and Thickness

Pipe diameter is reported as one of the main factors influencing break rates in water mains (Clark et al. 1982). It was found consistent in the previous studies that pipe diameter was inversely proportional to break rates in water mains (Berardi et al. 2008; Christodoulou et al. 2012).

The main reason for the increase in failure rate with a decrease in pipe diameter has been attributed to thinner pipe thickness, making them more vulnerable to failure following the loss of wall thickness due to corrosion or other deteriorations (Rezaei et al. 2015). Smaller pipes with thinner walls have a lower second moment of area, therefore, a reduced ability to resist internal or external stresses (UNESCO 2014).

Steel pipes manufactured in the ROK comply with the national standard specifications (e.g., pipe diameter and thickness) on steel pipes for waterworks. Figure 2.9 shows the relationship between pipe diameter and thickness stipulated in the Korea Standard, indicating that thickness in steel pipes increases with a diameter as follows:

$$T = 0.0079 \times D + 2.7544 \qquad \textit{(2-30)}$$

where:

T = thickness (mm); and

D = diameter (mm).

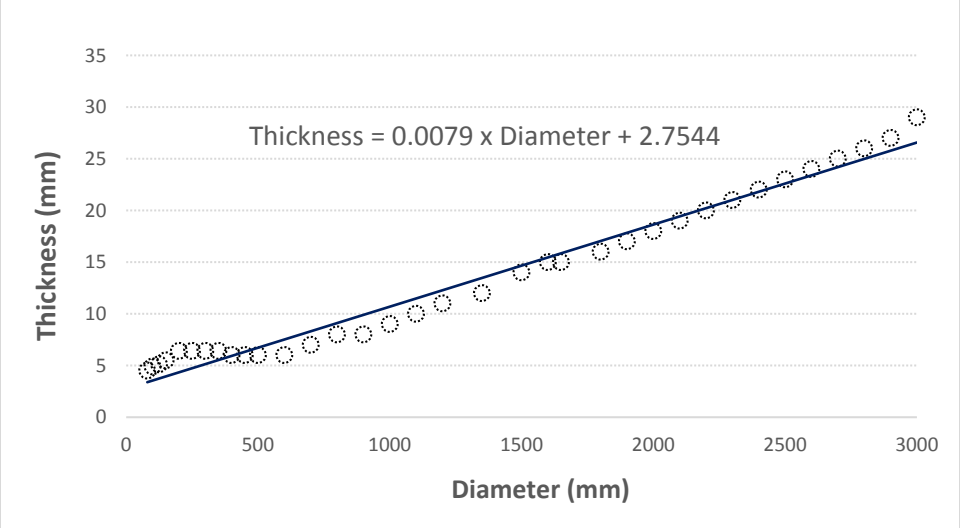

Figure 2.9. The relationship between thickness and diameter in steel pipe installed in the ROK [Modified from (Ministry of Environment of the ROK 2014)]

Internal pressure is one of the primary loads on WTMs. Barlow's formula is generally used to determine optimal pipe thickness or allowable stress commonly known as strength of pipes to withstand the internal operating pressure as follows (Wilmott and Sutherby 1998):

$$\sigma = \frac{P \times D}{2t} \qquad (2\text{-}31)$$

where:

σ = allowable stress;

P = pressure;

t = wall thickness; and

D = outside diameter.

The above equation can be expressed and simplified by entering Equation (2-30) as follows:

$$\sigma = \frac{P \times D}{2\,(0.0079\,D + 2.7544)} \qquad (2\text{-}32)$$

$$\sigma = \frac{P}{2\,(0.0079 + \frac{2.7544}{D})} \qquad (2\text{-}33)$$

Equation (2-33) indicates that the strength of steel pipes to withstand internal loads is proportional to diameter, thereby leading a reduction in break rate in steel WTMs.

As for external loads such as earth pressure or traffic, the strength of the buried pipes to withstand the effect of soil and surface forces, known as allowable bending stress pipes can be calculated as follows (ASCE 2001):

$$\sigma_b = 4E\,\frac{D_l K P}{\left(\frac{EI}{R^3} + 0.061E'\right)}\left(\frac{t}{D}\right) \qquad (2\text{-}34)$$

where:

σ_b = allowable bending stress;

D = outside diameter of pipe;

t = pipe wall thickness;

E = modulus of elasticity of pipe;

D = pipe outside diameter, inches;

Δy = vertical deflection of pipe, inches;

D_l = deflection lag factor (1.0 - 1.5);

K = bedding constant (0.1);

P = pressure on pipe due to soil load PV plus live load PP, psi;

R = pipe radius, inches;

E' = modulus of soil reaction, psi; and

$I = t^3/12$.

The above equation can be simplified as follows:

$$\sigma_b = 4E \frac{D_l K P}{\left(\frac{8E}{D^3}\frac{t^3}{12} + 0.061E'\right)} \left(\frac{t}{D}\right) \quad (2\text{-}35)$$

The allowable strength can be found to be a function of mainly diameter and thickness of buried pipes except for other coefficients and thereby simplified as follows:

$$\sigma_b \propto \frac{D^2}{t^2} \quad (2\text{-}36)$$

$$\sigma_b \propto \frac{D^2}{(0.0079D + 2.7544)^2} \quad (2\text{-}37)$$

$$\sigma_b \propto \frac{1}{(0.0079 + 2.7544/D)^2} \quad (2\text{-}38)$$

Therefore, Equation (2-38) analytically reveals that the strength of steel pipes to withstand external loads is proportional to diameter, thereby showing an inverse relationship between diameter and breakage rate in steel WTMs.

2.2.2.7 Burial Depth

The soil above a buried steel pipe exerts pressure on the pipeline. Earth pressure is one of the primary considerations when designing buried steel pipes (ASCE 2001). The pressure is mainly dependent on the burial depth of the pipeline (Washington State Department of Health 2006). If the burial depth is not sufficient, the pressure on the pipeline due to the earth can be greater than that causing the crushing of the side wall of the pipes and pipe bucking can occur (Rotterdam 2012).

The soil pressure acting on a buried pipeline is generally calculated using the following equation (ASCE 2001):

$$P_s = w\,H \qquad (2\text{-}39)$$

where:

P_s = soil pressure acting on the pipe;

W = unit weight of filling; and

H = height of fill above the top of the pipe.

When a pipeline is buried below the water table, the soil load pressure can be obtained as follows (ASCE 2001):

$$P_s = w_w h_w + R_w w_d H \qquad (2\text{-}40)$$

where:

P_s = soil pressure acting on the pipe;

w_d = dry unit weight of backfill;

H = height of fill above the top of pipe;

h_w = height of water above the pipe;

w_w = unit weight of water; and

R_w = water buoyancy factor = 1- 0.33(h_w /H).

The above equations indicate that soil pressure acting on the pipeline is a function of burial depth of a pipeline. Thus, the burial depth of pipes can affect significantly pipe failures. This is explained by the findings that the pipes with shallower burial depths appeared to show with higher break rate while the pipes with deeper burial depths tended to be with lower break rate in pipelines (Wilson et al. 2015).

2.2.2.8 Dissolved Oxygen

Corrosion is the primary process by which metals deteriorate. Dissolved oxygen (DO) in the water has a vital role in the corrosion of steel (Mabuchi et al. 1991). First, in natural waters, DO acts as an essential electron acceptor in the cathode of steel metal as follows:

$$Fe + 0.5O_2 + H_2O \rightarrow Fe^{+2} + 2OH^- \qquad (2\text{-}41)$$

The anode is generally the site of corrosion. The atoms of the steel are ionized and release electrons. The electrons react with DO in the water to form hydroxide ions. Simultaneously, the positive ferrous ions diffuse through the water to the cathode, starting to corrode. The negative hydroxide ions move from water to the anode and quickly precipitate as the form of ferrous hydroxide [$Fe(OH)_2$]. The ferrous ions may undergo a number of secondary reactions, in which DO can be involved in the secondary oxidation reaction of both ferrous ions (Fe^{2+}) and hydroxide ions (OH^-) as follows (AWWA Research Foundation 1996):

Secondly, DO plays a vital role in oxidizing ferrous compounds. With the availability of oxygen, the ferrous hydroxide forms iron (III) oxide-hydroxide ($Fe_2O_3 \cdot H_2O$)(Ahmad 2006):

$$4Fe(OH)_2 + O_2 \rightarrow 2Fe_2O_3 \cdot H_2O(s) + 2H_2O \quad (2\text{-}42)$$

The hydrated ferric oxides are formed from the reactions shown in Equations (2-42), (2-43), and (2-44). They are reddish and may cause "colored water" complaints. Tertiary reactions may take place as follows (AWWA Research Foundation 1996):

$$3FeCO_3\,(s) + 0.5O_2 \rightarrow Fe_3O_4\,(s) + 3CO_2 \quad (2\text{-}43)$$

$$4Fe_3O_4\,(s) + O_2 \rightarrow 6Fe_2O_3\,(s) \quad (2\text{-}44)$$

The process of steel corrosion depends primarily on DO concentration as described above. Thus, steel corrosion is highly associated with DO. It is also reported that the corrosion rate generally increases with increasing DO and water free of DO will not tuberculate (Rodolfo and Singley 2016).

2.2.2.9 Service type

Water treatment is customized to customer's preferences according to their diverse needs and purposes to use water. The customers are typically classified as local governments, industrial plants, and citizens. They have different preferences for water quality. To be specific, only raw water is supplied to drinking water treatment plants owned by local governments without their own water sources. Settled water is supplied to industrial plants for their cooling water use, not drinking water consumption. Most commonly, filtered water is provided to citizens through water networks after a final water treatment by K-water. Figure 2.10 illustrates the schematic diagram of drinking water treatment and the chemicals (chlorine and coagulants) depending on water service types.

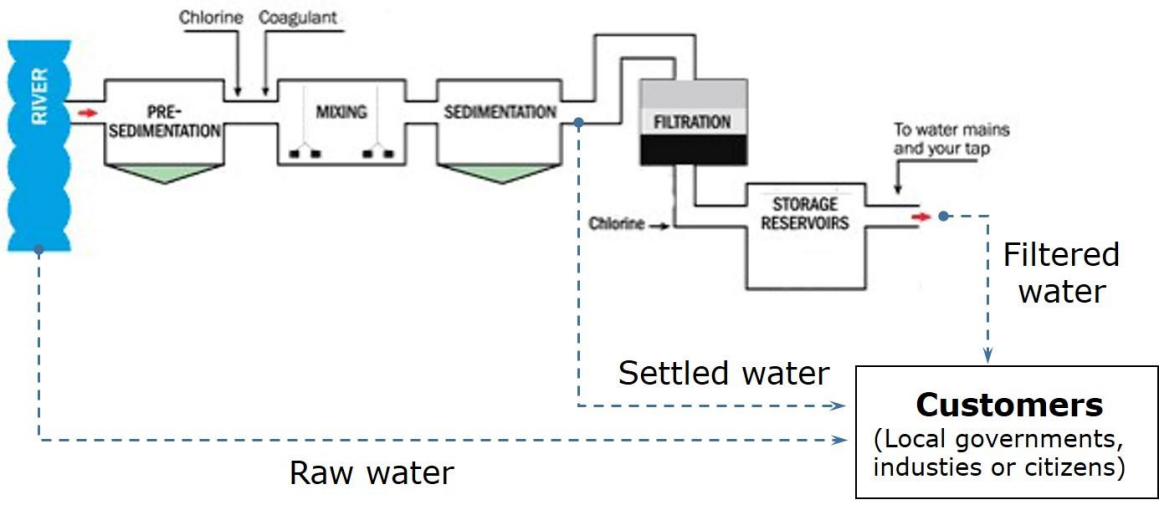

Figure 2.10. Schematic diagram of water service types

A couple of chemicals (coagulants and disinfectants) are mainly applied to drinking water treatment. First, chlorine is added to the raw water to oxide organics and help control taste & odor-causing substances as it enters. Secondly, coagulants such as alum [aluminum sulfate, $Al_2(SO_4)_3$] or PACs [poly aluminum chloride, $Al_2(OH)_3Cl_3$] are generally added to the water to destabilize, cluster, settle down and remove colloidal-size particulate matter suspended in water during the process known as coagulation. Then, chlorine is added to the purified water at the final step to deactivate microorganisms such as bacteria, protozoa, and viruses that may cause illness in humans.

While raw water does not contain any substance affecting a steel pipe corrosion, settled water as well as filtered water possess various corrosive ions resulting from water treatment chemicals added as shown in Figure 2.11. When chlorine is applied during prechlorination, it readily forms hydrochloric acid (HCl) and hypochlorous acid (HOCl) as described in Equation (2-23), escalating acidity of the water (Rodolfo and Singley 2016). HOCl reacts with ferrous ion, precipitating ferric hydroxide [$Fe(OH)_3$], and thereby increas-

ing corrosion rate as follows (Tuthill et al. 1998). Aluminum sulfate or poly aluminum chloride added during coagulation is dissociated into aluminum (Al^{3+}), sulfate (SO_4^{2-}), hydroxide (OH^-), and chloride (Cl^-) ions as follows:

$$Al_2(SO_4)_3 \cdot 18H_2O \rightarrow 2Al^{3+} + 3SO_4^{2-} + 18H2O \rightarrow 2Al(OH)_3 + 6H^+ + 3SO_4^{2-} + 12H_2O \quad (2\text{-}45)$$

$$Al_2(OH)_3Cl_3 \rightarrow 2Al^{3+} + 3OH^- + 3Cl^- \rightarrow Al(OH)_3 + 3H^+ + 3Cl^- \quad (2\text{-}46)$$

Thus, settled water can contain corrosive ions such as Cl^- or SO_4^{2-} forming ferrous chloride ($FeCl_2$) or ferrous sulfate ($FeSO_4$) as described in Equations (2-45), (2-46), and (2-47), resulting in further steel corrosion (Bohnet 2003; Ma 2012). Also, a decrease in pH increases the corrosivity of the settled water.

$$Fe^{2+} + SO_4^{2-} \rightarrow FeSO_4\ (s) \quad (2\text{-}47)$$

Chlorine is added during disinfection. It produces hydrochloric acid (HCl) and hypochlorous acid (HOCl), ultimately oxidizing iron as previously described (Rodolfo and Singley 2016). Therefore, filtered water can include a lot more corrosive ion as shown in Figure 3.7. The corrosivity of water increases over drinking water treatment resulting from the chemical addition.

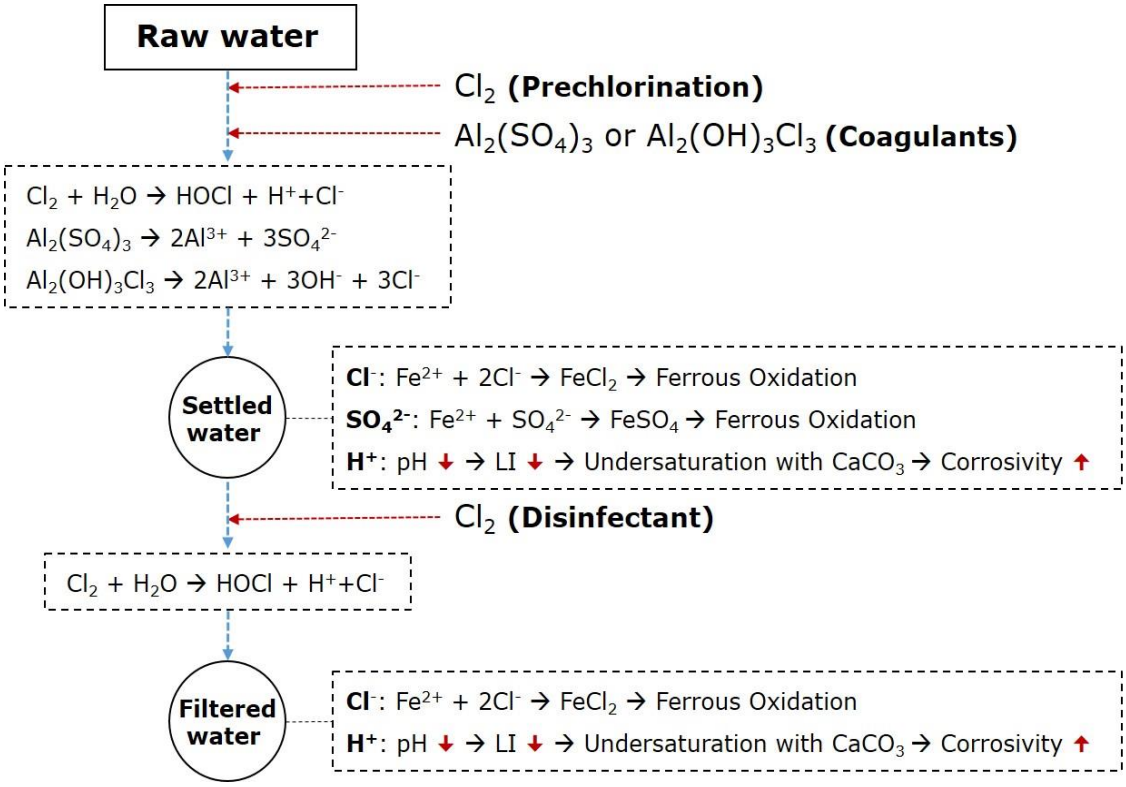

Figure 2.11. Schematic of anticipated reaction by adding chemicals in drinking water treatment process

2.2.2.10 Coatings

Corrosion has been well known as the most dominant cause of deterioration of steel WTMs (Hou et al. 2016) and it occurs as a result of the chemical reaction between the steel and electrochemical ions from the corrosive environment such as internal water and external soil as previously described. One of the effective ways to protect steel is by providing an impervious barrier coating that prevents the transfer of electrochemical ions from the corrosive environment to the steel since without moisture (electrolyte) there is no corrosion. Figure 2.12 illustrates how coatings perform as barrier layers and barrier coating cracks create corrosion.

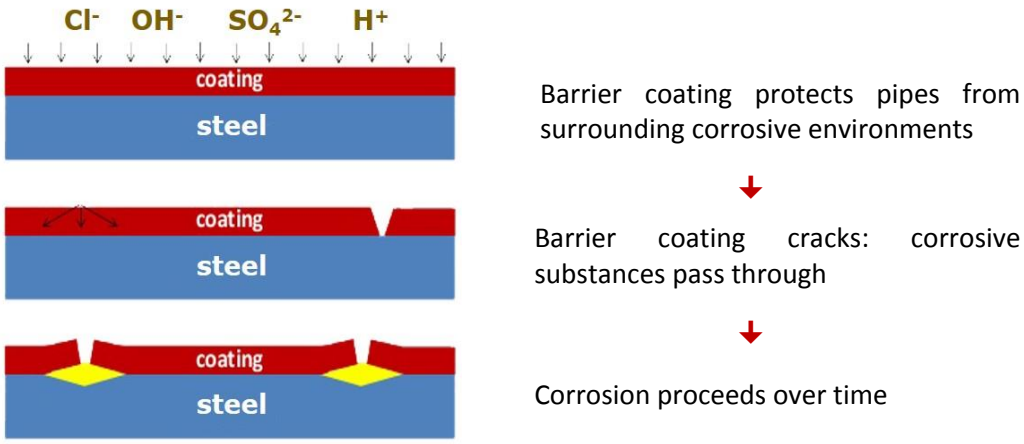

Figure 2.12. Barrier coating cracks and present opportunity for corrosive substances to react with steel [modified from (Lskiewicz 2014)]

Additionally, the electrochemical corrosion potential (ECP) of coated steel and uncoated steel was investigated in corrosive environments by conducting an immersion test. ECP implies the characteristics of metal to lose electrons in the presence of an electrolyte. ECP value increases over the progress of corrosion. The result shows that the coated steels have an active passivating and efficient barrier behavior against corrosion as shown in Figure 2.13 (Mobin and Tanveer 2011). This observation experimentally supports that coating contributes to anti-corrosion of steel WTMs.

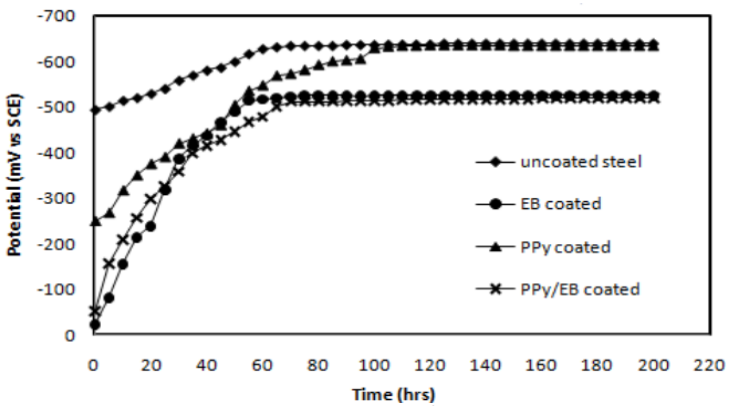

Figure 2.13. Electrochemical corrosion potential vs. time plot of uncoated and coated steels in 0.1 M HCl [Sourced from (Mobin and Tanveer 2011)]

2.2.3 Gaps in Knowledge

A review of published literature on pipe deterioration reveals that few studies have been undertaken on significant factors affecting failures in steel WTMs as well as on the deterioration mechanisms based on data in practice.

- **Lack of Comprehensive Factor Analysis**: Previous research has addressed physical factors such as pipe thickness and diameter and/or environmental factors such as soil characteristics when determining the leading causes of failure in aging WTMs. However, these studies did not address water quality factors that may lead to internal corrosion as contributors to the failure of pipes, although internal corrosion has been well known as the most dominant cause of deterioration of steel WTMs (Hou et al. 2016).
- **Limited to Small Diameter Iron and PVC Pipes**: Furthermore, management data and historical records of steel WTMs are scarce (Kleiner and Rajani 2007). Previous studies on the factors contributing to pipeline failure have been concentrated on small diameter water distribution networks composed of iron or PVC pipes. No studies have so far been conducted in investigating steel WTMs. The need for studies focused on steel water mains is further underscored by the fact that

the results of previous studies focusing on iron pipes may not be extrapolated. This is because iron and steel pipes are different in their composition, properties, lining and welding system, the chemical reactions associated with their corrosion and their failure characteristics (American Water Works Association Research Foundation 1996).

- **Lack of Comprehensive Study on Failure Mechanisms**: Lastly, the mechanisms that lead to pipe breaks are very complicated and not well understood (Kleiner and Rajani 2007). Furthermore, previous studies on the main factors affecting water main failure have not yet been conducted in connection with the failure mechanisms of the key factors derived. As a result, it was not possible to implement proper measures to extend the service life of WTMs. Thus, current knowledge about the mechanisms of the key factors and failure in steel WTMs is still limited, because it does not cover all factors contributing to water main failures comprehensively.

2.3 Previous Predictive Models

2.3.1 Statistical Models

Statistical models utilize historical break data to predict patterns from these data sets. Shamir & Howard (1979) were the first to develop a regression model in which a pipe breakage is exponentially associated with its age. Herz (1996) presented a lifetime probability distribution density model (known as the Cohort Survival Model), displaying expectancy values for a residual life-span, survival, and failure probabilities. A comprehensive review of research conducted using the traditional statistical predictive models can be found elsewhere (Kleiner and Rajani 2001).

2.3.2 Physical Models

Physical models predict pipe failure by modeling the mechanical performance of pipes. Physical models require data about pipe characteristics, material properties and additional environmental factors (Kleiner

and Rajani 2001). Rossum (1969) predicted the remaining wall thickness of pit cast mains and time to failure using a power law as a function of time and soil parameters such as pH and resistivity. Whereas physical models on the deterioration of pipes may be scientifically accurate, available data limits their utility because obtaining the data necessary for the physical models is costly and time-consuming (US EPA 2012a).

Figure 2.14 shows the previous physical and statistical models forecasting pipe failure, implicating that previous numerous researchers in the field have been focused on small diameter water distribution net-works (a cast iron or a PVC). Any relevant research on drinking WTMs made of steel not been conducted yet although it transports a large amount of water and its failure leads to tremendous damages. Iron and steel pipes are quite different in their composition, properties, lining and welding system, the chemical reactions associated with their corrosion and their failure characteristics (American Water Works Association Research Foundation 1996). Thus, the existing knowledge about lifespan prediction models associated with iron or plastic pipes can be determined not to be applied to steel WTMs.

One research dealing with gas and oil pipelines of steel using a physical model was carried out to predict its lifespan(Pandey 1998). But, applying this study to drinking WTMs is controversial, because it is thought that oil and gas affect pipe failure quite differently from water due to their dissimilar physical and chemical characteristics.

< Small Pipes (Iron, Concrete, PVC) >

Predictive Model

Physical Model (18 cases)

Doleac (1980): Remaining wall thickness of iron mains

Randall (1992): Remaining service life of iron mains

Rajani (2000): Reliability-based prediction of iron pipes

Rajani (2002): Rank deterioration of cast iron pipes

Rajani (2004): Pipe-soil interaction

Rajani (2007): Remaining service life of cast iron main

Moglia (2008): Failure in cast iron pipe

Davis (2008): Failure in asbestos cement pipes

Statistical Model (31 cases)

Shamir (1979): Time exponential model

Herz (1996): Cohort survival model

Lei (1997): Accelerated life-based models

Rostum (1999): Time duration (Herz distribution)

Dandy (2001): Power law increase in breakage

Kleiner (2004): Time exponential model

Kleiner (2006): Water mains (Fuzzy Markov process)

LeGat (2008): Model for drainage pipes (Markov chain)

< Large Pipes (Steel) >

- Prediction Model (physical, 1case)

Pandey (1998): Steel pipe (Gas & Oil)

※ No statistical model

Figure 2.14 Previous predictive models for failure in pipes

2.3.3 Artificial Neural Network-Applied Studies in Water Distribution Network

ANNs are inspired by interconnected neurons in biological systems. ANNs imitate the human brain functions based on learning and memory processes. It is regarded as a very effective prediction method because of its ability to learn automatically by example. ANNs are a prediction tool which is suitable for model development in areas where fundamental relationships among parameters are not clearly identified. The ANN is composed of many artificial neurons which are arbitrarily organized and linked in multiple-layers (input, hidden, and output). Figure 2.15 shows that input layers are connected to output layers through the hidden layers (Al-Barqawi and Zayed 2008).

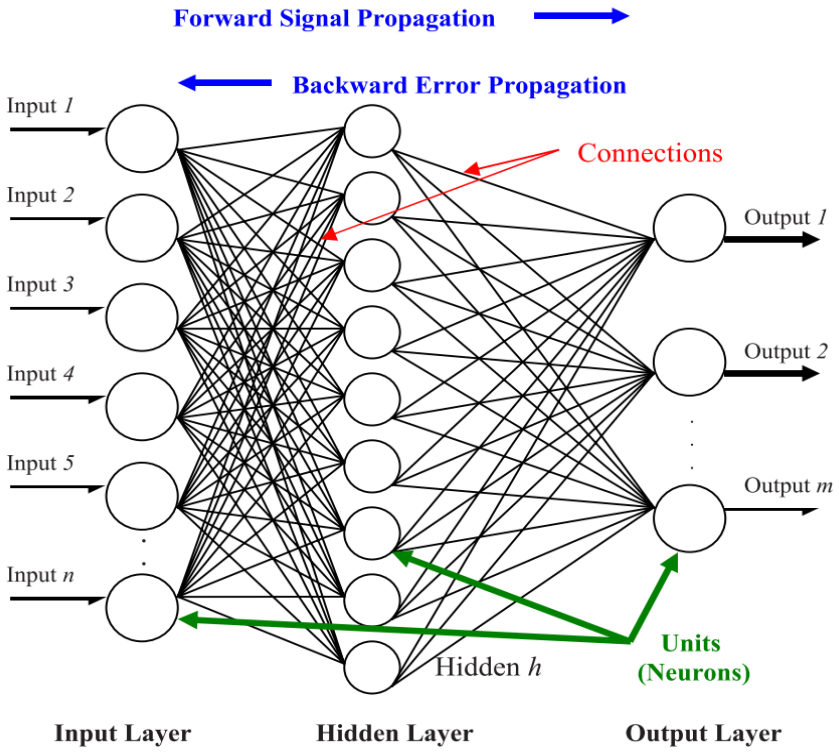

Figure 2.15 Schematic structure of the ANN (Al-Barqawi and Zayed 2008)

Each unit receives several real-value inputs and each unit produces a single real-value output. ANNs use an iterative method to minimize the errors between real and predicted data. Jafar at al (2010) employed ANNs to predict the number of failures of water distribution networks (composed of asbestos cement, PE and iron) using an observed number of failures, hydraulic pressure, soil types and pipe characteristics (material, diameter, length, age). Others have also used ANNs to predict failures of aging pipelines (iron or PVC) (Achim et al. 2007; Ahn et al. 2005; Al-Barqawi and Zayed 2006; Nishiyama and Filion 2014). The ANN technique has been extensively used and applied in various areas. The ANN modeling method has been employed to predict a lifespan or a break rate in a water distribution network. However, the previous ANN-based predictive models have been not only based on small pipes such as iron, PVC, etc., but they have also not addressed internal factors such as water quality variables as shown in Table 2-4.

Deep neural network (DNN) is an artificial neural network (ANN) with multiple hidden layers of units between the input and output layers as shown in Figure 2.16 . Like artificial neural networks with one hidden layer (Shallow ANNs), DNNs can model complex non-linear relationships. Additional layers allow DNNs to learn high-level features in data by using structures composed of multiple non-linear transformations (Bengio 2009). Deep learning algorithms include multi-layered Neural Networks (MLNNs), stacked Auto-encoders Neural Networks (ANNs), Deep Belief Networks (DBNs), Convolutional Neural Networks (CNNs), among others. DNN applications are as follows: prediction (time series prediction, fitness approximation and modeling), classification (pattern recognition), data processing (filtering, clustering, blind source separation, and compression), and robotics: directing manipulators, prosthesis control, including computer numerical control) (Venturescanner Inc. 2015).

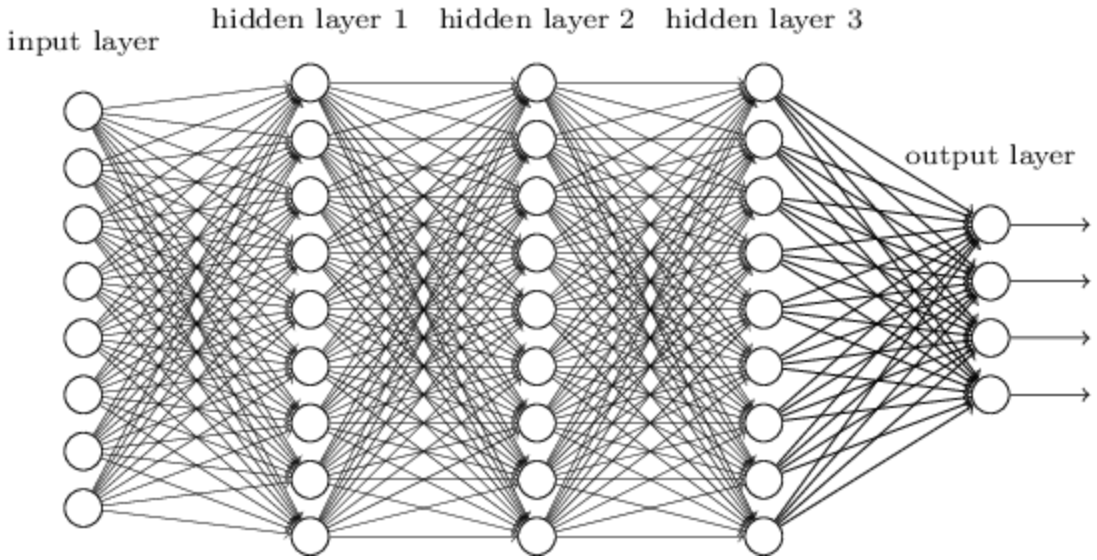

Figure 2.16. Schematic structure of the Deep Learning (Multi-Perceptron) Neural Network

Table 2-4 ANN-applied studies on water networks

Authors	Input variables	Target variables	Comments or Problems
(Nishiyama and Filion 2014)	- Observed number of failures, soil type - pipe characteristics (diameter, length, and age)	- Number of failures - Break rate (breaks/100 km/year)	- Only for iron pipe prediction. - Water quality is not included.
(Jafar et al. 2010)	- Observed number of failures, hydraulic pressure - soil type - pipe characteristics (material, diameter, length, and age) - pipe location (under sidewalk or road)	- Number of failures	- Hydraulic pressure calculated by a hydraulic model. - Material: asbestos cement, polyethylene, iron pipe. - Water quality is not included.

Authors	Input variables	Target variables	Comments or Problems
(Al-Barqawi and Zayed 2006)	- Pipe type & size - Pipe age, breakage rate - Hazen-Williams (C) factor - Excavation depth - Soil type. top road surface	- Pipe condition	- Water distribution (Asbestos cement, iron pipe); Not applicable to large steel pipe - Water quality is not included - Pre-processing for choosing data was not conducted
(Al-Barqawi and Zayed 2008)	- pipe type & size - Pipe age, breakage rate - Hazen-Williams (C) factor - Excavation depth, soil type - Groundwater level - Type of traffic & road - Operational pressure - Cathodic protection	- Pipe condition by pipe type (Iron, concrete)	- AHP used to calculate weighting factors for input data - Water distribution (Asbestos cement, iron pipe) - Water quality is not included
(Ahn et al. 2005)	- pipe type & size - Soil temperature - Water temperature - Atmospheric temp. - Number of pipe breaks	- Number of pipe breaks	- Water distribution (Asbestos cement, iron pipe, stainless steel) - Water quality is not included
(Achim et al. 2007)	- Pipe diameter - Year of construction - Age, pipe length - Geographical coordinates	- Failure of cast iron pipelines	- Iron pipe - Water quality is not included.

2.3.4 Gaps in Knowledge

A review of published literature on predictive models to forecast pipe failure reveals that few studies has been undertaken on forecasting failures in steel WTMs using comprehensive factors including water quality.

- **Lack of Comprehensive Factor Analysis**: Previous models have addressed physical factors such as pipe thickness and/or environmental factors such as soil characteristics. However, these studies

did not address water quality factors leading internal corrosion as contributors to the failure of pipes.

- **Limited to Small Diameter Iron and PVC Pipes**: Furthermore, previous studies have been based on small diameter water distribution networks composed of iron or PVC pipelines. No studies have so far been conducted in developing a predictive model for steel WTMs. As WTMs transport a much larger volume of water and their failure leads to even greater damages than those seen in small diameter water main breaks, such studies are much needed. The need for studies focused on steel water mains is further underscored by the fact that extrapolation of the results of previous studies focusing on iron pipes may not be valid. This is due to the fact that iron and steel pipes are different in their composition, properties, lining and welding systems, the chemical reactions associated with their corrosion, and their failure characteristics (American Water Works Association Research Foundation 1996).

2.4 Valuation of Intangible Public Services

2.4.1 Methods of Intangible Public Valuation

Economists have employed a variety of techniques to estimate various non-quantifiable benefits from public services into monetary units. Table 2-5 describes economic valuation techniques for non-market resources. Valuation methods can be broadly categorized into four categories.

First, the cost-based approach includes Damage Cost Avoided, Replacement Cost, and Cost of Saving methods. The Damage Cost Avoided method calculates either the cost of avoiding damages or the monetary value of property protected, as benefits made by public service (French Global Environment Facility 2015). The Replacement Cost method computes the cost required to replace existing resources or services as the value of the resources or the services. For example, in the event of water main breaks, the cost of

interrupted drinking water service can be replaced by the costs of bottled water or water tanker services. The Cost of Saving method quantifies a decrease in costs with the aid of a new service. For example, if an aging water main is rehabilitated, repair cost of breaks can be saved, which should be paid in case of water main breaks. Thus, the cost saved can be calculated by multiplying breaks reduction with repair cost per break.

Second, the Market Price method calculates the economic value of goods or services traded in markets (Bonnie et al. 2008). For instance, if a leaky pipeline is replaced with a new one and can prevent water loss through leaks, the benefit from the leaky pipe replacement activity, i.e., the amount of the saved water loss can be computed with the price of tap water billed to customers. However, the method is limited to only market goods and services (French Global Environment Facility 2015).

Third, the Revealed Preference approach estimates use information about a market recourse to estimate the value of a related, not-market resource (Bann 2002). This approach encompasses the Travel Cost method and Hedonic Price method. The Travel Cost method can be used to estimate the value of benefits provided by recreational services such as ecosystems. This method is limited to recreational activities and can be problematic for multiple destination trips (French Global Environment Facility 2015). The Hedonic Price method is used to estimate economic values for economic benefits or cost associated with environmental impacts. This method is most commonly applied to variations in real estate values affected by environmental policies or services (National Resources Council 2005).

Fourth, stated preference approach is based on responses to survey questions to ask willingness to pay (WTP) for new public services. This approach includes Contingent Valuation and Choice Experiment methods. These methods are used to estimate non-use values that public services such as environmental resources or ecosystems provide. However, these methods have a high risk of biases that may exaggerate WTP estimates (Brozovic et al. 2007). The Contingent Valuation method asks individuals directly what

their preferences are. The Choice Experiment method identifies implicit prices for service charges by asking a rating or ranking options (Bann 2002).

Lastly, the Benefit Transfer Approach estimates the benefits of public services by adopting an estimate of benefits from previous studies or practices of similar services. This approach can save funds and time to conduct an original valuation study. This approach includes Unit Value Transfer and Function Transfer methods. The Unit Transfer method transfers benefit estimates of similar services from previous studies. The Function Transfer method transfers a benefit function from studies completed in other public services (National Assembly Budget Office 2008).

Table 2-5 Economic valuation techniques for non-market resources [Modified from Yeom (2012)]

Categories	Valuation methods	Remarks
Cost-based Approach	• Damage Cost Avoided method • Replacement Cost method • Cost of Savings method	
Market-based Approach	• Market Price method	
Revealed Preference Approach	• Travel Cost method • Hedonic Price method	
Stated Reference Approach	• Contingent Valuation method • Choice Experiment method	**Survey required**
Benefit Transfer Approach	• Unit Value Transfer method • Function Transfer method	

2.4.2 Non-Market Benefits and Valuation Methods for Intangible Public Services

Intangible benefits of most public services such as transportation, environmental policies have been estimated and employed to carry out the economic feasibility studies of their projects, while a proper valuation methodology for improvement or rehabilitation projects of aging pipes has not been established yet, as described in Table 2-6.

Table 2-6. Non-market benefits and their valuation methods for public services

Organizations /Researchers	U.S. Department of Transportation	U.S. Water Resources Council	U.S. EPA
Applications	**Transportation**	**Water resources**	**Environmental policies and regulations**
Benefits	- **Vehicle cost savings** Fuel, tires, maintenance, repair, etc. - **Time savings** to transportation users - **Reduction in accidents, injuries, and fatalities** that would result from the use of new projects - **Improvement in access** to an important education, medical or recreational facility - **Decrease in evacuation time** required in the event of a disaster, etc. - **Reduction in emissions & noises**	- **Water supply** Water supply increase without & with the projects - **Hydropower** Energy produced by hydroelectric power plants - **Flood damage reduction** Reduction in actual or potential damages associated with land use (Transportation, buildings, labor, etc.) - **Recreation** - **Water quality improvements**	- **Human health improvements**: Mortality risk reductions (Cancer fatality, microbial illness) - **Avoided material damages**: A possible decline in pipe breakage; Water loss; a reduction to buy bottled water or purchase a filter - **Ecological improvements**: Market products (Food, timber, fuel, etc.) Recreation activities and aesthetics (Taste, odor, appearance) - **Valued ecosystem functions**: Climate moderation, flood moderation, ground recharge
Valuation Methods	- **Reduced vehicle ownership and use × Cost-per-mile value** for all affected travel - **Travel times before and after project implementation × cost** for each trip - **Accident frequency changes × unit accident costs** per crashes (Property damages, traffic days, medical care, etc.) - **Changes in vehicle-miles, vehicle-hours × emissions, noises × cost**	- **Contingent valuation method** (CVM) using WTP (Willingness to pay) for the increase in the value of goods and services attributable to water supply - **Reduced damages × dollar damages** to activities affected by flooding **or other market value data** - **Energy produced × market price or WTP** (Willing to pay)	- **Contingent valuation method** (CVM) using WTP (Willingness to pay) for non-market products - **Production functions** for market products benefits
Sources	(U.S. Department of Transportation 1998)	(US Water Resources Council, 1983)	(U.S. EPA 2014)

Table 2-6. Non-market benefits and their valuation methods for public services (Continued)

Organizations /Researchers	Hutton, Guy (Switzerland)	Griffin & Mjelde	P. Koss (U.S. Geological Survey)
Applications	**Water supply and sanitation services**	**Water supply in Texas**	**Water supply reliability in California**
Benefits	- **Health effects**: Reduction in incidence rates (cases reduced per year) or in deaths - **Economic benefits:** Transport costs to health services Lower morbidity, fewer deaths Time savings associated with closer water facilities	- **Avoidance of a current shortfall of water supply** as a standard annual shortage event	- **Avoidance of an occurrence of water shortages** of a given frequency and severity
Valuation Methods	- **Major values assumed:** $0.5 per return journey for health services - **Reduced deaths × income** (would be earned from averted fatalities)	- **Contingent valuation method** (CVM) using WTP (Willingness to pay) for non-market products	- **Contingent valuation method** (CVM) using WTP (Willingness to pay) for non-market products
Sources	(Hutton et al. 2007)	(Griffin and Mjelde 2000)	(Koss 2001)

Table 2-6. Non-market benefits and their valuation methods for public services (Continued)

Organizations /Researchers	Korea Development Institute (Korea)		European Commission (EU)
Applications	**Transportation**	**Water resources**	**Water supply improvement programs**
Benefits	- **Vehicle cost savings** Fuel, tires, maintenance, repair, etc. - **Time savings** to transportation users - **Reduction in accidents, injuries, and fatalities** that would result from the use of new projects - **Improvement in access** to an important education, medical or recreational facility - **Decrease in evacuation time** required in the event of a disaster, etc. - **Reduction in emissions & noises**	- **Water supply** Water supply increase without & with the projects - **Hydropower** Energy produced by hydroelectric power plants - **Flood damage reduction** Reduction in actual or potential damages associated with land use (Transportation, buildings, labor, etc.)	- **Reduction in operating costs** Customer complaints reduced operating costs at treatment works, etc. - **Improvements to service levels** Supply interruptions - **Health benefits** Reduced health cost associated with water quality problems - **Improved aesthetic qualities** Taste and odor
Valuation Methods	- **Reduced vehicle ownership and use ×Cost-per-mile value** for all affected travel (Purchase, insurance, fuel, oil, repairs, etc.) - **Travel times before and after project implementation × cost** for each trip - **Accident frequency changes × unit accident costs** per crashes (Property damages, traffic days, medical care, etc.) - **Changes in vehicle-miles, vehicle-hours × emissions, noises × cost**	- **Contingent valuation method** (CVM) using WTP (Willingness to pay) for the increase in the value of goods and services attributable to water supply - **Reduced damages × dollar damages** to activities affected by flooding **or other market value data** - **Energy produced × market price or WTP** (Willing to pay)	- **Contingent valuation method** (CVM) using WTP (Willingness to pay) for non-market products - **Production functions** for market products benefits
Sources	(KDI 2004)	(KDI 2001)	(Bonnie et al. 2008)

2.4.3 Gaps in Knowledge

A review of published literature on economic valuation of benefits from aging pipe improvements reveals that a comprehensive economic feasibility study framework suitable for aging pipe improvement projects has not been fully established yet and most of these studies have been limited to a small number of costs. There is a notable paucity of studies investigating the comprehensive impacts of pipe breakage including environmental aspects.

- **No Economic Feasibility Study Guideline on Pipe Improvements**: Various methods or guidelines to estimate intangible benefits from public services such as transportation or water resources developments have been established and instituted for their economic feasibility studies. Also, previous studies tried to identify the social impacts of pipe breaks. They have not, however, advanced to a framework or guideline for an economic feasibility study suitable for aging pipes replacements or improvement projects yet. To date, no such studies have so far been conducted in developing a methodology to valuate social intangible benefits from the pipe improvements. Thus, this gap has caused a water supply utility like K-water to face difficulty in justifying the needs and budgets on aging WTM improvement projects.
- **Limited to Scheduling Decision by Replacement Costs**: Furthermore, previous studies have been based on project costs or/and maintenance when scheduling aging pipeline improvements. However, these studies did not include indirect or social costs caused by pipe breakage, although indirect costs are well known to be higher than direct costs (Yerri 2016). As a result, such improvement plans made by decisions dependent on direct costs may lead to a biased or inappropriate prioritization of aging pipeline assets due to excluding social cost to the public and inconvenience to end-users. In addition, although some research has been carried out on quantifying intangible benefits from avoiding water service shortage or disruption, they have been limited to the CVM

methods based on WTM survey, which may cause a biased interpretation on economic feasibility study results.

- **Lack of Comprehensive Study on Impacts of Pipe Breakage**: Finally, previous models to estimate indirect or social consequences of pipe failure to the public did not include environmental impacts (e.g., sustainability, water quality, etc.), economic losses, and public distrust. The need for studies to develop a methodology to convert such social impacts into monetary values is further underscored by the fact that an economic feasibility study on pipe improvement projects should include social benefits to the public like the already-established feasibility study guidelines (U.S. Department of Transportation 1998; U.S. Water Resources Council 2009).

2.5 Summary

From a review of published literature on the management of water networks, the problems relating to the management of aging WTMs are found to be: (1) lack of study on understanding the main factors affecting steel WTMs in practice and their failure mechanisms, (2) lack of analysis on comprehensive factor affecting pipe failures, (3) no predictive model forecasting a service life of aging steel WTMs, and (4) no methodology to valuate the intangible benefits of water main improvement projects into monetary units to assess their economic feasibility study.

3 FACTORS AFFECTING STEEL WATER TRANSMISSION PIPE FAILURE AND PIPE FAILURE MECHANISMS

This chapter is based on the following research paper submission (amid review):

H. J. Jun, J. K. Park, C. H. Bae, “Factors Affecting Steel Water Transmission Pipe Failure and Pipe Failure Mechanisms,” Journal of Water Research (ISSN: 0043-1354)

3.1 Abstract

Breaks of water transmission mains (WTMs) transporting a much greater volume of water to smaller-diameter distribution networks cause water supply disruption, damage and flooding of roads and buildings, shut-down of business, the inconvenience of daily activities, and significant economic loss. However, there have been few detailed investigations of determining significant factors affecting failure in steel WTMs as well as the failure mechanisms based on field data, leaving reactive maintenance as the sole means of prevention. The objectives of the study are to evaluate the primary factors affecting deterioration installed steel WTMs by statistical correlation analysis, to explore and establish scientific causal relationships and mechanisms of the influential factors with the steel WTM failure, and to quantify the failure cause by the steel WTM failure cause analysis based on the historical break data. It was found that water quality (alkalinity, electoral conductivity, pH, temperature, and residual chlorine) along with pipe age, significantly affect steel pipe deterioration while external load contributed to a deterioration in steel pipes to a lesser extent unlike the previous studies based on small iron or plastic pipes. Besides, this study proposed the holistic model for chemistry-based mechanisms between the key factors and deterioration of

steel WTMs. Additionally, the failure cause analysis highlights corrosion as the most common failure cause accounting for approximately 52%, implicating large diameter steel WTMs are primarily deteriorated by corrosion and supporting the findings from the statistical correlation analysis. This study identified the primary factors affecting steel WTMs and modeled the failure mechanisms and causal relationships between failure in steel pipes and the influential factors. This will aid the systematic management of water networks.

3.2 Introduction

3.2.1 Background

A water network consists of transmission mains and distribution networks. Transmission mains are large diameter pipes (more than 300 mm in diameter) that transport large volumes of water, including raw source water from natural water sources destined for a treatment plant, as well as treated water en route to storage reservoirs or to smaller-diameter distribution networks connected to customers (Ji et al. 2017). Transmission mains include pipes of various diameters and compositions (steel, iron, concrete, etc.), chosen to suit the characteristics of the various regional water resources and supply systems. For example, in the United States (U.S.) which has abundant local water sources, non-steel pipes (iron and plastics) account for 96% of water networks (US EPA 2009); this is in contrast to the predominance (54%) of large diameter steel water transmission mains in the ROK where there is a relative paucity of local water supply and a consequent reliance upon long conveyance and a multi-regional water supply system (about 5,000 km and 50 water supply facilities).

As water networks get older, water main breaks become far more likely, resulting in water outage and considerable inconvenience to end users. In the U.S., water main breaks occur at the high rate of 240,000 per year (EPA 2007). Accordingly, it is not surprising that the reported infrastructure grade of the United

States in the drinking water category is “D (Poor: At Risk),” implicating that the infrastructure is approaching the end of its service life with a high risk of failure (American Water Works Association 2014). Similarly, in the ROK, the multi-regional water supply pipelines installed in the 1960s are experiencing increased water main breaks, as shown in Figure 1.5.

Failure in ferrous WTMs is a very complicated process and is usually caused by many factors. Their levels of influence can vary by location and operational conditions. The following factors are involved (US EPA 2009):

- Physical factors: Pipe material, thickness, age, diameter, length, type of joints, lining and coating, vintage, traffic load, and manufacturing processes.
- Environmental factors: Soil type, soil moisture, soil load, microbes, stray electrical currents, water quality (pH, residual chlorine, dissolved oxygen, etc.).
- Operational factors: Internal water pressure, flow velocity, and operational and maintenance practices.

If causes of failures in steel WTMs are identified, the causes may be managed more efficiently to extend their service life and used in predicting pipe failure for WTMs asset management. This ultimately makes it possible to minimize water outage, traffic congestion, and end-user inconvenience. It is necessary to determine the primary factors contributing to steel WTM failures based on field data and to investigate the deterioration mechanisms such that WTMs may be managed as economic as possible.

3.2.2 Previous Research

Major causes of reinforced concrete and cast iron pipes are found to be attributed to soil moisture content causing soil expansion and soil corrosivity, respectively (Pratt et al. 1996). It was reported that the factors

such as pipe material, pipe diameter, pipe installation vintage, and traffic loading, have a relatively substantial effect on the deterioration of iron, PVC, and concrete pipes (UNESCO 2014). It was identified that the diameter and burial depth have a relatively high impact on the failure in cast iron water mains, based on one city's limited data composed of 20 pipes with less than 500-mm diameter (Wilson et al. 2015). A comprehensive review of previous research investigating relationships between the physical characteristics of pipes, climatic conditions and pipe failure (iron and plastic) was performed by Kleiner and Rajani (2001).

Also, the studies on the identification of pipe deterioration mechanisms were carried out by various lab-scale experiments. The effect of water temperature on corrosion rate and tuberculation of cast iron samples was investigated through lab tests (McNeill and Edwards 2002). From the study of the effect of chlorides on pitting corrosion of steel specimens, the lifetime of steel pipes under the corrosive condition was found to be in a range of only 2.5 - 27% of that under the non-corrosive condition (Ma 2012).

3.2.3 Gaps in Knowledge

A review of published literature on pipe deterioration shows that few studies have been undertaken on significant factors affecting failures in steel WTMs as well as on the deterioration mechanisms based on data in practice.

- ***Lack of Comprehensive Factor Analysis***: Previous research has addressed physical factors such as pipe thickness and diameter and/or environmental factors such as soil characteristics when determining the leading causes of failure in aging WTMs. However, these studies did not address water quality factors that may lead to internal corrosion as contributors to the failure of pipes, although internal corrosion has been well known as the most dominant cause of deterioration of steel WTMs (Hou et al. 2016).

- ***Limited to Small Diameter Iron and PVC Pipes***: Furthermore, management data and historical records of steel WTMs are scarce (Kleiner and Rajani 2007). Previous studies on the factors contributing to pipeline failure have been concentrated on small diameter water distribution networks composed of iron or PVC pipes. No studies have so far been conducted in investigating steel WTMs. The need for studies focused on steel water mains is further underscored by the fact that the results of previous studies focusing on iron pipes may not be extrapolated. This is because iron and steel pipes are different in their composition, properties, lining and welding system, the chemical reactions associated with their corrosion and their failure characteristics (American Water Works Association Research Foundation 1996).
- ***Lack of Comprehensive Study on Failure Mechanisms***: Lastly, the mechanisms that lead to pipe breaks are very complicated and not well understood (Kleiner and Rajani 2007). Furthermore, previous studies on the main factors affecting water main failure have not yet been conducted in connection with the failure mechanisms of the key factors derived. As a result, it was not possible to implement proper measures to extend a service life of WTMs. Thus, current knowledge about the mechanisms of the key factors and failure in steel WTMs is still limited, because it does not cover all factors contributing to water main failures comprehensively.

3.2.4 Study Objectives

The objectives of the study are to:

- Determine key factors affecting failure in installed steel WTMs with analysis of general factors, which include both physical data as well as water quality data and
- Establish scientific causal relationships and mechanisms of the identified factors with WTM failure by literature review so that the results can be used for advancing failure prediction of steel pipes as well as for the management to extend a service life of WTMs.

3.3 Materials and Methods

Figure 3.1 describes the methodology used to determine the significant factors influencing the deterioration of steel WTMs and to investigate the mechanisms of the factors and degradation.

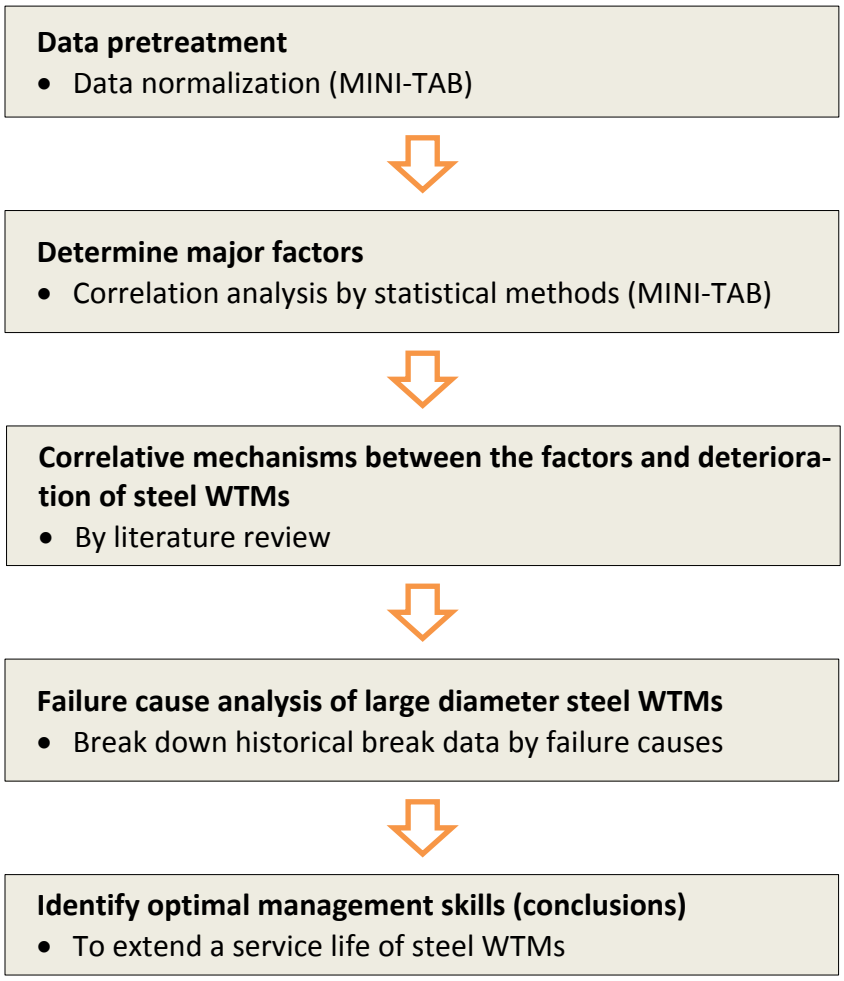

Figure 3.1 Flow overview of the methodology

3.3.1 Data Collection

Data were obtained from the database of K-water that maintains 32 drinking water treatment plants and supply facilities (50% of the ROK's drinking water) as a government-owned public utility. Data consisted of 855 historical breaks of steel WTMs from 1969 to 2015. The total length of WTMs is 2,783 km. The

collected data includes pipe diameter, pipe thickness, age, coating, service type, depth of cover, traffic loading, and water quality (pH, alkalinity, dissolved oxygen, residual chlorine, temperature, and electoral conductivity) for given variables, and a pipe break rate (number of breaks divided by total length of sectional pipelines of WTMs) for a target variable. The data used for statistical analysis are described in Table 3-1. It was assumed that the water quality data measured at the monitoring stations in the drinking water treatment plants (DWTP) are identical to the water quality throughout the WTMs. The break time of WTMs refers to the time to the first break of WTMs, in which the replacement should be considered before serious water service disruption occurs.

3.3.2 Data Pretreatment and Statistical Analysis

Real data are not at normal distribution while many statistical analyses including Neural Networks assume normality. However, The Box-Cox Power transformation can improve normality (Sakia 1992). The Box-Cox Power transformation was applied to improve statistical analysis representation of the collected data when forecasting water pipe asset life (Achim et al. 2007). Thus, this study applied the Box-Cox Power transformation method to the input factors to improve normality using MINITAB 2017 (Statistical S/W), which figures out lambda (λ) values to minimize the standard deviation of a standardized transformed variable. Figure 3.2 shows an example of the Box-Cox transformation applications. In the figure, the value of “-0.16” determined as λ indicates the power to which original data (pipe length) should be raised. The histogram in Figure 3.3 shows the resulting datum of “Burial depth of steel WTMs” from the Box-Cox Power Transformation is more normally distributed.

Table 3-1. Description of data on water transmission mains for statistical correlation analysis

Type	Factors	Descriptions
Given variables (13)	Pipe diameter	Internal diamter of of pipes
	Pipe thickness	Pipe manufacturing specifications
	Pipe age	Age of laid pipe
	Pipe coating	No coating, either internal or external coatings, and both coatings
	Service type	Raw water, settled water, and purified water
	Depth of cover	Earth load pressure
	Traffic loading	Traffic road and nontraffic road
	Six water quality parameters	pH, alkalinity, DO, residual chlorine, temperature, and conductivity
Target variable (1)	Break rate [Breaks/Km]	Number of breaks over the total length of sectional pipelines of WTMs

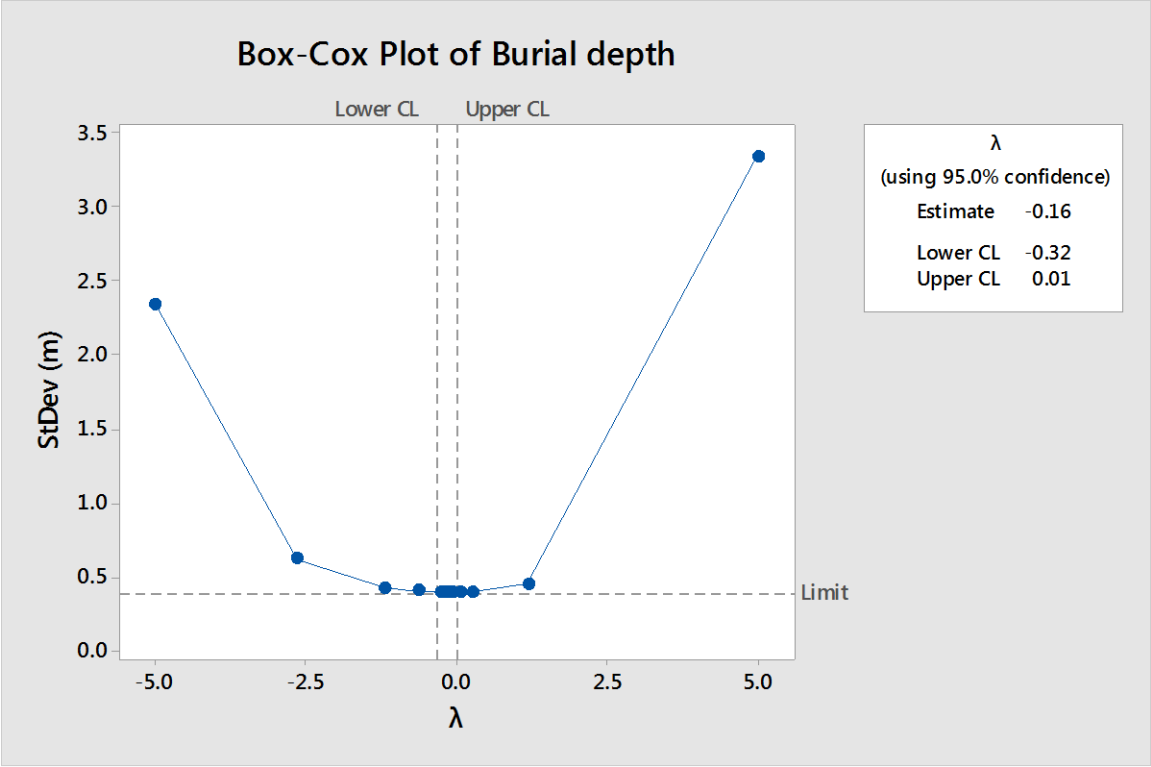

Figure 3.2. A sample of Box-Cox transformation for the input parameter (burial depth of pipes)

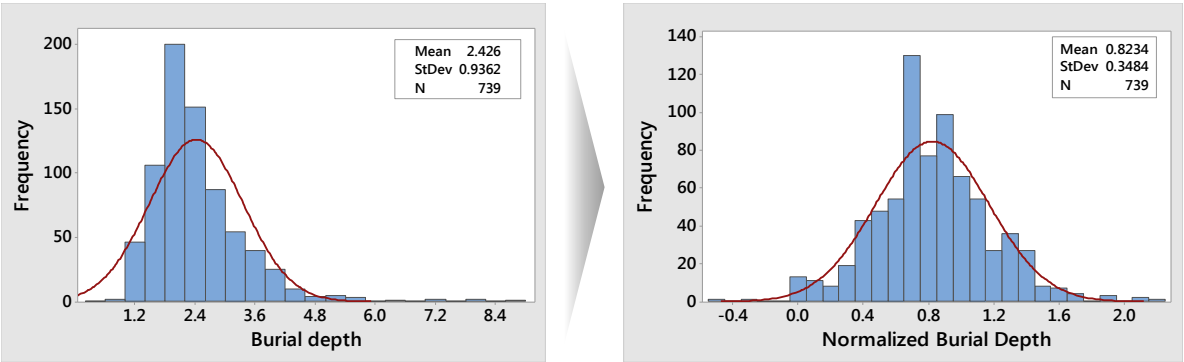

Figure 3.3. Normality test and data transformation for burial depth of WTMs by Box-Cox transformation

Influencing factors affecting a service life of steel WTMs were identified through the Pearson's correlation analysis using MINITAB 2017. Pearson's correlation coefficient (***r***) is the most commonly used correlation

statistic method in measuring the degree of the relationship between the two variables. The Pearson correlation coefficient (***r***) ranges from +1 to -1. As an absolute value of ***r*** approaches 1, this indicates a stronger relationship between two variables while a value of 0 shows that there is no association between the two variables. The correlation coefficients between each variable (pipe diameter, pipe thickness, pipe age, coating, service type, depth of cover, traffic loading, water pH, water alkalinity, dissolved oxygen, residual chlorine, water temperature, and electoral water conductivity) and the time to first failure were calculated from SPSS software based on the following formula (Chok 2010):

$$r = \frac{N \sum xy - \sum(x)(y)}{\sqrt{[N \sum x^2 - \sum(x^2)[N \sum y^2 - \sum(y^2)]}} \quad (3\text{-}1)$$

where:

r = Pearson r correlation coefficient;

N = number of value in each data set;

$\sum xy$ = sum of the products of paired scores;

$\sum x$ = sum of x scores;

$\sum y$ = sum of y scores;

$\sum x^2$ = sum of squared x scores; and

$\sum y^2$ = sum of squared y scores.

3.3.3 Establishment of Failure Mechanisms of the Main Factors in Steel WTMs

A comprehensive literature review was performed to investigate the relationship between various factors and their resulting deterioration. The results from this literature review can be used effectively for practical applications such as asset management in large diameter steel WTMs.

3.4 Results and Discussion

3.4.1 Significant Factors Influencing Deterioration in Steel WTMs

The effect of each factor on the break rate of large diameter steel WTMs was investigated using the Pearson correlation analysis method. The magnitude of the correlation coefficient determines the strength of the relationship between two variables. It was reported that the absolute value of the correlation coefficient more than 0.8 represented “very strong” correlation, from 0.6 to 0.79 “strong” correlation, from 0.4 to 0.59 “moderate” correlation, and more than 0.2 “weak” correlation (Evans 1996). Therefore, it is reasonable to consider the variables with the absolute correlation coefficient of greater than or equal to 0.2 as the significant factors affecting breakage of large diameter steel WTMs from a statistical perspective.

Figure 3.4 shows the absolute correlation coefficients of factors influencing break rate of steel WTMs obtained from the correlation analysis. This result reveals that there appeared to be a moderate correlation between the breakage of steel WTMs and pipe age, the alkalinity of water, and the conductivity of water, respectively in the statistical point of view. Also, it shows that the breakage of steel WTMs has a weak correlation with water pH, residual chlorine, pipe thickness, burial depth of pipes, pipe diameter, and water temperature.

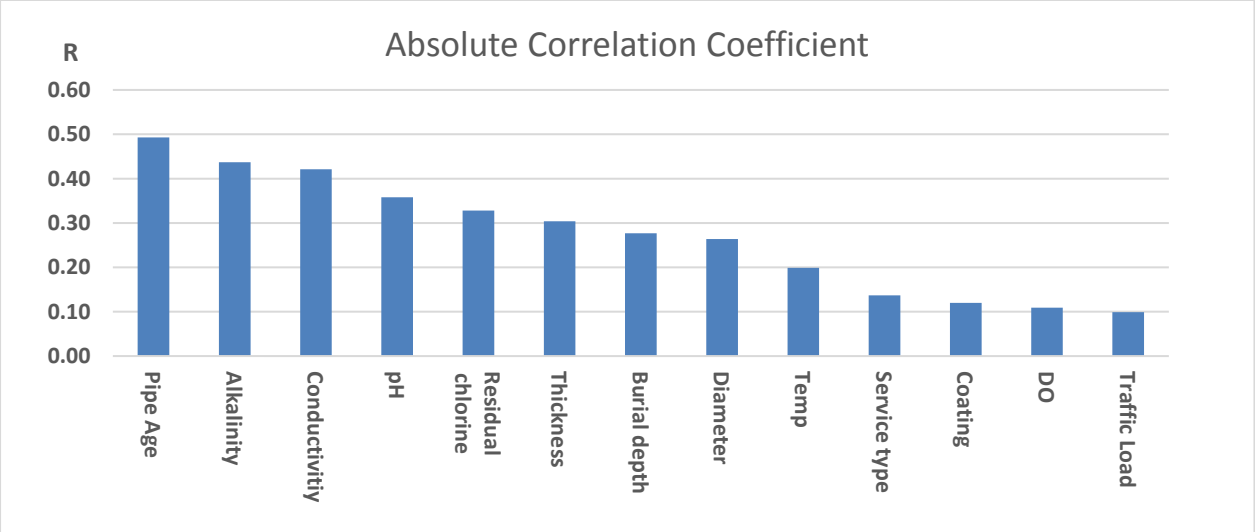

Figure 3.4. Absolute correlation coefficients of factors affecting breakage of steel WTMs

Nine factors such as pipe age, water alkalinity, electoral conductivity in water, water pH, residual chlorine, pipe thickness, burial depth of pipelines, pipe diameter and water temperature have correlation coefficient value greater than or equal to 0.2, indicating that those nine factors have a significant effect on deuteriation in large diameter steel WTMs in the statistical point of view, while other factors such as service type, coating, dissolved oxygen (DO), and traffic load, appeared to contribute relatively little to steel WTM deterioration in this study, unlikely previous studies reporting that those factors have a relatively substantial effect on deterioration of iron, PVC, and concrete pipes (UNESCO 2014).

No significant correlation was found between breakage in steel WTMs and traffic load as found in the previous studies on other pipe materials such as iron pipes. Steel pipes contain fewer carbon contents (0.08 ~ 0.25%) than iron pipes in excessive of 2%. Steel pipes also exhibit substantially better mechanical characteristics (ductility, toughness and tensile elongations) than iron pipes (Keil and Devletian 2011). These properties are thought to make steel WTMs less affected by the factors relating to external surface live loads such as traffic loads.

No significant correlation was found between breakage in steel WTMs and water DO amongst water quality parameters, although DO was recognized as an important factor affecting steel corrosion. This is because the waters served through steel WTMs in the ROK contain a high level of DO concentration ranging from 8.7 to 11.3mg/L, i.e., greater than the critical DO concentration (7 or 8 mg/L). This is explained by the previous study in which corrosion rate in steel did not increase significantly with DO level above 7 or 8 mg/L while the corrosion rate increased with DO concentration below that level (Speller 1935 in Schaschl and Marsh 1956). This result implies that DO changes in large diameter steel WTMs of the ROK does not influence deterioration in steel pipes, and that DO is not a good parameter to predict steel WTM failure.

Notably, it was implied that coating appears to influence to a lesser extent to breakage in the steel WTMs unlikely coating has been recognized as the best ways to protect steel by providing an impervious barrio preventing the transfer of electrochemical ions from the corrosive environment to the steel pipe wall. Coating failure and defects may happen in various situations: The reason why coating has a lower correlation with failure in steel WTMs might be that: improper installation or pipelining adhesion (Appalachian Underground Corrosion Short Course 2017): cathodic disbanding; weld defects; handling damages in lifting, loading, or storage; etc. Therefore, further investigation into the effect of coating on steel corrosion is thought to be needed to clearly clarify this relationship.

Figure 3.4 shows that pipe age has the highest correlation with WTMs deterioration. It also reveals that WTP failure is significantly affected by water quality parameters such as alkalinity, electoral conductivity, pH, residual chlorine, and water temperature) and physical variables (thickness and diameter of pipes, burial depth of pipelines). These correlations between water quality and deterioration in steel WTMs are close to the finding that iron corrosion is controlled by water quality factors which may exert their influ-

ence when the metal corrodes (American Water Works Association Research Foundation 1996). This implicates that water quality factors can be a good indicator to assess failure or deterioration in steel WTMs and used for WTM asset management such as corrosion control to extend a service life of steel WTMs, and substantial predictors for the prediction of steel WTM breaks.

It was found that water alkalinity was the primary factor amongst water quality factors, implicating that the steel corrosion of WTMs in the study site appears to be governed by alkalinity than other water quality parameters. This is because alkalinity as $CaCO_3$ coats a surface of steel pipes, forming $CaCO_3$ films (calcites) and passivated, and thereby inhibiting the corrosion rate (Ahmad 2006).

For new pipe installation, the similar approach can be used. As expected (result not shown), the order of the factors affecting pipe breakage was the same as the result shown in Figure 3.4. Alkalinity was most important, followed by conductivity, pH, and residual chlorine. This indicates that corrosion control is most effective in reducing pipe failure.

Consequently, failure in large diameter steel WTMs was significantly affected by water quality and their relationships were statistically verified through data in practice. It is essential that water quality should be considered when assessing WTM failure even though water quality has been overlooked and not been included in key factors used for the prediction of a service life of water networks.

Furthermore, the in-depth and detailed failure mechanisms of the derived main factors through the statistical method will be explained and discussed in the next subchapter.

3.4.2 Correlative Mechanisms between Significant Factors and Deterioration in Large Diameter Steel WTMs

Pipe failure occurs when the stresses (operational and environmental) acting on pipes exceed their residual strength where corrosion, degradation, or manufacturing defects has lowered the physical strength of

the pipes at their manufacturing stage. The mechanisms of failures in WTMs are associated with many influential factors (Rezaei et al. 2015).

Figure 3.5 shows the main factors affecting deterioration in steel WTMs, which were identified through statistic correlation analysis. The main factors can be divided into three main categories: physical factors (pipe thickness, pipe diameter, and burial depth of pipelines), environmental factors (water alkalinity, electrical water conductivity, residual chlorine, water pH and water temperature), and operational factors [pipe age and break rate (number of breaks over sectional length of pipelines)].

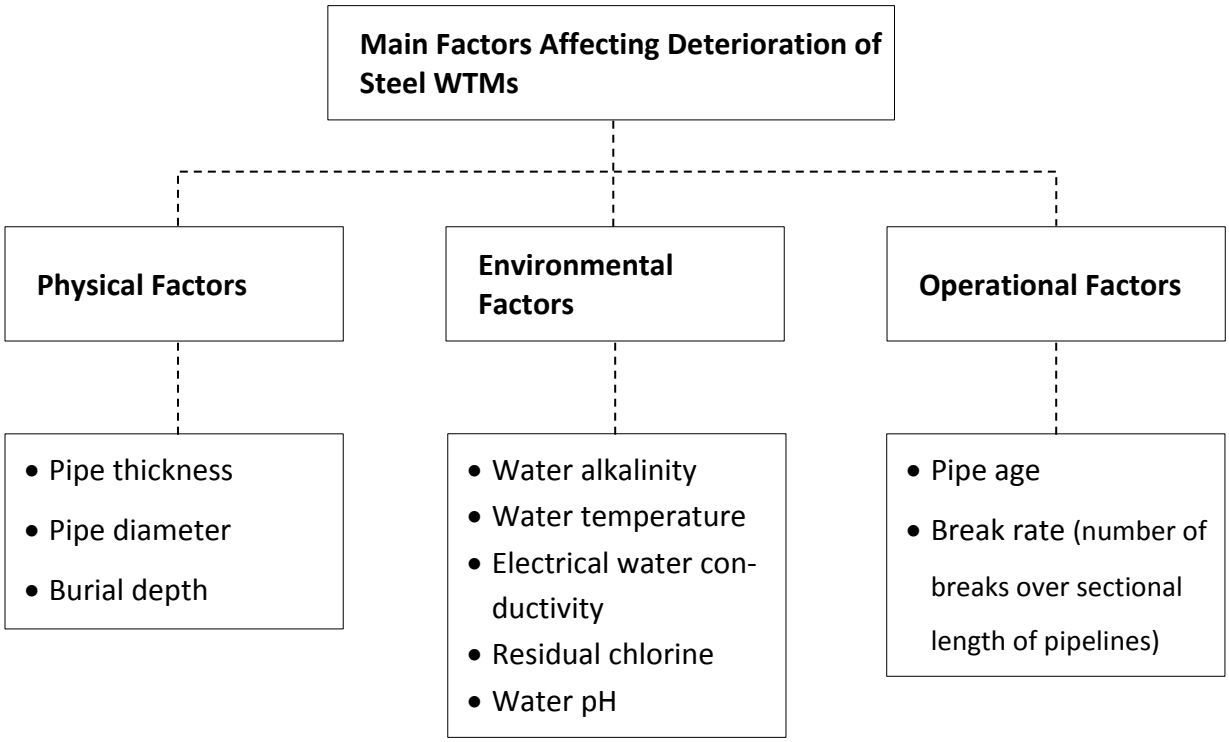

Figure 3.5. Main factors affecting deterioration in steel WTMs through statistic correlation analysis

3.4.2.1 pH and Alkalinity

pH and alkalinity are known as key water quality factors that affect steel corrosion (McNeill 2000).

First, iron is oxidized through the following steps in which OH^- takes part in (Bockris et al. 1961):

$$Fe + OH^- \rightarrow FeOH + e^- \quad (3\text{-}2)$$

$$FeOH \rightarrow FeOH^+ + e^- \quad (3\text{-}3)$$

$$FeOH^+ \rightarrow Fe^{2+} + OH^- \quad (3\text{-}4)$$

$$Fe \rightarrow Fe^{2+} + 2e^- \text{ (Overall reaction)} \quad (3\text{-}5)$$

Secondly, OH^- is commonly generated in drinking water networks by a reduction reaction as follows:

$$e^- + \tfrac{1}{4}O_2 + \tfrac{1}{2}H_2O \rightarrow OH^- \quad (3\text{-}6)$$

This reaction forms $CaCO_3$, coating a steel surface with passivating films (calcites), thereby inhibiting the corrosion rate as follows (AWWA Research Foundation 1996):

$$OH^- + HCO_3^- \rightarrow CO_3^{2-} + H_2O \quad (3\text{-}7)$$

$$Ca^{2+} + CO_3^{2-} \rightarrow CaCO_3\,(s) \quad (3\text{-}8)$$

Third, as pH increases, HCO_3^- is converted into CO_3^{2-} as shown in Equation (3-9), producing insoluble $CaCO_3$ and $FeCO_3$ as shown in Equation (3-8) and (3-10), respectively. The pipe wall is coated with the buildup of the precipitates ($CaCO_3$ and $FeCO_3$), thereby retarding the iron corrosion (American Water Works Association Research Foundation 1996).

$$HCO_3^- \rightarrow H^+ + CO_3^{2-} \quad (3\text{-}9)$$

$$Fe^{2+} + CO_3^{2-} \rightarrow FeCO_{3(S)}\text{(siderite)} \quad (3\text{-}10)$$

As pH increases, OH^- concentration increases prompting precipitations of ferrous hydroxide [$Fe(OH)_2$] and ferric hydroxide [$Fe(OH)_3$], developing protective scales and inhibiting corrosion as follows (American Water Works Association Research Foundation 1996):

$$Fe^{+2} + 2OH^- \rightarrow Fe(OH)_2\,(s) \qquad (3\text{-}11)$$

$$Fe^{2+} + \tfrac{1}{4}\,O_2 + \tfrac{1}{2}\,H_2O + 2OH^- \rightarrow Fe(OH)_3\,(s) \qquad (3\text{-}12)$$

Alkalinity refers to water's buffering capacity against a pH drop in the water. Total alkalinity includes bi-carbonate (HCO_3^-), carbonate (CO_3^{2-}) and hydroxide (OH^-) ions (Muylwyk et al 2014).

First, bicarbonate forms a protective carbonate film on a steel surface inhibiting the corrosion rate as follows (AWWA Research Foundation 1996):

$$Ca^{2+} + HCO_3^- \rightarrow CaCO_3(s) + H^+ \qquad (3\text{-}13)$$

Second, high alkalinity provides a less corrosive condition and encourages the formation of a protective film such as $CaCO_3$ or $FeCO_3$ against oxygen diffusion on a steel surface, thereby eventually limiting corrosion rate (American Water Works Association Research Foundation 1996). The reactions taking place at the anode and cathode of the steel surface in the absence and the presence of a buffer are described in Table 3-2.

At the anode with a buffer, ferrous ions react with carbonate ion (HCO_3^-), producing carbonic acid (H_2CO_3) as shown in Equation *(3-15)* . The hydroxide ions at the cathode are consumed through a neutralization reaction, thereby leading to the buildups of the precipitates such as $CaCO_3$ or $FeCO_3$, as shown in Equations *(3-19)* and *(3-20)*. As a result, the catholyte in a buffer system does not become as basic as it is in the absence of a buffer. Thus, steel in the water without alkalinity comes to be relatively more easily corroded while, in the alkaline condition with sufficient Ca^{2+} ions, $CaCO_3$ can be deposited and can retard steel corrosion (Rodolfo and Singley 2016).

Table 3-2. Reactions taking place at the anode and cathode of the steel surface without / with a buffer

Category	In the absence of a buffer	In the presence of a buffer
Anode	$Fe \rightarrow Fe^{2+} + 2e^-$ (3-5)	$Fe \rightarrow Fe^{2+} + 2e^-$ (3-5)
	$2Fe^{2+} + ½\ O_2 + 5H_2O \rightarrow 2Fe(OH)_3 + 4H^+$ (3-14)	$2Fe^{2+} + ½\ O_2 + 4HCO_3^- + 5H_2O \rightarrow 2Fe(OH)_3 + 4H_2CO_3$ (3-15)
Cathode	$Fe^{+2} + 2OH^- \rightarrow Fe(OH)_2\ (s)$ (3-11)	$O_2 + 2H_2O + 4e^- \rightarrow 4OH^-$ (3-16)
	$O_2 + 2H_2O + 4e^- \rightarrow 4OH^-$ (3-17)	$2H_2O + 2e^- \rightarrow H_2 + 2OH^-$ (3-18)
	$2H_2O + 2e^- \rightarrow H_2 + 2OH^-$ (3-18)	$2OH^- + 2Ca^{2+} + 2HCO_3^- \rightarrow 2CaCO_3(s) + 2H_2O$ (3-19)
		$2OH^- + 2Fe^{2+} + 2HCO_3^- \rightarrow 2FeCO_3(s) + 2H_2O$ (3-20)

In addition, the oxidation of ferrous (Fe^{2+}) to ferric ions (Fe^{3+}) and the formation of ferric oxides (e.g., $Fe(OH)_3$) produce a more fragile scale while siderite ($FeCO_3$) forms to a tight and more protective scale. pH and alkalinity play a role in deciding whether siderite forms or not (American Water Works Association Research Foundation 1996). As pH increases, the rate of formation of ferrous (Fe^{2+}) to ferric ions (Fe^{3+}) becomes faster, escalating the formation of nonprotective scale layers as shown in Equation (3-21), with the aid of hydroxide ions (OH^-). High alkalinity offsets this tendency, keeping the pH in a range where siderite formation might be kinetically favored over iron oxidation (Rossum 1983).

$$Fe^{3+} + 3OH^- \rightarrow Fe(OH)_3\ (s) \qquad (3\text{-}21)$$

3.4.2.2 Temperature

Temperature is expected to affect the corrosion of steel pipes by influencing several factors: electrochemical potential, DO solubility, thermal expansion, diffusivity, viscosity, and biological activity of iron-oxidizing bacteria.

3.4.2.2.1 Electrochemical Potential

In the view of electrochemistry, metals corrode only if the potential is above the equilibrium potential. The potential can be calculated by using the Nernst equation for the reaction as follows (AWWA Research Foundation 1996):

$$E_H = E^0 - \frac{RT}{zF} ln\, aMe^{z+} \qquad (3\text{-}22)$$

where E_H = potential relative to a standard hydrogen electrode (SHE); E_0 = standard potential, a constant that can be obtained from tables of electrochemical data; R = ideal gas constant; T = absolute temperature, K; z = number of electrons transferred in the reaction; F = Faraday constant; and $a\ Me^{z+}$ = activity of the ion Me^{z+}.

It is noted that an increase in temperature leads to a decrease of the equilibrium potential since the potential is a function of temperature, i.e., corrosion rate decreases as temperature increases.

3.4.2.2.2 DO Solubility

The solubility of oxygen in water decreases as temperature increases, because increased temperature causes an increase in kinetic energy, leading to more motion in the oxygen molecules which break intermolecular bonds and escape from solution (Buckley 1971). The temperature dependence of the equilibrium constant K (solubility product) can generally be described with the Van't Hoff equation as follows:

$$ln \frac{K_T}{K_{To}} = - \frac{\Delta H_R^o}{R} \left(\frac{1}{T} - \frac{1}{T_0}\right) \qquad (3\text{-}23)$$

where K_T and K_{T0} = equilibrium constants at temperatures T and T_0, respectively; ΔH_R^o = enthalpy of reaction which can be regard as constant between 5 - 35°C (Stumm and Morgan 1996); and R = gas constant (8.314 J/K/mole).

According to the Van't Hoff equation, solubility analytically decreases as temperature increases. As water temperature increases, it is more likely to inhibit the roles of DO in both accepting electrons and oxidizing ferrous compounds. Therefore, changes in DO solubility can have a significant impact on chemical reactions associated with steel corrosion such as oxidation and reduction as well as precipitation reactions.

3.4.2.2.3 Thermal Expansion and Constriction

WTM systems including various oxides and steel are subject to thermal expansion: a tendency to expand or constrict with a change in temperature. Ferrous compounds have a different coefficient of thermal expansion compared to metal as shown in Table 3-3. The differential thermal expansion properties of the scales lead to their physical stresses and deformation as temperature changes and can develop critical crack propagation (Schutze 1997). In addition, the cracks might expose the unprotected bare metal surface to the external corrosive environments.

Table 3-3. Coefficients of thermal expansion (α) values [Source from (Schutze 1997)]

Components	Coefficients of thermal expansion values
Fe	15.3×10^{-6}
FeO	12.2×10^{-6}
Fe_2O_3	10.96×10^{-6}
Fe_3O_4	10.5×10^{-6}

3.4.2.3 Residual Chlorine

Water chlorination is the final drinking water process. When chlorine is liquefied, it readily forms hydrochloric acid (HCl) and hypochlorous acid (HOCl) or hypochlorite (OCl^-) as follows (Rodolfo and Singley 2016):

$$Cl_2 + H_2O \rightarrow HOCl + HCl \, (pH < 7.5) \qquad (3\text{-}24)$$

$$HOCl \rightarrow H^{+} + OCl^{-} \ (pH > 7.5) \qquad (3\text{-}25)$$

HCl increases the acidity of the water and HOCl reacts with ferrous ion, precipitating ferric hydroxide [$Fe[OH]_3$], and thereby increasing corrosion rate as follows (Tuthill et al. 1998):

$$2Fe^{2+} + HOCl + 5H_2O \rightarrow 2Fe(OH)_3(S) + Cl^{-} + 5H^{+} \qquad (3\text{-}26)$$

HOCl as Cl_2 stoichiometrically oxidizes 1.56 mg of iron (Reckhow 2009). Also, the above reactions accelerate a decrease in pH, rising corrosivity.

In addition, chloride ion causes pitting corrosion with deep holes. Iron is dissolved into ferrous ion inside the pit through the anodic reaction and the electrons flow to the cathodes. The water enclosed in the pit has a net positive charge. The positively charged pit attracts negative chloride ions (Cl^{-}), reacting with ferrous ion, as follows (Ma 2012):

$$Fe^{2+} + 2Cl^{-} \rightarrow FeCl_2 \qquad (3\text{-}27)$$

The formed $FeCl_2$ increases acidity of the water, resulting in further iron corrosion as follows (Ma 2012):

$$FeCl_2 + 2H_2O \rightarrow Fe(OH)_2\,(S) + 2HCl \qquad (3\text{-}28)$$

3.4.2.4 Electrical Conductivity

Electrical conductivity (EC) is water's ability to allow the transport of charged ions (Ionode 2017):

$$EC = \frac{1}{R} \times \frac{D}{A} = \frac{I}{V} \times \frac{D}{A} \qquad (3\text{-}29)$$

where EC = electrical conductivity (S/cm); R = Resistance of the solution (ohms = 1/S); V = voltage (volts); I = current (amperes); D = distance between the electrodes (cm); and A = area of the electrodes (cm^2).

The above equation implicates that EC is proportional to the concentration of ions present in the water (US EPA 2012b). These ions originate from dissolved salts and inorganic materials such as alkalis (OH^-), chlorides (Cl^-), sulfides (SO_4^{2-}) and carbonate compounds (CO_3^{2-}) (Miller et al. 1988).

EC is often associated with the corrosivity of steel in the water. Because the corrosion current must pass through the water by ionic conduction, EC will influence the way in which corrosion occurs in the water (Ahmad 2006). It is known that highly conductive water tends to be more corrosive than less conductive waters (Rossum 1983) and a positive relationship was identified between EC and corrosion rate (Rodolfo and Singley 2016). Consequently, the higher the dissolved salts, the higher the ionic strength, i.e., EC, and faster steel is corroded (Muylwyk et al. 2014).

The ions contributing to EC contain their different corrosive characteristics. To be specific, some ions such as chlorides (Cl^-) and sulfides (SO_4^{2-}) are contributors to corrosion. These ions react with ferrous ion, forming ferrous chloride ($FeCl_2$) or ferrous sulfate ($FeSO_4$) as described in Equations (3-27) and (3-30). This eventually increases the acidity of the water (Bohnet 2003; Ma 2012), accelerating steel corrosion and pitting as shown in Equation (3-28) (Illinois State Water Survey 1975):

$$Fe^{2+} + 2Cl^- \rightarrow FeCl_2 \qquad (3\text{-}27)$$

$$FeCl_2 + 2H_2O \rightarrow Fe(OH)_2\,(S) + 2HCl \qquad (3\text{-}28)$$

$$Fe^{2+} + SO_4^{2-} \rightarrow FeSO_4\,(s) \qquad (3\text{-}30)$$

Also, experimental evidence supports that the corrosion rate of steel WTMs increases as EC in the water increases because potable water passing through steel WTMs holds ions contributing to corrosion (Ribeiro et al. 2012).

3.4.2.5 Pipe Age

Pipe age indicates the length of time that WTMs have been in operation, exposed to the surrounding environment. The relationship between pipe failure and age is typically described by a so-called “bathtub curve” as illustrated in Figure 3.6. The rate of occurrence of a failure (ROCOF) is usually associated with its age. This curve includes three phases in the life of a buried pipe: 1) Burn-in phase; 2) In-usage phase; and 3) Wear-out phase, in which breaks increase due to aging over time (Kleiner and Rajani 2001).

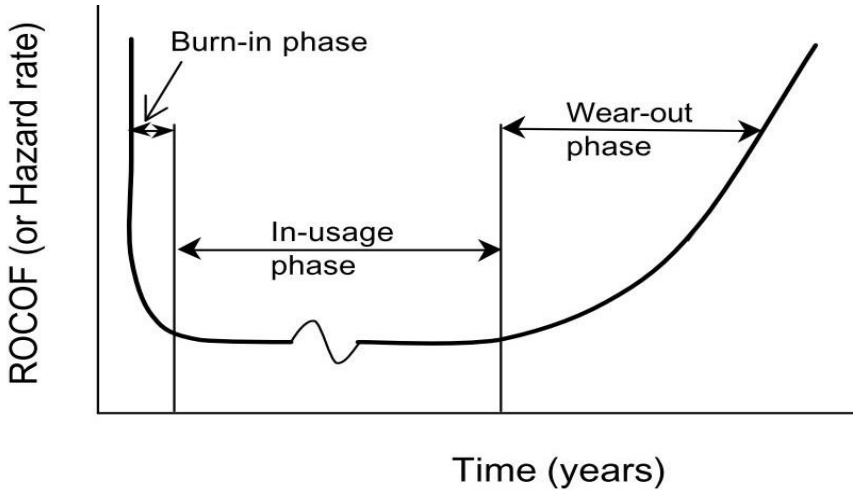

Figure 3.6. The bathtub curve of the life cycle of a buried pipe [Sourced from (Kleiner and Rajani 2001)]

It was found that the number of breaks in water mains increased with age (Gerhold 1976). Also, it was reported that corrosion-induced breaks increase over time, while breaks resulting from other causes were hard to find a relevance to pipe age (Fitzgerald 1968). The increase in metallic pipe break rates with age is generally ascribed to strength reduction because of corrosion (Boxall et al. 2007). Additionally, This observation experimentally supports that pipe age is associated with an increase in breakage of steel WTMs (Romanoff 1964).

3.4.2.6 Pipe Diameter and Thickness

Pipe diameter is reported as one of the main factors influencing break rates in water mains (Clark et al. 1982). It was found consistent in the previous studies that pipe diameter was inversely proportional to break rates in water mains (Berardi et al. 2008; Christodoulou et al. 2012).

The main reason for the increase in failure rate with a decrease in pipe diameter has been attributed to thinner pipe thickness, making them more vulnerable to failure following the loss of wall thickness due to corrosion or other deteriorations (Rezaei et al. 2015). Smaller pipes with thinner walls have a lower second moment of area, therefore, a reduced ability to resist internal or external stresses (UNESCO 2014).

The relationship between steel pipe diameter and thickness stipulated in the Korea Standard, indicating that thickness in steel pipes increases with a diameter as shown in Equation (3-31):

$$T = 0.0079 \times D + 2.7544 \qquad (3\text{-}31)$$

where T = thickness (mm) and D = diameter (mm).

Internal pressure is one of the primary loads on WTMs. Barlow's formula is generally used to determine allowable stress commonly known as strength of pipes to withstand the internal operating pressure as shown in Equation (3-32) (Wilmott and Sutherby 1998):

$$\sigma = \frac{P \times D}{2t} \qquad (3\text{-}32)$$

where σ = allowable stress; P = pressure; t = wall thickness; and D = outside diameter.

The above equation can be expressed and simplified by entering Equation (3-31) as follows:

$$\sigma = \frac{P}{2\,(0.0079 + \frac{2.7544}{D})} \qquad (3\text{-}33)$$

Equation (3-33) indicates that the strength of steel pipes to withstand internal loads is proportional to diameter, thereby leading a reduction in break rate in steel WTMs.

As for external loads such as earth pressure, the strength of the buried pipes to withstand the effect of soil and surface forces, known as allowable bending stress pipes can be calculated as follows (ASCE 2001):

$$\sigma_b = 4E \frac{D_l K P}{\left(\frac{EI}{R^3} + 0.061E'\right)} \left(\frac{t}{D}\right) \qquad (3\text{-}34)$$

where σ_b = allowable bending stress; D = outside diameter of pipe, mm; t = pipe wall thickness, mm; E = modulus of elasticity of pipe; Δy = vertical deflection of pipe, mm; D_l = deflection lag factor (1.0 - 1.5); K = bedding constant (0.1); P = pressure on pipe due to soil load and live load, psi; R = pipe radius, mm; E' = modulus of soil reaction, psi; and $I = t^3/12$.

The allowable strength can be simplified as a function of mainly diameter and thickness of buried pipes except for other coefficients and thereby simplified as follows:

$$\sigma_b \propto \frac{1}{(0.0079 + 2.7544/D)^2} \qquad (3\text{-}35)$$

Therefore, Equation (3-35) analytically reveals that the strength of steel pipes is proportional to diameter, thereby showing an inverse relationship between diameter and breakage rate in steel WTMs.

3.4.2.7 Burial Depth

The soil above a buried steel pipe exerts pressure on the pipeline. The pressure is mainly dependent on the burial depth of the pipeline (Washington State Department of Health 2006). If the burial depth is not sufficient, the pressure on the pipeline due to the earth can be greater than that causing the crushing of the side wall of the pipes and pipe bucking can occur (Rotterdam 2012).

The soil pressure acting on a buried pipeline is generally calculated using the following equation (ASCE 2001):

$$P_s = w\ H \qquad (3\text{-}36)$$

where P_s = soil pressure acting on the pipe; W = unit weight of filling; and H = height of fill above the top of the pipe.

The above equation indicates that soil pressure acting on the pipeline is a function of burial depth of a pipeline. Thus, the burial depth of pipes can affect pipe failures. This is explained by the findings that the pipes with shallower burial depths appeared to have higher break rates (Wilson et al. 2015).

3.4.2.8 Other Factors

3.4.2.8.1 Dissolved Oxygen

DO acts as an essential electron acceptor in the cathode of steel metal as follows:

$$Fe + 0.5O_2 + H_2O \rightarrow Fe^{+2} + 2OH^- \qquad (3\text{-}37)$$

The atoms of the steel are ionized and release electrons. The electrons react with DO in the water to form hydroxide ions. Simultaneously, the positive ferrous ions diffuse through the water to the cathode, starting to corrode.

Secondly, DO plays a vital role in oxidizing ferrous compounds. With the availability of oxygen, the ferrous hydroxide forms iron (III) oxide-hydroxide ($Fe_2O_3{\cdot}H_2O$)(Ahmad 2006):

$$4Fe(OH)_2 + O_2 \rightarrow 2Fe_2O_3{\cdot}H_2O(s) + 2H_2O \qquad (3\text{-}38)$$

The hydrated ferric oxides are formed as follows (AWWA Research Foundation 1996):

$$3FeCO_3\,(s) + 0.5O_2 \rightarrow Fe_3O_4\,(s) + 3CO_2 \qquad (3\text{-}39)$$

$$4Fe_3O_4\,(s) + O_2 \rightarrow 6Fe_2O_3\,(s) \qquad (3\text{-}40)$$

Thus, steel corrosion is associated with DO. It is also reported that the corrosion rate generally increases with increasing DO and water free of DO will not tuberculate (Rodolfo and Singley 2016).

3.4.2.8.2 Service type

Water treatment is customized to customer's preferences according to their diverse needs and purposes to use water. The customers are typically classified as local governments, industrial plants, and citizens. They have different preferences for water quality. To be specific, only raw water is supplied to drinking water treatment plants owned by local governments without their own water sources. Settled water is supplied to industrial plants for their cooling water use, not drinking water consumption. Most commonly, filtered water is provided to citizens through water networks after a final water treatment by K-water.

A couple of chemicals (coagulants and disinfectants) are mainly applied to drinking water treatment. First, chlorine is added to the raw water to oxidize organics and help control taste & odor-causing substances. Secondly, coagulants such as alum [aluminum sulfate, $Al_2(SO_4)_3$] or PACs [poly aluminum chloride, $Al_2(OH)_3Cl_3$] are added to the water to destabilize, cluster, settle down and remove colloidal-size particulate matter suspended in water during the process known as coagulation. Then, chlorine is added to the purified water at the final step to deactivate microorganisms such as bacteria, protozoa, and viruses that may cause illness in humans.

While raw water does not contain any substance affecting a steel pipe corrosion, settled water as well as filtered water possess various corrosive ions resulting from water treatment chemicals added as shown in Figure 3.7. When chlorine is applied during prechlorination, it readily forms hydrochloric acid (HCl) and hypochlorous acid (HOCl) as described in Equation (3-24), escalating acidity of the water (Rodolfo and

Singley 2016). HOCl reacts with ferrous ion, precipitating ferric hydroxide [$Fe(OH)_3$], and thereby increasing corrosion rate as follows (Tuthill et al. 1998). Aluminum sulfate or poly aluminum chloride added during coagulation is dissociated into aluminum (Al^{3+}), sulfate (SO_4^{2-}), hydroxide (OH^-), and chloride (Cl^-) ions as follows:

$$Al_2(SO_4)_3 \cdot 18H_2O \rightarrow 2Al^{3+} + 3SO_4^{2-} + 18H2O \rightarrow 2Al(OH)_3 + 6H^+ + 3SO_4^{2-} + 12H_2O \quad (3\text{-}41)$$

$$Al_2(OH)_3Cl_3 \rightarrow 2Al^{3+} + 3OH^- + 3Cl^- \rightarrow Al(OH)_3 + 3H^+ + 3Cl^- \quad (3\text{-}42)$$

Thus, settled water can contain corrosive ions such as Cl^- or SO_4^{2-} forming ferrous chloride ($FeCl_2$) or ferrous sulfate ($FeSO_4$) as described in Equations (3-41), (3-42), and (3-43), resulting in further steel corrosion (Bohnet 2003; Ma 2012). Also, a decrease in pH increases the corrosivity of the settled water.

$$Fe^{2+} + SO_4^{2-} \rightarrow FeSO_4\ (s) \quad (3\text{-}43)$$

Chlorine is added during disinfection. It produces hydrochloric acid (HCl) and hypochlorous acid (HOCl), ultimately oxidizing iron as previously described (Rodolfo and Singley 2016). Therefore, filtered water can include a lot more corrosive ion as shown in Figure 3.7. The corrosivity of water increases over drinking water treatment resulting from the chemical addition.

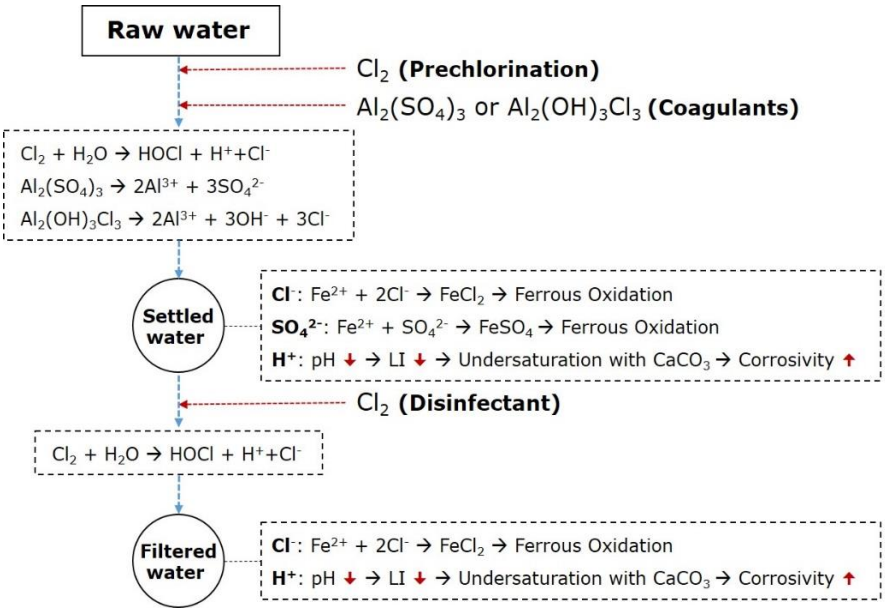

Figure 3.7. Flow diagram of reactions by adding chemicals in drinking water treatment process

3.4.2.8.3 Coatings

One of the effective ways to protect steel against corrosion is by providing an impervious barrier coating that prevents the transfer of electrochemical ions from the corrosive environment to the steel since without moisture (electrolyte) there is no corrosion.

Additionally, the electrochemical corrosion potential (ECP) of coated steel and uncoated steel was investigated in corrosive environments by conducting an immersion test. The result shows that the coated steels have an active passivating and efficient barrier behavior against corrosion (Mobin and Tanveer 2011). This observation experimentally supports that coating contributes to anti-corrosion of steel WTMs.

3.4.2.9 Summary

Based on the theoretical review above, the holistic model for chemistry-based mechanisms between the key factors and deterioration of steel WTMs were proposed in

Figure 3.8 Mechanism model between the main factors and deterioration in steel WTMs proposed in this study

.

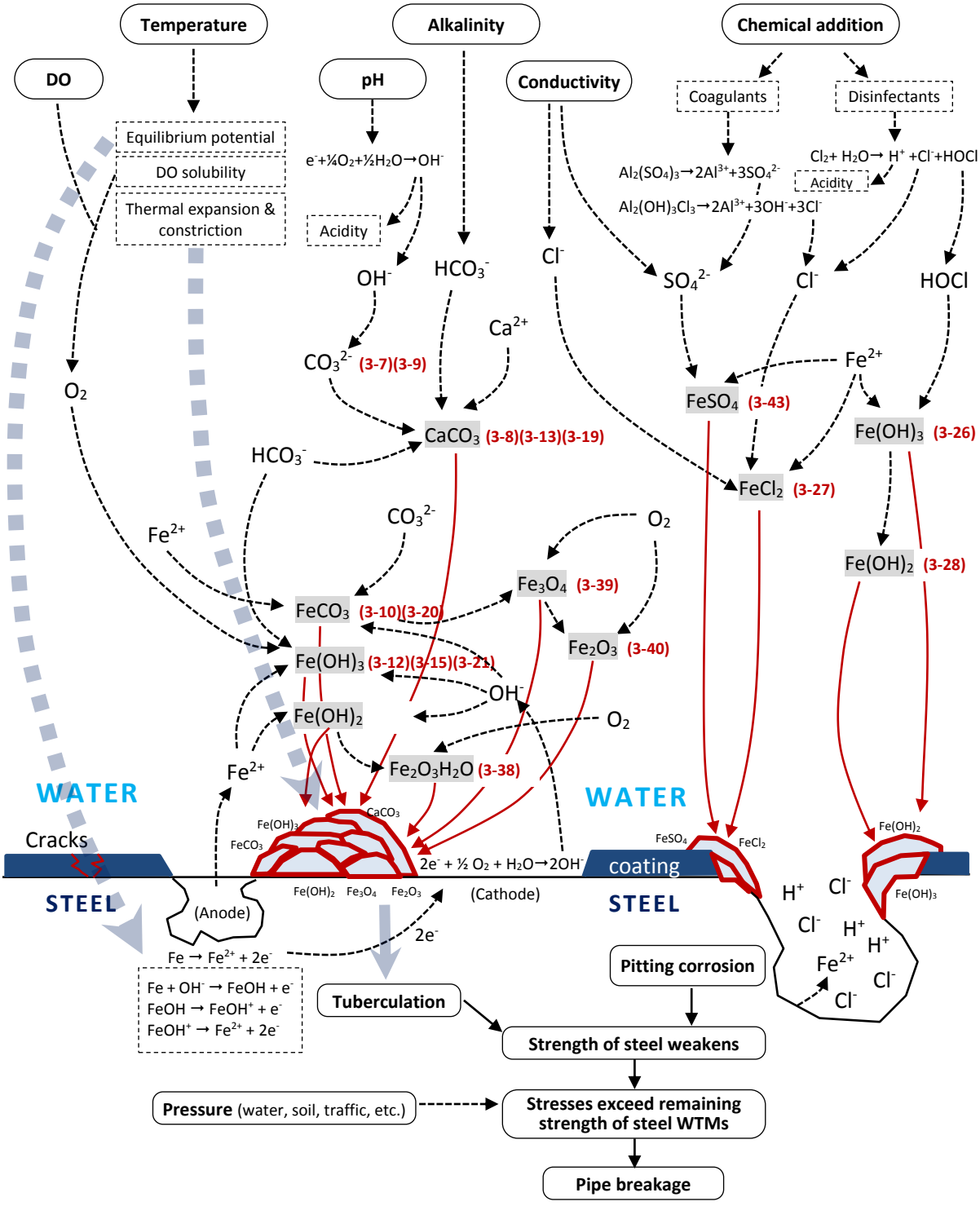

Figure 3.8 Mechanism model between the main factors and deterioration in steel WTMs proposed in this study

(3-#) denotes the relevant chemical reaction equation.

3.4.2.10 Breakage and Deterioration in Large Diameter Steel WTMs (Sourced from K-water)

Figure 3.9 through Figure 3.28 show breakage or deterioration in large diameter steel WTMs in the study area that resulted from various causes such as corrosion.

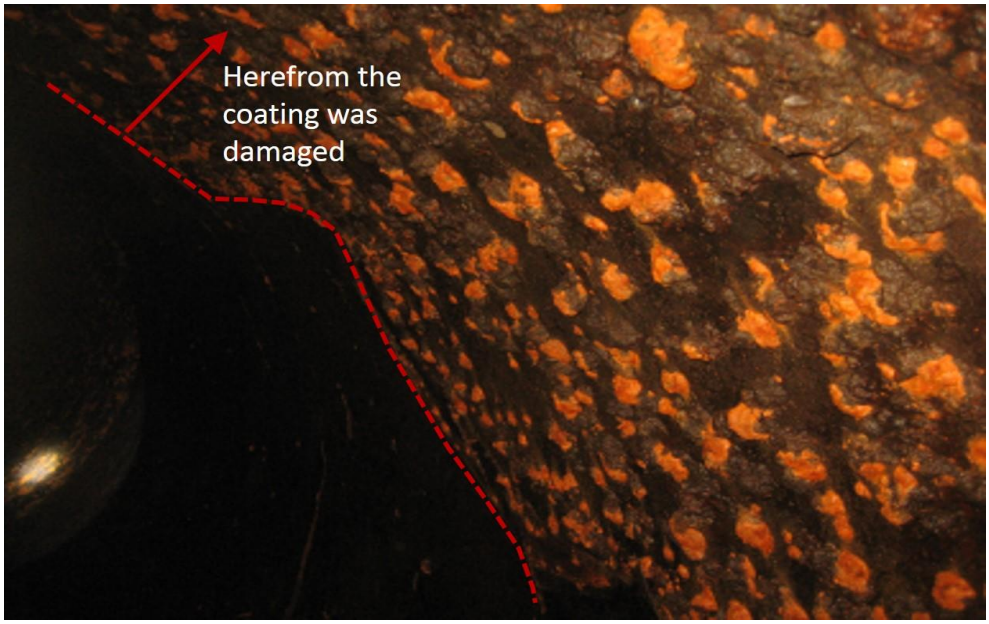

Figure 3.9. Tubercles are developing around the damaged area of the coating material Inside a 1,650-mm diameter steel WTM.

Figure 3.10. The internal coating material was cracked and detached at a pipe joint. The slime was developing across the 1,650-mm diameter steel WTM.

Figure 3.11. Corrosion developing at a pipe joint of a 1,650-mm diameter steel WTM.

Figure 3.12. Corrosion developing inside a 1,650-mm diameter steel WTM.

Figure 3.13. A pipe sample of a 1,650-mm diameter steel WTM before sandblasting for pipe cleaning

Figure 3.14. A pipe sample of a 1,650-mm diameter steel WTM after sandblasting for pipe cleaning.

Numerous holes are developing intensely due to corrosion.

Figure 3.15. Corrosion forming around the longitudinal weld caused a pipe break in a 1,350-mm diameter steel WTM. Numerous tubercles and thick scales were built up.

Figure 3.16. A hole due to corrosion around the weld caused a pipe break in a 350-mm diameter steel WTM.

Figure 3.17. A pipeline leak in a 900-mm diameter steel WTM before sandblasting for pipe cleaning

Figure 3.18. Appearance inside a 900-mm diameter steel WTM after sandblasting for pipe cleaning, in which the hole developed by corrosion caused a pipe break

Figure 3.19. A pipe sample of a 200-mm diameter steel water main before sandblasting for pipe cleaning

Figure 3.20. A pipe sample of a 200-mm diameter steel water main after sandblasting for pipe cleaning.

Corrosion developing around the longitudinal weld caused a pipe break.

Figure 3.21. Appearance outside a 700-mm diameter steel WTM before sandblasting for pipe cleaning

Figure 3.22. A 700-mm diameter steel WTM after sandblasting for pipe cleaning, in which numerous holes due to corrosion around a pipe joint weld caused a pipe break

Figure 3.23. A sample of straight portion in a 700-mm diameter steel WTM before sandblasting for pipe cleaning

Figure 3.24. An example of a straight pipe in a 700-mm diameter steel WTM after sandblasting for pipe cleaning, in which a big hole due to corrosion went through a pipe wall, causing a pipe break

Figure 3.25. A joint weld in a 900-mm diameter steel WTM before sandblasting for pipe cleaning

Figure 3.26. A pipe joint in a 900-mm diameter steel WTM after sandblasting for pipe cleaning, in which a few holes due to corrosion occurred on the joint weld and went through a pipe wall

Figure 3.27. A crack on the pipe hole cover in a 2,000-mm diameter steel WTM, which was caused by temperature expansion and constriction, resulted in a flood in Pyungtack City, the ROK, in 2015.

Figure 3.28. Broken water main floods homes, roads and cars in Pyungtack City in 2015 [source from (SBS NEWS 2015)]

3.4.3 Failure Cause Analysis of Large Diameter Steel WTMs Breaks

Failure cause analysis was performed to quantify the failure mechanisms of each case as well as to visualize break records by failure causes. This analysis was based on the total of 624 historical break data of steel WTMs relating to identified deterioration or failure causes.

Buried pipes are affected by corrosion, external loads (soil pressure, traffic load), internal water pressure, movement of the surrounding soil, etc. (US EPA 2012a). Based on the previous studies, seven failure cause categories were established as follows: Corrosion; Deterioration of accessories (valves, fittings, etc.); Movement of the surrounding soil; Temperature expansion and constriction; Water pressure; Traffic load; and Soil pressure. Table 3-4 shows the summary of the failure causes of historical steel WTM breaks incidents from 1969 to 2015.

Table 3-4. Summary of failure causes of steel WTM breaks from 1969 to 2015

Category	Failure Causes	Number of steel WTM breaks	Ratio
Break data with specified failure causes	Corrosion	324	51.9%
	Accessory deterioration	110	17.6%
	Movement of the surrounding soil	32	5.1%
	Temperature expansion and constriction	77	12.3%
	Soil pressure	2	0.3%
	Traffic load	27	4.3%
	Water pressure	52	8.3%
Total		**624**	**100%**

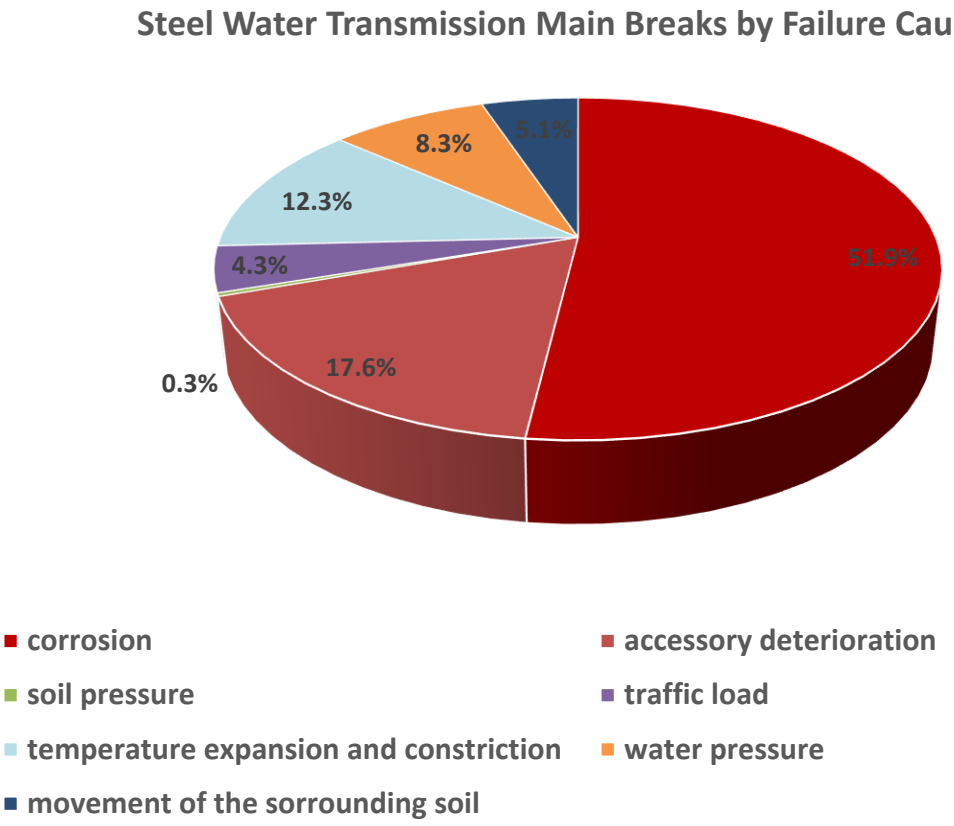

Figure 3.29 Pie chart of the steel WTMs breaks broken down by failure causes

The result in Figure 3.29 highlights corrosion as the most common failure cause in large diameter steel WTMs, amounting to approximately 52%. The next failure cause is accessory deterioration, followed by temperature expansion and constriction, water pressure, movement of the surrounding soil, traffic load, and soil pressure in descending order of the fraction of the failure causes. Thus, it is noted that large diameter steel WTMs are mainly affected by corrosion.

Also, this result is in line with the finding that pipe age and water quality (alkalinity, electoral conductivity, pH, and residual chlorine) were identified as the significant factors affecting failure in steel WTMs as described in the correlation analysis. Therefore, this finding strongly supports that water quality causes steel corrosion and ultimately deterioration in steel WTMs.

3.4.4 Application of the Outcomes

The significant factors affecting steel WTM deterioration were determined from the statistical correlation analysis method, using the various physical and water quality data set collected during 1969–2015. This result can guide water supply utilities into monitoring and collecting the identified main factors (pipe age, water alkalinity, electoral water conductivity, water pH, residual chlorine, pipe thickness, burial depth of pipes, and water temperature) for an efficient steel WTM management.

If water main breaks were accurately anticipated, water service outage, traffic congestion, and end-user inconvenience could all be minimized. To this end, a reliable prediction model is needed to make the process of water main replacement as economical as possible. In this best sense, the identified main factors can be employed to develop a computational model and contribute to improving its accuracy and reliability.

Moreover, steel pipe deterioration is extremely complicated and affected by practically various parameters in WTM systems. This study, however, provides theoretical and technical information on the causal mechanisms between steel WTM deterioration and the key factors as shown in

Figure 3.8 Mechanism model between the main factors and deterioration in steel WTMs proposed in this study

. This outcome can make water supply engineers and consultants easy to understand the scientific corrosion chemistry and failure phenomena occurring in large diameter steel WTMs.

Finally, the result can be directed to a steel WTM management guideline connected with drinking water treatment. Therefore, the findings will provide drinking water utilities practicing proactive steel WTM management with a scientific framework and operational skills to extend a service life of steel WTMs.

3.5 Conclusions and Recommendations

The statistical correlation analysis method was performed to determine the significant factors contributing to failure in steel WTMs, using the various physical and water quality data set collected during 1969–2015. In addition, the correlative mechanisms between the influential factors and failure or deterioration in steel WTMs were investigated and established by reviewing published literature on pipe deterioration. Accordingly, the following conclusions can be drawn:

- The significant factors affecting steel WTM deterioration in the research area, which were determined through the statistical correlation analysis, include pipe age, water alkalinity, electoral water conductivity, water pH, residual chlorine, pipe thickness, pipe diameter, burial depth of pipes, and water temperature. Thus, it is suggested that these parameters be monitored and collected to manage steel WTM assets efficiently.
- The results of this empirical study based on historical break records and operation data imply that water quality (alkalinity, electoral conductivity, pH, residual chlorine, pH, and water temperature) causes steel corrosion and ultimately deterioration in steel WTMs. They also present statistical evidence to support the previous theoretical and experimental studies on the relationships between water quality and steel pipe corrosion. Thus, water quality parameters must be employed to predict a service life of steel WTMs.
- It was found that water alkalinity was the primary factor amongst water quality factors, implicating that the steel corrosion of WTMs in the research site appears to be governed by water alkalinity relatively higher than other water quality parameters. This implies that alkalinity consisting of bicarbonate and carbonate plays a significant role in forming a protective carbonate film as a barrier against steel corrosion.

- This study reveals that control of water quality parameters covered by this study can help in extending a service life of large diameter steel WTMs in the study area, ultimately making it possible that water outage, traffic congestion, operational costs, and end-user inconvenience can all be minimized. It is essential that strategic directions on steel WTM management contain water quality management in DWTPs, including control of water quality such as adjustment of pH and residual chlorine in DWTPs, the addition of a corrosion inhibitor, or change of water treatment chemicals (e.g., coagulants).
- External load (traffic activities) appears to contribute to deterioration in steel WTMs to a lesser extent, unlike previous studies reporting that those factors have a relatively substantial effect on deterioration in pipes (iron, PVC, and concrete). This is thought to be because of the stronger material and mechanical properties of steel pipes. This study shows that the causes and influential factors affecting steel pipe deterioration might be different from the factors influencing deterioration in iron pipes although they are the same ferrous pipes. It was found that the main factors, causes, and characteristics of pipe breakage may vary depending on pipe materials. Thus, studies on steel pipes should be further advanced.
- Failure cause analysis based on the historical steel WTM break data highlights corrosion as the most common failure cause in large diameter steel WTMs in the research area, amounting to approximately 52%, followed by accessory deterioration, temperature expansion and constriction, water pressure, movement of the surrounding soil, traffic load, and soil pressure in descending order of the fraction of the failure causes. Thus, this result coincides with the statistical correlation analysis between break rate in steel WTMs and the factors, strongly supporting that water quality causes steel corrosion and ultimately deterioration in steel WTMs.
- Scientific failure mechanisms and causal relationships between failure in steel WTMs and the influential factors determined by statistical analysis were established. They are informative enough

for water utilities to be aware of the possible importance and effects of the factors as well as a better understanding of failure phenomena in steel WTMs.

- The primary approach to better management of steel WTM asset should be the change of the water characteristics chemically, i.e., make it less corrosive because it is not easy to manage pipelines already buried physically. The practical and feasible water quality management based on the influential factors can include: pH adjustment by chemicals (e.g., NaOH); addition of corrosion inhibitors (phosphates or silicates); introduction of selective water intake system to minimize daily or seasonal temperature variation (if the water source is a reservoir); and change of drinking water treatment chemicals into less corrosive coagulants (e.g., a pre-hydrolyzed coagulant such as poly aluminum silicate sulfate, poly aluminum hydroxy chloral silicate, and poly aluminum hydroxy chloral sulfate) and disinfectants (e.g., chloramines). Thus, it is suggested that water network asset management should be in line with drinking water treatment plant management.

Steel pipe deterioration is extremely complicated and is affected by practically various parameters in WTM systems. This study presents causal mechanisms between steel WTM deterioration and the key factors, which utilities must evaluate to mitigate failure in steel WTMs. The findings of this study are expected to help water supply engineers and consultants to broaden their understanding of failure in steel WTMs. Especially, the results are valuable because management data and historical records of steel WTMs are scarce.

3.6 Future Research Plans

It was reported that the usage of $FeCl_3$ as a coagulant was determined to be one of the crucial factors of aggravating corrosion of water distribution system, especially composed of lead. Water crisis occurred in Flint, Michigan, USA was blamed to be caused by the use of $FeCl_3$ (Olson 2016). As understood in the case of Flint's water crisis, the research is required on the effects of coagulants on pipe corrosion in water

networks. Thus, it is proposed to K-water that a study on the effect of various coagulants in DWTPs on corrosion in water networks be conducted further to extend a service life of water systems.

4 FORECASTING A BREAK RATE OF STEEL WATER TRANSMISSION PIPE USING DEEP NEURAL NETWORKS

This chapter is based on the following publications:

H. J. Jun, J. K. Park, C. H. Bae, “Deep Learning Neural Networks for Determining Replacement Timing of Steel Water Transmission Pipes,” International Journal of Neural Networks and Advanced Applications (ISSN: 2313-0563).

H. J. Jun, J. K. Park, C. H. Bae, “Deep Learning Neural Networks for Determining Replacement Timing of Steel Water Transmission Pipes,” Proceedings of the International Conference on Control, Artificial Intelligence, Robotics and Optimization, Prague, Czech Republic, May 20-22, 2017

4.1 Abstract

Water main breaks are an ongoing concern in developed nations. Large-diameter steel main transmission mains (WTMs) transport a much larger volume of water and their failure leads to even greater damages than those seen in water networks which are composed of small diameter pipes such as iron or PVC. However, there is no predictive model for large-diameter steel WTMs so that this leads to reactive maintenance on WTMs. This paper presents the established methodology to model a break rate of aging large-diameter steel WTMs based on physical and environmental factors. The model was developed in four steps: (1) set up various scenarios for predictive models, (2) determine the best Deep Neural Network (DNN) algorithm by comparing performances of three NNs (a shallow Artificial Neural Network, multiple hidden layered NN, stacked autoencoder NN), (3) bundle data into homogeneous groups by ANN-based

clustering technique, and (4) perform the developed model for each cluster. It is found that the multiple hidden layered NN is the best Deep Neural Network Algorithm in a regression field like forecasting a break rate of aging WTMs. Additionally, it is recommended that such an ANN-based clustering method should be used in predicting a more accurate breakage of aging water networks.

4.2 Introduction

4.2.1 Background

A water network consists of transmission mains and a distribution network. Transmission mains are large-diameter pipes (more than 300 mm in diameter) that transport large volumes of water, including both raw water from natural water sources destined for a treatment plant, as well as treated water en route to storage reservoirs or to smaller-diameter distribution networks connected to customers (Ji et al. 2017). Transmission mains include pipes of various diameters and compositions (steel, iron, plastics, etc.), chosen to suit the characteristics of the various regional water resources and supply systems. For example, in the United States (U.S.), relatively small-diameter iron pipes account for 57.6% of transmission mains since there are many local water supplies; this contrasts with the predominance (54%) of large-diameter steel transmission mains in the Republic of Korea (ROK) where there is a relative paucity of local water supply and a consequent reliance upon long conveyance and a multi-regional water supply system (about 5,000 km and 50 water supply facilities).

As water networks get older, water main breaks become far more likely, resulting in water service interruption, traffic disruption, and considerable inconvenience to end users. In the U.S., water main breaks occur at the high rate of 240,000 per year (EPA 2007). Accordingly, it is not surprising that the reported infrastructure grade of the United States (U.S.) in the drinking water category is “D (Poor: At Risk)”, implicating that the infrastructure is approaching the end of its service life with a high risk of failure

(American Water Works Association 2014). Similarly, in the ROK, the multi-regional water supply pipelines installed in the 1960s are experiencing increased water main breaks, as shown in Figure 1.5. If water main breaks could be accurately anticipated, water service interruption and end-user inconvenience could all be minimized. Thus, a reliable prediction model is needed to make the process of water main replacement projects as economical as possible.

4.2.2 The Ideal Predictive Model for Water Main Breaks

The ideal predictive model should address historical break data and other factors, both internal and external to the pipes themselves. Specifically, the factors affecting a service life of pipes can be categorized into three groups as follows:

- Physical factors: Pipe material, thickness, age, diameter, length, type of joints, lining and coating, vintage, traffic load, and manufacturing processes.
- Environmental factors: Soil type, soil moisture, soil load, microbes, stray electrical currents, water quality (pH, residual chlorine, dissolved oxygen, etc.).
- Operational factors: Internal water pressure, flow velocity, and operational and maintenance practices.

4.2.3 Shortcomings of Previous Predictive Models

- ***Lack of Comprehensive Factor Analysis***: Previous models have addressed physical factors such as pipe thickness and/or environmental factors such as soil characteristics. However, these studies did not address water quality factors leading internal corrosion as contributors to the failure of pipes.
- ***Limited to Small Diameter Iron and PVC Pipes***: Furthermore, previous studies have been based on small diameter water distribution networks composed of iron or PVC pipelines. No studies

have so far been conducted in developing a predictive model for steel WTMs. As WTMs transport a much larger volume of water and their failure leads to even greater damages than those seen in small diameter water main breaks, such studies are much needed. The need for studies focused on steel water mains is further underscored by the fact that extrapolation of the results of previous studies focusing on iron pipes may not be valid. This is due to the fact that iron and steel pipes are different in their composition, properties, lining and welding systems, the chemical reactions associated with their corrosion, and their failure characteristics (American Water Works Association Research Foundation 1996).

4.2.4 Artificial Intelligence-Based Predictive Models

Traditional studies have used statistical models that utilize historical break data to predict patterns. Shamir & Howard (1979) were the first to develop a regression model in which a pipe breakage is exponentially associated with its age. A comprehensive review of research conducted using the traditional statistical models can be found elsewhere (Kleiner and Rajani 2001).

The complex, multifactorial nature of WTM breaks requires a highly-sophisticated system to develop a reliable predictive model. Artificial NNs are an attractive modality for this purpose due to their impressive capacity to solve complex, real-world problems. Jafar et al. (2010) employed ANNs to predict the number of failures of water networks (composed of asbestos cement, PE, and iron) and others have used ANNs to predict failures of aging pipelines (iron or PVC) (Achim et al. 2007; Ahn et al. 2005; Al-Barqawi and Zayed 2006; Nishiyama and Filion 2014). However, studies using deep neural networks (DNNs) have not so far been used to predict WTM breaks.

A DNN is an artificial neural network (ANN) with multiple hidden layers of units between the input and output layers. Like ANNs with one hidden layer (Shallow ANNs), DNNs can model complex non-linear relationships. Additional layers allow DNNs to learn high-level features in data by using structures composed

of multiple non-linear transformations (Bengio 2009). DNNs include multi-layered NNs (MLNNs), stacked auto-encoders NNs (ANNs), deep belief networks (DBNs) and convolutional NNs (CNNs), among others.

DNNs are thought to be an ideal modality for predicting large-diameter steel WTM breaks. DNNs have already been used successfully to solve numerous complex tasks, such as character recognition and stock market predictions. Their previous success has led to the recognition of DNNs as powerful tools that can be used to predict outcomes in complex systems involving multiple parameters accurately.

4.2.5 Study Objective

In summary, the objective of the study is to develop a predictive model for large diameter steel WTM breaks by assessing the predictive performance of three NNs (shallow NN, MLNN, and Stacked Autoencoder NN) with the aid of the NN-based clustering technique for each scenario, which includes both physical factors as well as water quality factors.

4.3 Assumptions

Figure 4.1 shows the locations of monitoring water quality in WTMs of the ROK in which the pipelines in blue represent WTMs and water quality of WTMs is typically measured at a position just before raw water arrives drinking water treatment plants (DWTPs), at a place right after the whole treatment (after disinfection unit process, typically), and at a pump station. Additionally, it is not common and reasonable to measure water quality flowing inside WTMs by taking a sample from buried pipelines from the point of economic and technical view. Thus, this study assumes that the water quality is constant throughout and the water quality data measured at monitoring stations such as DWTPs and pump stations are considered as the water quality throughout WTMs.

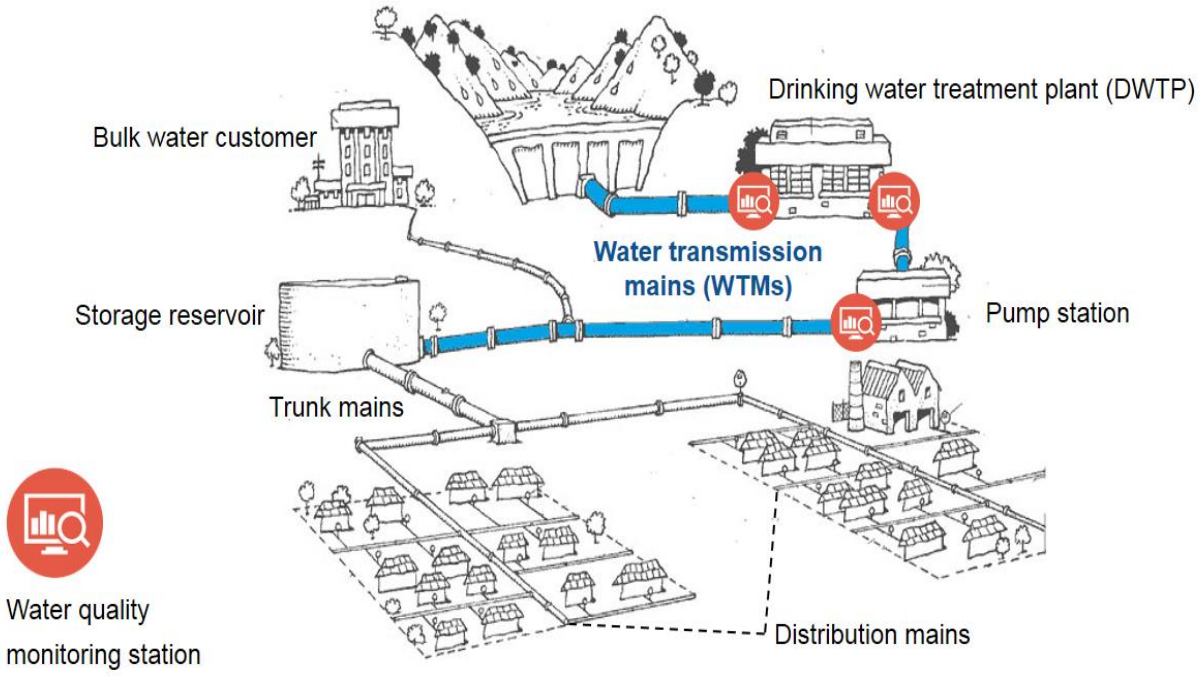

Figure 4.1. Typical locations of monitoring water quality in WTMs of the ROK

4.4 Material and Methods

Figure 4.2 describes the methodology of model development including data pretreatment, determination of significant factors affecting breaks of WTMs, comparison of DNNs, and potential improvements when employing an NN-based clustering method.

4.4.1 Data Collection

Data were obtained from the database of Korea Water Resources Corporation (K-water), which maintains 32 drinking water treatment plants and supply facilities (50% of the ROK's drinking water) as a government-owned public utility.

Data consisted of 855 historical breaks of steel WTMs over the observation period (1969 – 2015) with a total length of 2,783 km. The collected data includes pipe diameter, thickness, pipe age, coating, service type, depth of cover, traffic loading, and water quality (pH, alkalinity, dissolved oxygen, residual chlorine,

temperature, and electoral conductivity) for given variables, and break rate (number of breaks divided by total length of sectional pipelines of WTMs) for a target variable as shown in Table 3-1.

4.4.2 Determination of the Major Factors and Scenarios for Models

As described in Chapter 3, Box-Cox Power Transformations were applied to the input factors to improve normality using MINI-TAB 2017 (statistical software). Then, factors affecting a break time of steel WTMs were identified through the Pearson's correlation analysis using MINI-TAB 2017. The nine factors (pipe age, water alkalinity, electoral water conductivity, water pH, residual chlorine, pipe thickness, pipe diameter, burial depth, and water temperature) were identified as the primary factors through the work in Chapter 3.

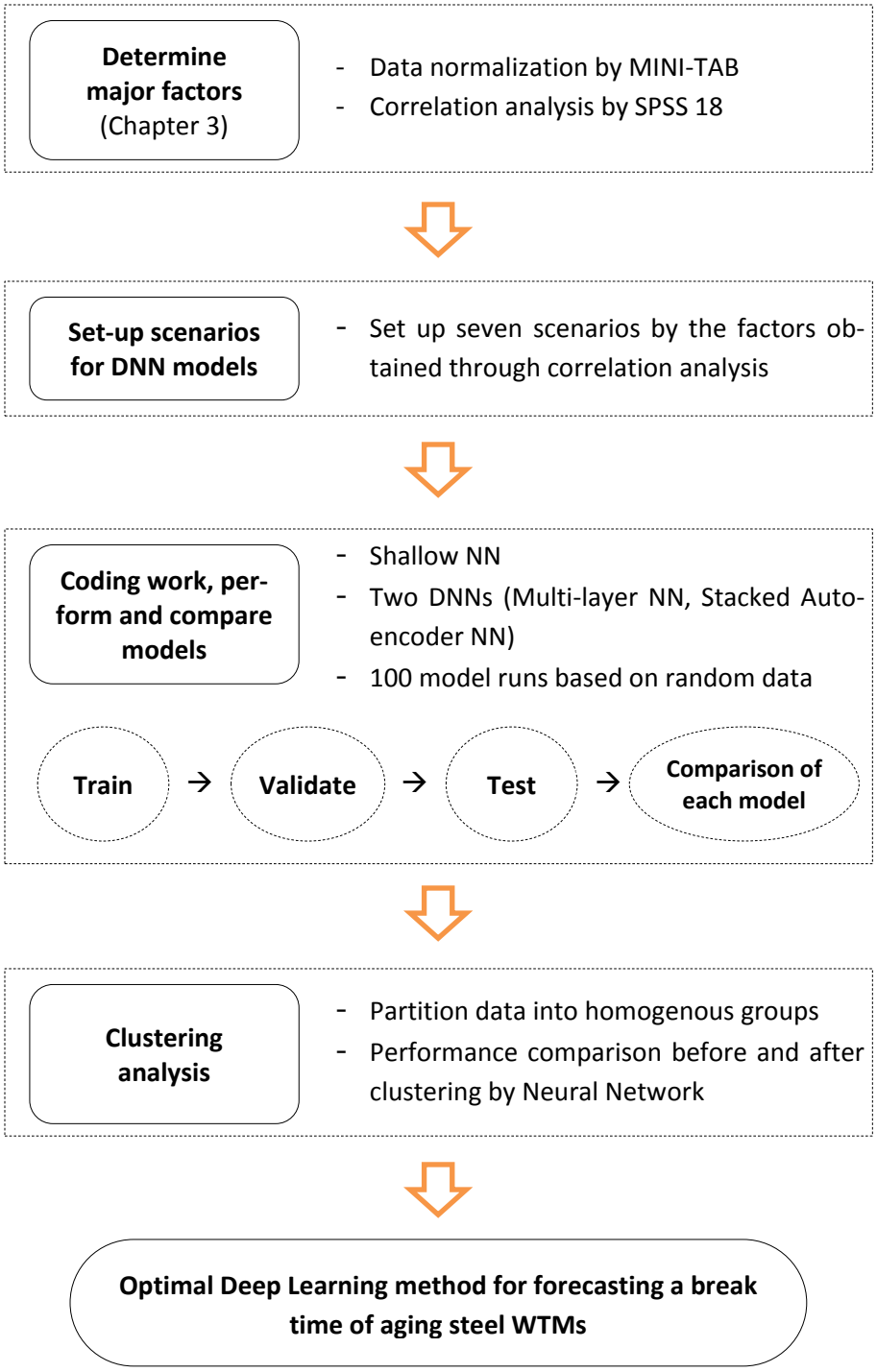

Figure 4.2. The methodology of model development

4.4.3 Construction of DNN Models

Two DNN methods (MLNNs and stacked ANNs) were used and compared with Shallow ANN to determine the optimal model. The NN Toolbox of MATLAB (Mathworks 2016) was used in all programming. Input data were randomly divided into three data sets: training (70%), validation (15%), and test dataset (15%) to build and test the model. Each model was run a hundred times using a hundred different data sets of initial random weights. The performance of each model has averaged over a hundred runs of the test data set for each scenario.

4.4.3.1 Shallow ANN and MLNN

A typical MLNN is shown in Figure 4.3. Mathematically, an MLNN with p, S1, S2, and S3 as the number of input, 1st hidden, 2nd hidden, and output nodes, respectively, is based on the following equation:

$$a_{s3}^{3} = f^{3}\left[\sum_{k=1}^{s2} w_{s3s2}^{3} \times f^{2}\left\{\sum_{j=1}^{s1} w_{s2s1}^{2} \times f^{1}\left(\sum_{i=1}^{R} w_{s1R}^{1} \times P_{R} + b_{s1}^{1}\right) + b_{s2}^{2}\right\} + b_{s3}^{3}\right] \tag{4-1}$$

where a_{s3}^{3} is the output values; P_R is the input values; w_{s1R}^{1}, w_{s2s1}^{2}, and w_{s3s2}^{3} are the weights of connections of the input layer and the first hidden layer, of the 1st hidden layer and the 2nd hidden layer, and of the 2nd hidden layer and output layer, respectively; b_{s1}^{1}, b_{s2}^{2}, and b_{s3}^{3} are the biases at the 1st hidden layer, the 2nd hidden layer, and output layer, respectively; f^{1} and f^{2} are sigmoid activation functions; and f^{3} are the linear activation functions. The used sigmoid activation function is as follows:

$$f(x) = \frac{1}{1 + e^{-x}} \tag{4-2}$$

The learning process of MLNN is based on a series of connection weight adjustments to minimize errors between the predicted and target values. Inputs are first propagated forward through each layer of the network. The process of training an NN involves tuning the values of the weights and biases of the network

to minimize the mean square error between the predicted values (a_{s3}^3) and the target values (t_{s3}). It is defined as follows:

$$Error = \frac{1}{N}\sum_{i=1}^{N}(t_{s3} - a_{s3}^3)^2 \tag{4-3}$$

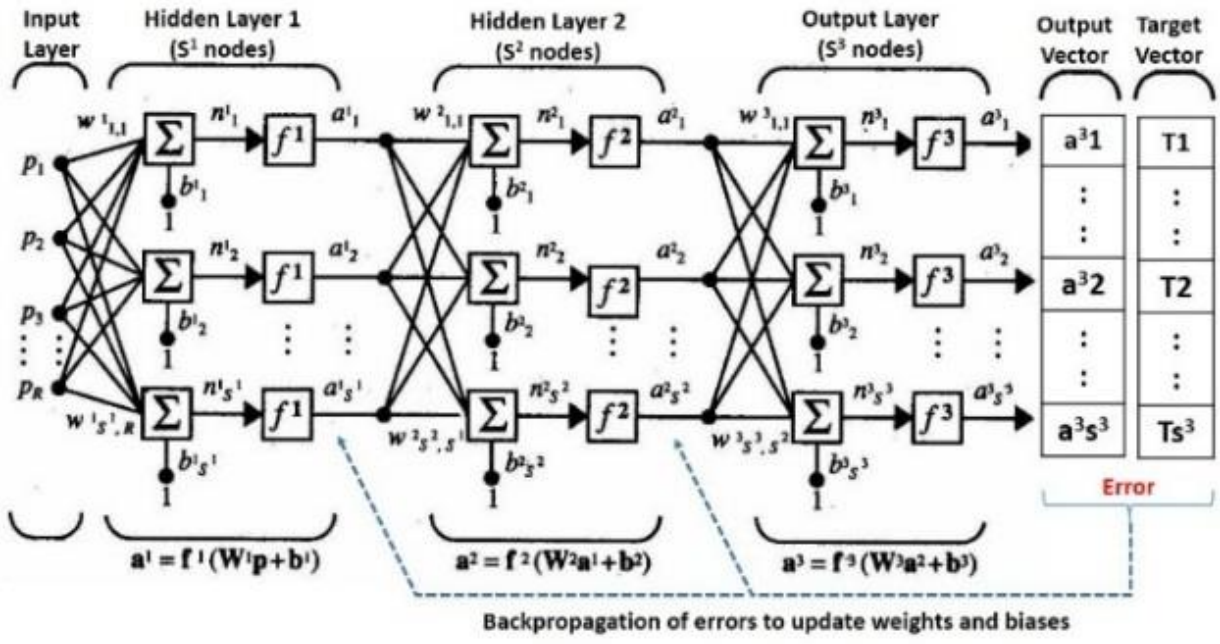

Figure 4.3. Typical multi-hidden layered Neural Networks (Sourced from (Beale et al. 2015))

A first-order iterative optimization algorithm aimed at finding a minimum in the error surface was used to perform gradient-descents in weights and biases. This process was iterated for each epoch until convergence within a given tolerance (Hagan et al. 1995).

Weights are updated using the Gradient Descent with Momentum algorithm as follows:

$$W_{i,new} = \alpha\, W_{i,old} - \eta\left(\frac{\partial E}{\partial W_i}\right) \tag{4-4}$$

where W is the weights; α is a momentum; η is a learning rate; $\partial E/\partial W$ is the gradient error function.

As the architecture for MLNN models is shown in Figure 4.4, the data (pipe diameter, thickness, age, coating, service type, depth of cover, traffic loading, water pH, water alkalinity, dissolved oxygen in water, residual chlorine, water temperature, and electoral water conductivity) depending on scenarios were used for inputs, and break rate (number of breaks divided by total length of sectional pipelines of WTMs) was used for target. The calculation procedures of Shallow ANN are the same as MLNN except for the number of hidden layers.

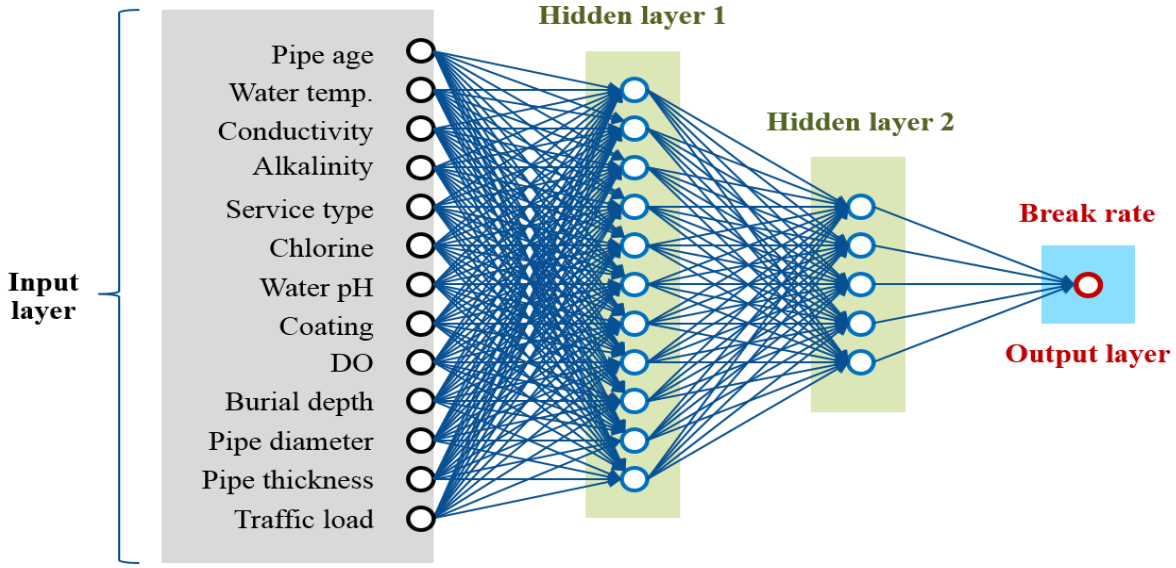

Figure 4.4. A representative architecture for MLNN models

4.4.3.2 Stacked Autoencoder Neural Network (Stacked ANN)

Stacked ANN uses an unsupervised learning method for pretraining to help to initialize network with good parameters. An autoencoder is pretrained to reconstruct the input as its output. After the pretraining, stacked ANN can run backpropagation on the entire network to finetune weights for the supervised task (Baldi 2012). Because this backpropagation starts with good weights, its credit assignment is better, and the learned model is likely to be better if backpropagation is run initially as shown in Figure 4.5 (Craven

2016). The following calculation method and procedures after the pretraining are identical to MLNN. Figure 4.6 shows a representative structure of Stacked Autoencoder NN obtained from MATLAB. The structure includes two hidden encoder layers and one output layer.

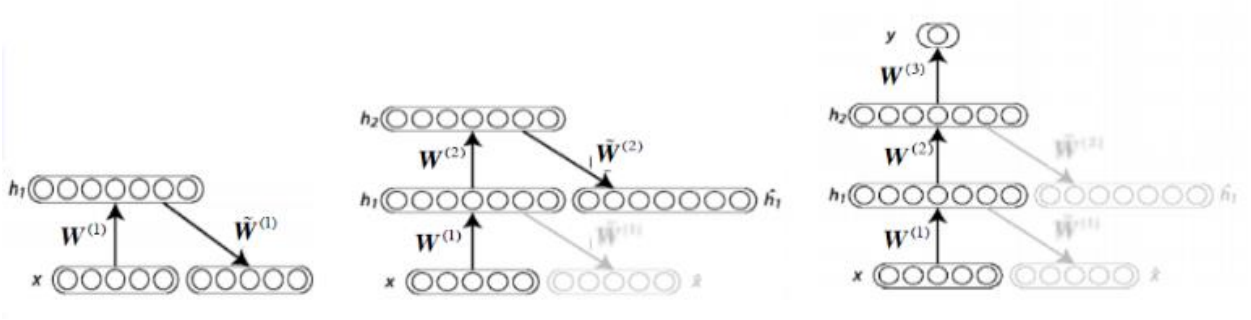

Figure 4.5. Typical Stacked ANN (Source from (Craven 2016))

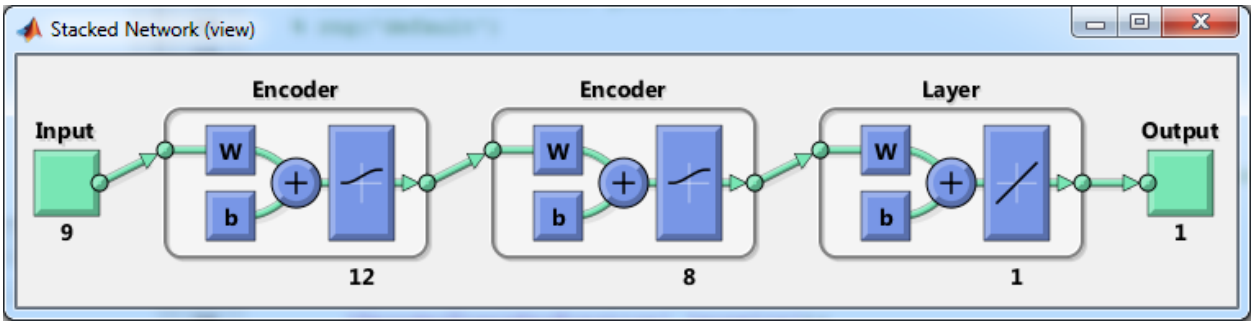

Figure 4.6. A representative architecture for Stacked Autoencoder NN models obtained from MATLAB

4.4.3.3 Overfitting Avoidance

DNNs with multiple hidden layers are powerful tools to learn complicated relationships between inputs and outputs. However, overfitting can be detrimental to such networks (Caruana et al. 2000). Early Stopping, known as an empirically better approach, was used to improve generalization of DNNs and avoid overfitting (Craven 2016). The error on the validation set is monitored during the training process. However, when the error on the validation set begins to rise, indicating they are overfitting as shown in Figure

4.7, the network returns the weights and biases, resulting in the least validation-set error (Beale et al. 2015).

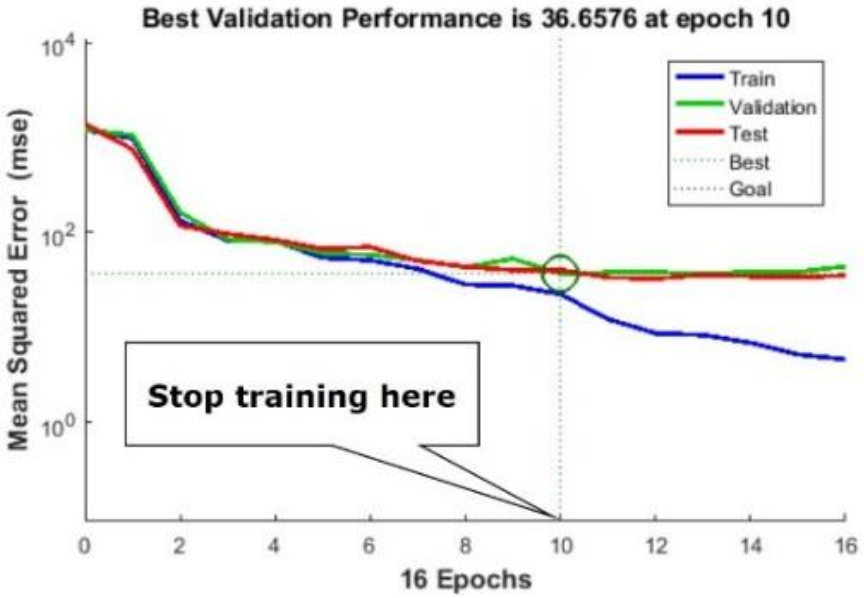

Figure 4.7. An exemplary application of the Early Stopping technique

4.4.3.4 DNNs with Clustering Analysis

A better prediction was achieved by clustering water main data into homogenous groups (Male et al. 1990). The Self-Organizing Map (SOM) is a clustering tool. Data can be automatically organized into a meaningful two-dimensional order in which similar models are closer to each other in the grid than the more different ones (Kohonen 1998). For clustering analysis, the Neural Network Toolbox of MATLAB (Mathworks 2016) was used, which is based on the Kohonen learning algorithm (Beale et al. 2015).

The SOM is trained iteratively. The topology of the Kohonen SOM network is shown in Figure 4.8. For each input (X), the Euclidean distance between inputs and all the synaptic weights is calculated as follows (Bullinaria 2004):

$$d_j(X) = \sum_{i=1}^{n} (x_i - w_{ji})^2 \quad (4\text{-}5)$$

where X is input vectors with units(xi); w_{ji} is the synaptic weights between input units *i* and the neurons *j* in the output layer; and $d_j(X)$ is the squared Euclidean distance between X and w_i for each neuron *j*.

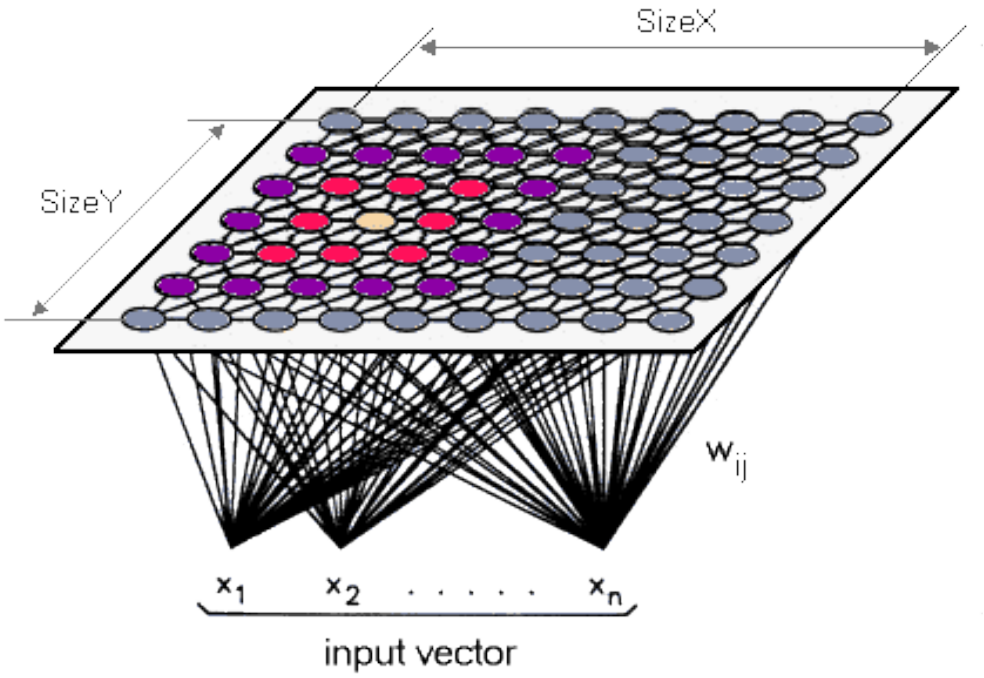

Figure 4.8. Kohonon SOM topology [Source from (SDL Component Suite 2012)]

The neuron closest to X is declared the best matching neuron I(X). After I(X) is recognized, the weights of I(X) are updated so that they are moved closer to the input vector in the input space. The vectors are updated following the Kohonen learning rule as follows (Kohonen 1998):

$$w_j(t+1) = w_j + a(t)(x_i - w_j(t)) \quad (4\text{-}6)$$

where I(X) between the I(X) and the neurons j in the output layer; t is time (epoch); α is the learning rate ($0 < a < 1$). This learning process continues until the two-dimensional output map stops changing. Eventually, the inputs are grouped into clusters (Huanga et al. 2007).

4.4.3.5 Performance measures and comparison

In this study, two commonly used errors are measured to compare the predictive performance of each model: the root-mean-squared-error (RMSE) and the mean absolute percentage error (MAPE). These accuracies are measured as follows:

$$RMSE = \sqrt{\frac{\sum(T-Y)^2}{N}} \tag{4-7}$$

$$MAPE = \frac{1}{N}\sum\left|\frac{T-Y}{T}\right| \times 100 \tag{4-8}$$

where T is the observed break rate; Y is the predicted one; and N is the number of predictions. The best model was judged by RMSE, which has been known as the standard error of the regression.

4.5 Results and Discussions

4.5.1 Application of DNNs

4.5.1.1 Setting-up Seven Scenarios for Models

The scenarios established by the factors obtained through the correlation analysis are presented in Table 4-1. It consists of seven scenarios. Scenario 1 includes all 13 factors. Scenario 2 includes pipe age, alkalinity, electoral conductivity, pH, residual chlorine, thickness, burial depth, pipe diameter, and water temperature. The input data was sequentially excluded one by one in descending order of its relativity for determining the input data for other following five scenarios.

Table 4-1. Scenarios for DNN models

Category	Factors
Scenario 1	Pipe age, alkalinity, electoral conductivity, pH, residual chlorine, pipe thickness, burial depth, pipe diameter of pipelines, water temperature, service type, coating, DO, and traffic load
Scenario 2	Pipe age, alkalinity, electoral conductivity, pH, residual chlorine, pipe thickness, burial depth of pipelines, pipe diameter, and water temperature
Scenario 3	Pipe age, alkalinity, electoral conductivity, pH, residual chlorine, pipe thickness, burial depth of pipelines, and pipe diameter
Scenario 4	Pipe age, alkalinity, electoral conductivity, pH, residual chlorine, pipe thickness, and burial depth of pipelines
Scenario 5	Pipe age, alkalinity, electoral conductivity, pH, residual chlorine, and pipe thickness
Scenario 6	Pipe age, alkalinity, electoral conductivity, pH, residual chlorine
Scenario 7	Pipe age, alkalinity, electoral conductivity, pH

4.5.1.2 Performance Comparison of Models by Scenarios

Shallow ANN, MLNN, and Stacked Autoencoder NN were performed for each scenario. Table 4-2 summarizes the performances of the models by scenarios based on the test data set, including correlations (R) and rooted mean squared errors (RMSE) in breaks per km.

Table 4-2. Performances of models by scenarios based on test data set

Scenarios		Shallow ANN	Deep NN	
			MLNN	Stacked Autoencoder NN
Scenario 1	R value	0.9461	0.9869	0.8922
	RMSE (breaks/km)	0.4709	0.2771	0.4700
Scenario 2	R value	0.9450	0.9890	0.9102
	RMSE (breaks/km)	0.5142	0.2280	0.5360
Scenario 3	R value	0.9497	0.9881	0.8902
	RMSE (breaks/km)	0.5407	0.2683	0.6117
Scenario 4	R value	0.9319	0.9481	0.9118
	RMSE (breaks/km)	0.4422	0.2516	0.6836
Scenario 5	R value	0.9258	0.9658	0.9008
	RMSE (breaks/km)	0.4402	0.2992	0.6767
Scenario 6	R value	0.9188	0.9071	0.8249
	RMSE (breaks/km)	0.7390	0.6403	0.7890
Scenario 7	R value	0.9283	0.9287	0.9039
	RMSE (breaks/km)	0.7210	0.6390	0.7974

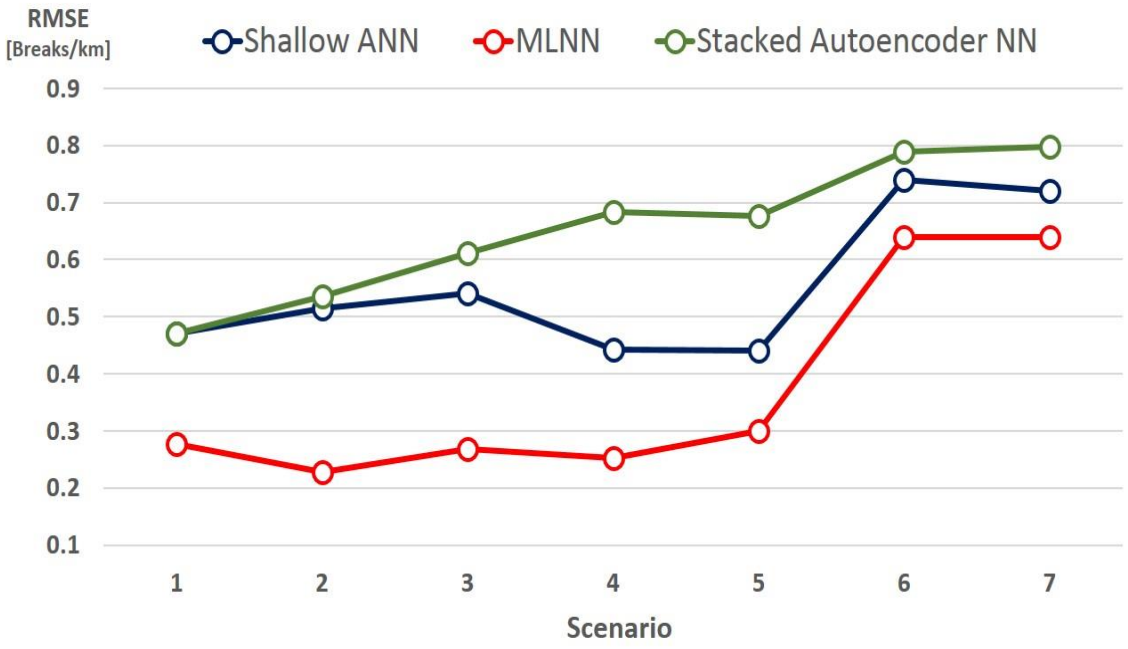

Figure 4.9. Performance comparison of models by scenarios

Figure 4.9 shows that MLNN has better accuracy with the lesser error than any other two algorithms (Shallow ANN and Stacked Autoencoder NN) across the scenarios. MLNN algorithm in Scenario 2 reveals the best forecasting performance in a break rate of steel WTMs with 0.989 in R-value and 0.2280 break/km in RMSE, respectively, amongst the seven scenarios. Also, it is observed that the predictive performances represented as RMSE of three algorithms tend to decrease as input variables decrease, notably illustrating the bigger errors at scenario 6 to 7 (i.e., four or five parameters for inputs), rather than those in the scenarios with more input parameters.

The Shallow NN algorithm appears to have the least error in scenario 5, which has six input variables (Pipe age, alkalinity, conductivity, pH, residual chlorine, and thickness) while the Stacked Autoencoder NN has a better performance in Scenario 1, which has the most input variables, implicating that it appears to be the better predictive algorithm with many input variables. However, for the most scenarios, the Stacked Autoencoder NN algorithm seems to have lower performances than the shallow NN, unlikely that DNNs

have better performances than shallow NNs in previous studies. It is important to note that each of the three NN algorithms has its critical condition (input variable) from Figure 4.9, respectively.

Thus, it can be drawn that it is essential to determine an optimal condition for each DNN because predictive performances of DNNs may vary based upon both modeling conditions such as the number of input variables and applicable fields such as regression or image recognition. In addition, it was implicated that DNNs such as the Stacked Autoencoder NN algorithm may not have a better performance in a regression field and the performance of DNNs can vary depending on applications or tasks.

4.5.1.3 Sensitivity Analysis

Each model by scenarios is verified and tested as previously described. Randomly-chosen 15% of the available data and another 15% of the data were used to validate and test each model as shown in Figure 4.10 and Figure 4.11. The performance of each model was averaged over a hundred runs with a randomly chosen data set for each scenario. Figure 4.10 depicts representative scatter plots and R values of the observed and predicted values of MLNN model for each dataset (training, validation, test, and overall) at scenario 2 in forecasting a break rate of multi-regional steel WTMs. The R-value is an indicator of the relationship between the outputs and targets. If R = 1, this indicates that there is an exact linear relationship between outputs and targets. If R is close to zero, then there is no linear relationship between outputs and targets. Figure 4.10 shows that the training data indicates a good fit and the validation and test results also show R values of greater than 0.95, suggesting that R values of the model performed on validation and test data are consistent with that of the model during learning. Also, this implicates that no significant overfitting happened during the training. This is because an error on validation data set is monitored during the training process and the network stops training, returning the weights and biases with the least validation-set error, right after the error on validation set begins to rise, implicating overfitting.

Other scatter plots and R values of the observed and predicted values of the Shallow NN and the Stacked autoencoder NN model can be referenced to in Figure 8.2 and Figure 8.3 of Appendix as well.

Figure 4.11 illustrates a representative error histogram of the observed and predicted values of the training, the validation, and the test, which were implemented in the MLNN model in scenario 2. The error histogram plot shows the distribution of the network errors, in which the blue, green and red bars signify training data, validation data, and testing data respectively. The histogram can indicate outliers, which are data where the error distribution is non-normalized, illustrating whether the data are bad. The most considerable part of data coincides with zero error line, and the errors are typically distributed implicating that the outlier data don't exist, and the model has a good fit. Consequently, Figure 4.10 and Figure 4.11 shows that the model is robust and capable to be used as a prediction tool.

For the new pipe installation, the effect of pipe age on the prediction of scenario 2 was investigated. The R-value, rooted mean square error, and percentile error of the prediction without pipe age were slightly lower than those with pipe age as shown in Table 4-3 but the prediction is anticipated to be accurate enough to use in practice.

Table 4-3. Impact of excluding pipe age on prediction

Items		**MLNN model**
With pipe age at scenario 2 (9 factors)	**R-value**	0.9890
	RMSE (breaks/km)	0.2280
	Percentile error (%)	21.32
Without pipe age at scenario 2 (8 factors)	**R-value**	0.9299
	RMSE (breaks/km)	0.2915
	Percentile error (%)	22.37

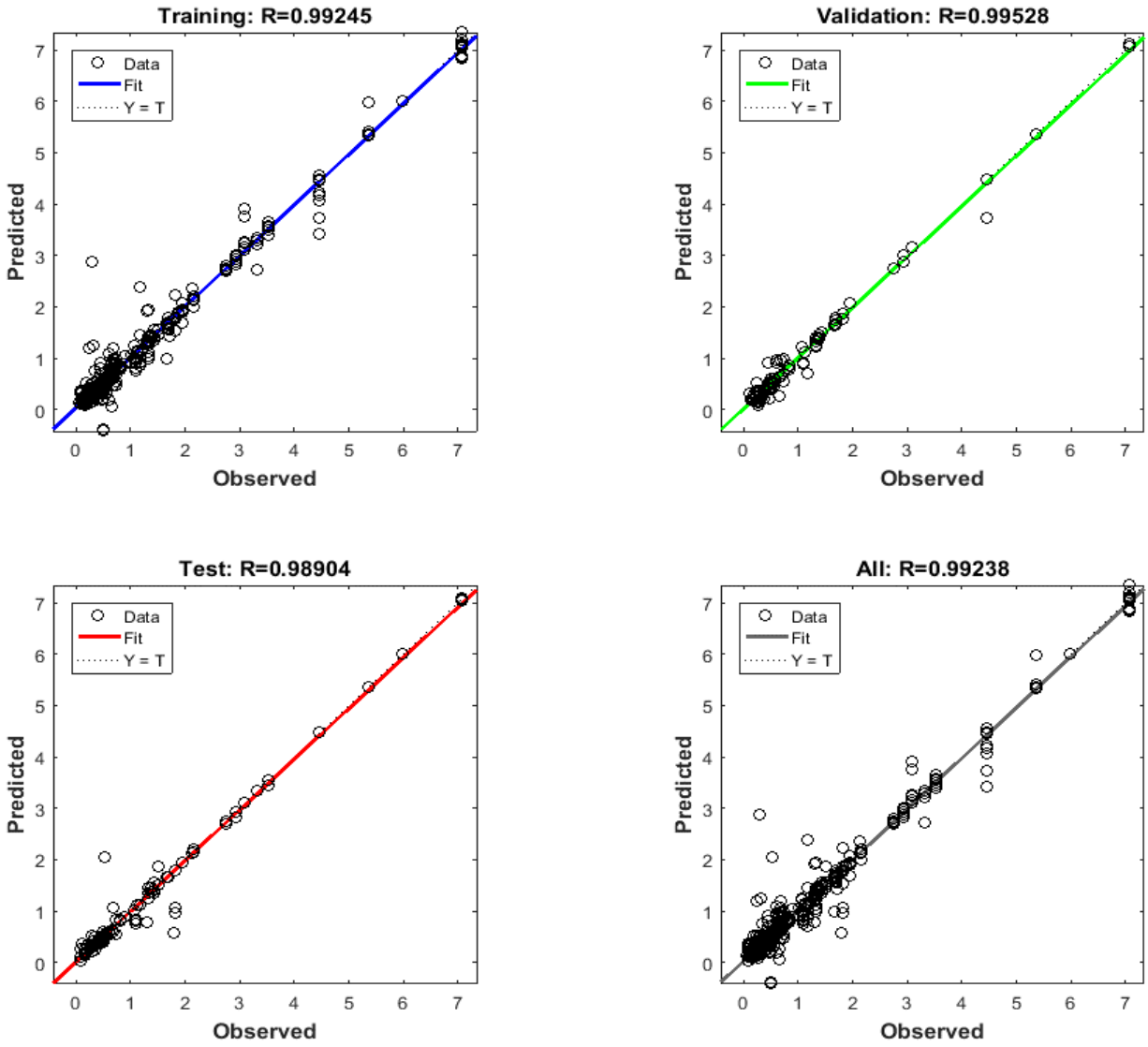

Figure 4.10. Scatter plots and R values of the observed and predicted values of the MLNN model for each dataset (training, validation, test, and overall) at scenario 2 in forecasting a break rate of multi-regional steel WTMs

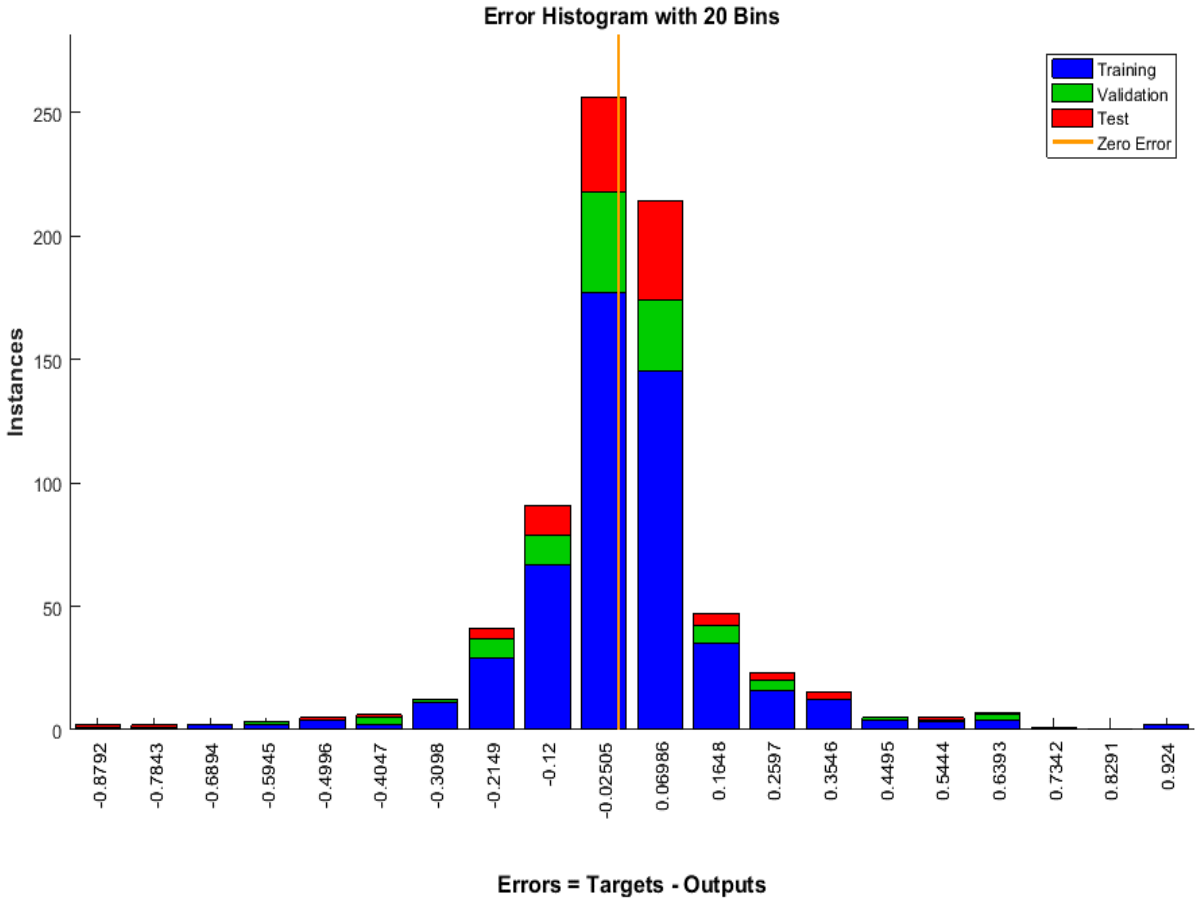

Figure 4.11. Error histogram of the observed and predicted values of the MLNN model for each dataset (training, validation, and test) at scenario 2 in forecasting a break rate of multi-regional steel WTMs

4.5.2 Clustering WTM Data by ANN

Dataset was partitioned by similarity using the SOM algorithm. Figure 4.12 shows that dataset was classified with 2D topology with 81 neurons, the red lines indicate the distances between neurons, and the darker colors represent larger distances on the SOM Neighbor Weight Distance map. The figures in the hexagonal neuron represent the number of homogeneous data on the Hits map of Figure 4.12. The SOM map shows data are clustered into three homogeneous groups.

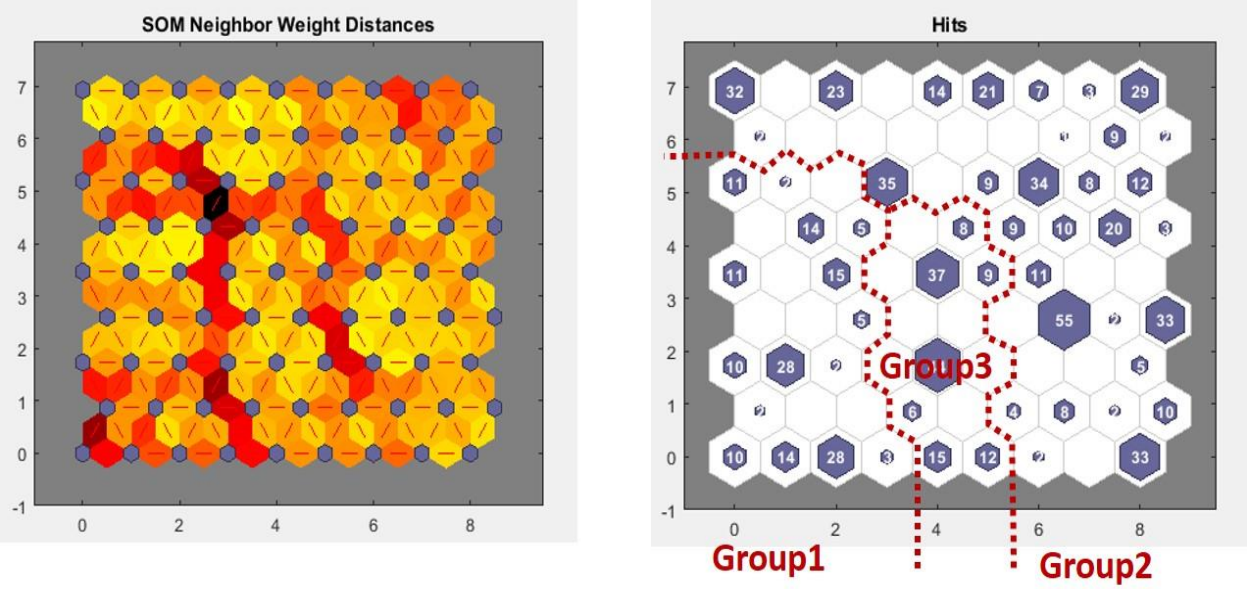

Figure 4.12. Data clustered into similar groups by Neural Network-based SOM algorithm

4.5.3 Performance Comparison Before and After Clustering

The MLNN in Scenario 2 was performed for each of three clustered groups. Table 4-4 shows the performance improvements before and after clustering by ANNs. The clustered group 1 has 0.9996 in R-value, 0.0313 breaks/km in RMSE, and 4.68% in mean absolute percentile error (MAPE). The clustered group 2 shows 0.9962 in R-value, 0.1970 breaks/km in RMSE, and 14.92% in MAPE. The clustered group 3 tells 0.9971 in R-value, 0.1939 breaks/km in RMSE, and 16.65% in MAPE. Thus, the performance for each group after partitioning into homogeneous group was improved by: 1.07%, 0.73%, and 0.83% in R values; 70.3%, 13.6%, and 15.0% in RMSE (breaks/km); and 78.0%, 30.0%, and 21.9% in MAPE, respectively.

Figure 4.13 depicts representative scatter plots and R values of the observed and predicted values of the MLNN model for each dataset (training, validation, test, and overall) of the clustered group 2 at scenario 2 in forecasting a break rate of multi-regional steel WTMs. These plots illustrate that the training, validation, and test data indicate good fits showing R values of greater than 0.99, which is higher than those before clustering. This demonstrates that R values of the validation and test data are almost precisely

consistent with that of the model during learning. Thus, any overfitting was not taken place during the training. Scatter plots of other clustered groups show similar accuracy to those of cluster 1 as depicted in Figure 8.4 and Figure 8.6 in the Appendix.

Figure 4.14 illustrates the representative scatter plots and R values of the predicted and the observed values for shallow ANN, Stacked Autoencoder NN, MLNN before clustering, and MLNN after clustering in Scenario 2 in forecasting a break rate of multi-regional steel WTMs in the ROK. When all data points in a scatter plot lie exactly along a straight dotted line, the R-value becomes 1. In the figure, the data lie more closely to the straight dotted line with higher R values from shallow ANN, to Stacked Autoencoder NN, to MLNN before clustering, and to MLNN after clustering. Notably, it can be clearly identified that nearly all data points of each gathered group are lie exactly along a straight dotted line, depicting that the clustering analysis was carried out successfully.

Table 4-4. Performance comparison before and after clustering

Groups	**MLNN for Scenario 2**		**Improvements**
	Before clustering	**After Clustering**	
Group 1 (160 data)	R value: 0.9890 RMSE (breaks/km): 0.2280 Mean Absolute Percentile error (MAPE): 21.32%	R value: 0.9996 RMSE: 0.0313 MAPE: 4.68%	1.07% ↑ 70.3% ↓ 78.0% ↓
Group 2 (589 data)		R value: 0.9962 RMSE: 0.1970 MAPE: 14.92%	0.73% ↑ 13.6% ↓ 30.0% ↓
Group 3 (131 data)		R value: 0.9971 RMSE: 0.1939 MAPE: 16.65%	0.82% ↑ 15.0% ↓ 21.9% ↓

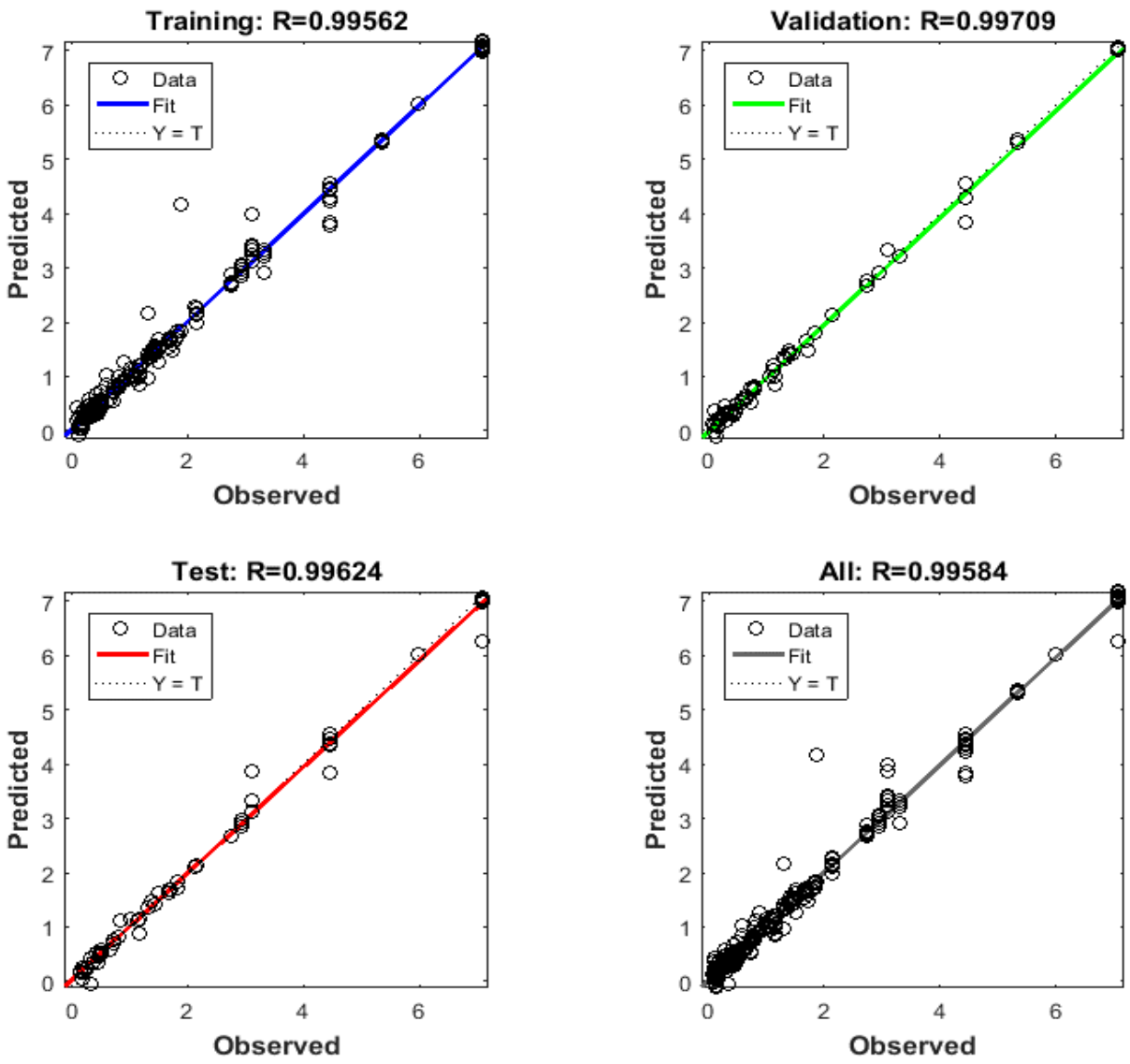

Figure 4.13. Scatter plots and R values of the observed and predicted values of the MLNN model for each dataset (training, validation, test, and overall) of the clustered group 2 at scenario 2 in forecasting a break rate of multi-regional steel WTMs

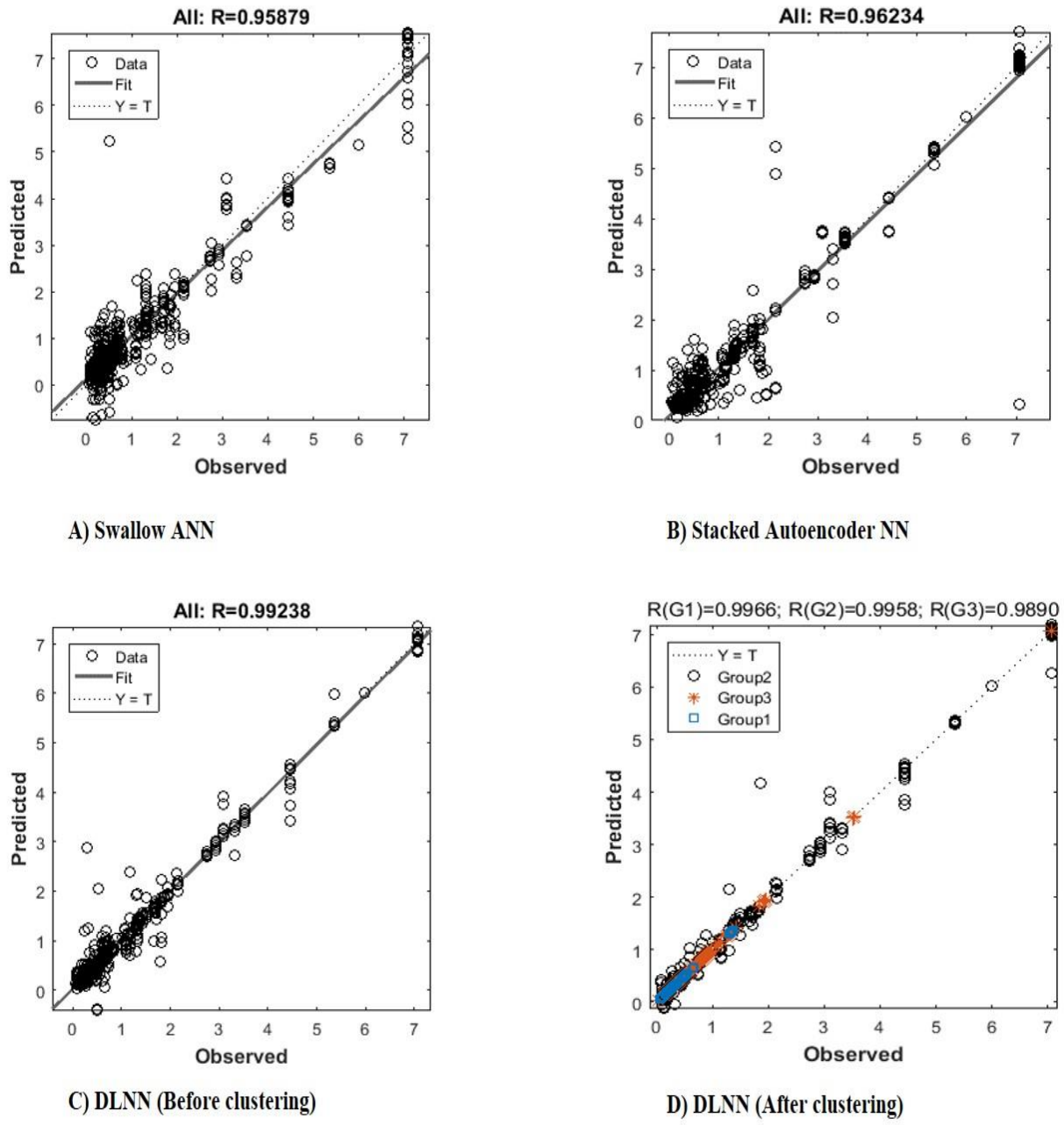

Figure 4.14. Representative scatter plots and R values of the predicted and the observed values for Shallow ANN, Stacked Autoencoder NN, MLNN before clustering, and MLNN after clustering at Scenario 2 in forecasting a break rate of multi-regional steel WTMs

4.5.4 Usefulness of the Developed MLNN Model

From the results presented in the previous sections, it can be concluded that the developed model was both reliable and robust in predicting a break rate of aging large-diameter steel WTMs. It is thought that this model can be supplemented to the "Man Entry and Visual Inspection" methodology currently in use. Specifically, if water supply engineers enter data (pipe age, water alkalinity, electoral water conductivity, water pH, residual chlorine, pipe thickness, pipe diameter, burial depth of pipes, and water temperature) for each segment of the operating WTMs, they can estimate when each of WTMs would experience their following WTM breaks. Additionally, the predictive model may be used to create better-operating conditions to extend the break time of WTMs by adjusting factors (e.g., residual chlorine) that affect WTMs deterioration.

4.6 Conclusions and Recommendations

The Shallow ANN and DNNs (MLNN and Stacked Autoencoder NN) were performed with the various physical and water quality data collected during 1969–2015 and used to forecast a break rate of large-diameter steel WTMs using statistical methods and clustering technique, as compared with each NNs. The following conclusions can be drawn:

- MLNN algorithm was found to be the best Deep NN for large diameter steel WTMs, while the Stacked Autoencoder NN appears to fit a predictive model with many input variables. MLNN had the better accuracy than the Stacked Autoencoder NN in a regression field like forecasting a break rate of aging WTMs, although the Stacked Autoencoder NN has been known as one of the most efficient Deep Learning algorithms in the areas of mainly classification and image processing.

- The optimal prediction model was established to estimate a break rate of aging large-diameter steel WTMs based on historical water main break records and available physical and environmental data using DNNs. The model was developed in four steps: (1) determine significant factors and set up scenarios for models, (2) determine the best scenario and DNN by comparing performances, (3) classify data into similar groups by ANN-based clustering technique, and (4) perform the developed model for each group.
- The SOP clustering method using ANN was applied first time to the WTM management area. The technique improved prediction accuracy significantly. It is thought to be a useful tool for clustering data. Also, such an ANN-based clustering method is recommended to be used in the field of water networks with big data.

The DNN-based predictive model proposed in this study is robust and can be used to reliably predict the first break time for aging large-diameter steel WTMs, reducing the amount of time and money spent on the direct inspection of existing WTMs and preventing unwanted water service interruption, operational costs and end-user inconvenience resulting from WTM breaks. This model is expected to benefit both drinking water consumers and water supply engineers and consultants.

5 ECONOMIC VALUATION OF AGING WATER MAIN IMPROVEMENTS

This chapter is based on the following research paper submission (amid review):

H. J. Jun, J. K. Park, C. H. Bae, "Economic Valuation of Aging Water Main Improvements," Journal of Pipeline Systems Engineering and Practice (ASCE) (ISSN: 1949-1204)

5.1 Abstract

Water main failure causes water disruption, damage and flooding of roads and buildings, the inconvenience of daily activities, and significant economic loss. There are few studies on economic valuation to justify aging water pipeline improvements. The objectives of the study were to assess benefits from aging pipeline improvements by economic valuation techniques (e.g., Damage Cost Avoided method) for intangible benefits and to develop an economic feasibility study framework on water pipeline improvement programs. A pilot test demonstrated that this economic feasibility study framework was robust and reliable. Thus, water utilities should be able to conduct economic feasibility studies successfully on aging pipelines improvements, clearly revealing hidden social benefits in monetary values. This framework will lead to practicing proactive water pipeline management to prevent costly water service outages. One of the intangible benefits, public distrust, was most significant in economic valuation on the study site, i.e., the benefit-cost ratio (BCR), followed by economic loss and future water demand. The least significant benefit was found to be sustainability improvement through the reduction of CO_2 emission.

5.2 Introduction

5.2.1 Background

As water mains age, they become far more likely to fail, resulting in water service interruption, traffic disruption, and considerable inconvenience to end users. In the United States (U.S.), water main breaks occur at the high rate of 240,000 per year (EPA 2007). Accordingly, it is not surprising that the reported infrastructure grade of the U.S. in the drinking water category is "D (Poor: At Risk)", implying that the infrastructure is approaching the end of its service life with a high risk of failure (American Water Works Association 2014). Similarly, in the Republic of Korea (ROK), the multi-regional water transmission pipelines installed in the 1960s are experiencing increased breaks. In general, the breaks of those large-diameter water transmission pipes transporting a large volume of water cause more catastrophic damages with far-reaching effects to water consumers than small-diameter based water distribution networks.

In the wake of the increased breaks, in 2015, Korea Water Resources Corporation (K-water) initiated the Aging WTM Improvement Plan (estimated at 3.3 billion USD), which replaces aging pipes and converts existing single to double-track pipelines in order to ensure the stability of the water supply. The scale of the multi-regional WTM improvement projects is so large that the economic feasibility for each project (43.7 million USD or more) must be conducted and approved by Ministry of Strategy and Finance of Republic of Korea (ROK) according to relevant statutes. However, surprisingly, a guideline or methodology on aging pipeline improvement has not been established yet, which causes their economic feasibilities to be commonly under-assessed (i.e., BCR < 1), due to their unrecognized social benefits. As a result, K-water has suffered from difficulty in justifying the need for WTM improvement projects funded by the government, such that a preventive replacement on aging WTMs has not been promoted proactively.

Thus, if a new methodology were developed to convert incalculable social benefits from aging WTM improvements into monetary values, it would be easier to justify aging WTM improvement projects, securing the economic validities in those projects to be funded, thereby, minimizing water service outages and end-user inconveniences. To this end, a novelty methodology or framework – that can valuate the hidden social benefits into dollar – is needed in order to make the process of water main replacement as economical as possible and aid in computing an economic validity (i.e., BCR > 1).

5.2.2 Previous Research

It has been reported that a variety of methodologies to estimate various intangible benefits from public services have been developed, instituted, and studied. Non-market and intangible benefits from transportation such as time savings to users or a reduction in accidents and fatalities have been estimated for the feasibility study of public transportation services (U.S. Department of Transportation 1998). The methodology to estimate the benefits such as water supply and flood damage reduction from water resources (e.g., dam) has been established to guide the feasibility studies of water resource development projects (U.S. Water Resources Council 2009). The U.S. EPA has evaluated the impacts of environmental policies and regulations on intangible benefits such as human health improvements have been estimated (U.S. EPA 2014). Economic benefits (e.g., reduction in deaths or reduced transport costs to health services) from water supply and sanitation services were estimated (Hutton et al. 2007). The benefits from avoiding water shortage through water supply facilities were valuated using the Contingent Valuation Method (CVM) by willingness-to-pay (WTP) surveys to service users (Griffin and Mjelde 2000; Koss 2001). Also, a framework for benefit-cost analysis (BCA) in water supply services was proposed, in which the methods to estimate the intangible social benefits (improved water supply service, reduced health costs associated with water quality problems, etc.) into monetary values using the CVM method were suggested (Bonnie et al. 2008).

Besides, most decision-making tools or frameworks designed to help water supply utilities to schedule or prioritize aging pipe replacement are largely based on project costs, maintenance costs, and generally, do not take into account social impacts or benefits. (Boulos 2017; Shamir and Howard 1979; Ugarelli and Di Federico 2010; Xu et al. 2013).

Furthermore, several attempts have been made to estimate the indirect and social consequences of pipe breakage. Economic impacts (repair costs, revenue losses to the water utility, economic losses suffered by customers, etc.) from water pipelines disruption resulting from earthquakes were estimated (Chang et al. 1996). The impacts of water infrastructure failures on water supply utility and society, which included legal and administrative costs, emergency repair and return to service costs, water service outage costs, traffic delay costs, health impacts, and property damages were calculated (Cromwell et al. 2002). A study on the consequences from large diameter water main breaks was carried out based on Cromwell et al's model, in which six types of the impacts including lost product costs, repair and return to service costs, supply outage and substitution costs, travel delay costs, health risk, and property damages were calculated based on 20 water main break case studies in the U.S. (Yerri 2016).

5.2.3 Gaps in Knowledge

A review of published literature on economic valuation of benefits from aging water supply pipeline improvements reveals that a comprehensive economic feasibility study framework suitable for aging pipe improvement projects has not been fully established yet and most of these studies have been limited to a small number of costs. There is a notable paucity of studies investigating the comprehensive impacts of pipe breakage including environmental aspects.

- **No Economic Feasibility Study Guideline on Pipe Improvements**: Various methods or guidelines to estimate intangible benefits from public services such as transportation or water resources developments have been established and instituted for their economic feasibility studies. Also,

previous studies tried to identify the social impacts of pipe breaks. They have not, however, advanced to a framework or guideline for an economic feasibility study suitable for aging pipes replacements or improvement projects yet. To date, no such studies have so far been conducted in developing a methodology to valuate social intangible benefits from the pipe improvements. Thus, this gap has caused a water supply utility like K-water to face difficulty in justifying the needs and budgets on aging WTM improvement projects.

- **Limited to Scheduling Decision by Replacement Costs**: Furthermore, previous studies have been based on project costs or/and maintenance when scheduling aging pipeline improvements. However, these studies did not include indirect or social costs caused by pipe breakage, although indirect costs are well known to be higher than direct costs (Yerri 2016). As a result, such improvement plans made by decisions dependent on direct costs may lead to a biased or inappropriate prioritization of aging pipeline assets due to excluded social cost to the public and inconvenience to end-users. In addition, although some research has been carried out on quantifying intangible benefits from avoiding water service shortage or disruption, they have been limited to the CVM methods based on WTP survey, which may cause a biased interpretation on economic feasibility study results.
- **Lack of Comprehensive Study on Impacts of Pipe Breakage**: Finally, previous models to estimate indirect or social consequences of pipe failure to the public did not include environmental impacts (e.g., sustainability, water quality, etc.), economic losses, and public distrust. The need for studies to develop a methodology to convert such social impacts into monetary values is further underscored by the fact that an economic feasibility study on pipe improvement projects should include social benefits to the public like the already-established feasibility study guidelines (U.S. Department of Transportation 1998; U.S. Water Resources Council 2009).

5.2.4 Study Objectives

This study offers an economic feasibility study framework suitable for aging water supply pipeline improvement projects, based on valuation methods of direct benefits to water supply utilities as well as indirect (social) benefits to the public.

In accordance with this goal, the specific objectives of this study are to:

- Establish valuation methodologies of benefits from aging pipeline improvements after deducing hidden indirect (social) impacts and subsequent consequences of pipe breakage;
- Develop an economic feasibility study framework on aging water pipeline improvements; and
- Validate the newly developed methodology by conducting a pilot test on a pipeline improvement project and comparing its economic feasibility before and after the developed methodology.

5.3 Material and Methods

Figure 5.1 describes the procedure of this study, which involves identification of the impacts (damages or costs) of pipe breakage, determination of its social benefits, establishment/development of methodologies to valuate such identified benefits, application of the methods to an aging water pipeline improvement, and sensitivity analysis.

5.3.1 Impacts of Aging WTMs to the Public

As described in Chapter 3, aging water pipelines experience water quality deterioration such as reddish water when a sudden change of internal pressure or flow loosens or breaks free built-up tubercles caused by corrosion. Also, as water network gets older, the aging pipelines become prone to breakage. Water pipe breaks lead to significant water leaking and flooding, water service outages, and emergency repair work, with each impacting the public indirectly. These indirect effects of aging pipelines and pipe breakage

on the public include bottled-water consumption, disruption in manufacturing, traffic congestion, complaints or lawsuits, property damages, piping flushing, an increase in health risk, public distrust toward water quality of tap water, etc. Eventually, these significant impacts cause water supply utilities and the public to pay for higher direct or indirect costs, which involve Repair & Return to Service costs, water substitution expense, revenue loss, environmental costs (e.g., increased CO_2 emission), traffic congestion costs, water loss, maintenance, customer service costs, liability insurance costs, health costs and public distrust costs, and so on. Figure 5.2 illustrates the direct and indirect (social) damages and costs caused by breakage and deterioration of aging water pipelines through top-down deductive reasoning.

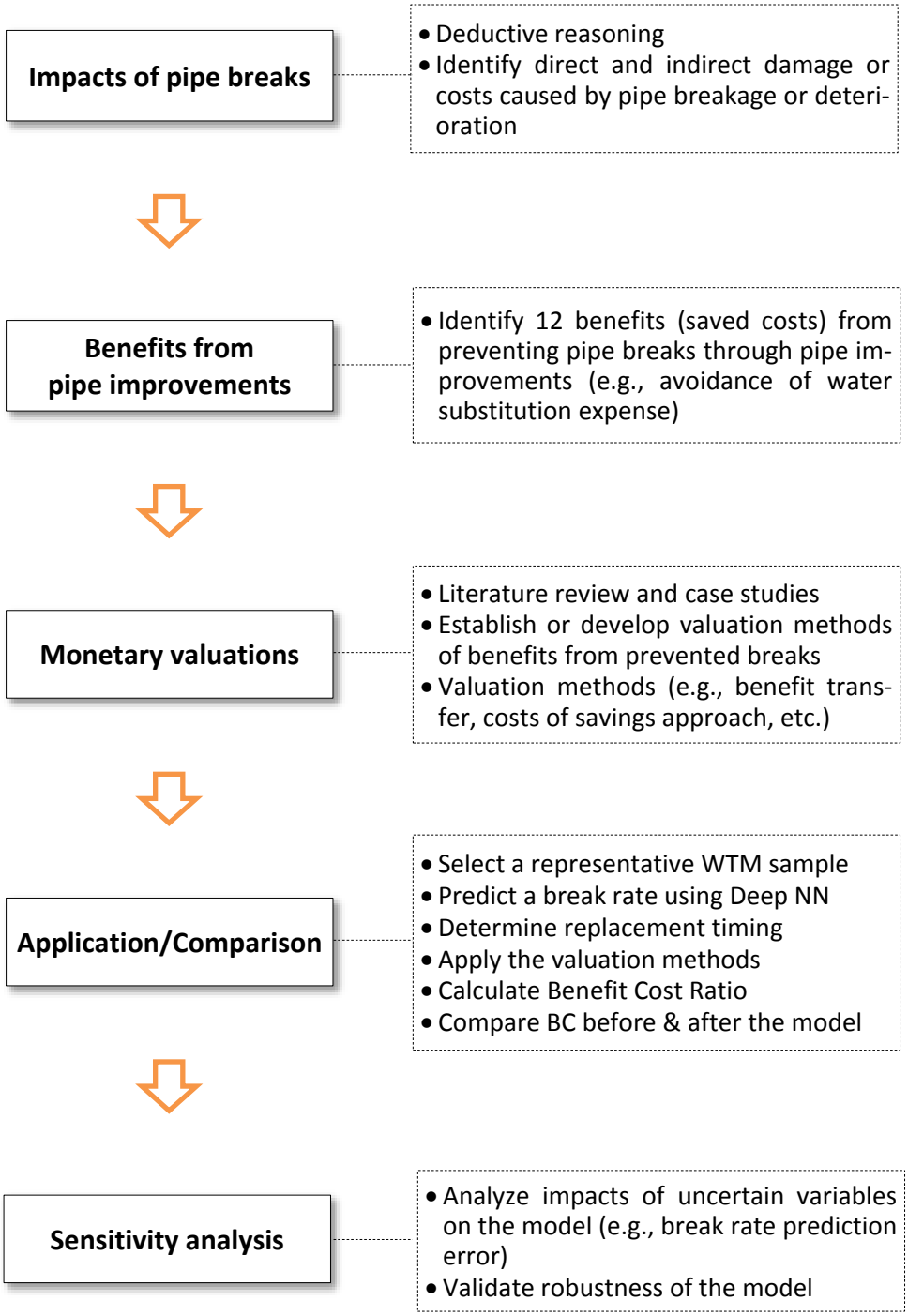

Figure 5.1. The procedure of estimation and application of the identified benefits from prevented pipe breaks through aging pipes improvements

Figure 5.2. Schematic of the damages and costs caused by breakage and deterioration of aging pipelines

Direct costs or indirect costs of water pipe breakage can be categorized in accordance with whether they are directly passed to the public or not (Yerri 2016). Specifically, direct costs are a cost paid by utilities such as lost product, repair and return to service. Indirect costs (social costs) are costs paid by the public or insurance companies, e.g., travel delay, supply outage and substitution expenses, health impact cost, and property damages.

5.3.2 Benefits from Aging Water Pipeline Improvements

Figure 5.3 shows the flowchart of conceptualizing the benefits of aging pipe improvement projects by preventing the damages and costs caused by pipe breakage that would happen without such improvement actions. The identified benefits from proactive pipeline improvement projects are categorized into direct benefits and indirect (social) benefits, according to beneficiaries as described in Table 5-1. These are the benefits that will be used to estimate monetary value in this study. To be specific, the direct benefits include savings in maintenance and operational costs, prevention of water loss, prevention of costs for emergency repair and return to service, reduction in economic losses, prevention of water quality deterioration (pipe-flushing programs), and revenue of water supply utilities by additional future water supply. The indirect benefits involve a reduction in traffic congestion, prevention of water supply outage and substitution, sustainability improvement, prevention of water quality deterioration (health risk), reduction in property damages, and reduction in public distrust costs.

While some valuation methods were introduced from literature review and case studies in similar applications (e. g., a study on estimating damages by natural disasters, a feasibility study guideline on other public services) and modified for water network application, others were developed by this study, which previous study or similar cases have not attempted yet so far. This benefit valuation study employed a variety of theoretical methods established by economists. These technical methods including a similar market price or replacement cost were applied through various approaches such as Cost Savings Approach,

Replacement Cost Approach, Market Demand Approach, and Benefit Transfer Approach as fully described in Literature Review section.

Table 5-1. Identified benefits and detailed savings from aging pipeline improvements

Benefits		Detailed savings
Direct Benefits to water utilities	Prevention of costs for emergency repair and return to service	- Costs of emergency repair work
	Prevention of water supply outage and substitution	- Water truck costs
	Prevention of water loss	- Water loss through leakage
	Reduction in maintenance and operational costs	- Intensified inspection and preventive maintenance programs - Pumping costs due to increased head loss
	Reduction in administrative and legal costs	- Administrative and legal costs caused by complaints or lawsuits
	Future extended water supply	- Revenue of water supply utilities resulted from increasing water demand
	Prevention of water quality deterioration	- Loss of water caused by pipeline flushing programs
Indirect Benefits to the public	Reduction in traffic congestion	- Traffic congestion costs (delay time, additional fuel)
	Reduction in economic losses	- Revenue losses of business water users (small commercial business customers, industrial customers)
	Sustainability improvement	- Environmental costs (air pollutants)
	Prevention of water quality deterioration	- Health risks due to exposure to waterborne infection and illness
	Reduction in property damages	- Property damages due to flooding
	Reduction in public distrust costs	- Costs of bottled-water consumption and water purifiers

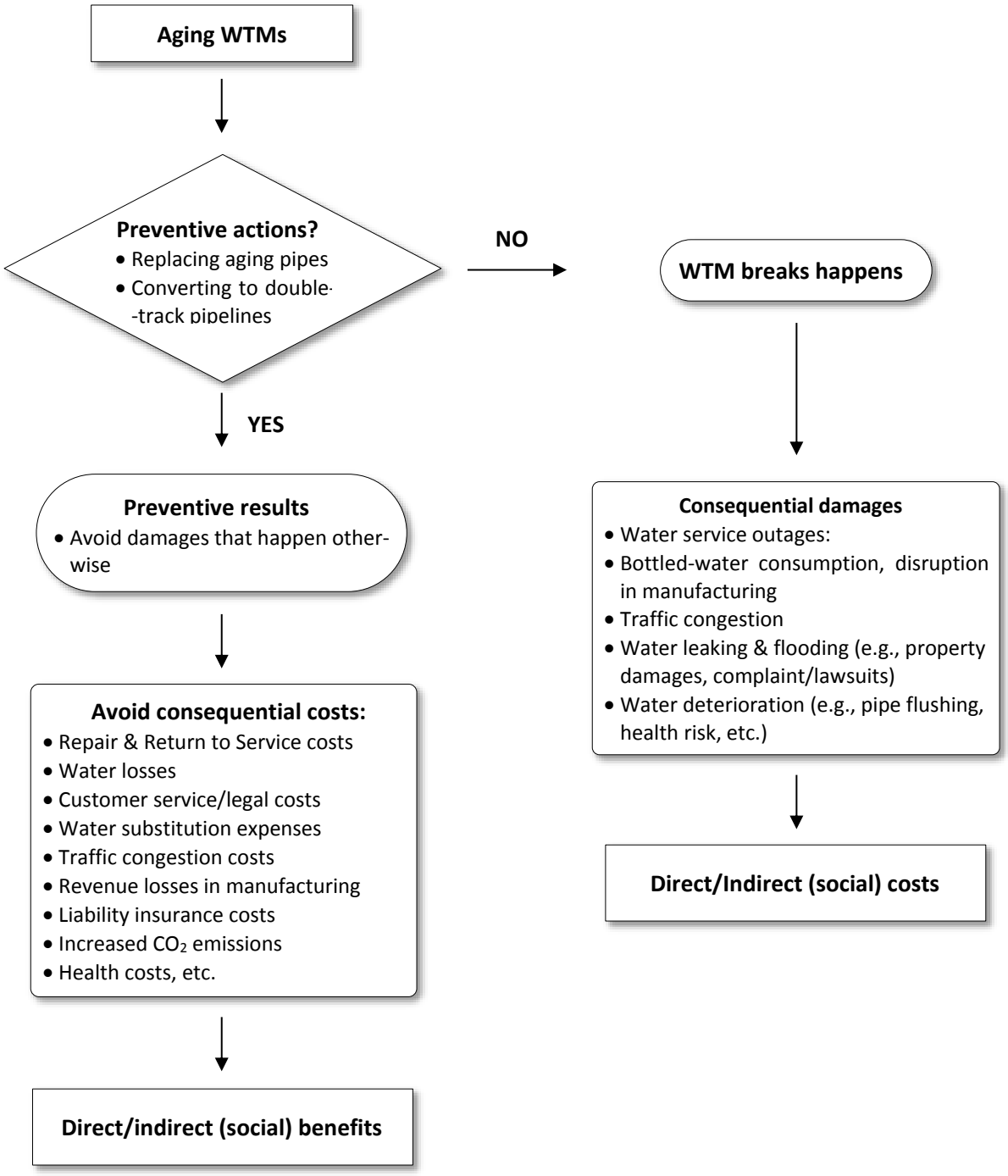

Figure 5.3. Flow chart of conceptualizing benefits of aging pipeline improvements from preventing the damages and costs caused by pipe breaks

5.3.3 Application of the Developed Valuations

The application of the established valuation methods involves forecasting a break rate of a sample pipeline chosen out of WTMs in the ROK with the aid of the Deep Neural Network model, deciding an economical service life of the pipeline, and computing the benefits from the improvement project into monetary values. Finally, the Benefit-Cost Ratios (BCRs) are calculated and compared before and after the developed valuation framework for an economic feasibility study on aging WTM improvements.

5.3.3.1 A Sample Pipeline and Assumptions for Feasibility Study

A representative large-diameter steel WTM was sampled out of the water transmission pipelines operated by K-water as depicted in red in Figure 5.4. The WTM (WTM Site D hereinafter) was installed in 1987 and its length is 23.36 km. On a daily average, 202,063 m^3/day of drinking water produced at a drinking water treatment is supplied to 479,100 people, 65,266 businesses, and two industrial complex facilities through 22 distributing reservoirs and a pumping station. Table 5-2 describes the detailed installation, customers, and operational information of WTM Site D (K-water 2018). In this study, the WTM Site D is assumed to be replaced for its improvement. The spatial boundary influenced by the benefits from the renewal project is assumed to be the water service area of the pipeline. The assumptions and calculation conditions for the application are described in Table 5-3.

5.3.3.2 Forecast a Break Rate of WTM Site D and Determine a Service Life

To predict a break rate of WTM Site D over the future years, we used the MLNN (Multiple-hidden Layered Neural Network) model developed and described in the previous chapter, with the structure composed of two hidden layers, with 12 nodes on the first layer and seven nodes on the second layer, with nine

installment and operational data elements (pipe age, alkalinity, electoral conductivity, pH, residual chlorine, pipe thickness, burial depth of pipelines, pipe diameter, and water temperature) are entered into the MLNN model as described in Table 5-2.

The “Minimum-Cost Life” analysis method was used in order to determine a replacement timing of WTM Site D. Economic service life (ESL) for a given asset is the number of years where the annual worth of the future costs is minimum, using the cost estimates for all possible years as illustrated in Figure 5.5 (Blank and Tarquin 2012).

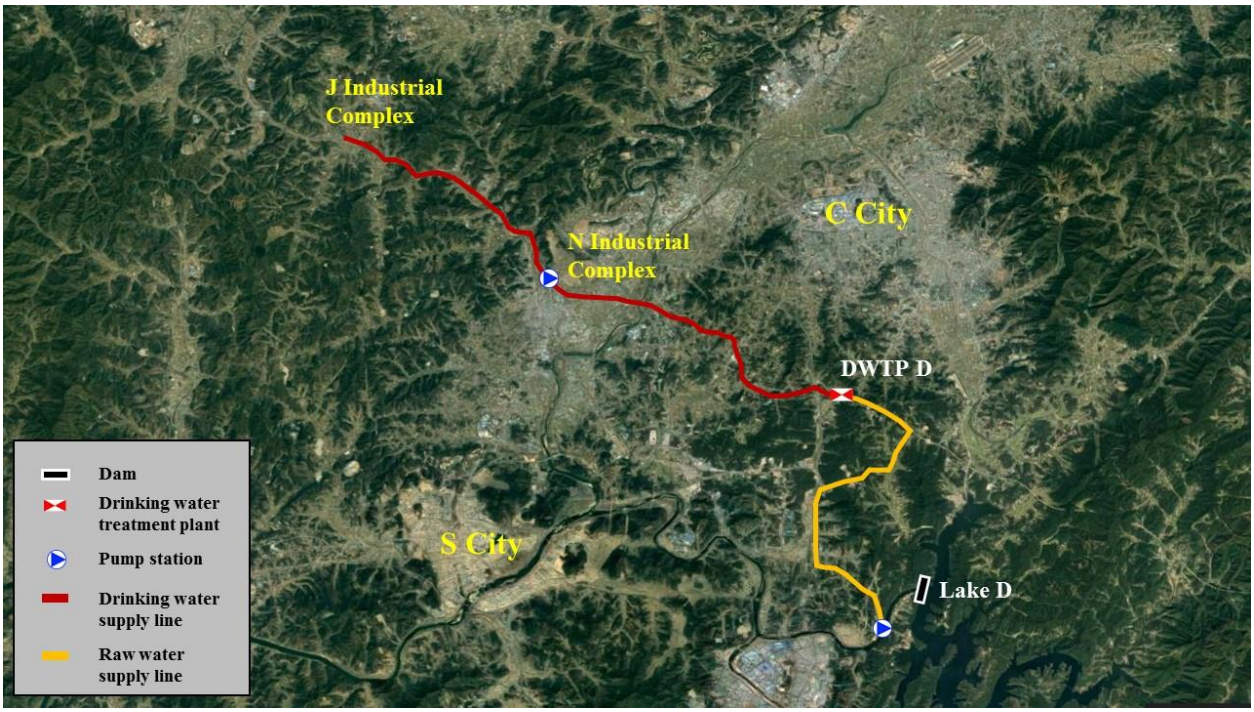

Figure 5.4. Pipeline map of the WTM Site D for an economic feasibility study

Table 5-2. Detailed installation, customers and operational information of the WTM Site D

Information specifications		Description
Installation	Age in operation	- 31 years old as of 2017
	Construction cost	- 8,600,470 USD as of 1987
	Pipeline length	- 23.36 km
	Pipe materials	- Steel
	Representative pipe diameter	- 1,100 mm
	Average burial depth	- 2.58 m
Customers and operational	Persons served	- 479,100 persons
	Average daily drinking water supplied	- 202,063 m^3/day
	The capacity of water distribution reservoirs	- 111,321 m^3/day
	Commercial businesses served	- 65,266 businesses (Ministry of Environment of the ROK 2017)
	Complex industrial facilities served	- Two complexes
	Operating water pressure	- 6 kgf/m^2
	Yearly average water quality	- pH 7.28; - Alkalinity 32.03 mg/L; - Residual chlorine 0. 8 mg/L; - Temperature 15.28°C; and - Electoral conductivity 130.19 mg/L;

Table 5-3. Assumptions and calculation conditions for the application

Details		Description
Assumptions	Normal traffic speed at the road	- 60 km/hr
	Traffic speed after WTM breaks	- 10 km/hr
	Length of the broken pipeline	- 1.0 km
	The diameter of the broken hole	- 10 cm
	Flushing duration after WTM breaks	- 4 hours
	Time elapsed between break and isolation of the broken section	- 2 hr
	Number of average complaints per break	- 1,000 complaints/break
	Duration of effort to deal with the complaints by each staff	- 0.1 hours
	Number of residential properties affected	- 10 counts/break
	Number of commercial properties affected	- 10 counts/break
	Number of vehicles affected	- 10 vehicles/break
Calculation conditions	Emergency repair work duration	- 23.94 hours (K-water 2017)
	Non-revenue water rate at normal time	- 0.5% (K-water 2017)
	The economic value of raw water for industrial water supply	- 0.51 USD/m^3 (KDI 2011)
	The economic value of settled water for industrial water supply	- 0.71 USD/m^3 (KDI 2011)
	Future residential water demand	- 10,000 m^3/day (K-water 2017)
	The infection rate of waterborne illness	- 0.0155% [0.21% (incidence rate of waterborne disease related to drinking water in the U.S) times 7.4% (distribution system-related rate out of waterborne diseases)] (Craun and Calderon 2001; Morris and Levin 1995)
	The marginal value of water for commercial business	- 4.65 USD/m^3 (KDI 2008)
	The fraction of households using a water purifier at home	- 47.6% (Ministry of Environment of ROK 2013)
	Uses of residential water purifiers	- 69% for purchase and 31% for rent (Jo 2008)
	A lifetime of a residential water purifier	- 7 years (Public Procurement Service of the ROK 2014)
	The fraction of households drinking bottled-water	- 10.3% (Ministry of Environment of ROK 2013)
	The fraction of drinking water out of average daily water use per capita	- 19.5% (Kim et al. 2008)

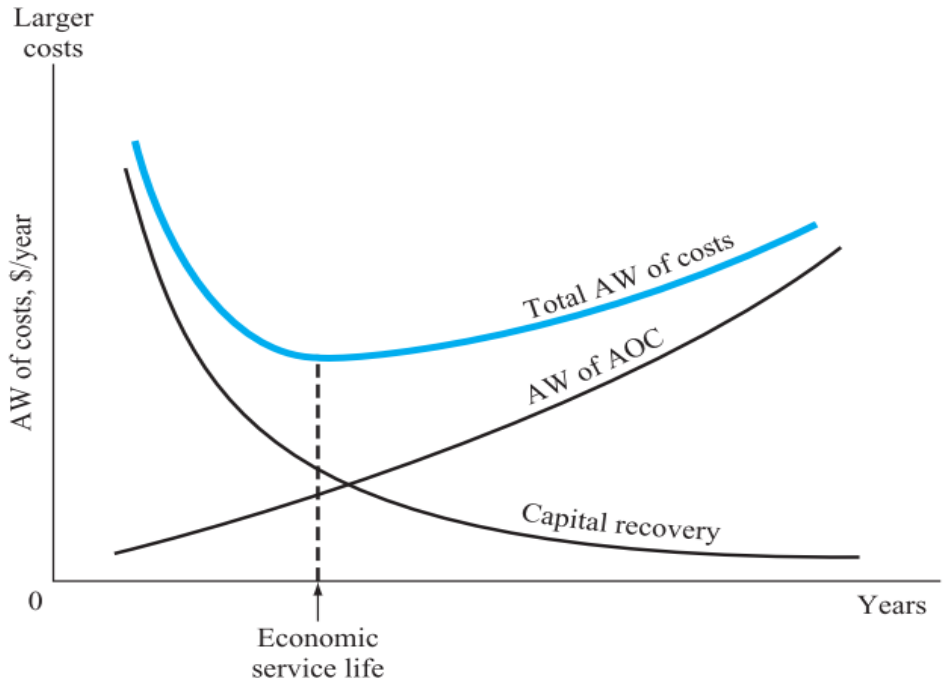

Figure 5.5. Annual worth curves of cost elements that determine the economic service life [source: Blank & Tarquin (2012)]

The ESL of WTM Site D was determined by computing the total annual worth of costs for the following 10 years when the asset is assumed to be useful. The total annual worth of costs is the sum of capital recovery, which is the sum of the annual worth of the initial capital cost (investment) and any salvage values, and the annual worth of the estimated annual future operating and maintenance costs. The equation for the total annual worth of costs over 10 years (k = 1, 2, 3, . . .) is expressed as follows (Blank and Tarquin 2012):

$$Total\ AW_k = -P(A/P, i, k) + S_k(A/F, i, k) - \left[\sum_{j=1}^{j=k} AOC_j(P/F, i, j)\right](A/P, i, k) \qquad (5\text{-}1)$$

where

P (A/P, i, k) = annualized present market value after k years at interest i, USD;

S_k (A/F, i, k) = annualized future salvage values after k years at interest i, USD; and

AOC_j (P/F, i, j) = Present values of future operating costs for year j (j = 1 to k), USD.

5.3.3.3 Economic Feasibility Study

An economic feasibility study (EFS) is carried out to determine whether an investment or decision is sound by comparing its costs with benefits (Office of Financial Management 2010). Benefit-Cost Ratios (BCR) are widely used to decide upon public sector projects, in which benefits and costs are estimated in terms of monetary values. If the ratio of the benefits to costs for a proposed project is greater than 1, indicating the benefits outweigh the costs, the investment is economically beneficial and project funding is justified (Bonnie et al. 2008).

The BCR is computed as (Office of Financial Management 2010):

$$BCR = \sum_{t=0}^{n} \frac{1}{(1+r)^t} \left(\frac{B_t}{C_t}\right) \qquad (5\text{-}2)$$

where

B_t = Benefits at year = t, USD;

C_t = Costs at year = t, USD; and

r = Discount rate, %.

5.3.4 Sensitivity Analysis

Sensitivity analysis aims to analyze how variation in independent parameters or assumptions would affect the results of the analysis. It aids in identifying the significance of variables in the decision process. The uncertain variables in this model are thought to be: the error in predicted break rates of aging pipelines, future water demand, discount rate, and the interest rate on construction loans. Thus, the sensitivity analysis was performed by letting these parameters vary by a percentile change. Table 5-4 shows the

given variable range of each parameter to measure the sensitivity of the developed valuation model. Also, the One-Way Sensitivity Analysis method was employed, in which the parameters change one at a time while holding all other variables fixed.

Table 5-4. Possible range of uncertain parameters in the developed valuation model

Parameters	Low	Base	High	Criteria
- Break rate due to prediction error (%)	-21.3%	0.0%	21.3%	Percentile error of the NN model: ±21.3%
- Future water demand (m^3/day)	8,500	10,000	11,500	Variable ratio: 15%
- Discount rate (%)	4.68%	5.50%	6.33%	
- Interest rate on construction loans (%)	2.83%	3.33%	3.83%	

5.4 Results and Discussion

5.4.1 Monetary Valuations of the Benefits from Aging Pipeline Improvements

The valuation models of the 12 identified benefits led by aging pipeline improvements were established for an economic feasibility study.

5.4.1.1 Prevention of Costs for Emergency Repair and Return to Service

When water supply pipes break, emergency repair work is needed to resume water supply service. In the case of K-water, this effort costs water supply utilities between 8,008 USD and 51,948 USD, depending on pipe diameter and pavement type over pipelines (K-water 2016). This cost is comprised of labor, material, and equipment cost. Aging pipeline improvements save the costs of emergency repair and return to service by reducing pipe breakage probability, which benefits water supply utilities. Thus, according to the Cost of Savings Approach valuation method, this benefit can be computed as:

$$B_{SR} = N_{RB} \times \sum_{i=1}^{2} \sum_{j} \{(L_{i,j} \times C_{i,j})/L_D\} \quad (5\text{-}3)$$

where

B_{SR} = Yearly benefits from cost savings of repair and return to service, USD/year;

N_{RB} = Number of reduced breaks [(BR_{BI} - BR_{AI}) × L_T], breaks/year;

BR_{BI} = Break rate before pipeline improvements, breaks/km/year;

BR_{AI} = Break rate after pipeline improvements, breaks/km/year;

L_T = Sectional length of a broken pipeline in total, km;

L_D = Length of the damaged section (= L_1 + L_2), km;

$L_{i,j}$ = Length of the damaged section by pipe diameter and by driveway type, km;

$C_{i,j}$ = Average cost of repair and return to service by pipe diameter by driveway per break [Table 8-7] (K-water, 2016), USD/break;

i = Type of roadway pavement (1: paved; 2: unpaved); and

j = Pipe diameter.

5.4.1.2 Prevention of Water Supply Outage and Substitution

In the event of water supply pipe breakages, a water supply utility may provide water tanker truck service for customers to prevent a water service outage. More specifically, the water tanker trucks convey purified water from a drinking water treatment plant to distributive reservoirs affected by pipe breaks. Otherwise, the customers are forced to purchase bottled-water to avoid water service outage hardship. Thus, the water supply outage caused by water pipe breaks can be substituted by water truck service or bottled-water. In this study, water tanker truck service is assumed to be a substitute for potable water. The cost of water service outage and substitution (USD/break) can be estimated by the products of disrupted water supply (m^3/day), water truck cost (USD/m^3), and outage duration (hours/break). Therefore, the benefits

of aging pipe improvements from preventing water outage can be computed using the Replacement Cost Approach valuation method as:

$$B_{OS} = N_{RB} \times Q_D \times OD \times C_{WT} \quad (5\text{-}4)$$

where

B_{OS} = Yearly benefit from preventing water outage and substitution costs, USD/year;

N_{RB} = Number of reduced breaks [(BR_{BI} - BR_{AI}) × L_T], breaks/year;

BR_{BI} = Break rate before aging pipeline improvements;

BR_{AI} = Break rate after aging pipeline improvements;

Q_d = Disrupted water supply, m^3/day;

OD = Outage duration [= emergency repair time – retention time of water distribution reservoirs (capacity of reservoir/daily water supply demand) + flushing duration after repair], hours/break; and

C_{WT} = Cost of water tanker truck service, 3.5 USD/m^3 (K-water 2017).

5.4.1.3 Prevention of Water Loss

Aging water pipelines experience both sudden pipe breakage as well as minor leaks that are undetected over years, i.e., a continuous leak. Pipe breakage results in a tremendous amount of treated water leaking out of the supply pipe. Additionally, produced water may be lost continuously through the continuous leaks during the normal operating period of pipelines. Thus, the total water loss throughout pipelines is computed as the sum of water lost through pipelines breaks and water lost through continuous leaks during the normal operating period.

First, the water loss throughout pipeline breaks is defined as the volume of water lost during the time elapsed between the pipe break and isolation of the failed pipeline section for emergency repair. Applying

Bernoulli's equation from a point inside the water pipe to the exit of the pipe break and assuming steady, constant density, and frictionless flow as follows:

$$\frac{P_0}{\rho} + \frac{1}{2}V_0^2 + g(0) = \frac{P_A}{\rho} + \frac{1}{2}V_E^2 + gh_E \qquad (5\text{-}5)$$

where

P_0 = Internal water pressure at the center inside of the water pipe, kgf/m^2;

V_0 = Velocity in the pipe, which can be negligible compared to V_E, m/s^2;

g (0) = Gravitational potential energy at the center inside of the pipe, m^2/s^2;

ρ = Density of water, 1,000 kg/m^3 (at 4°C);

P_A = Atmospheric pressure at the external break of the pipe, 10,332.27 kgf/m^2;

V_E = Exit velocity at the hole of the pipe, m/s^2; and

gh_E = Gravitational potential energy at the hole of the pipe, m^2/s^2.

Ignoring the slight change in gravitational potential energy over the height h_E, the above Bernoulli's equation can be simplified and solved for the exit velocity at the hole of the pipe as follows:

$$V_E = \sqrt{\frac{2(P_0 - P_A)}{\rho}} \qquad (5\text{-}6)$$

Thus, the volume of the water lost throughout pipeline breaks can be computed as follows:

$$V_B = A \times t_E \times \sqrt{\frac{2(P_0 - P_A)}{\rho}} \qquad (5\text{-}7)$$

where

V_B = Volume of water lost throughout pipeline break per break, m^3/break;

A = Surface area of the break, split or pipe burst through which water flows, m^2; and

t_E = Time elapsed between failure and isolation of the pipe section per break, hour/break.

Secondly, the water lost through the continuous leaks during the normal operating period can be calculated by multiplying yearly water products with non-revenue water rate throughout pipelines as follows:

$$V_L = V_P \times R_{NR} \quad (5\text{-}8)$$

where

V_L = Yearly water product lost throughout leakage, m^3/year;

V_P = Yearly water product, m^3/year; and

R_{NR} = Non-revenue water rate through pipelines, which can be provided from the Database of Ministry of Environment of the ROK, %.

Consequentially, using the Replacement Cost Approach valuation method, the benefit of pipeline improvements from preventing water loss can be valued as follows:

$$B_{WL} = (N_{RB} \times V_B + Q_L) \times P_W \quad (5\text{-}9)$$

where

B_{WL} = Yearly benefit from preventing water loss, USD/year;

N_{RB} = Number of reduced breaks [(BR_{BI} - BR_{AI}) × L_T], breaks/year;

V_B = Volume of water lost throughout pipe breaks, m^3/break;

Q_L = Yearly water product lost throughout continuous leaks, m^3/year; and

P_W = Price of water, USD/m^3.

5.4.1.4 Reduction in Maintenance and Operational Costs

As WTMs age over time, their maintenance costs increase because water supply utilities commonly carry out an intensified inspection or preventive maintenance programs on aging pipes as a security measure. Aging pipeline improvements play a role in reducing these maintenance costs. Annual maintenance cost can be estimated by multiplying yearly average maintenance cost per unit pipeline (USD/km/year) with

the sectional length of pipelines (km) to be replaced. Thus, using Damage Function Approach valuation method, the maintenance savings from proactive pipelines improvements can be computed as follows:

$$B_{MS} = YAM \times L_T \times P_{BCA} \quad (5\text{-}10)$$

where

B_{MS} = Benefits from maintenance savings, USD;

YAM = Yearly averaged maintenance per unit length, 243 USD/km/year (K-water 2016);

L_T = Sectional length of pipelines in total, km; and

P_{BCA} = Period for benefit-cost analysis, year.

As pipes get older, headloss increases due to scale built-up inside the pipe walls, decreasing the cross-sectional area of flow. As a result, operational costs (i.e., pumping cost) throughout water networks increase over the years. In this study, pumping cost is assumed to be an operational cost of pipelines. The operational cost (USD) can be calculated by multiplying pumping flow rate (m^3/day) with electricity price (USD/kWh) and a unit conversion constant (0.0027). Thus, using Damage Function Approach valuation method, the operational cost savings from aging pipeline improvements can be computed in accordance with Eq. *(5-11)*, based on the Hazen-Williams formula, Eq. *(5-12)* (Shaughnessy et al. 2005) and Hazen-Williams Coefficient formula by pipe age, Eq. *(5-13)* [Walski et al. (1990) cited in Kwon (2015)]. The total savings in maintenance and operational costs are a combination of the calculated maintenance savings and operational savings.

$$B_{OS} = \sum_{Y} \left(\frac{0.0027 \times Q \times \Delta h_L}{\eta_P} \times P_E\right) \quad (5\text{-}11)$$

$$h_L = 10.666\, C^{-1.85} D^{-4.87} Q^{1.85} L \quad (5\text{-}12)$$

$$C = 18.0 - 37.2 \log \frac{0.1819 + 0.0945 \times y}{D} \quad (5\text{-}13)$$

where

B_{OS} = Benefits from operational savings, USD;

Δh_L = Reduced head loss (old pipe h_L – new pipe h_L), m;

η_p = Pump efficiency;

Q = Water pumping flow rate, m^3/day;

P_E = Price of electricity per kWh, USD/kWh;

Y = Year;

h_L = Loss of head, m;

10.666 = Unit conversion constant;

C = William Hazen coefficient;

D = Pipe inner diameter, m;

Q = Water pumping flow rate, m^3/sec;

L = Pipe length, m; and

y = Pipe age, year.

5.4.1.5 Reduction in Administrative and Legal Costs

Flooding and water supply outages caused by pipe breaks result in various types of property damages (e.g., flood-damaged housings or vehicles), end user inconvenience, and economic loss such as revenue loss by a disruption in business sales or manufacturing. Various complaints or lawsuits associated with these damages and inconveniences can be filed against water supply utilities. As a result, the utilities can be subject to administrative and legal expenses to respond to these claims. The administrative and legal costs can be estimated as a combination of legal fees based on the average lawsuit payouts per failure event (USD/break) and the administrative expense calculated by multiplying average number of complaints (complaints/break) with number of customer service staff (persons), the duration of effort by each staff (hours/person/complain), and the average hourly wage rate (USD/hour).

Aging pipeline improvement projects can save these administrative and legal costs by preventing pipe breaks. Thus, using the Cost of Savings Approach valuation method, the valuation model to estimate the benefits of pipeline improvements from preventing administrative and legal costs in this study is defined as:

$$B_{LA} = N_{RB} \times (C_{LF} + N_C \times N_{CSS} \times D_{ES} \times HR) \quad (5\text{-}14)$$

where

B_{LA} = Yearly benefit from legal and administrative cost reduction, USD/year;

N_{RB} = Number of reduced breaks [$(BR_{BI} - BR_{AI}) \times L_T$], breaks/year;

BR_{BI} = Break rate before aging pipeline improvements;

BR_{AI} = Break rate after aging pipeline improvements;

C_{LF} = Cost of legal fee depending on average legal claims per break, USD/break;

N_C = Number of average complaints, complaints/break;

N_{CSS} = Number of customer services staff, persons;

D_{ES} = Duration of effort by each staff, hours/person/complaint; and

HR = Average hourly wage rate of staff, USD/hour;

5.4.1.6 Future Extended Water Supply

In general, aging pipeline improvement projects include updates on water supply network systems. Specifically, a new pipeline can be installed to meet future extended water demand such as future city expansion or a planned industrial complex. Additionally, the pipeline improvement can be in conjunction with replacing the previous pipes with a larger-diameter pipe for the regions where the water network cannot afford extended water demand. Thus, aging pipeline improvements can produce a benefit for the future extended water supply. Using Market Demand Approach and Benefit Transfer Approach valuation methods, this benefit can be computed as:

$$B_{FW} = \sum_{k} FRQ_k \times WP + \sum_{l} \sum_{m}^{3} FIQ_{l,m} \times EV \quad (5\text{-}15)$$

where

B_{FW} = Benefits from future extended water supply, USD;

FRQ_k = Future residential water demand, m^3;

WP = Water price, USD/m^3;

FIQ_M = Future industrial water demand, m^3;

EV = Economic value of industrial water supply (KDI 2011), USD/m^3;

k = Number of districts with future extended water demands;

l = Number of planned industrial complexes; and

m = Water service type (1 = raw water, 2 = settled water, and 3 = purified water).

5.4.1.7 Prevention of Water Quality Deterioration

As pipelines age, various chemical reactions form deposits and the build-up of scales accumulate on the inner surface of the old pipes, causing water quality deterioration such as reddish water under the unexpected pressure fluctuation within pipelines in operation. Customers often claim a complaint about water quality deterioration. Typically, water supply utilities are forced to flush the contaminated section of pipelines to deal with the water quality issues. This water quality recovery cost can be calculated by multiplying the number of reduced failures (failures/year) with the volume of water lost while flushing (m^3/failure) and the price of water (USD/m^3). Thus, timely aging pipeline improvements can prevent water quality deterioration through pipelines, thereby benefiting water utilities by saving the water quality recovery cost. Using Cost of Savings Approach valuation method, the benefit of aging pipeline improvements from reducing water quality recovery cost can be calculated as:

$$B_{WR} = N_{RB} \times FV \times VF \times P_W \quad (5\text{-}16)$$

where

B_{WR} = Yearly benefit from reducing water quality recovery costs, USD/year;

N_{RF} = Number of reduced water quality failures, failures/year;

FV = Flushing volume (= $\pi/4 \times \sum_k D_k^2 L_k$), m^3/failure;

D_k = Pipe inner diameter, m;

L_k = Length of sectional pipelines for each pipe diameter, m;

VF = Volume factor (i.e., the repeating number of flushing), in which five times of water as pipeline volume is assumed to be flushed to reach a proper water quality; and

P_W = Price of water, 0.27 USD/m^3 (K-water).

Also, the water quality failure throughout pipelines can put the public at risk of exposure to waterborne infection and illness (Cromwell et al. 2002). Thus, aging pipeline improvements benefit the public by reducing the health risk. It is noted that this health risk and its benefit are extremely low in modern water network systems. Nonetheless, it is included with this study for comprehensive inclusion of valuating all possible benefits from aging pipeline improvements. The health risk costs can be estimated by Cromwell's model, which are composed of lost wages and hospital expenses (Cromwell et al. 2002). In the model, the lost wages (USD/failure) is estimated by multiplying population served with risk population rate, infection ratio, the severity of illness, average hospital days, and daily wage rate. The hospital expense is calculated by multiplying population at risk, infection ratio, the severity of illness, average hospital days, and average daily hospital charge. The final health risk cost is computed by multiplying the sum of the above expenses with a probability of water supply contamination. Therefore, using Cost of Savings Approach based on the methods and the assumption of the Grand Central Model (Cromwell et al. 2002), the health risk reduction benefit can be calculated in Equation *(5-17)*. It is assumed that the number of waterborne illness outbreaks due to water quality failure follows the pattern of the predicted pipe breaks

and the inputs for health risk estimation (e.g., infection percentages, hospital days, etc.) follow the assumptions of GCM model (Cromwell et al. 2002).

$$B_{HR} = N_{RWF} \times P \times IR \times \left\{ \sum_{i}^{2} \sum_{j}^{3} (RP_i S_j HD_j) \times WR + \sum_{i}^{2} \sum_{j}^{3} (RP_i S_j HD_j HC_j) \right\} \quad (5\text{-}17)$$

where

B_{HR} = Yearly benefit from health risk reduction, USD/year;

N_{RWF} = Number of reduced water quality failures, failures/year;

P = Population affected by water quality failure, persons;

IR = Infection rate, %/failure;

RP_i = High/low risk population, %;

S_j = Severity of illness (mild/moderate/severe infection percent), %;

HD_j = Average hospital days depending on illness severity, days;

WR = Average daily wage rate, USD/day/person; and

HC_j = Average Hospital charges depending on illness severity, USD/day/person.

Finally, the total benefit from preventing water quality deterioration can be computed as the sum of the savings in water quality recovery costs and the benefit from health risk reduction.

5.4.1.8 Reduction in Traffic Congestion

In the wake of the water supply pipe breaks, a tremendous amount of water flows out onto the roadway. This is followed immediately by emergency repair work, with closing a traffic lane to repair the damaged underground pipelines. This interrupts traffic flow, thereby resulting in travel delay. The traffic congestion causes the costs of the travel time delay and the additional fuel costs (The Korea Transport Institute 2014).

Pipe failures cause the passengers in the vehicles to experience the travel time delay due to the closed lanes. Under normal conditions, passengers can reach the destination at their desired time and have an opportunity for individual economic activities to create goods. Thus, the loss of such opportunity lost due to the traffic delay can be estimated in monetary units. This cost can be estimated by multiplying repair duration (hour/break) with a delay time (hour), monetary values of time by vehicles (USD/vehicle/hour), and traffic flow (vehicles/hour) (KDI 2004). In this study, it is assumed that the duration of travel delay is equal to the duration that the water system is out of service due to the emergency repair work. Using the Benefit Transfer valuation method of Guideline for Feasibility Study on Roads and Rails, the benefit from saving the travel delay time can be computed as (KDI 2004)**:**

$$B_{TD} = N_{RB} \times D_{EF} \times DT \times \sum_{k=1}^{2} (VT_k \times Q_k) \qquad (5\text{-}18)$$

where

B_{TD} = Yearly benefit from a reduction in traffic delay, USD/year;

N_{RB} = Number of reduced breaks [$(BR_{BI} - BR_{AI}) \times L_T$], breaks/year;

BR_{BI} = Break rate before aging pipeline improvement;

BR_{AI} = Break rate after aging pipeline improvement;

L_T = Sectional length of a broken pipeline in total, km;

D_{EF} = Duration of emergency repair work [Table 8-1], hours, which includes pipe repair and road recovery, etc.;

DT = Delay time on the damaged section (normal travel time – travel time after pipe break), hours/break;

VT_k = Values of travel time per vehicles [Table 8-2], USD/vehicle/hour; and

Q_k = Traffic flow (annual average daily volume of traffic) [Table 8-3], vehicles/day.

The traffic congestion causes idling or low-speed operation of vehicles, increasing vehicular fuel consumption. The additional fuel cost can be estimated by multiplying the length of the damaged pipeline (km/break) with fuel cost per unit distance (L/km) and fuel price (USD/L) (KDI 2004). Thus, Using Benefit Transfer valuation method of Guideline for Feasibility Study on Roads and Rails, the benefit from preventing additional fuel consumption can be determined as (KDI 2004)**:**

$$B_{FC} = N_{RB} \times \sum_{k=1}^{3} \{L_D \times (FC_{k,r} - FC_{k,n}) \times FP\} \quad (5\text{-}19)$$

where

B_{FC} = Yearly benefit from preventing additional fuel consumption, USD/year;

L_D = Length of the damaged section per break, km/break;

$FC_{k,r}$ = Fuel consumption at the vehicular velocity on the damaged section [Table 8-4], L/km;

$FC_{k,n}$ = Fuel consumption at normal velocity by vehicle [Table 8-4], L/km;

FP = fuel price, USD/L; and

k = Vehicle classification (1: sedans; 2: buses; and 3: commercial trucks)

The total benefit from a reduction in traffic congestion is calculated as the sum of the benefit from a reduction in traffic delay and the benefit from preventing addition fuel consumption.

5.4.1.9 Prevention in Economic Losses

Critical water availability cutoff caused by pipe failure may leave business inactivated, thereby affecting the revenue of such business water users as small commercial business customers and complex industrial facilities (Brozovic et al. 2007).

The revenue losses of complex industrial facilities can be estimated by multiplying the average daily revenue of each enterprise (USD/day) with outage duration (hr/break) (Chang et al. 1996). Thus, using Damage Function Approach valuation method, the valuation model for avoiding the revenue loss of complex industrial facilities can be represented as (Chang et al. 1996):

$$B_{RIF} = N_{RB} \times \sum_{N} R_N \times OD \qquad (5\text{-}20)$$

where

B_{RIF} = Yearly revenue loss of complex industrial facilities, USD/year;

N_{RB} = Number of reduced breaks [(BR_{BI} - BR_{AI}) × L_T], breaks/year;

R_N = Average daily revenue per enterprise, USD/day;

OD = Outage duration, hr/break; and

N = Numbers of enterprises in complex industrial facilities.

The revenue losses of commercial business customers can be estimated by multiplying the marginal value of water for commercial business (USD/m^3) with average daily water supply to commercial business districts (m^3/day) and outage duration (hr/break)(Chang et al. 1996; KDI 2008). Therefore, using Damage Function Approach valuation method, the benefit from preventing the revenue loss of commercial business customers can be computed as (Chang et al. 1996; KDI 2008):

$$B_{RCB} = N_{RB} \times MV_W \times Q_{CB} \times OD \qquad (5\text{-}21)$$

where

B_{RCB} = Yearly revenue loss of commercial business customers, USD/year;

N_{RB} = Number of reduced breaks [(BR_{BI} - BR_{AI}) × L_T], breaks/year;

MV_W = Marginal value of water for commercial business (5,583 KRW/m^3) (KDI 2008), USD/m^3;

Q_{CB} = Disrupted water supply to commercial business districts, m^3/day; and

OD = Outage duration, hr/break.

The benefits from preventing business loss due to the failure of aging pipelines can be obtained by summing up each preventable revenue loss (for complex industrial facilities and small commercial business customers).

5.4.1.10 Sustainability Improvement

Emissions from vehicles can cause air pollution. The emitted pollutants include carbon monoxide (CO), sulfur dioxide (SO_2), hydrocarbons (HC), nitrogen oxides (NOx) and particulate matters (PM). Traffic and road conditions greatly influence the emissions of these pollutants, and when driving conditions are improved, air pollution is also reduced, improving environmental sustainability (Wallington et al. 2008). Traffic congestion causes idling or low-speed operation of vehicles, thereby increasing the emissions of air pollutants such as NOx. If traffic congestion caused by pipeline breaks can be reduced or avoided, the incremental emission of pollutants from vehicles would also be reduced and eliminated. The air pollution costs can be estimated by multiplying the length of the damaged pipeline (km/break) with air pollutant emission factors (g/km) and environmental costs per unit pollutant emissions (USD/kg) (KDI 2004). Thus, using the Benefit Transfer method from Guideline for Feasibility Study on Roads and Rails, the benefit of sustainability improvement by preventing air pollution due to traffic congestion can be computed as (KDI 2004):

$$B_{AP} = N_{RB} \times \sum_{k=1}^{3} \{L_D \times (EF_{k,r} - EF_{k,n}) \times EC\} \quad (5\text{-}22)$$

where

B_{AP} = Yearly benefit from preventing air pollution, USD/year;

N_{RB} = Number of reduced breaks [$(BR_{BI} - BR_{AI}) \times L_T$], breaks/year;

BR_{BI} = Break rate before aging pipeline improvement;

BR_{AI} = Break rate after aging pipeline improvement;

L_T = Sectional length of a broken pipeline in total, km;

L_D = Length of the damaged section per break, km/break;

$FC_{k,r}$ = Emission factors of air pollutants at the vehicular velocity on the damaged section [Table 8-5], g/km;

$FC_{k,n}$ = Emission factors of air pollutants at normal velocity by vehicle [Table 8-5], g/km;

EC = Environmental cost per unit air pollutants, USD/kg; and

k = Vehicle classification (1: sedans; 2: buses; and 3: commercial trucks)

5.4.1.11 Reduction in Property Damage

Flooding caused by pipeline breaks may damage such properties as vehicles and buildings adjacent to the pipeline breakage. Thus, aging pipeline improvements may save the property damage costs by preventing pipe breaks. In this study, the valuation of this benefit follows the COWAMB model proposed by Cromwell based on Cost of Savings Approached method and his assumptions. The model includes the damaged value of residential properties, damaged non-residential property values, and damaged vehicle values (Cromwell et al. 2002). Thus, the benefits from reducing property damage risk can be computed as:

$$B_{PD} = N_{RB} \times \{N_{RP} \times V_{RP} + N_V \times V_V + \sum_i (N_{NRP_i} \times V_{NRP_i})\} \times DP_P \quad (5\text{-}23)$$

where

B_{PD} = Yearly benefit from property damage risk reduction, USD/year;

N_{RB} = Number of reduced breaks [$(BR_{BI} - BR_{AI}) \times L_T$], breaks/year;

BR_{BI} = Break rate before aging pipeline improvements;

BR_{AI} = Break rate after aging pipeline improvements;

N_{RP} = Number of residential properties affected, counts/break;

V_{RP} = Average value of residential properties, USD/count;

N_V = Number of vehicles affected, vehicles/break;

V_V = Average value of vehicles, USD/vehicle;

N_{NRPi} = Numbers of each non-residential properties (restaurants, offices, school, hospitals, etc.) affected, counts/break;

V_{NRPi} = Average values of each non-residential properties, USD/count; and

DP_P = Damaged percentage of property, %.

5.4.1.12 Reduction in Public Distrust Costs

Reddish tap water can often be supplied to end-user customers through corroded water networks during unsteady flow (e. g., a sudden change in operating water pressure). These aesthetic concerns may create distrust in public water companies over the safety of drinking water from the tap, causing the customers to prefer using a water purifier or consuming bottled-water at home rather than drinking tap water. In this study, it is assumed that this social cost (e. g., public distrust cost) includes the cost of purchasing or renting a drinking water purifier at home and the cost of purchasing bottled water.

The cost of using water purifiers can be obtained as a combination of purchase, rent, and maintenance of a water purifier. Using Cost of Savings Approach valuation method, the valuation model of the benefit from saving the cost of using a drinking water purifier can be represented as:

$$B_{PDC} = (N_H \times f_H + N_B \times f_B) \times \left\{ f_P \times \frac{P_Y}{L_{WP}} \times APP + f_R \times (R + AMC) \times P_M \right\} \qquad (5\text{-}24)$$

where

B_{WP} = Benefits from using water purifiers, USD;

N_H = Number of households served, households;

f_H = Fraction of households using a water purifier at home, units/household;

N_B = Number of commercial businesses, businesses;

f_B= Fraction of using a water purifier at business, units/business;

f_P = Fraction of purchased water purifiers out of the total purifier being used;

f_R = Fraction of rental water purifiers ($f_R = 1 - f_P$);

P_y = Period of years for benefit-cost analysis, year;

L_{WP} = Lifetime of a water purifier, year;

APP = Average purifier price, USD/unit;

R = Average rent of a water purifier, USD/month/unit;

AMC = Average maintenance cost, USD/month/unit; and

P_m = Period of months for benefit-cost analysis, month.

Additionally, the benefit from saving the cost of bottled-water consumption can be computed as:

$$B_{BW} = N_H \times f_{BW} \times f_C \times WU \times f_{DW} \times P_d \times P_{BW} \quad (5\text{-}25)$$

where

B_{BW} = Benefits from purchasing bottled-water, USD;

N_H = Number of households served, households;

f_{BW} = Fraction of households drinking bottled-water;

f_C= Conversion factor to residential number, 4 persons/household;

WU = Average daily water use per capita, 152.6 L/day/person (Kim et al. 2008);

f_{DW} = Fraction of drinking water out of average daily water use per capita;

P_d = Period of benefit-cost analysis, days; and

P_{BW} = Price of bottled-water, USD/L.

5.4.2 Application of the Established Valuations

5.4.2.1 Forecasting a Break Rate of WTM Site D over Years

Table 5-5 presents the results obtained from forecasting a break rate of WTM Site D over the years using the MLNN (Multi-layered NN) model developed in Chapter 4. Also, Figure 5.6 depicts the predicted break rate of WTM Site D in black line with the error interval of 21.3% in red-dotted line over the years, implicating that the break rate increases non-linearly over the years.

Table 5-5. Predicted break rates of the WTM Site D over the years

Year	Simulated break rate (breaks/km)	Year	Simulated break rate (breaks/km)	Year	Simulated break rate (breaks/km)
2019 (Year 1)	0.110	**2034 (Year 16)**	0.754	**2049 (Year 31)**	2.357
2020 (Year 2)	0.119	**2035 (Year 17)**	0.882	**2050 (Year 32)**	2.371
2021 (Year 3)	0.131	**2036 (Year 18)**	1.025	**2051 (Year 33)**	2.384
2022 (Year 4)	0.144	**2037 (Year 19)**	1.179	**2052 (Year 34)**	2.397
2023 (Year 5)	0.160	**2038 (Year 20)**	1.341	**2053 (Year 35)**	2.416
2024 (Year 6)	0.180	**2039 (Year 21)**	1.504	**2054 (Year 36)**	2.442
2025 (Year 7)	0.202	**2040 (Year 22)**	1.661	**2055 (Year 37)**	2.482
2026 (Year 8)	0.229	**2041 (Year 23)**	1.808	**2056 (Year 38)**	2.538
2027 (Year 9)	0.261	**2042 (Year 24)**	1.938	**2057 (Year 39)**	2.616
2028 (Year 10)	0.299	**2043 (Year 25)**	2.050	**2058 (Year 40)**	2.724
2029 (Year 11)	0.345	**2044 (Year 26)**	2.142	**2059 (Year 41)**	2.866
2030 (Year 12)	0.401	**2045 (Year 27)**	2.214	**2060 (Year 42)**	3.053
2031 (Year 13)	0.467	**2046 (Year 28)**	2.269	**2061 (Year 43)**	3.291
2032 (Year 14)	0.547	**2047 (Year 29)**	2.309	**2062 (Year 44)**	3.588
2033 (Year 15)	0.643	**2048 (Year 30)**	2.337	**2063 (Year 45)**	3.953

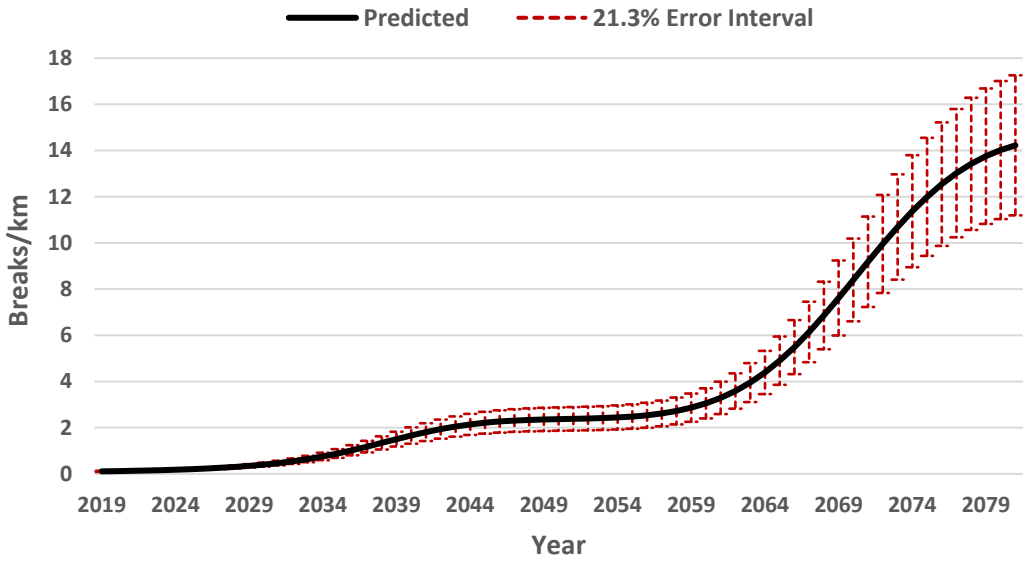

Figure 5.6. Predicted break rate of the WTM Site D over the years

5.4.2.2 Deciding Appropriate Replacement Timing of WTM Site D

The ESL of WTM Site D was estimated with "Minimum-Cost Life" analysis method to decide appropriate replacement timing of the pipeline. The analysis method requires the current book value, future book values, and operating and maintenance costs of WTM Site D over the analysis period (10 years). The book value of WTM Site D as of 2018 is 7,776,016 USD (K-water 2018) and the future book worth of the pipeline was computed based on the annual depreciation rate (2%), according to Economic Feasibility Study Guideline of KDI in the ROK. The annual operating costs of WTM Site D were obtained as the sum of the direct costs to a water supply utility, which involves costs of emergency repair and return to service, costs of water supply outage and substitution, water loss, maintenance, administrative and legal costs, and water recovery costs based on a predicted break rate for each year, using the developed valuation methodology. Table 5-6 shows the future book values and the annual operating costs of WTM Site D based on the predicted break rates over the analysis period.

Table 5-6. Future book values and the annual operating costs of the WTM Site D based on the predicted break rates over the analysis period

Year	Future book values (USD)	Annual operating costs (USD)
2019	7,366,752	192,286
2020	6,957,488	212,035
2021	6,548,224	233,728
2022	6,138,960	257,999
2023	5,729,696	285,740
2024	5,320,432	318,181
2025	4,911,168	356,956
2026	4,501,904	404,141
2027	4,092,640	462,217
2028	3,683,376	533,909

Also, the interest rate of 5.5% was assumed to compute the annual worth, which is composed of the capital recovery costs (the annual worth of the sum of opportunity costs and salvage values) of WTM Site D. The curves of annual worth, capital recovery cost, and annual operating cost of WTM Site D over the years are plotted in Figure 5.7 using Equation *(5-1)* for each year. These plots visualize that WTM Site D has the minimum total annual worth in 2021, at which time the pipeline needs to be replaced based upon economic considerations.

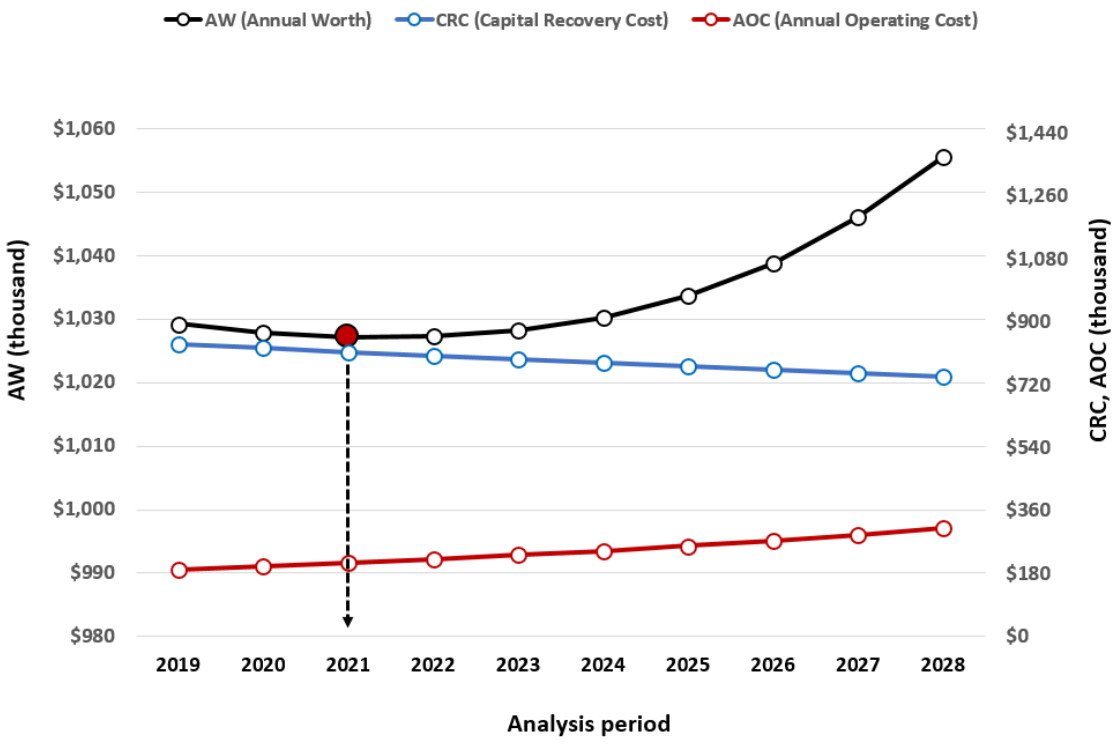

Figure 5.7. Plots of annual worth, capital recovery cost, and annual operating cost during the analysis period

5.4.2.3 Benefit-Cost Analysis

To compute the BCRs of WTM Site D improvement project, preventable breaks by the project were estimated, followed by the project cost measurement, followed by calculating the benefits from the project and followed by its BCR calculation.

5.4.2.3.1 Preventable Break Rate Estimation of WTM Site D by Improvement Project

Each model in this study to convert the intangible benefits from aging WTM improvements into monetary values is based on how many pipeline breaks would be avoided by a proposed WTM improvement project. Thus, in this study, an avoidable break rate over the years by the project for WTM Site D improvement

was computed by subtracting the predicted break rates with the project from the predicted ones without the project for each year, using the MLNN model as depicted in Figure 5.8, in which the diagonal stripes-patterned area implicates the preventable break rate by the improvement project.

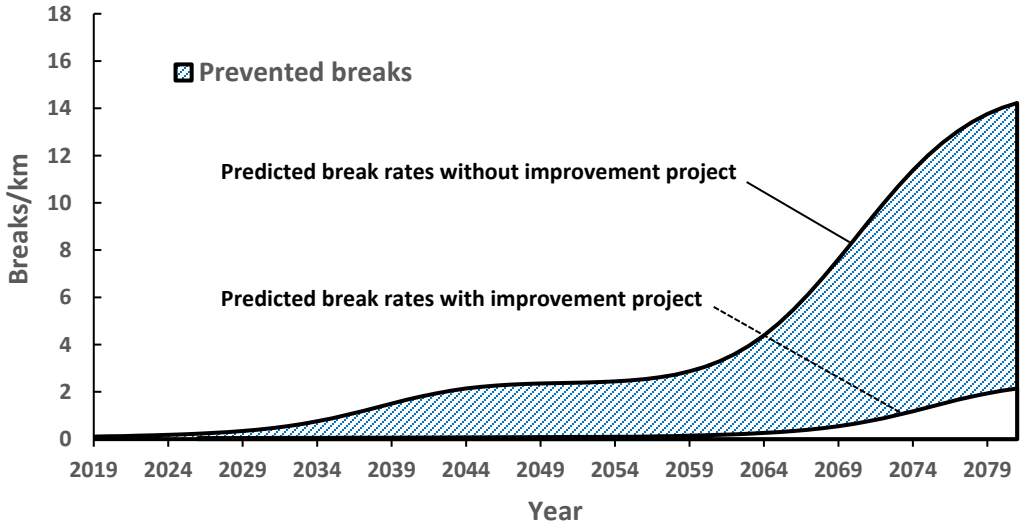

Figure 5.8. Preventable break rates resulted from the project for the WTM Site D improvement

5.4.2.3.2 Cost Measurement of WTM Improvement Project

In this study, aging WTM Site D is assumed to be replaced with a new pipeline. The project cost consists of purchased pipes, installation (unloading, welding, trenching, and backfilling, etc.), survey, design, and other construction expenses. The total project cost was estimated as 40,939,894 USD shown in Table 5-7.

Table 5-7. Details of the project cost for the WTM Site D improvement (K-water 2018)

Details	Cost (USD)
Purchased pipes (23.36 km)	17,289,950
Installation (unload, welding, trench/backfill, etc.)	14,309,328
Survey, design, and construction expenses	8,021,252
Finance interest cost (3.33%)	1,319,364
Total project cost	**40,939,894**

5.4.2.3.3 Valuation of Benefits from WTM Site D Improvement Project

Using the valuation methodologies developed or established by this study, the estimated benefits from the project for WTM Site D improvement involve prevention of costs for emergency repair and return to service, prevention of water supply outage and substitution, prevention of water loss, reduction in maintenance and operating costs, reduction in administrative and legal costs, future extended water supply, prevention of water quality deterioration, reduction in traffic congestion, prevention of economic losses, sustainability improvement, reduction in property damage, and reduction in public distrust costs.

The improvement project for WTM Site D (23.36 km) was assumed to be conducted for 4 years (2021 – 2024). The benefits would be taken into effect following 2024, the completion year of the project. Thus, the benefits from the project were computed during 2024 and 2053 (30 years) according to the relevant act (State Owned Corporation Act 2017). The discount rate of 5.5% was applied to the conversion of all benefit values estimated over the future years to the present value (KDI 2008).

Table 5-8 summarizes the result of the computed benefits from WTM Site D improvement project during the analysis period (30 years), using the developed valuation methodology on water supply networks improvement. The result indicates the total benefits during the analysis period amounted to $8,732,252,737 and $4,095,304,815 (net present worth as of 2018) at the discount rate of 5.5%. The unexpected finding

is that the benefit from public distrust reduction accounts for 98.68% of the total benefits, implicating that such a social cost as public distrust costs caused by not drinking tap water (i.e., using a drinking water purifier and drinking bottled-water) in the ROK is remarkably expensive compared to other costs. Since this study includes public distrust cost consisting of the costs of drinking bottled water and using purifiers at home, this result seems to come from a low percentage (1.3%) of drinking the water directly from the tap water in the ROK due to mistrust of the tap water safety, compared to other countries (e.g., 46% of the U.S.) (Ministry of Environment of ROK 2013; Sebastian et al. 2011). Therefore, this benefit can vary depending on nations and their portion of drinking tap water. For the case of the U.S. where the rate of drinking tap water is 61%, the BCR decreased to 22.7.

The second most significant benefit was the prevention of economic losses, followed by future extended water supply, reduction in property damage, prevention of water supply outage and substitution costs, savings in water loss, prevention of costs for emergency repair and return to service, reduction in administrative and legal costs, reduction in operational and maintenance costs, and reduction in traffic congestion. The least significant benefit was sustainability improvement reducing air pollution such as CO_2 in monetary terms. In addition, Figure 5.9 illustrates benefit distribution of the project except for the benefit from public distrust costs to break down each contribution of other components to the benefits more closely, as the benefit from public distrust costs is such a high percentage of the total benefits as to overshadow the other factors which we wish to compare.

Table 5-8. Results of the computed benefits from the WTM Site D improvement project for 30 years

Benefits	Benefits, USD	Benefits (Present worth), USD	Ratio, %
Reduction in traffic congestion	201,106	105,061	0.00%
Reduction in water loss	3,234,812	1,576,677	0.04%
Sustainability improvement	17	16	0.00%
Repair cost savings	1,222,390	638,593	0.02%
Savings in outage substitution costs	14,960,561	7,815,596	0.21%
Prevention of economic losses	37,981,809	19,842,202	0.47%
Savings in O & M	320,422	150,607	0.00%
Reduction in public distrust costs	8,619,814,744	4,041,231,965	98.68%
Future water demand	29,528,500	14,305,323	0.35%
Prevention of water quality deterio-ration	4,545,589	2,374,676	0.06%
Reduction in property damage	17,857,392	6,482,437	0.16%
Reduction in legal and complaints	1,243,754	624,527	0.02%
SUM	**8,732,252,737**	**4,095,304,815**	100.0%

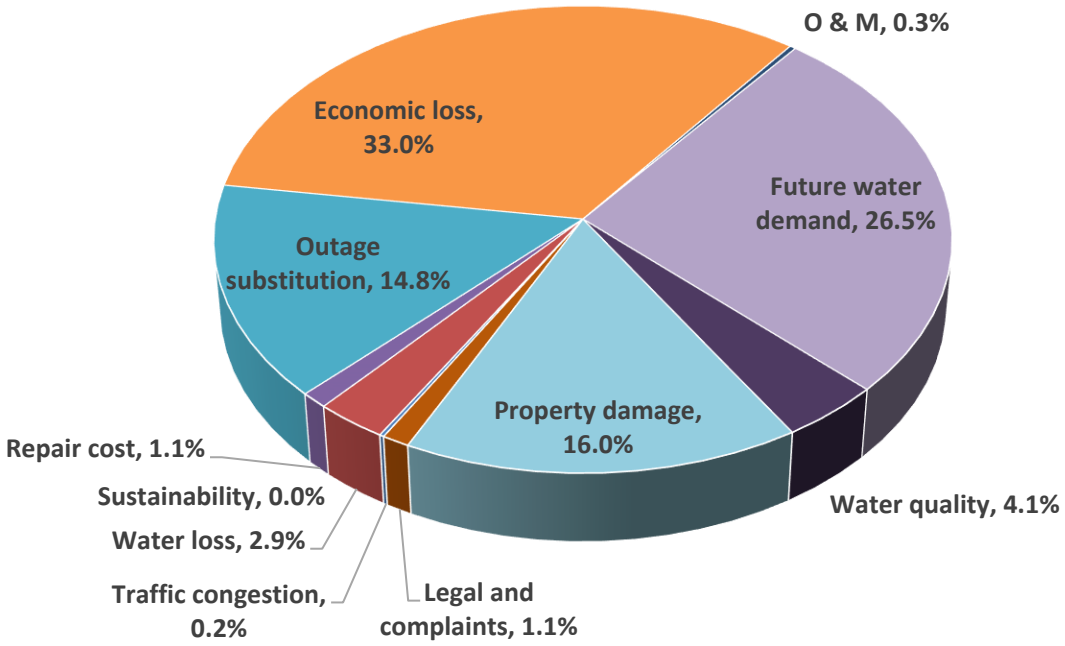

Figure 5.9. Pie chart of benefits of the project excluding the benefit from public distrust costs

Table 5-9 summarizes the breakdown of the benefits by the beneficiary. To be specific, the benefits were broken down by whether the advantages of the benefits from the WTM improvement project are taken by a water utility directly or the public indirectly as prescribed in this study. The total direct benefit to a water supply utility is calculated as 54,664,083 USD, which includes water loss savings, cost savings in emergency repair and return to service, savings in operational and maintenance costs, future extended water demand, savings in water quality recovery, reduction in legal and administrative costs, and savings in outage substitution cost. In contrast, the total indirect (social) benefits to the public can be calculated as 8,677,588,653 USD, which involves a reduction in traffic congestion, sustainability improvement, prevention of economic losses, reduction in public distrust, reduction of health risk, and reduction in property damage. This analysis implies that the social benefits to the public (99.37%) is more significant than the direct benefits to a water supply utility (0.63%). The details of the benefits over the years are as shown in Table 8-11 of Appendix section.

Table 5-9. Breakdown of the benefits by direct and indirect benefits

Benefits		Benefits for 30 years in USD	Ratio, %	Ratio of direct and indirect benefits, %
Direct benefits to a water supply utility	Water loss savings	3,234,812	5.92%	
	Cost savings in emergency repair and return to service	1,222,390	2.24%	
	O&M savings	329,300	0.60%	
	Future extended water demand	30,512,783	55.82%	
	Savings in water quality recovery cost	1,585,686	2.90%	
	Reduction in legal and Complaints	1,243,754	2.28%	
	Savings in outage substitution cost	16,535,357	30.25%	
	Sub-sum	54,664,083	100.00%	0.63%
Indirect (social) benefits to the public	Reduction in traffic congestion	201,106	0.00%	
	Sustainability improvement	17	0.00%	
	Prevention of economic losses	36,707,799	0.42%	
	Reduction in public distrust	8,619,814,744	99.33%	
	Reduction of health risk	3,007,595	0.03%	
	Reduction in property damage	17,857,392	0.21%	
	Sub-sum	8,677,588,653	100.00%	99.37%
Total		8,732,252,737	100.00%	100.00%

5.4.2.3.4 BCR Calculation

Table 5-10 provides the summary of BCR calculation using Equation *(5-2)* based on the estimated benefits and cost of the WTM Site D improvement project. The BCRs greater than 1 indicate that the investment on this project is economically worthwhile enough for funding to be justified. Also, the result notes that

the BCR including the benefit from a reduction in public distrust costs is calculated as 100.03 and the BCR excluding that benefit can be calculated as 1.32.

Table 5-10. BCR calculation of the WTM Site D improvement project

Items	Benefit from public distrust included	Benefit from public distrust excluded
Benefits	4,095,304,815 USD	54,072,850 USD
Costs	40,939,894 USD	40,939,894 USD
BCR	**100.03**	**1.32**

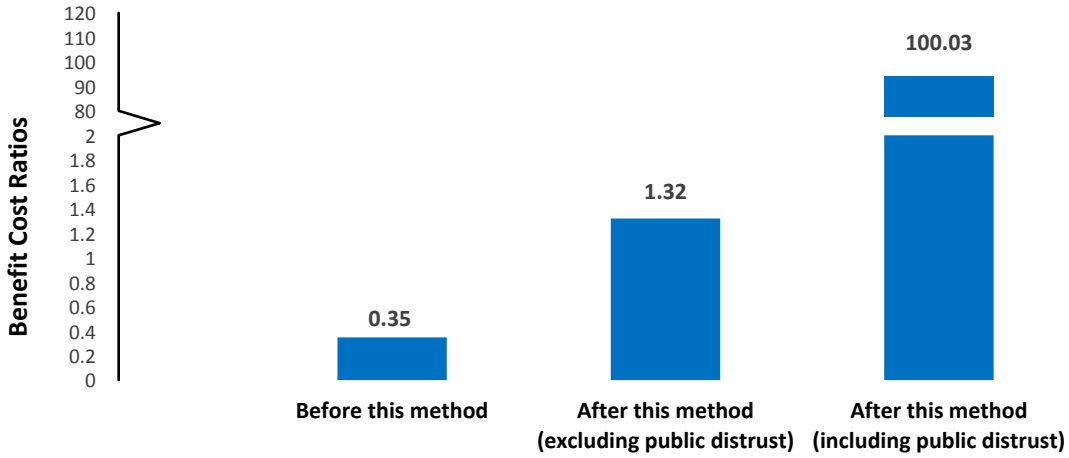

Figure 5.10. Comparison of BCRs before and after this developed valuation methodology

In addition, to validate the effectiveness of the valuation methodology developed in this study, the BCRs before and after establishing the method were compared as depicted in Figure 5.10. The BCR of the project is calculated as 0.35 before the valuation method was established while the BCR is calculated to be greater than 1 after the valuation method is applied to this economic feasibility study for the project. This

is a remarkable outcome of this established framework for an economic feasibility study on aging WTM improvements.

5.4.3 Sensitivity Analysis

Sensitivity analysis was performed to identify the results of an economic feasibility study on WTM Site D improvement project affected by the uncertain variables (the error of predicted break rates of aging pipeline improvements, future water demand, discounted rate, and the interest rate on construction loans) through One-Way sensitivity analysis method for multiple variables.

Figure 5.11 illustrates a spider diagram on BCR variation of the improvement project depending on the change in individual parameters under the calculation condition of excluding the benefit from a reduction in public distrust costs. If the BCR curve approaches horizontal over the total variation of a variable, there is little sensitivity of BCR to changes in the variable. This plot depicts that BCRs vary from 1.16 to 1.49, 1.27 to 1.37, 1.22 to 1.43, and 1.31 to1.33 over variation in prediction error on a break rate of WTM Site D, future water demand, discount rate, and interest on the construction loan, respectively. The spider diagram indicates that BCR is relatively more sensitive to a break rate of WTM Site D, which has a most vertical approach among other parameters.

Figure 5.12 depicts a spider diagram on percent BCR variation of the improvement project depending on the change in individual parameters under the calculation condition of excluding the benefit from a reduction in public distrust costs. This plot illustrates that BCRs vary between -12.43% and +12.55%, between -3.91% and +4.03%, between -7.23% and +8.24%, and between -0.50% and +0.47% over variation in prediction error on a break rate of WTM Site D, future water demand, discount rate, and interest on construction loan, respectively. The spider diagram supports that BCR is more sensitive to a break rate of WTM Site D. A reduction of 21.3% from the expected break rate reduces the BCR to −12.43%, while a 21.3% increase in the break rate raises the BCR to 12.55%.

Figure 5.13 shows a tornado diagram of BCRs under the same condition. Each bar in the diagram is a measure of uncertainty in BCRs. As a result, excluding the benefit from a reduction in public distrust cost, the parameter with the most impact on BCRs of the WTM Site D improvement project is prediction error on a break rate, followed by the discount rate, future water demand, and the interest rate on a construction loan in descending order. Furthermore, it is noted that the uncertainties do not influence the economic feasibility of this project because the least BCR is 1.16 across variations in uncertainties.

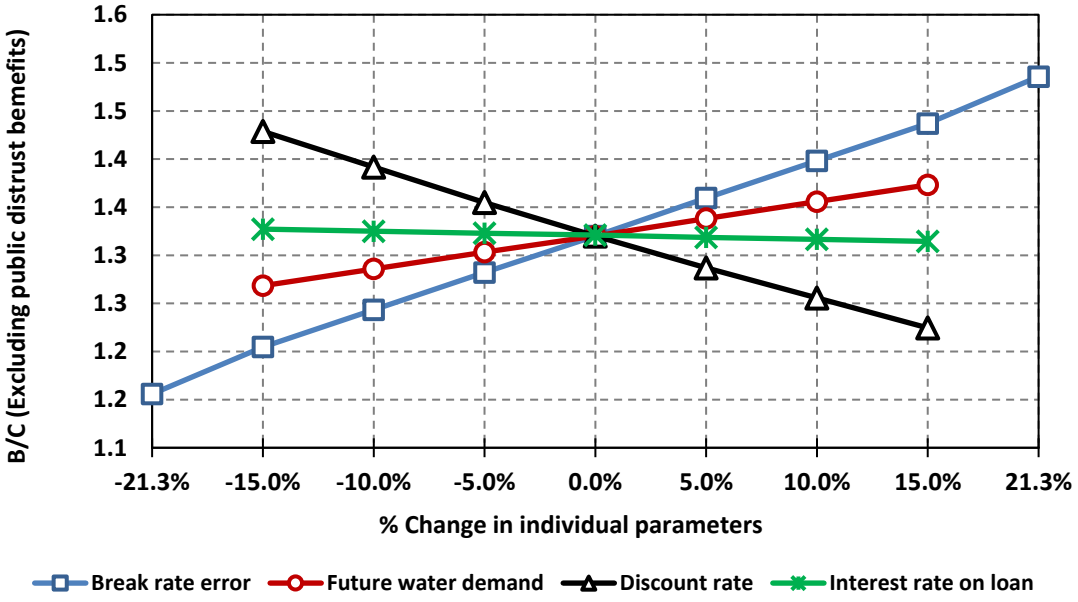

Figure 5.11. Spider plot of BCRs (excluding benefit from public distrust) variations from the most likely estimates

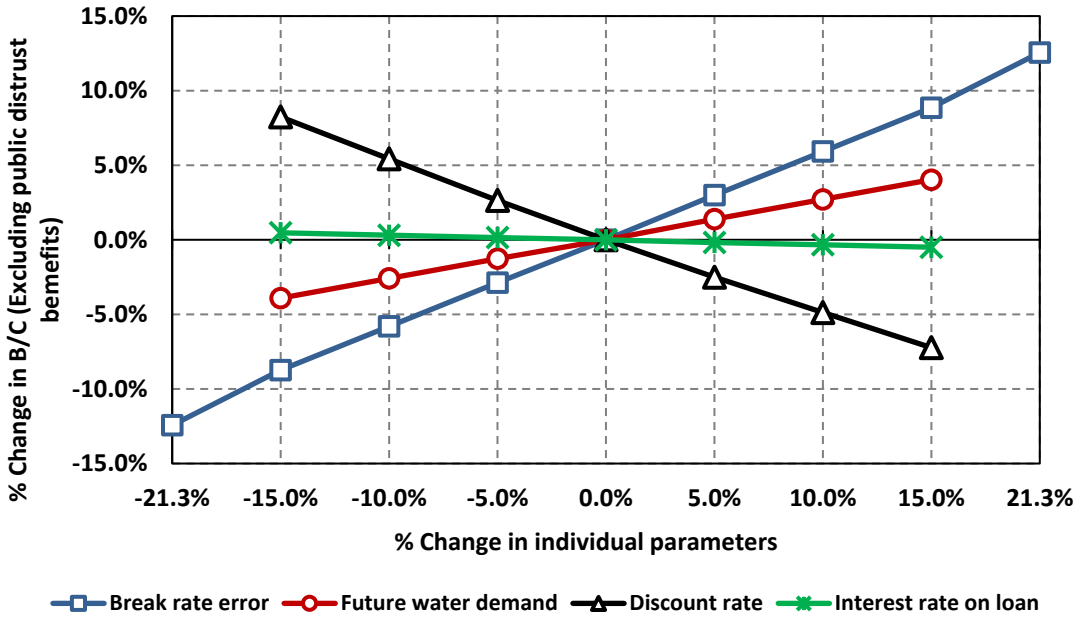

Figure 5.12. Spider plot of percent variation of BCRs (excluding benefit from public distrust) variation from the most likely estimates

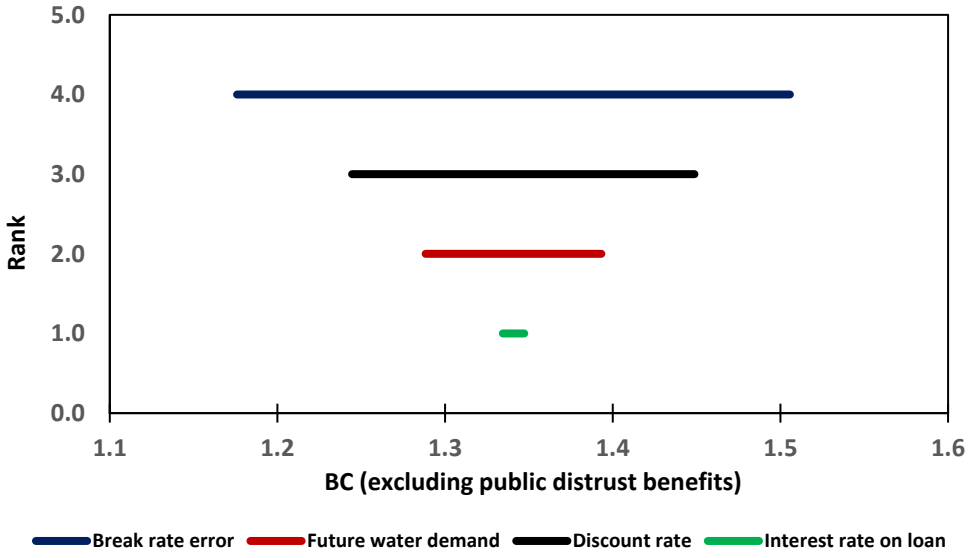

Figure 5.13. Tornado diagram of BCRs (excluding benefit from public distrust) variation depending on parameters

Figure 5.14 illustrates a spider diagram on BCR variation of the improvement project depending on the change in individual parameters under the calculation condition of including the benefit from a reduction in public distrust costs. This plot depicts that BCRs vary from 99.87 to 100.20, 99.98 to 100.08, 91.50 to 109.76, 99.55 to 100.52 over variation in prediction error on a break rate of WTM Site D, future water demand, discount rate, and interest on the construction loan, respectively. In the spider diagram, the BCR curves of a break rate, future water demand, and interest rate on loan are flat and approach horizontal over the total variation of a variable, indicating there is little sensitivity of BCR to changes in those variables. In contrast, it is revealed that BCR is relatively more sensitive to the discount rate.

Figure 5.15 depicts a spider diagram on percent BCR variation of the improvement project depending on the change in individual parameters under the calculation condition of including the benefit from a reduction in public distrust costs. This plot illustrates that BCRs vary between -0.16% and +0.16%, between -0.05% and +0.05%, between -8.53% and +9.72%, and between -0.48% and +0.49% over variation in prediction error on a break rate of WTM Site D, future water demand, discount rate, and interest on construction loan, respectively. The spider diagram supports that BCR is more sensitive to the discount rate. A reduction of 15% from the expected discount rate increases the BCR to 9.72%, while a 15% decrease in the discount rate reduces the BCR to -8.53%.

Figure 5.16 shows a tornado diagram of BCRs under the same condition. As a result, including the benefit from a reduction in public distrust cost, the most sensitive parameter to BCRs of the WTM Site D improvement project can be identified as the discount rate, followed by the interest rate on the construction loan, prediction error on a break rate of WTM, and future water demand in descending order. Additionally, it is noticed that the uncertainties do not influence the economic feasibility of this project because the least BCR is 91.50 over variations in uncertainties as well. This is because the benefit from a reduction in public

distrust cost constitutes most of the benefits (98.68%), in which discount rate cause the benefit to fluctuate more significantly rather than other uncertain variables do. Accordingly, the sensitivity analysis implies that the framework for an economic feasibility study on aging water pipes improvements, which is established in the study is robust.

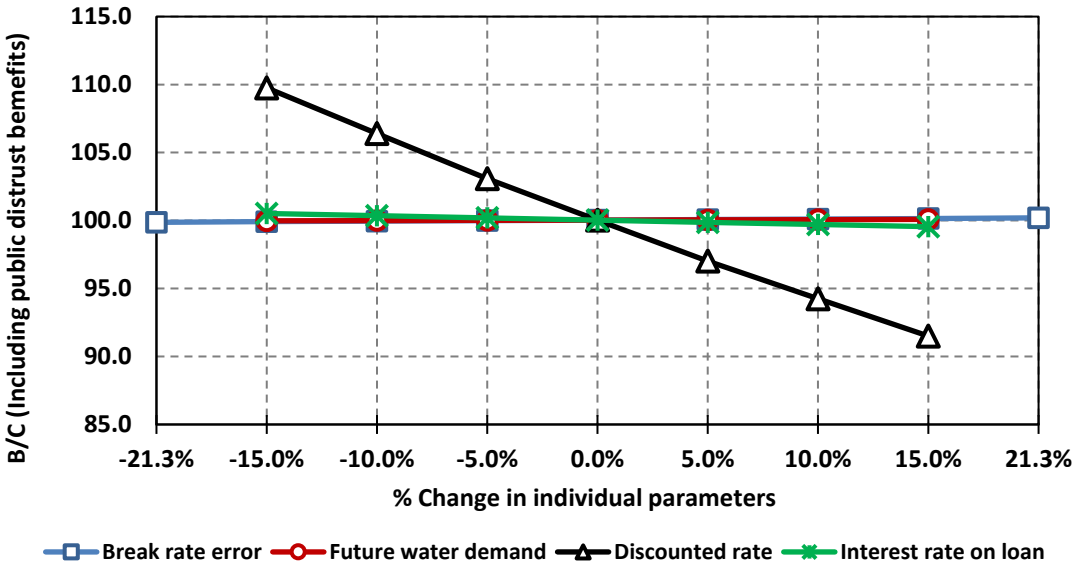

Figure 5.14. Spider plot of BC (including the benefit from public distrust) variation from the most likely estimates

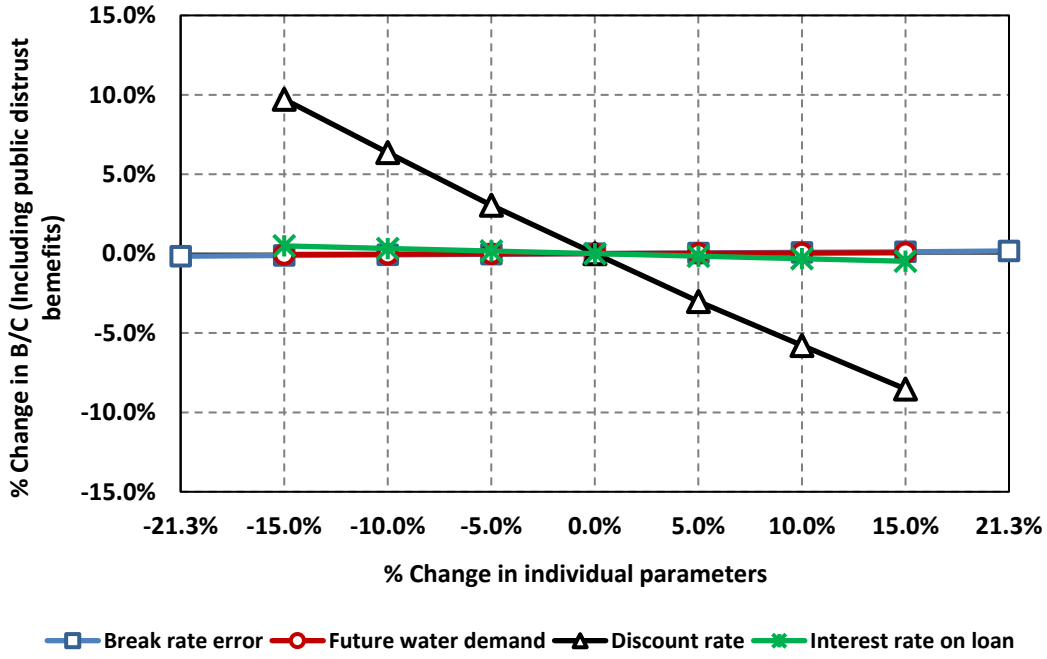

Figure 5.15. Spider plot of percent variation of BC (including the benefit from public distrust) variation from the most likely estimates

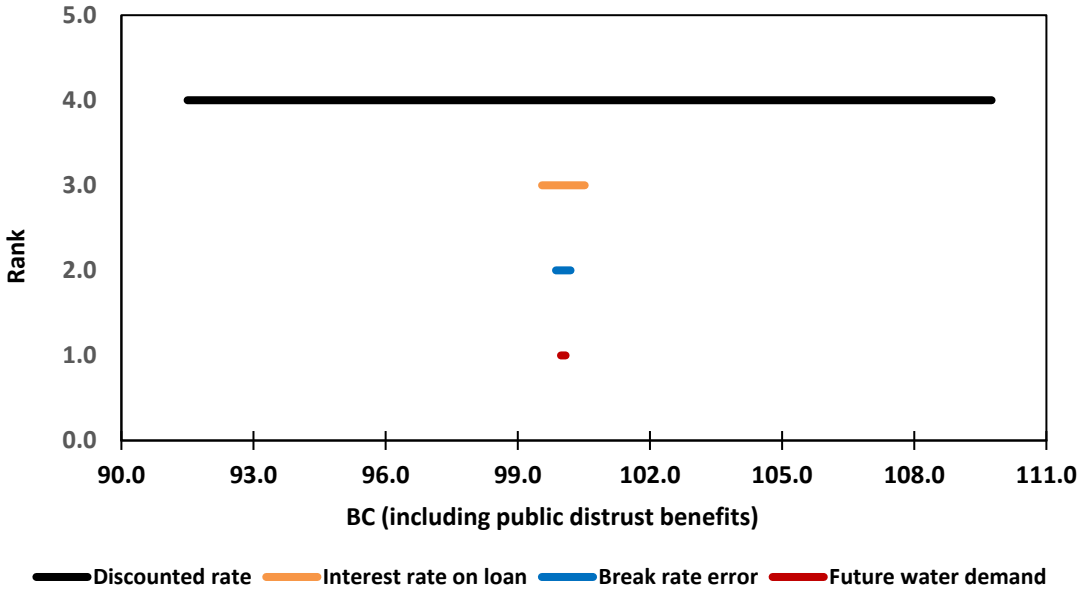

Figure 5.16. Tornado diagram of BC (including the benefit from public distrust) variation depending on parameters

5.4.4 Usefulness of the Outcomes

An economic feasibility study framework suitable for aging water pipeline improvement programs was established from this study. The framework provides the valuation methods to estimate dollar values for all-inclusive benefits from the renewed pipeline infrastructures. The resulting methodology makes it possible for water supply utilities to carry out successfully and reliably economic feasibility studies on improvement projects of aging water supply pipelines assets, clearly revealing hidden and intangible social benefits in monetary values, thereby leading to BCRs of greater than 1. Also, the outcomes can play a fundamental role as a guideline for an economic feasibility study on all water network assets as well as WTMs.

Notably, from this study, we created the methodologies for estimating costs of water loss throughout pipelines, operational costs of pipelines, water recovery costs while flushing disqualified water, and public distrust costs. These tools to measure direct and social costs help water supply utilities and researchers to advance the impact of drinking water supply on the public, contributing to reducing social costs.

Finally, the outcomes will provide drinking water utilities practicing proactive water pipeline management with an economic feasibility study framework to minimize water service outages, end-user inconveniences, and social costs.

5.5 Conclusions and Recommendations

This is the first study to establish valuation methodologies of benefits from aging pipeline improvements and to provide water supply utilities with an economic feasibility study framework suitable for analysis of water supply network renewal and replacement programs. Also, this study validated the robustness and effectiveness of the proposed valuation methodology by conducting an economic feasibility study on a sample pipeline in operation. Accordingly, the following conclusions can be drawn:

- The identified benefits from aging water pipes improvements include the following direct and indirect benefits to water supply utilities:
    - ✓ Direct benefits: Preventions of costs for emergency repair and return to service, prevention of water supply outage and substitution, prevention of water loss, reduction in maintenance and operating costs, reduction in administrative and legal costs, future extended water supply, and prevention of water quality recovery cost); and
    - ✓ Social benefits to the public: Reduction in traffic congestion, reduction in economic losses, sustainability improvement, reduction in health risks, reduction in property damages, and reduction in public distrust costs.
- The economic feasibility study framework developed as a tool to make investment decisions on aging water pipes is composed of five steps:
    1) Select an aging pipeline for improvements;
    2) Select the benefits and their valuation models established in this study;
    3) Forecast a break rate of the pipeline using Deep Learning algorithm-based predictive model;
    4) Decide a replacement timing of the pipeline by estimating its ESL using "Minimum-Cost Life" method; and
    5) Compute BCRs based on the valuation models.
- It was found that the BCR using the established valuation methods was determined to be greater than 1, compared with 0.35 before applying the methods. This pilot test validates that the developed framework for economic feasibility study successfully quantifies the hidden social values of aging pipeline improvement programs.
- This study reveals that indirect (social) benefits to the public appear to be significantly greater than direct benefits to water supply utilities. To be specific, the greatest benefit was reduction in

public distrust costs, followed by prevention of economic losses, future extended water supply, reduction in property damage, prevention of water supply outage and substitution costs, savings in water loss, prevention of costs for emergency repair and return to service, reduction in administrative and legal costs, reduction in operating and maintenance costs, reduction in traffic congestion, and sustainability improvement through the reduction of CO_2 emission in descending order.

- It was found that the benefit from public distrust reduction constitutes 98.7% of the total benefits from WTM Site D improvement project, implicating that such the social cost of public distrust costs caused by not drinking tap water is significantly greater than any other cost.
- The sensitivity analysis confirmed that the developed economic feasibility study model for aging water pipes improvements is robust and reliable, showing BCRs greater than 1 despite reasonable variation in the possible uncertain parameters.

Water supply utilities may have the difficulty of justifying governmental decision makers for the needs and funds to improve aging water network assets due to a lack of proper methods to convert hidden social benefits into dollar values, despite the importance of proactive improvements on aging water networks. However, the economic feasibility study framework for water networks improvements proposed in this study is robust and can be used to effectively assess the economic feasibility of improvement projects on aging water pipes. This framework will aid in the proactive and more cost-effective management of water networks, to minimize water service disruption, end-user inconveniences, and social costs.

It was assumed that some inputs such as infection percentage, hospital days, etc. based on the U.S. database would be the same as those of the ROK due to a lack of data, which might vary depending on counties. Thus, further research is needed to confirm the assumptions used in the economic feasibility study. In

addition, further work is recommended to develop a more user-friendly decision-making tool, which can perform economic feasibility studies automatically.

6 CONCLUSIONS AND RECOMMENDATIONS

6.1 Conclusions

This research identified four significant issues associated with WTM managements. The issues are: (1) lack of study on understanding the main factors affecting steel WTMs and their failure mechanisms, (2) lack of analysis on comprehensive factor affecting steel pipe failures, (3) no availability of predictive models to forecast breaks of aging steel WTMs, and (4) no methodology of valuating the intangible and incalculable public benefits of water main improvement programs into monetary terms to assess their economic feasibility study. In order to tackle these issues, the following four objectives were promulgated: (1) determination of primary factors affecting failures in installed steel WTMs, (2) establishment of scientific causal mechanisms of the identified factors with WTM failure, (3) development of a predictive model for steel WTM breaks that includes both physical factors as well as water quality factors, with the aid of Deep Neural Network algorithms, and (4) establishment of an economic feasibility study framework for the budget justification of water main improvement programs by developing methodologies to valuate hidden public benefits of water main improvements into monetary units.

From this study, the failure cause relationships between the key factors and deterioration of steel WTMs were established using their chemistry-based holistic model. In addition, developed were the DNN-based predictive model suitable for steel WTMs and the economic feasibility study framework using the economic valuation techniques.

First, from the study of the factors affecting steel WTM failure and pipe failure mechanisms, the following conclusions were drawn:

- Water quality (alkalinity, electoral conductivity, pH, temperature, and residual chlorine) as well as pipe age affected steel pipe deterioration significantly while external load was a minor factor unlike the previous studies on small iron or plastic pipes.
- Corrosion was found to be the most common failure cause (52%) of steel water transmission pipes through the failure cause analysis based on the historical break data, confirming that water quality causes steel corrosion and ultimately leads to steel pipe failures.
- The holistic model for chemistry-based failure mechanisms and causal relationships between failure in steel pipes and the influential factors was proposed.

Second, the following conclusions were drawn from developing the DNN-based model for steel WTMs:

- MLNN was found to be the best DNN algorithm for large diameter steel WTMs, while the Stacked Autoencoder NN appears to fit a predictive model with many input variables.
- The established methodology to develop a predictive model has the following steps: (1) determination of significant factors and the establishment of scenarios for models, (2) decision of the best scenario and DNN by comparing performances, (3) classification of data into similar groups by ANN-based clustering technique, and (4) performance of the developed model for each group.
- The SOP clustering method using ANN significantly reduced the prediction percentile errors by 21.9 ~ 78.0% p. It is thought to be a useful tool for clustering data. Also, the ANN-based clustering method is recommended to be used in predicting a replacement timing of water networks.

Last, from the economic feasibility study framework study, the following conclusions were drawn:

- The BCR using the established valuation methods was determined to be greater than 1, compared with 0.35 before applying the methods. This pilot test validated that the developed feasibility study framework successfully quantified the social values of aging pipeline improvements.
- Social benefits appear to be greater than direct benefits in BCR estimation. The greatest benefit was the reduction in public distrust costs, implicating that the social cost caused by not drinking tap water is significantly greater than any other costs in the case of the ROK. This benefit can vary depending on nations and their portion of drinking tap water. Also, no significant benefit was found in sustainability improvement contributing to reducing air pollution.
- The sensitivity analysis showed that the developed economic feasibility study model for aging water pipes improvements was robust and reliable, showing insignificant variation in BCR values when the uncertainty of the parameters was considered.

This study pioneered a major improvement in the WTM world. The outcomes are valuable in that management data and historical records of steel WTMs are scarce. The WTM management before and after this study is summarized in Figure 6.1. Consequentially, this study enables WTMs to be managed more proactively and cost-effectively, minimizing water disruption, end-user inconveniences, and social costs.

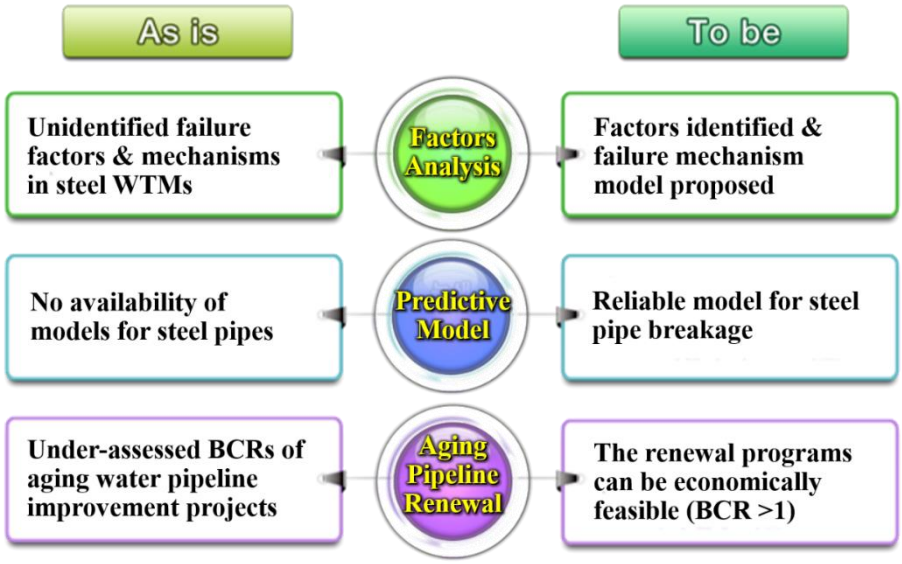

Figure 6.1. WTM management before and after this study

6.2 Recommendations for Further Study

It was reported that the usage of $FeCl_3$ as coagulant was found to be one of the crucial factors of accelerating corrosion of water distribution system, especially composed of lead. Water crisis occurred in Flint, Michigan, USA was found to be caused by switching to a more corrosive water source and use of $FeCl_3$ as a coagulant during water treatment (Olson 2016). As learned from the Flint water crisis, it is recommended that the research be conducted on the effects of coagulants on steel pipe corrosion in WTMs. It would be beneficial if large utilities such as K-water initiate the corrosion study in DWTPs to extend service life of water systems.

Also, during the development of the economic feasibility assessment framework, some inputs such as infection percentage, hospital days, etc. obtained from the U.S. database were used for the assessment in the ROK due to lack of data. Since these input values may vary depending on counties, further research is needed to confirm the assumptions used in the economic feasibility study.

Additionally, further work is recommended to develop a more user-friendly decision-making tool by combining all the models and framework developed in this study. This tool will allow for faster economic feasibility studies and thus will help utility engineers in planning WTM management more efficiently.

7 REFERENCES

Achim, D., GhotbK, F., and McManus, J. (2007). "Prediction of Water Pipe Asset Life Using Neural Networks." *Journal of Infrastructure Systems*, 13(1), 26–30.

Ahmad, Z. (2006). *Principles of Corrosion Engineering and Corrosion Control*. Elsevier Science & Technology Books, Amsterdam.

Ahn, J. C., Lee, S. W., Lee, G. S., and Koo, J. Y. (2005). "Predicting Water Pipe Breaks Using Neural Network." *Water Science and Technology: Water Supply*, 5(3–4), 159–172.

Ahonen, L., and Tuovinen, O. H. (1989). "Microbiological Oxidation of Ferrous Iron at Low Temperatures." *Journal of Applied and Environmental Microbiology*, 55(2), 312–316.

Al-Barqawi, H., and Zayed, T. (2006). "Condition Rating Model for Underground Infrastructure Sustainable Water Mains." *Journal of Performance of Constructed Facilities*, 20(2), 126–135.

Al-Barqawi, H., and Zayed, T. (2008). "Infrastructure Management: Integrated AHP/ANN Model to Evaluate Municipal Water Mains' Performance." *Journal of Infrastructure Systems*, 14(December), 305–318.

American Water Works Association. (2014). *2013 Report Card For America's Infrastructure*. Denver, CO.

American Water Works Association Research Foundation. (1996). *Internal Corrosion of Water Distribution Systems*. *American Water Works Association*, The Foundation, Denver, CO.

Appalachian Underground Corrosion Short Course. (2017). "Pipeline Coating Failures Corrosion

Protection." *Appalachian Underground Corrosion Short Course*, <https://www.aucsc.com/_aucsc speaker files/Coatings Period 11 AUCSC 2012 Jeff Didas.pdf> (Nov. 12, 2017).

ASCE. (2001). *Guidelines for the Design of Buried Steel Pipe*. Washington USA.

AWWA. (2012). "Buried No Longer: Confronting America's water infrastructure challenge." 37.

AWWA Research Foundation. (1996). *Internal Corrosion of Water Distribution Systems*. *American Water Works Association*, The Foundation, Denver, CO.

Baldi, P. (2012). "Autoencoders, Unsupervised Learning, and Deep Architectures." *Workshop on Unsupervised and Transfer Learning*, Washington USA, 37–50.

Bann, C. (2002). *An Overview of Valuation Techniques: Advantages and limitations*. *Asean biodiversity*.

Beale, M. ., Hagan, M. ., and Demuth, H. . (2015). *Neural Network Toolbox User's Guide*. *MathWorks*, Mathworks.

Bengio. (2009). "Learning Deep Architectures for AI." *Foundations and Trends® in Machine Learning*, 2(1), 1–127.

Berardi, L., Giustolisi, O., Kapelan, Z., and Savic, D. A. (2008). "Development of Pipe Deterioration Models for Water Distribution Systems Using EPR." *Journal of Hydroinformatics*, 10(2), 113–126.

Blank, L., and Tarquin, A. (2012). *Engineering Economy*. (M. Lange, ed.), McGraw-Hill, New York, NY.

Bockris, J. O., Drazic, D., and Despic, A. R. (1961). "The Electrode Kinetics of The Deposition and Dissolution of Iron." *Journal of Electrochimica Acta*, 4(2), 325–361.

Boffardi. (1992). "Corrosion and Deposit Control in Mill Water Supply." *Proceedings of the 1992 TAPPI Engineering*.

Bohnet, M. (2003). *Ullmann's Encyclopedia of Industrial Chemistry*. Wiley-VCH, Weinheim, Germany.

Bonnie, B. B., Harle, T., Glennie, E., and Dillon, G. (2008). *Framework for Operational Cost-Benefit Analysis*. Brussels, Belgium.

Boulos, P. F. (2017). "Optimal Scheduling of Pipe Replacement." *Journal - American Water Works Association*, 109(1), 42–46.

Boxall, J. B., O'Hagan, A., Pooladsaz, S., Saul, A. J., and Unwin, D. M. (2007). "Estimation of Burst Rates in Water Distribution Mains." *Proceedings of the Institution of Civil Engineers-Water Management*, ICE Virtual Library, London, UK, 73–82.

Brozovic, N., Sunding, D. L., and Zilberman, D. (2007). "Estimating Business and Residential Water Supply Interruption Losses from Catastrophic Events." *Water Resources Research*, 43(8), 1–14.

Buckley, W. H. W. D. (1971). "Temperature Coefficient of Gas Solubility for Regular Solutions." 49, 667–671.

Bullinaria, J. (2004). "Self Organizing Maps : Fundamentals." <http://www.cs.bham.ac.uk/~jxb/NN/l16.pdf> (Aug. 10, 2017).

Canada Pipe Compay. (2012). *Ductile Iron Pipe*. Ontario, CA.

Caruana, R., Lawrence, S., and Giles, L. (2000). "Overfitting in neural nets: Backpropagation, conjugate gradient, and early stopping." *the 13th International Conference on Neural Information Processing Systems*, MIT Press Cambridge, Denver, CO, 402–408.

Chang, S. E., Seligson, H. A., and Eguchi, R. T. (1996). *Estimation of the Economic Impact of Multiple Lifeline Disruption : Memphis Light, Gas and Water Division Case Study*. Buffalo, NY.

Chok, N. S. (2010). “Pearson’s Versus Spearman’s and Kendall’s Correlation Coefficients for Continuous Data.” *D-Scholarship*, University of Pittsburgh, Pittsburgh, PA.

Christodoulou, S., Gagatsis, A., Agathokleous, A., Xanthos, S., and Kranioti, S. (2012). “Urban Water Distribution Network Asset Management Using Spatio-Temporal Analysis of Pipe-Failure Data.” *14th International Conference on Computing in Civil and Building Engineering*, ICCCBE, Moscow.

Congressional Budget Office. (2015). *Public Spending on Transportation and Water Infrastructure, 1956 to 2014*.

Craun, G. F., and Calderon, R. L. (2001). “Waterborne Disease Outbreaks Caused by Distribution System Deficiencies.” *Journal of American Water Works Association*, 93(9), 64–75.

Craven, M. (2016). “Neural Networks.” <www.biostat.wisc.edu/~craven/cs760/%0ASome> (Sep. 24, 2016).

Cromwell, J., Reyonlds, H., and Young, K. (2002). *Costs of Infrastructure Failure*. AWWA Research Foundation, Denver, CO.

Davalos, J., and Gracia, M. (1991). “Corrosion of Weathering Steel and Iron Under Wet-Dry Cycling Conditions: Influence of the Rise of Temperature During the Dry Period.” *Hyperfine Interactions*, 69, 871–874.

EPA. (2002). *The Clean Water and Drinking Water Infrastructure Gap Analysis Message from EPA ’ s Assistant Administrator for Water*.

EPA. (2007). *Addressing the Challenge Through Innovation*. Cincinnati, OH.

EPA. (2013). *Drinking Water Infrastructure Needs Survey and Assessment Fifth Report to Congress*.

Evans. (1996). “Pearson’s Correlation.” *Statstutor*, <http://www.statstutor.ac.uk/resources/uploaded/pearsons.pdf> (Jan. 9, 2017).

Fitzgerald, J. H. (1968). “Corrosion as a Primary Cause of Cast-Iron Main Breaks.” *Journal of American Water Works Association*, 60(8), 882–897.

Fontana, M. G. (1988). *Corrosion Engineering*. (M. B. Bever, S. M. Copley, M. E. Shank, C. A. Wert, and G. L. Wilkes, eds.), McGraw-Hill Book Company, New York, NY.

French Global Environment Facility. (2015). *Sustainable Forest Management: Socio-economic assessment of goods and services provided by Mediterranean forest ecosystems*. Valbonne, FR.

Gerhold, W. F. (1976). “Corrosion Behavior of Ductile Cast-Iron Pipe in Soil Environments.” *Journal of American Water Works Association*, 68(12), 674–678.

Griffin, R. C., and Mjelde, J. W. (2000). “Valuing Water Supply Reliability.” *Journal of American Agricultural Economics Association*, 82(May), 414–426.

Hagan, M. T., Demuth, H. B., Beale, M. H., and Hayden, I. (1995). *Neural Network Design*. *Boston Massachusetts PWS*.

Herz. (1996). “Aging process and rehabilitation needs of drinking water distribution networks.”

Hou, Y., Lei, D., Li, S., Yang, W., and Li, C. Q. (2016). “Experimental Investigation on Corrosion Effect on Mechanical Properties of Buried Metal Pipes.” *International Journal of Corrosion*, 10(1), 13.

Huanga, R., Xia, L., Lib, X., Liuc, C. R., Qiud, H., and Lee, J. (2007). “Residual life predictions for ball bearings based on the self-organizing map and back propagation neural network methods.” *Mechanical Systems and Signal Processing*, 21(1), 193–207.

Hutton, G., Haller, L., and Bartram, J. (2007). “Global Cost-Benefit Analysis of Water Supply and Sanitation Interventions.” *Journal of Water and Health*, 5(4), 481–501.

Illinois State Water Survey. (1975). *Corrosion by Domestic Waters*. Urbana, Il.

Ionode. (2017). “Conductivity Theory.” <http://ionode.com/theory/conductivity-theory> (Feb. 1, 2017).

Jafar, R., Shahrour, I., and Juran, I. (2010). “Application of Artificial Neural Networks (ANN) to model the failure of urban water mains.” *Mathematical and Computer Modelling*, Elsevier Ltd, 51(9–10), 1170–1180.

Ji, J., Robert, D. J., Zhang, C., Zhang, D., and Kodikara, J. (2017). “Probabilistic Physical Modelling of Corroded Cast Iron Pipes for Lifetime Prediction.” *Journal of Structural Safety*, Elsevier Ltd, 64(3), 62–75.

Jo, J. (2008). “Water Taste.” <http://www.adic.co.kr/library/period/showPeriodBook.do?ukey=114367>.

KDI. (2001). *Guidelines for Water Resources Feasibility Studies*.

KDI. (2004). *Guidelines for Transporation Feasibility Studies*. KDI, South Korea.

KDI. (2008). *Guidelines for Water Resources Feasibility Studies*. KDI, Seoul, Korea.

KDI. (2011). *Guideline for Industrial Water Supply Benefits*. Seoul, Korea.

Keil, B., and Devletian, J. (2011). “Comparison of the Mechanical Properties of Steel and Ductile Iron Pipe Materials.” *Pipelines Conference 2011*, 2011 American Society of Civil Engineers, Seattle, Washington, 1301–1312.

Kim, H. S., Lee, D. J., Park, N. S., and Jung, K. S. (2008). “Analysis on Statistical Characteristics of Household Water End-uses.” *Journal of Korean Society of Civil Engineers*, 28(5), 603–614.

Kleiner, Y., and Rajani, B. (2001). "Comprehensive Review of Structural Deterioration of Water Mains: Statistical Models." *Journal of Urban Water*, 3(3), 131–150.

Kleiner, Y., and Rajani, B. (2007). "Static and Dynamic Effects in Prioritizing Individual Water Mains for Renewal." *SUWM 2007 Conference*, SUWM 2007 Conference, Leicester, UK, 1–8.

Knudsen, H. A. (1940). "Corrosion and Tuberculation." *AWWA*, 32(3), 387–393.

Kohonen, T. (1998). "The self-organizing map." *Neurocomputing*, 21(1–3), 1–6.

Koss, P. (2001). "The value of Water Supply Reliability in California: a Contingent Valuation Study." *Journal of Water Policy*, 3(2), 165–174.

Kwon, H. (2015). "Design Criteria of Hazen-Williams C Value of Water Pipe System." *Journal of Korean Society of Water and Wastewater*, 29(6), 659–666.

LAWnB. (2017). "Legal Fee." <http://www.lawnb.com/sosong/calculation/support_lawyer.asp>.

Lskiewicz, T. (2014). "Functional surfaces for corrosion protection." *Intercorr 2014 Conference*, <https://www.slideshare.net/TomaszLiskiewicz/functional-surfaces-for-corrosion-protection-current-challenges-and-future-trends> (Feb. 27, 2017).

Ma, F. Y. (2012). *Corrosive Effects of Chlorides on Metals*. *Pitting Corrosion*, (N. Bensalah, ed.), InTech.

Mabuchi, K., Horii, Y., Takahasi, H., and Nagayama, M. (1991). "Effect of Temperature and Dissolved Oxygen on the Corrosion Behavior of Carbon Steel in High-Temperature Water." *Corrosion Science*, 47(7), 500–508.

Makar, J. M., and Rajani, B. (2000). "Gray Cast-Iron Water Pipe Metallurgy." *Journal of Materials in Civil Engineering*, 12(3), 245.

Male, J. W., Walski, T. M., and Slutsky, A. H. (1990). “Analyzing water main replacement policies.” *Journal of water resources planning and management*, 116(3), 362.

Maughan. (2000). *Basics of Stator Collant Water Chemistry*. Clearwater, Florida.

McNeill, L. S. (2000). “Water Quality Factors Influencing Iron and Lead Corrosion in Drinking Water.” Virginia Polytechnic Institute of State University. Blacksburg, VA.

McNeill, L. S., and Edwards, M. (2002). “The Importance of Temperature in Assessing Iron Pipe Corrosion in Water Distribution System.” *Journal of Environmental Monitoring and Assessment*, 77(3), 229–242.

Miller, R. L., Bradford, W. L., and Peters, N. E. (1988). “Specific Conductance: Theoretical Considerations and Application to Analytical Quality Control.” *Journal of United States Geological Survey Water-Supply*, 2311(1), 1–16.

Milone, V. (2012). “The effect of temperature and material on mains pipe breaks in Gothenburg.”

Ministry of Environment of ROK. (2013). *Solution to Water Distrust and to Improve Potable Water Consumption Rate*. Gwachun, South Korea.

Ministry of Environment of S. Korea. (2014). “Korean Standard on Steel Pipes for Water Works.” <https://standard.go.kr/KSCI/standardIntro/getStandardSearchView.do>.

Misawa, T., Asami, K., Hashimoto, K., and Shimodaira, S. (1974). “The mechanism of atmospheric rusting and the protective amorphous rust on low alloy steel.” *Corrosion Science*, 14(4), 279–289.

Mobin, M., and Tanveer, N. (2011). “Corrosion Behavior of Chemically Deposited Single and Bi-layered Conducting Polymer Coatings on Mild Steel.” *Portugaliae electrochemical Acta*, 29(3), 139–154.

Morris, R. D., and Levin, R. (1995). “Estimating the incidence of waterborne infectious disease related to drinking water in the United States.” *Assessing and Managing Health Risks from Drinking Water Contamination: Approaches and Applications*, E. G. Reichard and G. A. Zapponi, eds., International Association of Hydrological Sciences, Rome, Italy, 75–88.

Muylwyk, Q., Sandvig, A., and Snoeyink, V. (2014). “Developing Corrosion Control for Drinking Water Systems.” *AWWA*, 40(11), 24–27.

National Assembly Budget Office. (2008). *Evaluation of non-market resources*. Seoul, ROK.

National Research Council. (2003). *Deterioration and Inspection of Water Distribution Systems*.

National Research Council. (2006). *Drinking Water Distribution Systems: Assessing and Reducing Risks*. The National Academies Press, Washington, D.C.

National Resources Council. (2005). *Valuing Ecosystem Service*. THE NATIONAL ACADEMIES PRESS, Washington, D.C.

Nimmo, B., and Hinds, G. (2003). “Beginners Guide to Corrosion.” *NPL, February*, 1(February), 1–10.

Nishiyama, M., and Filion, Y. (2014). “Forecasting breaks in cast iron water mains in the city of Kingston with an artificial neural network model.” *Canadian Journal of Civil Engineering*, 923(August), 918–923.

Office of Financial Management. (2010). *State Administrative & Accounting Manual*. U.S., 23.

Olson, T. (2016). “The science behind the Flint water crisis: corrosion of pipes, erosion of trust.” <http://theconversation.com/the-science-behind-the-flint-water-crisis-corrosion-of-pipes-erosion-of-trust-53776>.

Pandey, M. . D. (1998). “Probabilistic models for condition assessment of oil and gas pipelines.” *NDT & E International*, 31(5), 349–358.

Pratt, C., Yang, H., Hodkiewicz, M., and Oldham, S. (1996). “Factors Influencing Pipe Failures in the WA Environment.” *CEED Seminar 2011*, The National SEED Project, Crawley, WA, 43–48.

Reckhow, D. (2009). “Water and Wastewater Systems.” *Univ. of Massachusetts Amherst*, <http://www.ecs.umass.edu/cee/reckhow/courses/371/371l25/371l25print.pdf> (Jun. 13, 2017).

Rezaei, H., Ryan, B., and Stoianov, I. (2015). “Pipe Failure Analysis and Impact of Dynamic Hydraulic Conditions in Water Supply Networks.” *13th Computer Control for Water Industry Conference*, Elsevier, ed., Elsevier, Leicester, UK, 253–262.

Ribeiro, D. V., Labrincha, J. A., and Morelli, M. R. (2012). “Cement and Concrete Research Effect of the Addition of Red Mud on the Corrosion Parameters of Reinforced Concrete.” *Journal of Cement and Concrete Research*, Elsevier Ltd, 42(1), 124–133.

Rodolfo, P., and Singley, J. E. (2016). “Influence of Buffer Capacity, Chlorine Residual, and Flow Rate on Corrosion of Mild Steel and Copper.” *Journal of American Water Works Association*, 79(2), 62–70.

Roisemount Analytical Inc. (2010). *Theory and Application of Conductivity*.

Romanoff, M. (1964). “Exterior Corrosion of Cast-Iron Pipe.” *AWWA*, 56(9), 1129–1143.

Rossum. (1969). “PREDICTION OF PITTING RATES in ferrous metals from soil parameters.” 61(6), 305–310.

Rossum, J. R. (1983). “Fundamentals of Metallic Corrosion in Fresh Water.” *CiteSeerX*, <http://citeseerx.ist.psu.edu/viewdoc/similar?doi=10.1.1.565.778&type=ab> (Aug. 22, 2016).

Rotterdam. (2012). “Buried Piping.” <http://www.dynaflow.com/wp-content/uploads/2015/06/Lecture-08-03-2012-Buried-piping-by-Dynaflow.pdf>.

Sakia, R. M. (1992). “The Box-Cox Transformation Technique.” *Journal of Royal Statistical Society*, 41(2), 129–136.

SBS NEWS. (2015). “Broken Water Main Floods Roads.” <http://news.sbs.co.kr/news/endPage.do?news_id=N1002814131>.

Schaschl, E., and Marsh, G. (1956). “The Effect of Dissolved Oxygen on Corrosion of Steel and on Current Required for Cathodic Protection.” *Journal of National Association of Corrosion Engineers*, 13(3), 243–251.

Schutze, M. (1997). *Protective Oxide Scales and Their Breakdown*. (D. R. Holmes, ed.), Wiley, Hoboken, NJ.

SDL Component Suite. (2012). “Kohonen Network.” <http://www.lohninger.com/helpcsuite/kohonen_network_-_background_information.htm>.

Sebastian, R. S., Enns, C. W., and Goldman, J. D. (2011). *Drinking Water Intake in the United States*. Washington, D.C.

Shamir, U., and Howard, C. (1979). “An analytic approach to scheduling pipe replacement.” *Journal of American Water Works Association*, 71(5, May 1979), 248–258.

Shamir et al. (1979). “An Analytic Approach to Scheduling Pipe replacement.” *Journal of American Water Works Association*, 71(5), 248–258.

Shaughnessy, E. ., Katz, I. M., and Schaffer, J. P. (2005). *Introduction to Fluid Mechanics*. Oxford University Press, New York, NY.

Stumm, W., and Morgan, J. J. (1996). *Chemical Equilibria and Rates in Natural Waters*. *Aquatic chemistry*.

The Financial News. (2016). "Domestic Market Shares of Water Purifiers." *The Financial News*, <http://www.fnnews.com/news/201610190720169693> (Jul. 20, 2001).

The Korea Transport Institute. (2014). *Traffic Congestion Costs in 2011 and 2012*. Goyang, Korea.

Tuthill, A. H., Avery, R. E., Lamb, S., and Kobrin, G. (1998). "Effect of Chlorine on Common Materials in Fresh Water." *Journal of Materials Performance*, 37(11), 52–56.

U.S. Department of Transportation. (1998). "Procedural Guidelines for Highway Feasibility Studies." *U.S. Department of Transportation*, <http://www.fhwa.dot.gov/planning/border_planning/corbor/feastudy.cfm#7> (Aug. 20, 2004).

U.S. EPA. (2014). *Guidelines for Preparing Economic Analyses*. *U.S. EPA*, Cincinnati, OH.

U.S. Water Resources Council. (2009). *Economic and Environmental Principles and Guidelines for Water and Related Land Resources Implementation Studies*. U.S., 147.

Ugarelli, R., and Di Federico, V. (2010). "Optimal Scheduling of Replacement and Rehabilitation in Wastewater Pipeline Networks." *Journal of Water Resources Planning and Management*, 136(3), 348–356.

UNESCO. (2014). *Identification of Factors Contributing to the Deterioration and Losses in the Water Distribution System in Barbados*. Barbados.

US EPA. (2009). *State of Technology Review Report on Condition Assessment of Ferrous Water Transmission and Distribution Systems*. Cincinnati.

US EPA. (2012a). *Condition Assessment Technologies for Water Transmission and Distribution Systems*. Cincinnati.

US EPA. (2012b). "5.9 Conductivity." *Environmental Protection Agency*, <https://archive.epa.gov/water/archive/web/html/vms59.html> (Oct. 11, 2017).

Venturescanner Inc. (2015). "Artificial Intelligence At a Glance." <https://venturescannerinsights.wordpress.com/tag/artificialintelligence/>.

Videla, H. A., and Herrera, L. K. (2005). "Microbiologically influenced corrosion: looking to the future." *International microbiology : the official journal of the Spanish Society for Microbiology*, 8(3), 169–180.

Wallington, T. J., Sullivan, J. L., and Hurley, M. D. (2008). "Emissions of CO 2 , CO , NO x , HC , PM , HFC-134a , N 2 O and CH 4 from the global light-duty vehicle fleet." *Journal of Meteorologische Zeitschrift*, 17(2), 109–116.

Washington State Department of Health. (2006). *Pipeline Separation Design and Installation Reference Guide*. Olympia, WA.

Wilmott, M., and Sutherby, R. (1998). "The Role of Pressure and Pressure Fluctuations in the Growth of Stress Corrosion Cracks in Line Pipe Steel." *International Pipeline Conference*, ASME, ed., ASME, Calgary, Alberta, 409–422.

Wilson, D., Filion, Y. R., and Moore, I. D. (2015). "Identifying Factors That Influence the Factor of Safety and Probability of Failure of Large-Diameter, Cast iron Water Mains with a Mechanistic, Stochastic Model." *13th Computer Control for Water Industry Conference*, Elsevier, Leicester, UK, 130–138.

Xu, Q., Chen, Q., Ma, J., and Blanckaert, K. (2013). "Optimal Pipe Replacement Strategy Based on Break

Rate Prediction Through Genetic Programming for Water Distribution Network." *Journal of Hydro-Environment Research*, 7(2), 134–140.

Yeom, Y. S. (2012). *Application & reality of the feasibility study on public investment using CVM*. Junju, ROK.

Yerri, S. R. (2016). "Empirical Analysis of Large Diameter Water Main Break Consequences." *Resources, Conservation, and Recycling*, Clemson University.

Yu, H., and Bogdan, M. (2016). *Intelligent Systems*. (B. M. Wilamowski and J. D. Irwin, eds.), CRC Press, New York, NY.

8 APPENDICES

8.1 Scatter Plots of the Observed and Predicted Values of Each Model

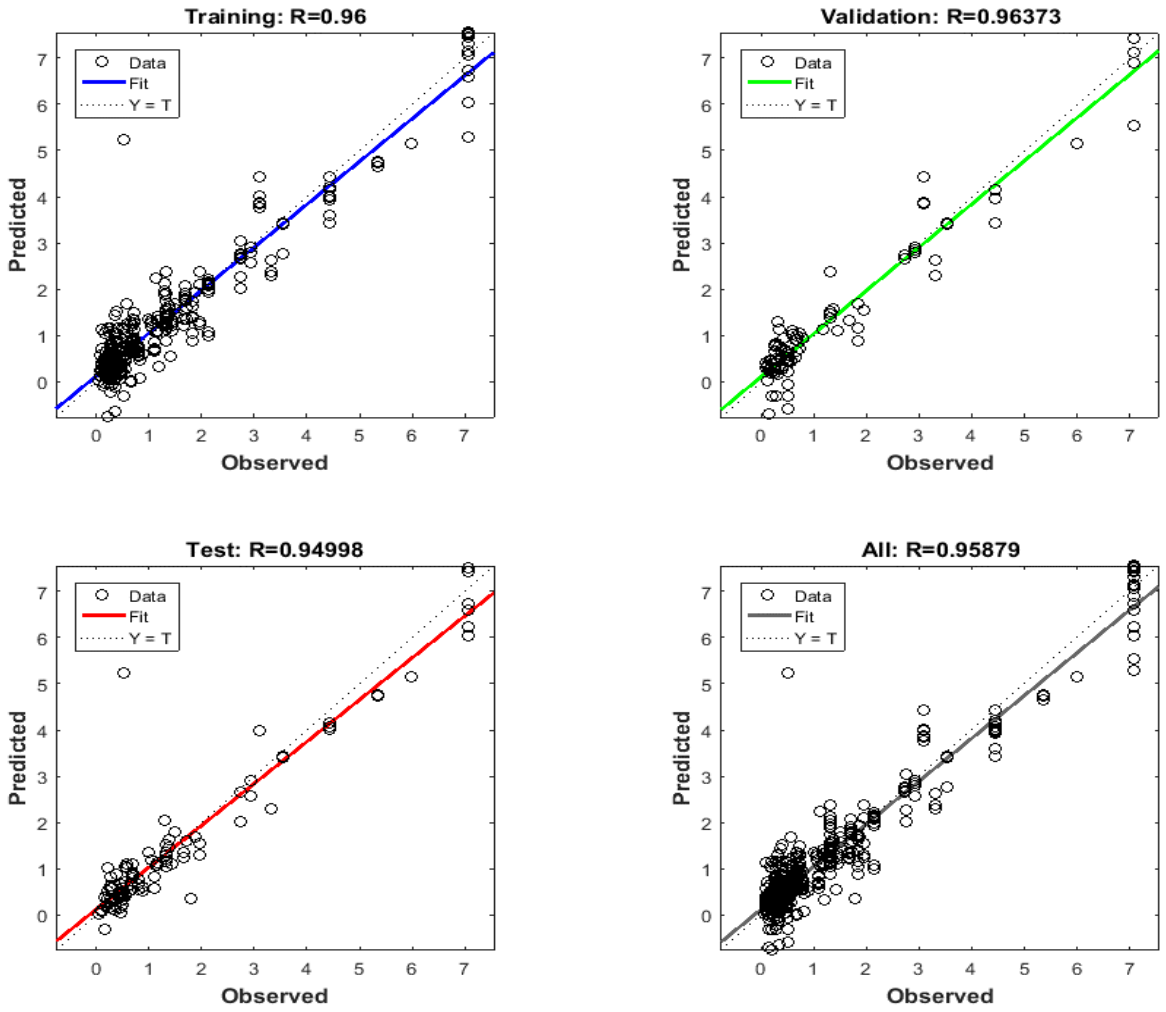

Figure 8.1. Scatter plots and R values of the observed and predicted values of the Shallow NN model for each dataset (training, validation, test, and overall) at scenario 2 in forecasting a break rate of WTMs

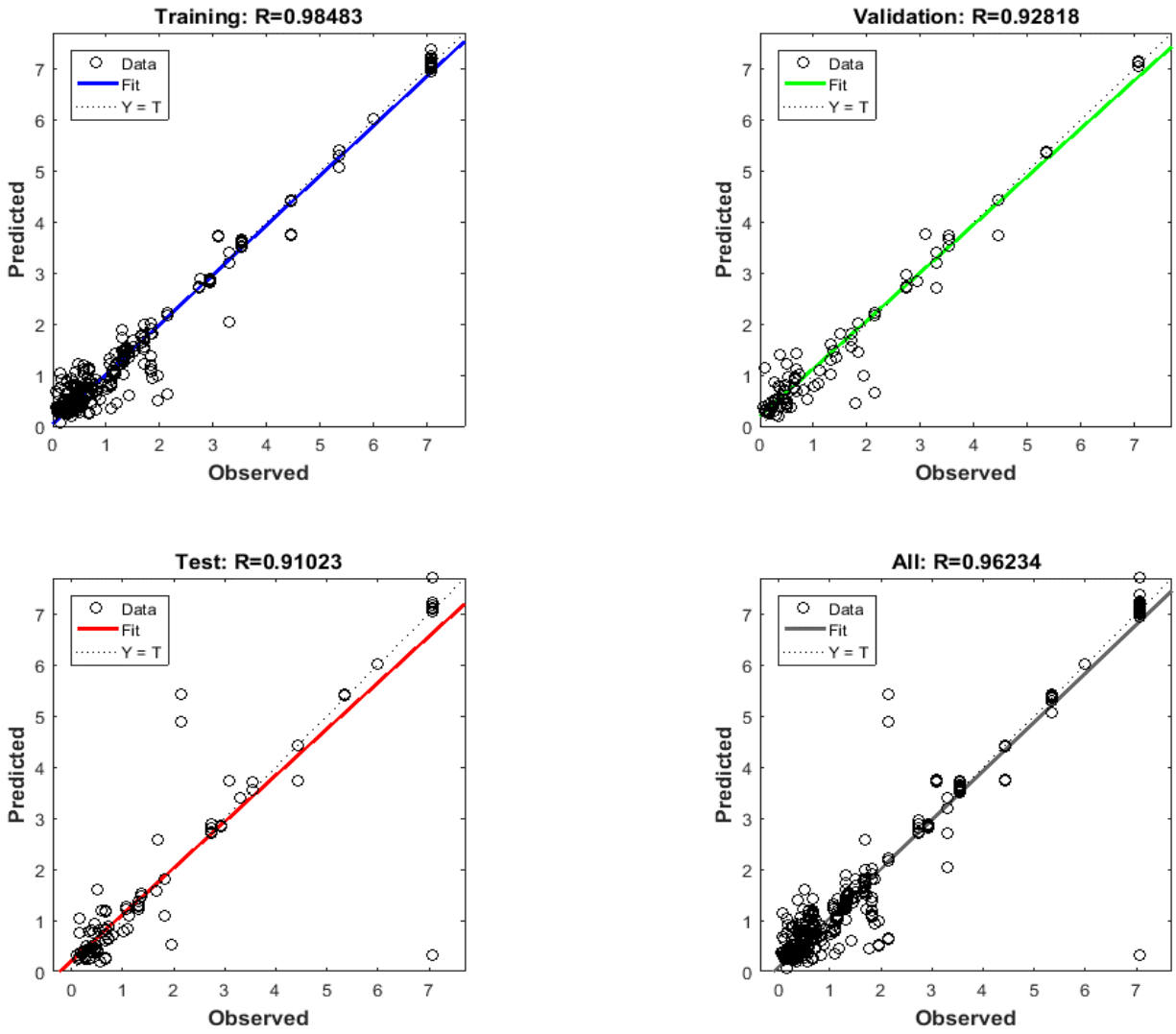

Figure 8.2. Scatter plots and R values of the observed and predicted values of the Stacked Autoencoder NN model for each dataset (training, validation, test, and overall) at scenario 2 in forecasting a break rate of multi-regional steel WTMs

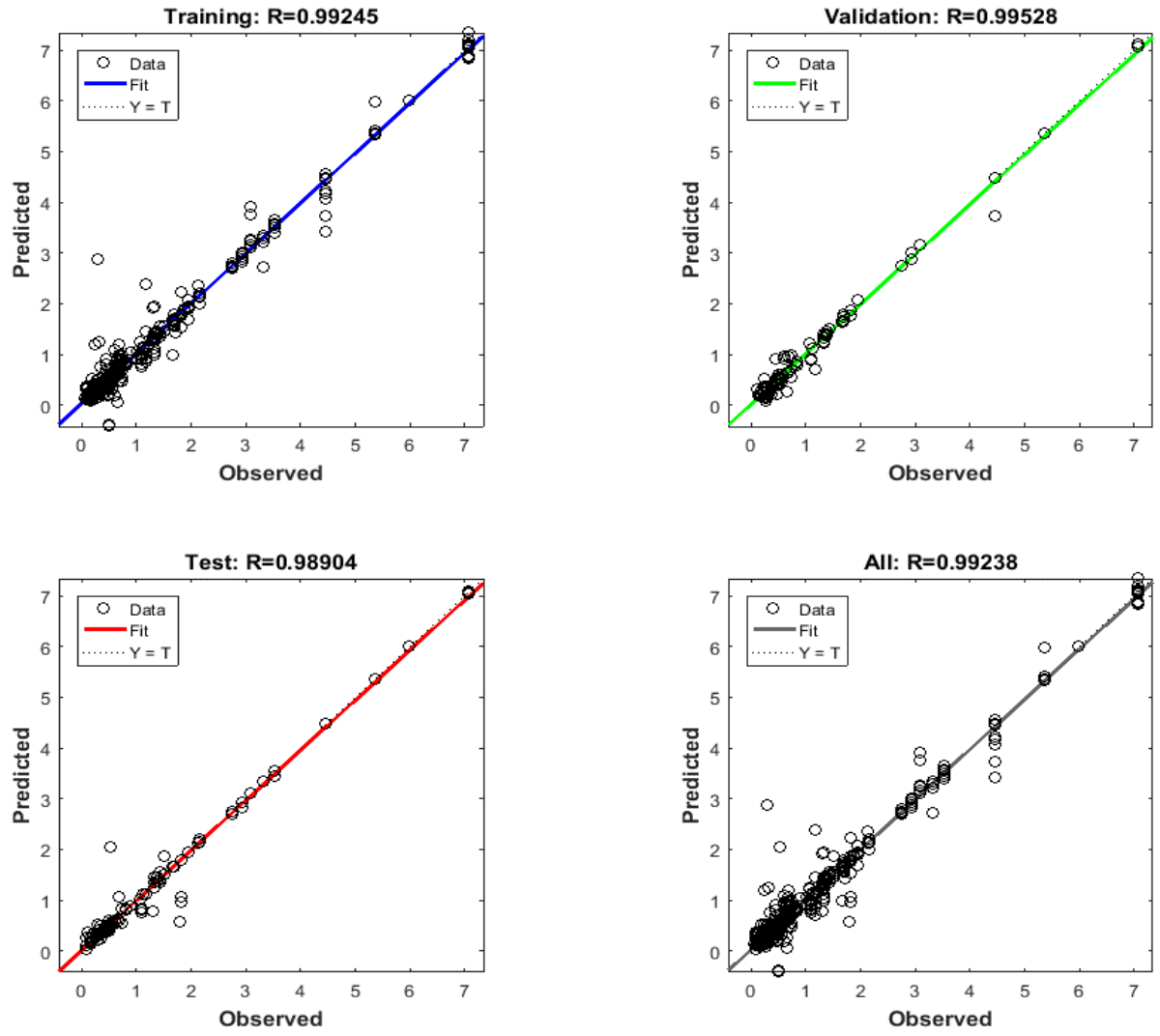

Figure 8.3. Scatter plots and R values of the observed and predicted values of the MLNN model for each dataset (training, validation, test, and overall) at scenario 2 in forecasting a break rate of multi-regional steel WTMs

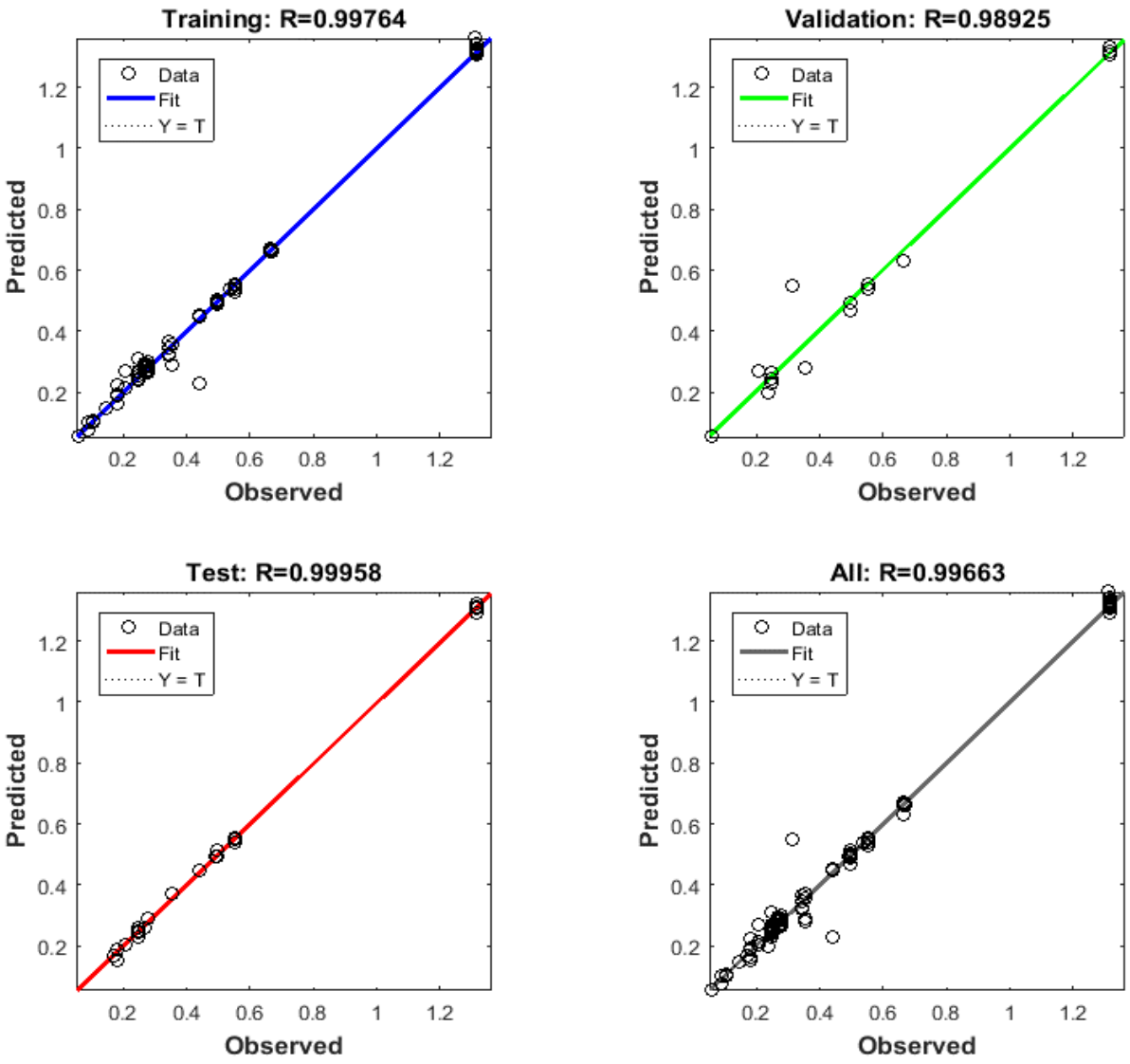

Figure 8.4. Scatter plots and R values of the observed and predicted values of the MLNN model for each dataset (training, validation, test, and overall) of the clustered group 1 at scenario 2 in forecasting a break rate of multi-regional steel WTMs

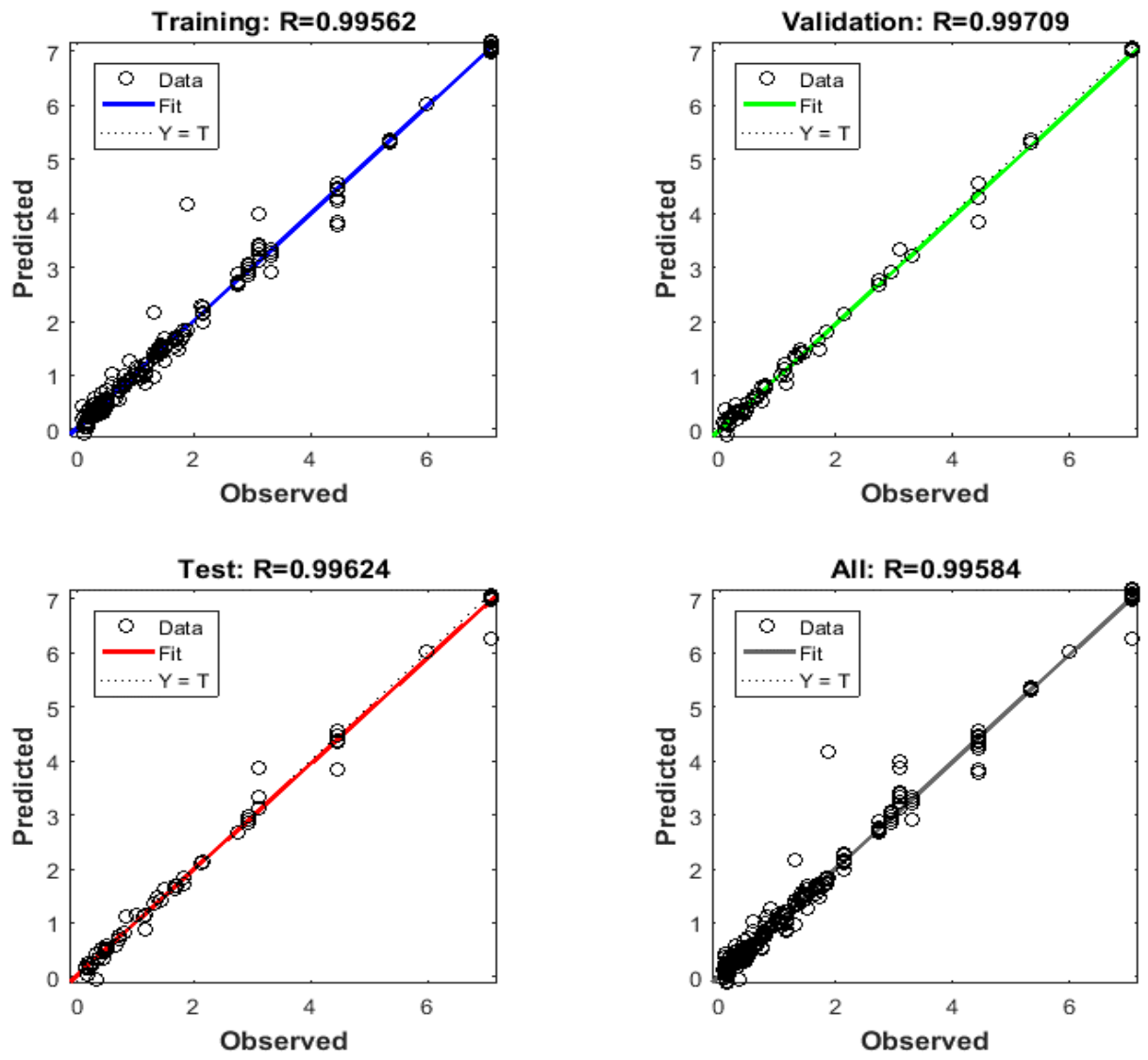

Figure 8.5. Scatter plots and R values of the observed and predicted values of the MLNN model for each dataset (training, validation, test, and overall) of the clustered group 2 at scenario 2 in forecasting a break rate of multi-regional steel WTMs

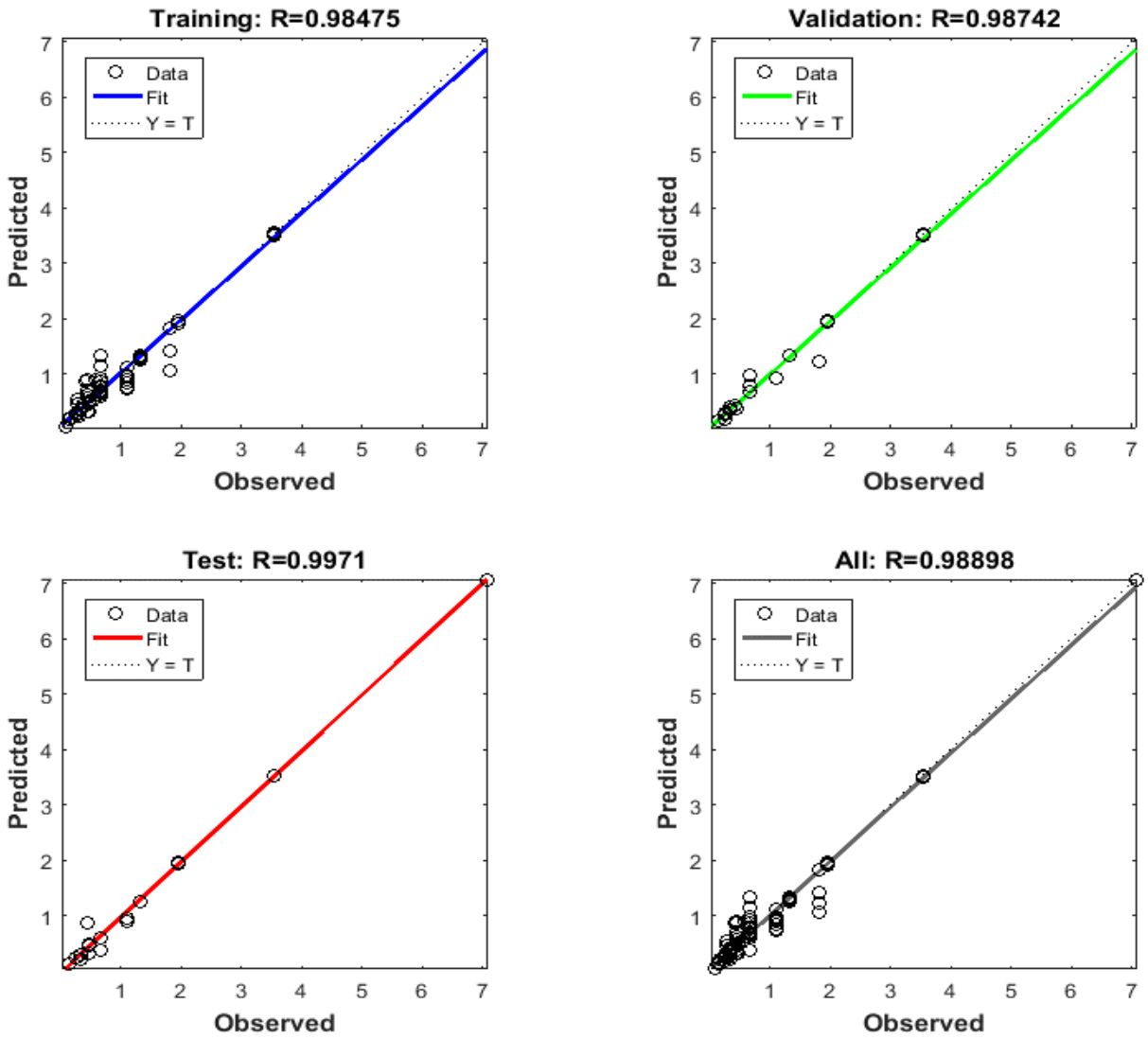

Figure 8.6. Scatter plots and R values of the observed and predicted values of the MLNN model for each dataset (training, validation, test, and overall) of the clustered group 3 at scenario 2 in forecasting a break rate of multi-regional steel WTMs

8.2 Data for Economic Valuation of Aging Water Main Improvements

8.2.1 Repair Time, Value of Travel Time, and Daily Traffic

Table 8-1. Average time to repair broken WTMs by diameter (K-water 2012)

Diameter (mm)	**~ 300**	**400**	**500**	**600**	**700**	**800**	**900**	**1,000**
Time (Hours)	14.57	15.61	16.64	17.67	18.71	19.45	20.8	22.9
Diameter (mm)	**1,100**	**1,200**	**1,350 ~ 1,600**		**1,650 ~ 2,000**		**2,000 ~**	
Time (Hours)	23.94	24.98	29.16		35.35		38.69	

Table 8-2. Annual average values of travel time by vehicles from (KDI 2004)

Categories	**Sedans**		**Bus**	
	Business	**Nonbusiness**	**Business**	**Nonbusiness**
Passengers, persons	0.39	1.61	3.60	18.40
Values of travel time, USD (KRW)	11.0(13,257)	3.6(4,335)	7.8(9,325)	1.8(2,160)
Values of travel time per vehicle, USD/vehicle/hr (KRW/vehicle/hr)	4.3(5,170)	5.8(6,979)	36.5(43,793)	33.1(39,744)
Average values of travel time per vehicle, USD/vehicle/hr (KRW/vehicle/hr)	**10.1(12,150)**		**70.0(83,537)**	

Exchange rate: 1 USD = 1,200 KRW

Table 8-3. Average daily traffic by road and vehicle types

Road and vehicle classifications	Daily traffic (vehicles per day)
Expressway	46,403
Sedans	32,593
Buses	1,586
Trucks	12,224
Highway	11,587
Sedans	8,660
Buses	270
Trucks	2,657
Provincial road	5,064
Sedans	3,500
Buses	155
Trucks	1,409

(Sourced from Statistical Year Book 2016 of the Ministry of Land, Infrastructure, and Transport)

Table 8-4. Fuel consumption by vehicle (KDI 2004)

Speed (km/hr)	Sedans [L/km]	Buses [L/km]	Trucks [L/km]
10	0.151629	0.410714	0.545454
20	0.091431	0.2875	0.428572
30	0.07777	0.188524	0.307692
40	0.070239	0.136905	0.226415
50	0.071743	0.129214	0.218182
60	0.074476	0.133721	0.244898
70	0.078579	0.151316	0.279070
80	0.080533	0.169118	0.324324
90	0.087599	0.188524	0.387097
100	0.094419	0.216981	0.461538
110	0.102164	0.255555	-
120	0.114544	-	-
130	0.126284	-	-

8.2.2 Emission Factors and Environmental Cost of Air Pollutants

Table 8-5. Air pollutant emission factors by vehicles and speed (KEI, 2002)

Vehicle types	Speed [km/hr]	CO [g/km]	NO_X [g/km]	HC [g/km]	PM [g/km]	CO_2 [g/km]
Sedans	10	4.341	1.168	0.691	0.000	380.437
	20	1.915	0.670	0.237	0.000	257.480
	30	1.187	0.483	0.127	0.000	204.913
	40	0.845	0.384	0.082	0.000	174.262
	50	0.649	0.321	0.058	0.000	153.682
	60	0.524	0.277	0.044	0.000	138.685
	70	0.437	0.245	0.034	0.000	127.152
	80	0.373	0.220	0.028	0.000	117.940
	90	0.324	0.200	0.023	0.000	110.371
	100	0.287	0.184	0.020	0.000	104.012
Buses	10	4.060	7.446	1.250	0.603	504.710
	20	2.641	4.894	0.798	0.350	388.390
	30	2.054	3.829	0.613	0.254	297.090
	40	1.718	3.217	0.509	0.203	230.810
	50	1.496	2.810	0.441	0.186	189.550
	60	1.336	2.517	0.391	0.174	173.310
	70	1.214	2.293	0.354	0.174	182.090
	80	1.118	2.114	0.325	0.186	215.890
	90	1.039	2.265	0.301	0.210	274.710
	100	0.973	2.927	0.281	0.246	358.550

Vehicle types	Speed [km/hr]	CO [g/km]	NO_X [g/km]	HC [g/km]	PM [g/km]	CO_2 [g/km]
Trucks	**10**	8.028	34.484	2.301	2.269	3142.430
	20	4.803	26.530	1.554	1.696	2398.414
	30	3.556	22.757	1.236	1.431	2047.782
	40	2.874	20.410	1.050	1.268	1830.554
	50	2.436	18.758	0.925	1.154	1678.059
	60	2.128	17.508	0.835	1.069	1562.940
	70	1.898	16.516	0.765	1.002	1471.792
	80	1.719	15.703	0.709	0.948	1397.144
	90	1.575	15.018	0.663	0.902	1334.449
	100	1.457	14.431	0.625	0.863	1280.754

Table 8-6. Environmental cost per unit air pollutant (KEI, 2002)

Pollutants	CO	NO_X	HC	PM	CO_2
Cost [KRW/kg]	6,376	7,410	7,671	25,045	34
Cost [USD/kg]	5.3	6.2	6.4	20.9	0.028

Exchange rate: 1 USD = 1,200 KRW

8.2.3 Average Cost of Repair and Return to Service

Table 8-7. Average cost of repair and return to service (K-water, 2016)

Unit: thousand KRW/break

Steel pipe			Other pipes		
Diameter (mm)	Driveway over pipelines		Diameter (mm)	Driveway over pipelines	
	Paved	Unpaved		Paved	Unpaved
3,000	62,337	48,200	**3,000**		
2,800	60,527	46,800	**2,800**		
2,600	58,717	45,400	**2,600**		
2,500	56,907	44,000	**2,500**		
2,400	55,699	43,066	**2,400**		
2,300	54,492	42,133	**2,300**		
2,200	53,285	41,200	**2,200**		
2,100	51,474	39,800	**2,100**		
2,000	49,664	38,400	**2,000**		
1,900	47,853	37,000	**1,900**		
1,800	46,043	35,600	**1,800**		
1,650	42,421	32,800	**1,650**	41,750	32,800
1,500	38,800	30,000	**1,500**	38,800	30,000
1,350	35,850	27,719	**1,350**	35,850	27,719
1,200	32,900	25,438	**1,200**	32,900	25,438
1,100	31,601	24,434	**1,100**	31,601	24,434
1,000	30,300	23,428	**1,000**	30,300	23,428
900	28,600	22,113	**900**	28,600	22,113
800	25,341	16,342	**800**	25,341	16,342
700	22,081	13,571	**700**	22,081	13,571
600	19,467	11,413	**600**	19,467	11,413
500	17,205	9,610	**500**	17,205	9,610
450	16,163	8,794	**450**	16,163	8,794
400	15,098	7,957	**400**	15,098	7,957
350	13,910	7,004	**350**	13,910	7,004
300	12,952	6,270	**300**	12,952	6,270
Less than 300	12,149	5,685	**Less than 300**	12,149	5,685

8.2.4 Costs of a Residential Water purifier

Table 8-8. Market shares and costs of water purifiers in the ROK (The Financial News 2016)

Providers		Average	Company W	Company CH	Company CU	Company D
Market share [%]			40	15	10	10
Purchase Price	[KRW]	1,397,320	1,570,000	1,870,000	1,125,180	1,024,100
	[USD]	**1,164**	1,308	1,558	938	853
Monthly rent	[KRW]	32,650	41,800	39,000	28,900	20,900
	[USD]	**27**	35	33	24	17

Exchange rate: 1 USD = 1,200 KRW

8.2.5 Data Ranges for Property Damage Estimation Inputs

Table 8-9. Suggested data ranges for property damage data inputs (Yerri 2016)

No. of properties due to flooding	Suggested Data Range	
	Lower bound	Upper Bound
Residential	10	500
Office	10	500
Restaurants	10	500
Hospitals	1	20
Schools	1	20
Average value of the property:		
Residential	$20,000.00	$300,000.00
Office	$3,000,000.00	$25,000,000.00
Restaurants	$500,000.00	$6,000,000.00
Hospitals	$15,000,000.00	$40,000,000.00
Schools	$5,000,000.00	$30,000,000.00

8.2.6 Typical Legal Fee of the Republic of Korea

Table 8-10. Typical legal fee of the ROK (LAWnB 2017)

Settlement amount (X)	Legal fee (USD)
8,333 USD – 16,667 USD	[667 + (X – 8,333) x 7/100]
16,667 USD – 25,000 USD	[1,250 + (X – 16,667) x 6/100]
25,000 USD – 41,667 USD	[1,750 + (X – 25,000) x 5/100]
41,667 USD – 58,333 USD	[2,583 + (X – 41,667) x 4/100]
58,333 USD – 83,333 USD	[3,250 + (X – 58,333) x 3/100]
83,333 USD – 166,667 USD	[4,000 + (X – 83,333) x 2/100]
166,667 USD – 416,667 USD	[5,667 + (X – 166,667) x 1/100]
416,667 USD -	[8,167+ (X – 416,667) x 0.5/100

8.2.7 Details of the Benefits from the WTM Site D Improvement Project

Table 8-11. Details of the full benefits from the WTM Site D improvement project over the years

Year	Direct benefits									Indirect (social) benefits						Total benefits	Total benefits (Present worth)
	Pre-vented breaks	Water loss	Repair cost	Revenue loss of utility	O&M	Future water demand	Water quality recovery	Com-plaints	Outage sub-stitution	Traffic	Sustaina-bility	Economic loss	Public distrust	health risk	Property damage		
	[Breaks]	[USD]	[USD]	[USD]	[USD]	[USD]	[USD]	[USD]	[USD]	[USD]	[USD]	[USD]	[USD]	[USD]	[USD]	[USD]	[USD]
2023	0.0	0	0	0	8,879	984,283	21,044	0	0	0	0	0	278,058,540	0	0	279,072,747	279,072,747
2024	0.7	102,885	16,726	0	9,148	984,283	25,293	13,280	226,251	2,752	0	502,269	278,058,540	41,153	51,532	280,034,111	265,435,176
2025	0.9	103,580	20,103	0	9,358	984,283	30,543	16,280	271,934	3,307	0	603,683	278,058,540	49,462	52,562	280,203,637	251,749,634
2026	1.0	104,438	24,276	0	9,534	984,283	36,991	20,053	328,380	3,994	0	728,990	278,058,540	59,729	80,420	280,439,628	238,826,219
2027	1.3	105,493	29,400	0	9,687	984,283	44,782	24,771	397,700	4,837	0	882,877	278,058,540	72,337	109,372	280,724,080	226,605,178
2028	1.5	106,767	35,592	0	9,824	984,283	53,945	30,588	481,459	5,856	0	1,068,819	278,058,540	87,572	139,449	281,062,695	215,050,724
2029	1.8	108,265	42,875	0	9,948	984,283	64,318	37,585	579,979	7,054	1	1,287,530	278,058,540	105,492	170,685	281,456,555	204,125,194
2030	2.2	109,961	51,120	0	10,062	984,283	75,467	45,708	691,498	8,410	1	1,535,096	278,058,540	125,776	203,115	281,899,038	193,787,775
2031	2.6	111,785	59,981	0	10,168	984,283	86,653	54,703	811,368	9,868	1	1,801,203	278,058,540	147,579	266,371	282,402,503	184,013,152
2032	2.9	113,614	68,871	0	10,268	984,283	96,857	64,068	931,629	11,331	1	2,068,176	278,058,540	169,453	301,887	282,878,977	174,714,334
2033	3.3	115,282	76,981	0	10,361	984,283	104,907	73,044	1,041,330	12,665	1	2,311,708	278,058,540	189,406	369,510	283,348,019	165,880,595
2034	3.6	116,599	83,379	0	10,450	984,283	109,692	80,697	1,127,877	13,717	1	2,503,840	278,058,540	205,148	439,717	283,733,942	157,446,944
2035	3.7	117,381	87,183	0	10,534	984,283	110,411	86,066	1,179,324	14,343	1	2,618,050	278,058,540	214,506	480,548	283,961,171	149,358,328
2036	3.8	117,499	87,754	0	10,615	984,283	106,779	88,363	1,187,058	14,437	1	2,635,219	278,058,540	215,913	555,514	284,061,975	141,622,132
2037	3.6	116,905	84,867	0	10,692	984,283	99,106	87,165	1,148,007	13,962	1	2,548,527	278,058,540	208,810	599,955	283,960,821	134,191,185
2038	3.4	115,650	78,769	0	10,766	984,283	88,231	82,520	1,065,519	12,959	1	2,365,408	278,058,540	193,806	679,949	283,736,402	127,094,911
2039	3.0	113,872	70,126	0	10,838	984,283	75,320	74,934	948,593	11,537	1	2,105,837	278,058,540	172,538	728,225	283,354,644	120,307,023
2040	2.6	111,760	59,864	0	10,907	984,283	61,628	65,248	809,782	9,849	1	1,797,682	278,058,540	147,290	778,160	282,894,995	113,850,109
2041	2.1	109,522	48,982	0	10,974	984,283	48,288	54,455	662,582	8,058	1	1,470,905	278,058,540	120,516	793,724	282,370,831	107,714,844
2042	1.6	107,340	38,379	0	11,039	984,283	36,177	43,521	519,162	6,314	1	1,152,517	278,058,540	94,430	809,598	281,861,302	101,915,144
2043	1.2	105,360	28,753	0	11,101	984,283	25,877	33,258	388,950	4,730	0	863,454	278,058,540	70,746	863,326	281,438,379	96,457,084
2044	0.9	103,675	20,567	0	11,163	984,283	17,705	24,264	278,208	3,384	0	617,609	278,058,540	50,603	842,306	281,012,307	91,290,101
2045	0.6	102,339	14,072	0	11,222	984,283	11,787	16,934	190,352	2,315	0	422,574	278,058,540	34,623	898,204	280,747,247	86,449,283
2046	0.4	101,371	9,368	0	11,280	984,283	8,135	11,499	126,722	1,541	0	281,317	278,058,540	23,049	876,335	280,493,440	81,868,369
2047	0.3	100,774	6,466	0	11,337	984,283	4,981	8,095	87,459	1,064	0	194,156	278,058,540	15,908	934,492	280,407,555	77,576,589
2048	0.2	100,258	3,959	0	11,392	984,283	9,085	5,055	53,549	651	0	118,876	278,058,540	9,740	953,182	280,308,571	73,506,355
2049	0.3	100,929	7,221	0	11,446	984,283	11,260	9,405	97,675	1,188	0	216,834	278,058,540	17,766	972,245	280,488,793	69,719,066
2050	0.4	101,285	8,949	0	11,499	984,283	15,873	11,890	121,057	1,472	0	268,741	278,058,540	22,019	991,690	280,597,300	66,109,988
2051	0.5	102,039	12,616	0	11,551	984,283	23,207	17,097	170,656	2,076	0	378,849	278,058,540	31,040	967,545	280,759,500	62,699,718
2052	0.8	103,239	18,444	0	11,602	984,283	33,652	25,496	249,499	3,034	0	553,878	278,058,540	45,381	986,896	281,073,945	59,497,574
2053	1.1	104,947	26,746	0	11,652	984,283	47,693	37,711	361,797	4,400	0	803,174	278,058,540	65,807	960,877	281,467,629	56,474,795